Mass spectrometric analysis of signal dependent protein modifications

Dissertation

zur Erlangung des akademischen Grades

doctor rerum naturalium

(Dr. rer. nat.)

im Fach Biologie / Molekularbiologie

eingereicht an der

Lebenswissenschaftlichen Fakultät

der Humboldt-Universität zu Berlin

von

Günther Kahlert, Dipl. Biologe

Präsident der Humboldt-Universität zu Berlin

Prof. Dr. Jan-Hendrik Olbertz

Dekan der der Lebenswissenschaftlichen Fakultät

Prof. Dr. Richard Lucius

Gutachter:

1. Prof. Dr. Achim Leutz

2. Prof. Dr. Matthias Selbach

3. Prof. Dr. Udo Heinemann

Eingereicht am: 27.03.2015

Tag der mündlichen Prüfung: 10.08.2015

For my parents Silvia and Charles,
and for
Joanna Narog and Dr. R. Hauser.

Contents

ZUSAMMENFASSUNG

Zellproliferation und Zelldifferenzierung sind streng kontrollierte Prozesse, die von Transkriptionsfaktoren gesteuert werden. C/EBPα und C/EBPβ sind Transkriptionsfaktoren, die diese Prozesse in Hepatozyten, Adipozyten und myeloischen Zellen regulieren. Darüber hinaus spielen C/EBPα und C/EBPβ eine onkogene Rolle in akuter myeloischer Leukämie und anaplastisch-großzelligen Lymphomen. In dieser Studie wird C/EBPα auf neue posttranslationalen Modifikationen, wie zum Beispiel Arginin-Methylierungen und Citrullinierungen, sowie Lysin-Methylierungen und Acetylierungen mit neusten massenspektrometrischen Mitteln untersucht. Es werden eine ausgewählte modifizierbare C/EBPα-Arginin-Citrullinierungsposition und die C/EBPα-Lysinsumoylierung eingehend auf ihren Einfluss auf C/EBPα-Proteininteraktionsnetzwerk überprüft. Dabei wurden neue modifikationsabhängige Proteine wie PML, ARIP4 und NUP358 als Partner der sumoylierten C/EBPα-Transaktivierungsdomäne 3 identifiziert. Außerdem wurde im Verlauf dieser Studie ein Hochdurchsatz-Screening-Verfahren entwickelt, das wir Protein Interaktions-Screening auf einer Peptid Matrix (PrISMa) nennen. Dieses Verfahren dient der Aufklärung des modifikationsabhängigen Proteininteraktionsnetzwerkes von C/EBPβ. PrISMa basiert auf einer Peptidmembran, auf der C/EBPβ-Peptide synthetisiert sind. Die C/EBPβ-Peptidsequenzen decken C/EBPβ vom N-Terminus bis zum C-Terminus ab und bieten die Möglichkeit überlappende Aminosäureinteractionsmotive zu entdecken. Viele dieser Peptide sind mehrfach auf der Peptidmembran vertreten mit dem Unterschied, dass sie methylierte Arginine und Lysine, acetylierte Lysine, citrullinierte Arginine und phosphorylierte Serine, Tyrosine und Threonine enthalten. Mittels PrISMa konnten Interaktionen von C/EBPβ mit Histonacetyltransferasen, dem Mediatorkomplex, Proteinen des nucleären Transports und RNA bindenden und spleißenden Proteinen verifiziert und auf kurze C/EBPβ-Aminosäuresequenzen kartiert werden. Darüber hinaus, konnte mit Hilfe von PrISMa eine große Anzahl der von C/EBPβ publizierten Interaktionspartner spezifischen C/EBPβ-Sequenzen zugeordnet werden. C/EBPβ ist in ALK positiven anaplastischen-großzelligen Lymphomen in hohem Maße exprimiert und ist essentiell für die

Zellproliferation dieser Krebsart. In dieser Studie wird das C/EBPβ Proteininteraktionsnetzwerk in einer anaplastischen-großzelligen Lymphom Zelllinie aufgeklärt, um tiefere Einsichten über die Funktion von C/EBPβ als Onkogen zu erlangen.

Stichworte: C/EBPα, C/EBPβ, posttranslationale Proteinmodifikation, Protein Interaktions-Screening auf einer Peptide Matrix (PrISMa), Sumoylierung, Proteininteraktionsnetzwerk

SUMMARY

Cell proliferation and differentiation are highly controlled processes managed by transcription factors. C/EBPα and C/EBPβ are two transcription factors that regulate cell proliferation and differentiation in multiple cell types, such as hepatocytes, adipocytes and cells of the myeloid lineage. Moreover, C/EBPα and C/EBPβ are known to play oncogenic roles in acute myeloid leukemia and anaplastic large cell lymphomas. In this study C/EBPα is screened for novel posttranslational modifications (PTMs), such as arginine methylation and citrullination, as well as lysine methylation and acetylation by using state of the art mass spectrometry. A in this survey identified C/EBPα site of arginine citrullination and the C/EBPα lysine sumoylation are scrutinized for their impact on C/EBPα protein interaction network. Among others, the novel C/EBPα interaction partners PML, ARIP4 and NUP358 were detected to interact with the sumoylated C/EBPα transactivation domain 3. A new high-throughput method named Protein Interaction Screen on peptide Matrices (PrISMa) is introduced in this study. This method was developed to determine the C/EBPβ protein interaction network in a PTM dependent manner. The PrISMa survey is based on a peptide membrane spotted with C/EBPβ peptides. These synthetic C/EBPβ peptide sequences were designed in a tiled manner from C/EBPβ N-terminus to the C-terminus containing multiple peptides for amino acid sequences comprising arginine and lysine methylation, lysine acetylation, arginine citrullination and serine, tyrosine and threonine phosphorylation. By means of PrISMa the C/EBPβ interplay with histone acetyltransferases, the mediator complex, proteins of the nucleoplasmic transport and RNA processing proteins is verified and specified by mapping these interactions to short C/EBPβ amino acid sequences. Furthermore, PrISMa provides a map of C/EBPβ protein interaction patterns for a great number of the up to date published C/EBPβ protein interaction partners. C/EBPβ is highly expressed in ALK positive anaplastic large cell lymphoma (ALK+ALCL) cell lines and is essential for the cell proliferation of this type of cancer. In this study the C/EBPβ protein-protein interaction pattern in an anaplastic large cell lymphoma cell line is unraveled providing valuable insight into

the protein interaction network of C/EBPβ as an oncogene.

Keywords: C/EBPα, C/EBPβ, posttranslational modification, Protein Interaction Screen on peptide Matrices (PrISMa), sumoylation, protein interaction network

INTRODUCTION

1.1 The C/EBP family of transcription factors

Transcription factors are nodes of the transcription machinery. Their binding to deoxyribonucleic acid (DNA) and their protein-protein interaction pattern plays a remarkable role in transcription determining if a gene is transcribed or not.

The CCAAT/enhancer-binding protein (C/EBP) family is a family of six transcription factors. The members of the C/EBP family are highly conserved amongst species from human to fish (Leutz et al., 2011). The six members are named C/EBPα, C/EBPβ, C/EBPγ, C/EBPδ, C/EBPε and C/EBPζ (Cao et al., 1991, Tsukada et al., 2011). C/EBPs have a highly conserved basic leucine zipper domain (bZIP) consisting of a DNA binding region (DB) and a leucine zipper (LZ) at the protein C-termini. The LZ is important for forming homo- or heterodimers with proteins. The protein N-termini of C/EBPα, C/EBPβ, C/EBPδ and C/EBPε are made up of a transactivation domain (TAD) and a regulatory domain (RD). The TAD and the RD can be subdivided into multiple conserved regions (CRs) linked by low complexity regions (LCR). C/EBPs play a pivotal role in cell proliferation and differentiation by binding to ATTGCGCAAT nucleotide sequences (Johnson et al., 1989; Miller et al., 2003; Schmidt et al., 2010).

1.2 C/EBPα and C/EBPβ are key regulators in multiple tissues

C/EBPα and C/EBPβ are two key players of the C/EBP family determining cell proliferation or cell differentiation of multiple tissues. A fine-tuned interplay of C/EBPα and C/EBPβ is important for hepatocyte differentiation and liver regeneration (Takayama et al., 2013; Michalopoulos et al., 2014). C/EBPα and C/EBPβ are part of a transcription factor cascade guiding mesenchymal stem

cell differentiation into preadipocytes followed by the transformation into adipocytes (Tang et al., 2012). C/EBPα and C/EBPβ are expressed in skin and are essential for terminal differentiation of keratinocytes (Maytin et al. 1998; Lopez et al., 2009). C/EBPα and C/EBPβ take part in the complex process of hematopoiesis (Laiosa et al., 2006). Both of these C/EBPs are involved in granulopoiesis and have been shown to play a role in the transdifferentiation of fibroblasts or B cells into macrophages (Fiedler et al., 2012; Xie et al., 2004; Graf et al., 2009).

Mice knockout studies showed that C/EBPα$^{-/-}$ mice die shortly after birth from hypoglycemia due to the decreased or delayed expression of the glucogen synthase, glucose-6-phosphatase and phosphoenolpyruvate carboxykinase (Wang et al., 1995). These C/EBPα$^{-/-}$ mice lack mature neutrophil granulocytes (Zhang et al., 1997). C/EBPβ$^{-/-}$ mice are viable but present lymphoproliferative disorders, an altered CD4^{+} T-helper response and are severely limited in bactericidal activities of macrophages (Tanaka et al., 1995; Screpanti et al., 1995). Female C/EBPβ$^{-/-}$ mice are infertile as C/EBPβ expression is critical in granulosa cells for normal oocyte development (Sterneck et al., 1997). C/EBPα,β$^{-/-}$ mice die during embryogenesis due to embryonic development arrest (Bégay et al., 2004).

C/EBPα and C/EBPβ display redundancy to a certain degree in the gene activation necessary for embryonic development and tissue specific gene activation. C/EBPα deficient mice, which have the *CEBPA* gene replaced in the *CEBPA* gene locus with the *CEBPB* gene are viable and fertile (Chen et al., 2000). The C/EBPα $^{\beta/\beta}$ phenotype shows no abnormalities in liver development or granulocyte differentiation but has reduced white adipose tissue revealing C/EBPα essential functions in adipogenesis (Jones et al., 2002).

1.3 C/EBPα and C/EBPβ involvement in cancer

Acute myeloid leukemia (AML) is a cancer characterized by myeloid neoplasm in the bone marrow and blood (Hasserjian et al., 2013). C/EBPα plays an oncogenic role in AML. 10-15 % of all AML patients have a mutation in the *CEBPA* gene (Paz-Priel et al., 2011). Many of the AML patients have biallelic *CEBPA* mutations. The mutations of C/EBPα lead to an impaired hematopoietic

differentiation (Gaidzik et al., 2008). Acute lymphoblastic leukemia is a cancer characterized by the overproduction of lymphoid neoplasm in the bone marrow. C/EBPα expression levels and gene regulatory functions are atypically upregulated in acute lymphoblastic leukemia (Akasaka et al., 2011; Slamova et al., 2014).

C/EBPβ aberrant expression and functions are associated with cancer types arising from various tissue types. C/EBPβ is expressed in colorectal cancer and has been suggested to support the tumor invasion capability of this cancer type (Rask et al., 2000). Human and murine studies revealed that the atypical expression of C/EBPβ is connected with mammary gland abnormalities in breast cancer (Zahnow et al., 2002). Furthermore, elevated C/EBPβ mRNA levels have been shown to be prominent in aggressive subsets of breast cancers (Zahnow et al., 2009). C/EBPβ is an important transactivator during hematopoiesis and has been shown to play an oncogenic part in lymphoma survival. Anaplastic large-cell lymphomas (ALCLs) are a type of lymphoma originating from malignant T-cells. C/EBPβ is highly expressed in some types of ALCL and has been shown to be vital for the cell proliferation of the lymphoma carrying the NPM-ALK fusion gene (Quintanilla-Martinez et al., 2006; Anastasov et al., 2010).

Interestingly, C/EBPβ has not only been shown to display oncogenic functions in various cancers but also activates cell senescence during oncogenic stress (Sebastian et al., 2005). The C/EBPβ induced cell senescence is RB-E2F dependent and was suggested to be cell type specific. C/EBPβ induced cell senescence is potentially controlled by the varied spatial translation of C/EBPβ mRNA in different parts of the cytosol (Basu et al., 2011). Recently, mouse knockin studies by Bégay et al. revealed that the expression of only the short C/EBPβ isoform LIP (C/EBPβ $^{LIP/LIP}$) instead of a cell type specific balanced expression of all three C/EBPβ isoforms promotes tumorigenesis (Bégay et al., 2015).

1.4 C/EBPα and C/EBPβ mRNA is transcribed into multiple isoforms

C/EBPα and C/EBPβ are transcribed from intronless messenger ribonucleic acids (mRNAs) (Lin et al., 1993; Descombes et al., 1991). Both of these mRNAs lead to the translation of several protein isoforms. The C/EBPα mRNA is translated into three isoforms, the C/EBPα extended isoform (C/EBPα Ext), p42 and p30 (Figure 1) (Ossipow et al., 1993; Calkhoven et al., 2000). C/EBPβ is expressed as the three isoforms LAP*, LAP and LIP (Figure 1). The C/EBPα and C/EBPβ isoforms vary in their length of the protein N-terminus. C/EBPα and C/EBPβ have a highly conserved bZIP domain comprising a basic acidic (BA) region, a DNA binding region (DB), a fork region (FORK), the leucine zipper (LZ) and a C-terminal peptide (CP) (Leutz et al., 2011). C/EBPα N-terminus is subclassified into the transactivation domain 1 (TF-1), the transactivation domain 2 (TF-2) and the transactivation domain 3 (TF-3) (Nerlov et al., 1994; Johnson et al., 2005). The C/EBPβ N-terminus is subclassified into the functional domains TAD and RD comprising the conserved regions (CRs) 1 to 7. C/EBPβ CR 2 to 7 are conserved in C/EBPα as well, providing a rationale as why these two transcription factors are interchangeable (Leutz et al., 2011; Jones et al., 2002). The C/EBPα Ext isoform is translated from a CUG or GUG codon, whereas p42 and p30 are initiated from an AUG initiation codon (Calkhoven et al., 2000; Müller et al., 2010). The non-AUG initiation codon of the C/EBPα Ext isoform was suggested to be a mechanism to limit the expression of this C/EBPα isoform.

The C/EBPα and C/EBPβ mRNA contain an upstream open reading frame (uORF) (Lincoln et al., 1998). The C/EBPα uORF resides in the 5´untranslated region (UTR) of C/EBPα mRNA, whereas C/EBPβ uORF is located between the AUG initiation codons of the LAP* and LAP isoforms (Lincoln et al., 1998; Calkhoven et al., 2000; Wethmar et al., 2010b). The translation of the C/EBPα and C/EBPβ isoforms is uORF-regulated and is affected by the mTOR signaling pathway (Calkhoven et al., 2000). In murine knockout studies it was shown that the C/EBPβ $^{\Delta uORF}$ mice do not express the LIP isoform (Wethmar et al., 2010a). These C/EBPβ $^{\Delta uORF}$ mice display cell differentiation defects and stunted osteoclast differentiation. As reviewed by Wethmar et al. the C/EBPα p42 isoform is important for the cell differentiation

of hepatocytes, adipocytes, and granulocytes, whereas the short isoforms is predominant in still proliferating cell types such as preadipocytes, prehepatocytes and AML (Wethmar et al., 2010b). The C/EBPβ LAP isoform is the main isoform expressed in macrophages, lymphocytes and the mammary gland, whereas the LIP isoform is primarily expressed in osteoclasts and mammary tumors. The N-terminal truncated C/EBP isoforms p30 and LIP are regarded as antagonists of the corresponding longer C/EBPα and C/EBPβ isoforms.

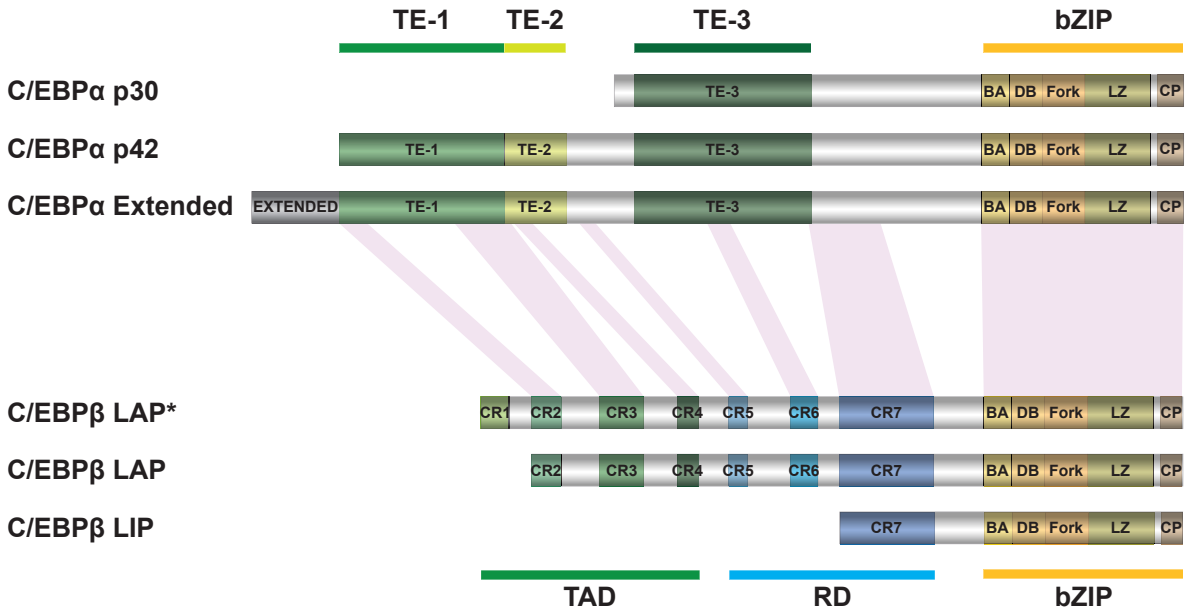

Figure 1: C/EBPα and C/EBPβ are expressed each with three isoforms from a single intronless mRNA. C/EBPα is translated into the three isoforms C/EBPα Extended, p42 and p30. C/EBPβ is translated into the three isoforms LAP*, LAP and LIP. C/EBPα and C/EBPβ have a highly conserved bZIP comprising a basic acidic (BA) region, a DNA binding region (DB), a fork region (FORK), the leucine zipper (LZ) and a C-terminal peptide (CP). C/EBPα N-terminus is subclassified into the transactivation domain 1 (TF-1), the transactivation domain 2 (TF-2) and the transactivation domain 3 (TF-3). C/EBPβ N-terminus is subcassified into a transactivation domain (TAD) and a regulatory domain (RD) comprising the conserved regions (CRs) 1 to 7. The light red coloring connecting C/EBPβ LAP* with C/EBPα Extended depicts regions of high amino acid sequence overlap or similarity. This figure is adapted from Leutz et al., 2011 and Johnson et al., 2005.

Apart from the expression of the C/EBPβ isoforms guided by the uORF C/EBPβ mRNA contains an Adenylate-uridylate-rich (AU-rich) element in the 3´UTR as well (Jones et al., 2007). ELAV1, a RNA binding protein, binds to C/EBPβ AU-rich element and regulates the nuclear export of the C/EBPβ mRNA. The binding of ELAV1 to C/EBPβ mRNA increases C/EBPβ

mRNA stability and C/EBPβ protein levels (Bergalet et al., 2011). Furthermore, it was suggested that the binding of ELAV1 to C/EBPβ mRNA controls, in which area of the cytosol C/EBPβ is translated (Basu et al., 2011). C/EBPβ mRNA is transcribed in the perinuclear cytoplasmic region when ELAV1 is not bound to C/EBPβ AU-rich element leading to C/EBPβ activation after translation due to phosphorylation via the Ras-Raf-MEK-ERK pathway. The perinuclear cytoplasmic region harbors important kinases, such as activated ERK1/ERK2. When ELAV1 binds to C/EBPβ AU-rich element C/EBPβ mRNA gets transported away from the perinuclear cytoplasmic region. The interaction of C/EBPβ AU-rich element with ELAV1 has been proposed as a possible mechanism for regulating C/EBPβ induced cell senescence.

1.5 PTM writers, readers and erasers

C/EBPα and C/EBPβ are highly modified by PTMs (Tsukada et al. 2011). The same set of enzymes that mark histones or erase histone marks modify numerous proteins featuring a variety of cellular functions. C/EBPα and C/EBPβ belong to the group of proteins, which are guided by PTMs during cell proliferation and cell differentiation.

There are numerous types of PTMs discovered in recent years. Among these are phosphorylated serines, threonines or tyrosines, methylated arginines and lysines, citrullinated arginines and acetylated lysines (Rothbart et al., 2014). The modification of proteins, such as histones and transcription factors, is carried out by a large set of enzymes. Some of these amino acid modifications lead to conformational changes of the nucleosome architecture caused by charge effects, whereas other PTMs are essential for the attraction or rejection proteins and their corresponding protein complexes (Wozniak et al., 2014).

Histone acetyltransferases (HATs) are enzymes that acetylate histones leading to the decondensation of chromatin in a transcriptionally activating manner (Lee et al., 2007). The acetyltransferases CBP, P300, GCN5 and KAT5 play a key role in protein complexes. These enzymes create the histone marks that are recognized by proteins containing a bromodomain (Zeng et al., 2002). Many of these bromodomain containing proteins are vital for transcriptional

regulation, chromatin-remodeling or like CBP, P300 and GCN5 are histone acetyltransferases themselves (Filippakopoulos et al., 2012). Histone deacetylases (HDACs) remove the lysine-acetylation pattern on histones leading to the condensation of chromatin and the loss of the protein-PTM interaction of the bromodomain containing proteins (De Ruijter et al., 2003). HDAC1 and HDAC2 are two prominent histone deacetylases known to be components of multiple chromatin-remodeling complexes, for example the transcriptionally repressive Mi2/NuRD complex or the SIN3A complex (Gregoretti et al., 2004).

Histone methylases are grouped into two classes of enzymes methylating either arginines or lysines. The class of human protein arginine methyltransferases (PRMT) consists of eleven proteins that methylate arginines (Pal et al., 2007). After monomethylating arginines these enzymes subsequently either asymmetrically or symmetrically dimethylate their substrates, depending on which enzymatic subtype these PRMTs belong to. Apart from methylating histones these PRMTs have been shown to associate with chromatin-remodeling complexes such as the Mi2/NuRD, the SWI/SNF and INO80 complex. PRMTs are associated with transcriptional regulation as well. Arginine methylation marks are erased by protein-arginine deiminases (PADIs) leaving behind citrullinated arginines (Mohanan et al., 2012). Additionally, these enzymes have the capacity to citrullinate non-modified arginines.

Lysine methyltransferases (KMTs) are enzymes that mono-, di- or trimethylate lysines (Black et al., 2012). Histone lysine methylation is associated with transcriptional repression or transcriptional activation depending on whether a lysine is singly, doubly or triply methylated and which histone residue is modified (Varier et al., 2011). Lysine demethylases (KDMs) remove the histone marks on lysines and by this reverse the effects of KMTs on the corresponding histone residues (Klose et al., 2007). JmjC domain containing proteins are one important group of KDMs (Shi et al., 2007). They play a significant part in the regulation of the transcription and the cell cycle (Del Rizzo et al., 2014). Many proteins belonging to the tudor protein family have been shown to read arginine or lysine methylation marks (Chen et al., 2011; Gayatri et al., 2014). These tudor domain containing proteins interact with modified histones, to impact RNA metabolism and participate in the DNA damage response (Pek et al., 2012).

1.6 C/EBPα and C/EBPβ are highly modified by PTMs

C/EBPα is highly post-translationally modified by phosphorylation and sumoylation (Figure 2) (Tsukada et al. 2011; Wang et al., 1995; Zhang et al., 1997). Phosphorylation of C/EBPα S21 restricts granulocyte differentiation (Radomska et al., 2006). C/EBPα S193 is phosphorylated as well (Wang et al., 2004). Downstream of the PI3K/Akt signaling pathway PP2A dephosphorylates C/EBPα S193 and abolishes C/EBPα growth arrest ability. The loss of growth has been suggested to be brought about by the disruption of C/EBPα interaction with the E2F-Rb complex in favor of an E2F independent Rb binding to C/EBPα (Wang et al., 2005). C/EBPα is phosphorylated at T222 and T226 by GSK3, depending on blood glucose levels (Liu et al., 2006; Pedersen et al., 2007). S248 phosphorylation as a result of RAS signaling is important for granulocyte differentiation (Behre et al., 2002). C/EBPα DNA binding ability is sensitive to the phosphorylation of S299 by PKC (Mahoney et al., 1992). Furthermore, the phosphorylation of S299 stimulates nucleolar retention of C/EBPα influencing the synthesis of ribosome RNA (Müller et al., 2010). C/EBPα is sumoylated at K159 with SUMO-1, SUMO-2 and SUMO-3 (Kim et al., 2002; Golebiowski et al., 2009; Subramanian et al., 2003). The decline of sumoylated C/EBPα and the increased availability of the non-sumoylated C/EBPα has been associated with terminal cell differentiation (Khanna-Gupta et al., 2008).

C/EBPβ is intensely modified by phosphorylation, acetylation and methylation (Figure 2) (Tsukada et al., 2011; Leutz et al. 2011). C/EBPβ is dimethylated by PRMT4 at R3 (Kowenz-Leutz et al., 2010). This R3 dimethylation abrogates the interaction of C/EBPβ with the chromatin-remodeling SWI/SNF complex impacting transcriptional regulation. C/EBPβ K39 (rat) is a diversely modified amino acid. K39 is acetylated by P300 (Cesena et al., 2007). The acetylation of K39 affects the transcriptional activation of C/EBPβ downstream targets. Aside from being acetylated, K39 is methylated by G9a as well (Pless et al., 2008). Mutational analysis by site-directed mutagenesis of C/EBPβ R3 and K39 revealed that these amino acids affect C/EBPβ dependent lympho-myeloid trans-differentiation (Stoilova et al., 2013). C/EBPβ S65 (rat) is phosphorylated by CDK2 as a consequence of the RAS pathway induction (Shuman et al., 2004). C/EBPβ is acetylated at K99 (rat), K102 (rat) and K103 (rat) by PCAF and GCN5 (Wiper-Bergeron et al., 2007). The acetylation of these lysines of the C/EBPβ TAD is linked

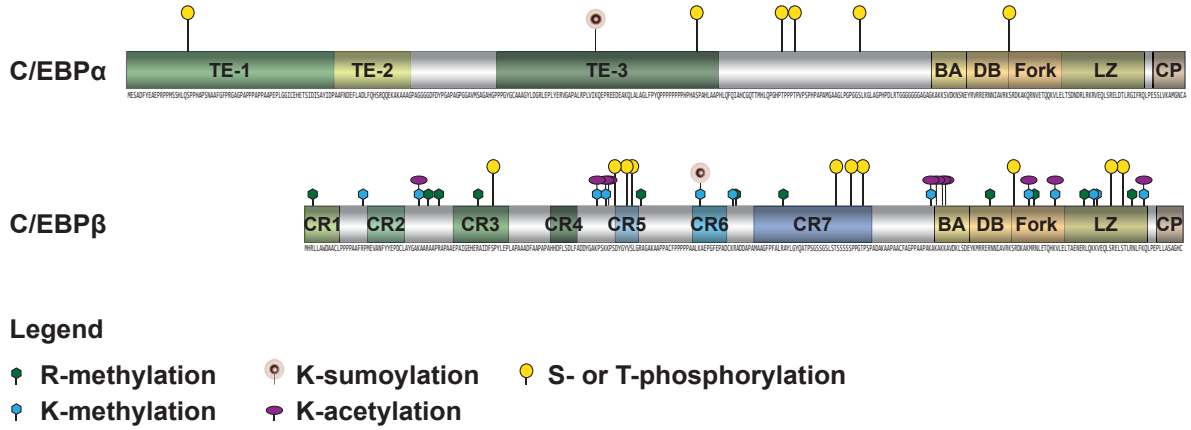

Figure 2: C/EBPα and C/EBPβ are highly modified by PTMs. Schematic presentation of C/EBPα and C/EBPβ (*Rattus norvegicus*) and their corresponding modification pattern. C/EBPα is highly modified by serine and threonine phosphorylation of the TE-1, the TE-3, the bZIP and the amino acid stretch between the TE-3 and the BA. C/EBPα TE-3 is modified by SUMO-1, SUMO-2 and SUMO-3. All parts of C/EBPβ are thoroughly modified by serine and threonine phosphorylation, arginine and lysine methylation and lysine acetylation. C/EBPβ CR6 is modified by SUMO-1, SUMO-2 and SUMO-3. For C/EBPα and C/EBPβ PTM annotation vide legende at the bottom. The figure is adapted from Tsukada et al., 2011, Leutz et al., 2011, and Johnson et al., 2005.

to preadipocyte differentiation. C/EBPβ S105 (rat), S240 (rat) and S277 (rat) are phosphorylated as well (Wegner et al., 1992; Trautwein et al., 1994). S105 are S240 are phosphorylated by PKA, a kinase that plays an essential role in glycogen and lipid metabolism. S105 phosphorylation is associated with TGFα induced hepatocyte proliferation as well (Buck et al., 1999). One of the most significant PTMs of C/EBPβ is the phosphorylation of T189 (rat) located in C/EBPβ RD (Nakajima et al., 1993). T189 is phosphorylated by ERK1 or ERK2, components of the Ras-Raf-MEK-ERK pathway. The phosphorylation of T189 putatively characterizes an active state of C/EBPβ (Kowenz-Leutz et al., 1994). The phosphorylation of the T189 abrogates the R3 methylation enabling the interaction of the SWI/SNF complex with C/EBPβ in a transcriptionally activating manner (Kowenz-Leutz et al., 2010). Furthermore, the T189 phosphorylation is accompanied by the phosphorylation of C/EBPβ T180 (rat) (Shen et al., 2009). C/EBPβ is phosphorylated at S185 (rat) by GSK3 (Piwien-Pilipuk et al., 2001). C/EBPβ bZIP is acetylated by P300 at K216 (rat) and K217 (rat) leading to impaired DNA binding of C/EBPβ (Cesena et al., 2007). On the contrary, C/EBPβ K216 (rat) and K217 (rat) are

deacetylated by HDAC1 restoring the DNA binding capacity of C/EBPβ (Xu et al., 2005). The Ras-Raf-MEK-ERK pathway induces C/EBPβ S273 (rat) phosphorylation facilitating C/EBPβ DNA binding. The same C/EBPβ activation by Ras leads to the phosphorylation of C/EBPβ T109 (rat) and S111 (rat) and the methylation of R114 (rat) as well (Lee et al., 2010c). By means of the Ras-Raf-MEK-ERK pathway C/EBPβ is phosphorylated at T217 (mouse) by RSK (Buck et al., 2001a). The T217 only exists in mouse and human C/EBPβ and is absent in rat C/EBPβ. The T217 phosphorylation is crucial for TNFα induced proliferation of hepatic stellate cells during liver regeneration (Buck et al., 1999). C/EBPβ arginines and lysines are frequent targets of methylases and acetylases. A mass spectrometric screening revealed that C/EBPβ can be methylated at K20 (rat), R42 (rat), R59 (rat), K99 (rat), K102 (rat), R114 (rat), K134 (rat), K145 (rat), R146 (rat), R162 (rat), K212 (rat), R232 (rat), K245 (rat), R247 (rat), R264 (rat), K267 (rat), K268 (rat), R280 (rat) and K284 (rat) and C/EBPβ K212 (rat), K214 (rat), K245 (rat), K254 (rat), K268 (rat) and K284 (rat) can be acetylated (Leutz et al. 2011). Apart from being methylated C/EBPβ K134 (rat) is sumoylated by SUMO-1, SOMO-2 and SUMO-3 as well (Kim et al., 2002; Eaton et al., 2003). C/EBPβ was shown to be sumoylated in breast cancer cells (Atwood et al., 2011). The sumoylation of C/EBPβ has been shown to be T189 phosphorylation dependent.

PTMs play a crucial role in the structure of C/EBPs, such as the Ras-Raf-MEK-ERK pathway triggered phosphorylation of C/EBPβ T189 leading to an activating conformational change of C/EBPβ (Kowenz-Leutz et al., 1994; Mo et al. 2004). So far only the structure of the bZIP-DNA complex of C/EBPs has been thoroughly unraveled by cristallization (Miller et al., 2003). Moreover, C/EBPα and C/EBPβ have been classified as intrinsically disordered proteins (Miller et al., 2009). Intrinsically disordered proteins are proteins that lack at least partially a well-ordered tertiary structure. In the case of C/EBPβ, intrinsically disordered regions have been predicted for the TAD and the RD. C/EBPβ intraprotein interactions of the TAD and RD are managed by short α-helical sequences and have been suggested to be liable to PTM dependent charge repulsion mechanisms (Lee et al., 2010b; Lee et al., 2010c). The transient but highly specific interactions of transcription factors with transcriptionally activating or repressing cofactors and complexes have been suggested to rely on the structural convertibility of intrinsically disorderd proteins (Miller et al., 2009).

1.7 C/EBPα and C/EBPβ interplay with proteins and protein complexes

C/EBPα is known to induce cell differentiation and inhibit cell proliferation by the interaction with components of the transcription machinery, chromatin-remodeling complexes and by the dimerization with other transcription factors. The TATA-box-binding protein (TBP) and Transcription initiation factor IIB (TF2B) bind to C/EBPα TE-1 and TE-2 promoting transcription (Nerlov et al., 1995). TE-1 and TE-2 are crucial for the binding of the histone acetyltransferases CBP and P300 as well (Kovacs et al., 2003). The chromatin-remodeling complex SWI/SNF interacts with C/EBPα TE-3 (Pedersen et al., 2001). The interaction of C/EBPα with the SWI/SNF complex is essential for C/EBPα dependent cell proliferation inhibition (Müller et al., 2004). CDK2 and CDK4 interact with the C/EBPα TE-3 as well (Wang et al., 2001). This interaction prevents the formation of CKD2/Cyclin complexes necessary for cell proliferation. The transcription factor E2F is a protein partner of C/EBPα (Slomiany et al., 2000). This E2F interaction via C/EBPα bZIP represses E2F mediated cell proliferation in adipocytes and granulocytes promoting terminal cell differentiation (Porse et al., 2001). Recently, a mass spectrometric survey of C/EBPα interactome revealed novel C/EBPα interactions with components of the mediator complex, the PAF complex, the mRNP complex, the Sin3a-HDAC1 complex, the MLL-SWI/SNF complex, the DNA repair-replication complex, the Nono-SFPQ complex, the DBIRD complex and the Spliceosome complex (Giambruno et al., 2013). The interaction of these complexes with C/EBPα emphasizes the importance of this transcription factor in transcriptional regulation. Moreover, C/EBPα supposedly interacts with complexes that process mRNAs and mediate DNA repair.

C/EBPβ can replace C/EBPα when transcribed from the *CEBPA* gene locus (Jones et al., 2002) and C/EBPα and C/EBPβ share regions of high amino acid sequence overlap or similarity (Figure 1). Therefore, it comes at no surprise that the protein interaction pattern of these two transcription factors overlaps significantly. A vital part of the transcription machinery

is the mediator complex. The mediator complex is essential for the expression of most of the RNA polymerase II target genes (Poss et al., 2013). The Mediator complex has been shown to interact with C/EBPβ TAD (Mo et al., 2004). The Mediator complex links C/EBPβ with the RNA polymerase II either in a transcriptionally activating way containing MED26 or in a transcriptionally repressive way containing CDK8 (Eastburn et al., 2004). C/EBPβ CR3 and CR4 of the TAD contain the same amino acid sequence motifs for the interplay with TBP, TF2B and P300 as found in C/EBPα (Nerlov et al., 1995, Mink et al., 1997). P300 interacts with C/EBPβ acting as a transcriptional coactivator. The C/EBPβ TAD interacts with components of the SWI/SNF complex as well (Kowenz-Leutz et al., 1999). The C/EBPβ cooperation with the nucleosome remodeling SWI/SNF complex was shown to be transcriptionally activating. C/EBPβ CR1, only present in the long LAP* isoform, is a conserved region important for the SWI/SNF complex interaction. C/EBPβ is a protein interaction partner of members of the Mi2/NuRD complex as well as of INO80 chromatin-remodeling complex members (Steinberg et al., 2012). All three of these C/EBPβ interacting chromatin-remodeling complexes effectively modulate the nucleosome structure to activate or repress transcription. Likewise to C/EBPα, C/EBPβ has been screened for interaction partners using mass spectrometry (Steinberg et al., 2012; Siersbæk et al., 2014). These surveys suggested that C/EBPβ has protein partners executing numerous functions, for example mRNA processing, regulation of transcription and cell cycle maintenance.

1.8 Mass spectrometry a useful tool to detect PTMs and PTM dependent protein interaction networks

Mass spectrometers are used to unravel protein PTM sites, to elucidate protein networks and to detect alterations in protein abundances on a proteome level. The detection of proteins using mass spectrometers is either conducted using top-down or bottom-up techniques. The top-down approach involves analyzing entire proteins, whereas bottom-up mass spectrometry relies on the identification of peptides (Chait et al., 2006). The bottom-up procedure requires the digestion of proteins by endoproteinases to peptides. Almost all high-throughput proteomic measurements done today depend on the identification of peptides, which are assigned to their corresponding

proteins during data analysis (Nilsson et al., 2010).

The mass spectrometric detection of peptides is either done by shotgun proteomics or by targeted proteomics. Shotgun proteomics methods harness the benefits of high-resolution mass spectrometers, such as time-of-flight or Fourier transform analyzers (Zubarev et al., 2013). These analyzers are able to perform MS^2 analysis by determining the exact mass of a peptide, detected by a mass spectrometer as the mass-to-charge ratio (m/z), and subsequently fragment the peptide ion for the spectra acquisition (Aebersold et al., 2003). The mass spectrometric scan for the peptide m/z is often referred to as the MS1 scan and the acquisition of the peptide ion fragmention is frequently termed a MS2 scan. Using shotgun proteomic methods tens of thousands of peptides can be detected and quantified during a single measurement.

The site-specific identification of PTMs is based on MS^2 analysis. First the modification containing peptide is scanned for with high mass accuracy, then the peptide fragmention spectra reveals, which amino acid has a mass shift matching with the sought-after modification mass. Shotgun proteomics has become the key tool in quantifying protein abundances. The mass spectrometric quantification of proteins is used to unravel protein networks or to show protein abundance alterations of entire proteomes of diverse cell types. One way to quantify proteins is by stable-isotope labeling by amino acids in cell culture (SILAC) (Mann et al., 2006). In SILAC experiments the cell culture medium that is used to feed the analyzed cells is either ´light´or ´heavy´. The heavy SILAC medium contains arginines and/or lysines partially made up of ^{13}C and ^{15}N instead of ^{12}C and ^{14}N, whereas the light SILAC medium contains arginines and/or lysines consisting of ^{12}C and ^{14}N. The cells or the Co-IPs of SILAC experiments are mixed 1:1. Due to the high-resolution power of present-day mass spectrometers the ´light´and the ´heavy´peptides isotope clusters can be distinguished yielding a ratio useful for the detection of alterations in protein abundances. An alternative way to relatively quantify protein abundances is stable isotope incorporation at a protein or a peptide level (Gevaert et al., 2008). A third way to quantify proteins is the label-free quantification (LFQ) approach (Bantscheff et al., 2007). The mass spectrometric peptide signals gathered from multiple mass spectrometric measurements are quantified using LFQ algorithms either by spectral counting, which involves the comparison and counting fragment spectra of the MS2 scans, or by comparison of peptide precursor ion intensities of the MS1 scans. LFQ based on MS1 intensities requires high mass resolution as the

contamination of the MS1 signals by close by *m/z* signals leads to inaccurate intensity readouts (Cox et al., 2014). MS1 based LFQ has the advantage that the steady intensity readout of peptide precursor ion intensities is more reliable and information-rich than MS2 scan based LFQ. LFQ is still preferably used for small data sets, such as Co-IPs, as handling variations and chromatographic discrepancies substantially affect LFQ analysis in comparison to sample analysis from metabolic labeling experiments (Bantscheff et al., 2007; Cox et al., 2014). The LFQ disclosure of protein-protein interaction networks is usually based on the independent observations of a peptide in multiple samples as label-free Co-IPs are validated according to the resulting P value emanating from a t-test (Hubner et al., 2011).

Targeted proteomics is used to quantify peptides with a high sensitivity and reproducibility (Marx et al., 2013). Selected reaction monitoring (SRM) is a targeted proteomics method. SRM takes advantage of the selectivity of triple quadrupole mass spectrometers (QQQs) acting as mass filters (Picotti et al., 2012). The first quadrupole (Q1) scans for the *m/z* of the peptide, the second quadrupole (Q2) is a collision cell and fragments the peptide at the peptide bonds by collision-activated dissociation and the third quadrupole (Q3) selects the most prominent fragment ions of the in the Q2 dissociated peptide and guides them to the detector. The increased sensitivity of SRM in comparison to a shotgun proteomics approach is based on the non-scanning nature of the operation mode of QQQs and that only a preselected set of peptides are targeted during SRM measurements (Lange et al., 2008). In comparison to shotgun proteomic methods, where thousands of proteins can be quantified by the analysis of a single measurement, the number of targeted proteins is limited and depends on transition intensities and the corresponding dwell times and cycle times needed to aquire them (Picotti et al., 2012). Another downside of SRM compared to MS^2 based methods is that the SRM methods have to be established in advance, as the most prominent Q1 and Q3 masses have to be obtained for each peptide prior to sample analysis. On top of that, the exact retention time of the peptide and the optimal collision energy (CE) and declustering potential for all the Q3 masses have to be determined during method development. To establish SRM methods synthetic peptides are used (Picotti et al., 2010). These synthetic peptides can be either isotopically labeled or non-labeled. The isotopically labeled peptides are more beneficial than the non-labeled synthetic peptides as they are used as spike-in references being added directly to samples for retention time and fragmentation validation. With

the help of isotopically labeled and prequantified synthetic peptides standards absolute protein quantification by SRM is performed (Schnatbaum et al., 2011). Absolutely quantified isotopically labeled standards are more precise when they contain an endoproteinase cleavable C-terminal tag. These types of peptide standars are added before protein digestion and the C-terminal tags reduce absolute quantification variations by limiting the effects of fluctuating protein digestion rates.

1.9 Aim of this study

C/EBPα and C/EBPβ play a part in the downstream regulation of protein abundances, the proliferation and the differentiation of cells from diverse tissues and are known to play an oncogenic part in cancer cells. This study focuses on the effects of signal dependent protein modifications on the C/EBPα and the C/EBPβ protein-protein interaction networks.

This study intends to test C/EBPα for novel PTMs, such as arginine methylation and citrullination and lysine methylation and to verify them with tandem mass spectrums. As PTMs are known to impact protein-protein interactions this study aims to elucidate the protein interaction pattern of a novel C/EBPα arginine citrullination site. C/EBPα sumoylation pattern has been been associated with terminal cell differentiation (Khanna-Gupta et al., 2008). The aim of this study is to shed light on the C/EBPα sumoylation specific protein interaction pattern.

C/EBPβ has been thoroughly examined for PTMs over the last two decades and a recent mass spectrometric survey conducted by Leutz et al. showed that C/EBPβ has numerous sites of lysine and arginine methylation (Leutz et al., 2011). As the C/EBPβ PTM dependent protein-protein interaction network cannot be traced with conventional Co-IP methods a new in vitro method is devised in this study termed ´protein interaction screen on peptide matrices´(PrISMa) using a synthetic peptide matrix for protein interaction. This peptide matrix will cover the C/EBPβ amino acid sequence from the N-terminus to the C-terminus in a tiled manner including the most prominent C/EBPβ PTMs. With the aid of PrISMa this study aims to elucidate C/EBPβ protein interaction network by mapping proteins to specific C/EBPβ amino acid sequences and at the same time scrutinizing them for their dependency towards C/EBPβ PTM pattern. Apart from intending to map published and novel C/EBPβ protein interactions to specific C/EBPβ short amino acid sequences this study also aims to depict the collaboration of C/EBPβ with its protein interaction network.

C/EBPβ has been published to interact with the transcriptional coactivators P300/CBP (Kovacs et al., 2003). Furthermore, C/EBPβ has been shown to associate with members of chromatin-remodeling complexes, such as the members of the Mi2/NuRD complex (Steinberg et al., 2012). The aim of this study is to identify the CRs and PTMs of C/EBPβ that regulate the interplay of C/EBPβ with the HATs P300/CBP and the members of the Mi2/NuRD complex.

C/EBPβ is strongly expressed in many ALK+ALCL cell lines (Quintanilla-Martinez et al., 2006). Moreover, C/EBPβ has been shown to be essential for the cell proliferation and cell survival of the ALK+ALCL cell line SU-DHL-1 (Anastasov et al., 2010; Bonzheim et al., 2013). The aim of this study is to provide a thorough survey of the C/EBPβ protein interactome in SU-DHL-1 and to elucidate the C/EBPβ protein interaction pattern that is most likely regulating pathways crucial for the survival of this lymphoma cell line. This survey also intends to compare the outcome of C/EBPβ in vivo protein interactome in SU-DHL-1 with the in vitro mapping of C/EBPβ peptide-protein interactions to obtain a better insight of how C/EBPβ conserved regions (CRs) and domains are involved in the oncogenic functions of C/EBPβ in a prominent cancer line.

MATERIAL AND METHODS

2.1 Chemicals, solvents and materials

Acetic anhydrid (Sigma-Aldrich, Germany)

Acetonitrile (ACN) hypergrade for MS (Merck, Germany)

4-Alkoxy-2-hydroxybenzaldehyde (Sigma-Aldrich, Germany)

Ammoniumhydrogencarbonat (Roth, Germany)

Benzotriazolyl-oxytripyrrolidinophosphonium-hexafluorophosphat (PyBOB) (Merck,Germany)

Biopsy punch 2 mm (Stiefel, NC, USA)

Bromophenol blue (Sigma-Aldrich, Germany)

2,3-Butanedione (Sigma-Aldrich, Germany)

C18 reversed-phase beads Reprosil-Pur120 C18-AQ 3 µm (Dr. Maisch GmbH, Germany)

Capillary tubing OD 360 / ID 75 µm (Polymicro Technologies, PHO, USA)

C/EBPε TAD peptides with biotin-tag (PSL Peptide Specialty Laboratories GmbH, Germany)

2-Choroacetamide (Sigma-Aldrich, Germany)

Dimethylformamide (Sigma-Aldrich, Germany)

Dithiothreitol (DTT) (Sigma-Aldrich, Germany)

Dulbecco´s modified Eagle medium (PAA/GE Healthcare, United Kingdom)

DynaMag^{TM}-2 magnetic rack (Invitrogen, WI, USA)

Ethylenedinitrilotetraacetic acid disodium salt (EDTA) (Merck, Germany)

Fetal bovine serum (PAA/GE Healthcare, United Kingdom)

Fmoc-amino acid starter kit 20x (25g) (Intavis AG, Germany)

Formic acid (FA) for analysis (Merck, Germany)

Glycerol (Merck, Germany)

Hydrochloric acid 37 ⅞ (HCl) (Sigma-Aldrich, Germany)

L-Lysine (Sigma-Aldrich, Germany)

L-Lysine-D_4 hydrochloride (Cambridge Isotope Laboratories Inc., MA, USA)

L-Lysine-$^{13}C_6$,$^{15}N_2$ hydrochloride (Sigma-Aldrich, Germany)

Methanol hypergrade for LC-MS (Merck, Germany)

N-(2-Hydroxyethyl)piperazine-N´-2 ethane sulfonic acid (HEPES) (SERVA, Germany)

N-methylmorpholine (Intavis, Germany)

N-methyl-2-pyrrolidone (Sigma-Aldrich, Germany)

Penicillin/Streptomycin (PAA/GE Healthcare, Little Chalfont, United Kingdom)

Piperidine (Sigma-Aldrich, Germany)

Potassium chloride (KCl) (Roth, Germany)

PrISMa spotted peptide filter (JPT Peptide Technologies GmbH, Germany)

Octadecyl C18 solid phase extraction disks (Empore 3M, MN, USA)

RPMI 1640 (Invitrogen, CA, USA)

SILAC DMEM (PAA/GE Healthcare, United Kingdom)

SILAC fetal bovine serum dialyzed (Sigma-Aldrich, Germany)

SILAC RPMI 1640 (PAA/GE Healthcare, United Kingdom)

Sodium dodecyl sulfate (Merck, Germany)

SpikeTides TQL peptides (JPT Peptide Technologies GmbH, Germany)

Tert-butyl-methyl-ether (Sigma-Aldrich, Germany)

ThermoFast 96 well robotic PCR-plate (Thermo Scientific, Denmark)

Thiourea (Roth, Germany)

Trichloromethane / Chloroform for HPLC (Roth, Germany)

Trifluoroacetic acid (TFA) for spectroscopy (Merck, Germany)

Triisopropylsilane (Sigma-Aldrich, Germany)

Tris-(hydroxymethyl)-aminomethan (TRIS) (Roth, Germany)

Urea (VWR International, Belgium)

Water for chromatography (Merck, Germany)

2.2 Enzymes, tRNA and cell extract

HeLa nuclear protein extract (CILBiotech, Belgium)

Endoproteinase Lys-C (Wako, Japan)

Modified trypsin, sequencing grade (Promega, WI, USA)

Yeast tRNA (Invitrogen, WI, USA)

2.3 Laboratory equipment

Centrifuge 5415D (Eppendorf, Germany)

Heating block DRI-Block DB 2A (Techne, United Kingdom)

Laser-based micropipette puller P-2000 (Sutter Instruments, CA, USA)

Microscope Sedival (Carl Zeiss Jena Microscopes, Germany)

Orbital shaker Rotamax 120 (Heidolph, Germany)

PAL HTS-*xt* autosampler (custom pipetting robot) (CTC-Analytics AG, Switzerland)

pH-meter CG 842 (Schott Instruments, Germany)

Pipet-lite XLS (1000-100µl, 200-20 µl, 20-2 µl, 2-0.5µl) (Rainin Instrument LCC, CA, USA)

Pressure injection cell for column packing (Biostep GmbH, Germany)

Refridgerated vapor trap RVT4104 (Savant, Thermo Scientific, United Kingdom)

Scale XA 105 DualRange (Mettler-Toledo GmbH, Germany)

Scale EW (Kern, Germany)

Speed vac SPD11V (Savant, Thermo Scientific, United Kingdom)

Thermomixer compact (Eppendorf, Germany)

Vortex-Genie 2 (Scientific Industries, NY, USA)

2.4 Mass spectrometers, HPLCs, autosampler and peptide synthesizer

AB Sciex Nano Spray II source (AB Sciex, MA, USA)

Eksigent nanoLC-ultra 1D plus (Eksigent, CA, USA)

Orbitrap electrospray ion source (Proxeon, Thermo Scientific, Denmark)

Orbritrap Velos (Thermo Scientific, MA, USA)

PAL 5500 HTC-*xt* (CTC-Analytics AG, Switzerland)

Proxeon EASY-nLC II (Thermo Scientific, Denmark)

Q Exactive (Thermo Scientific, MA, USA)

QTRAP 5500 (AB Sciex, MA, USA)

ResPepSL peptide Synthesizer (Intavis, Germany)

2.5 Methanol-chloroform precipitation of the C/EBPα,β and P300 Co-IPs and the C/EBPα-TE3 and C/EBPε peptide pull-downs

Proteins were eluted from magnetic Co-IP beads by adding 50 µl of laemmli buffer (1.3 ⁒ (w/v) sodium dodecyl sulfate (SDS), 10 mM TRIS, pH 6.8, 0.1 M Dithiothreitol (DTT), 8 ⁒ (w/v) glycerol, 0.1 mM bromophenol blue) and boiling the samples at 95 ℃ for 3 minutes. The denaturated proteins were separated from the beads using a magnetic rack. Detergents like SDS ionize during electrospray ionization quenching and overlaying peptide signals. Moreover, SDS contaminates the reversed-phase columns used for the peptide separation during mass spectrometric measurements. To remove the SDS from the proteins the samples were methanol-chloroform precipitated (Wessel and Flügge, 1984; Puchades et al., 1999) by adding 800 µl of methanol, then adding 200 µl chloroform and 600 µl H_20. Samples were vortexed and spun-down at 10.000 revolutions per minute (rpm) / 8161 g with a tabletop centrifuge for phase separation.

The supernatant was discarded and the protein interphase was precipitated by adding 600 µl methanol. The protein pellets were spun-down at 13.200 rpm / 14.200 g for 5 minutes. The supernatants were discarded and the air-dried pellets were reconstituted in urea buffer (10 mM HEPES, pH 8.0, 6 M urea, 2 M thiourea).

2.6 In-solution digests of purified C/EBPs, C/EBPα,β and P300 Co-IPs, the C/EBPα-TE3 and C/EBPε peptide pull-downs and the PrISMa peptide spots

Proteins were digested in a two-step protocol using the Lysyl endopeptidase (Lys-C) and the endopeptidase trypsin or exclusively Lys-C. The difference between these two endoproteinases is the cleavage site. Lys-C cleaves proteins into peptides at the carboxyl side of lysines, whereas trypsin cleaves at the carboxyl side of lysines and arginines. For the digestion procedure the protein samples were dissolved in 20 µl urea buffer (10 mM HEPES, pH 8.0, 6 M urea, 2 M thiourea). Disulfid bonds were reduced and cysteines were alkylated by first adding DTT with a final concentration of 1 mM for 30 minutes, thereafter topping up the samples with 2-chloroacetamide with a final concentration of 5.5 mM for 20 minutes. Subsequently, 1 µg Lys-C for 50 µg of protein was added to the samples for protein digestion. After three hours the samples were diluted four times with ABC buffer (50 mM ammoniumhydrogencarbonat). Then a second portion of endoproteinase was added. For a Lys-C digest Lys-C was added for a second time, whereas for a tryptic digest trypsin was added. For both the Lys-C and the tryptic digest a ratio of 1 µg endoproteinase was added to 50 µg of protein. The digestion was stopped after ten hours by acidifying the samples with 0.125 ٪ trifluoroacetic acid (TFA). The in-solution digest was performed using a PAL HTS-xt autosampler custom pipetting robot in-house programmed to perform in-solution digests. Subsequently, the acquired peptides were purified by stop-and-go-extraction tip (StageTip) purification.

2.7 StageTip purification of purified C/EBPs, C/EBPα,β and P300 Co-IPs, the C/EBPα-TE3 and C/EBPε peptide pull-downs and the PrISMa peptide spots

The peptides aquired by in-solution digest were desalted using non-polar interaction disks using StageTips (Rappsilber et al. 2007). 2 mm octadecyl C18 solid phase extraction disks from Empore 3M were punched out and packed into plastic pipette tips. Subsequently, the disks were wetted with 100 ℅ methanol. Then disks were prepared for peptide contact by rinsing them with washing buffer (1 ℅ TFA, 2 ℅ acetonitrile (ACN)). Thereafter, the samples were loaded onto the disks and thoroughly washed with washing buffer again. The StageTips carrying the purified peptides are storable at 4 ℃ for several months. The peptides were eluted from the StageTips by using an elution buffer (0.1 ℅ formic acid (FA), 80 ℅ ACN). Eluted peptides were dryed in a speed-vac and were reconstituted for mass spectrometric measurements in resuspension buffer (3 ℅ TFA, 5 ℅ ACN).

2.8 Modification of the citrulline residues of C/EBPα by 2,3-butanedione

Protein-arginine deiminases (PADIs) citrullinate arginines and methylated arginines. The citrullination of these arginines causes a mass shift of plus one Dalton (Da). The loss of the charge of the guanidinium group of arginines is a common artifact during peptide ionization, for this reason the citrullinated arginines of C/EBPα were chemically modified with 2,3-butanedione on a peptide level before the mass spectrometric measurement (De Ceuleneer et al., 2011). For that the C/EBPα peptides acquired from a Lys-C in-solution digest were eluted from a StageTip. The peptides were dryed in a speed-vac and reconstituted in 10 µl of 50 mM 2,3-butanedione. Then 30 µl of 100 ℅ TFA was added. The reaction was carried out at 37 ℃ for 16 hours. After 16 hours the sample was purified by a StageTip once more. The chemical modification

of citrullinated guanidinium group with 2,3-butanedione leads to formation of an imidazolone derivate leading to a mass shift of plus 50 Da.

2.9 C/EBPβ Protein Interaction Screen on peptide Matrices (PrISMa)

The spotted peptide matrix for the detection of C/EBPβ peptide-protein interactions was designed comprising 57 tiled peptides covering C/EBPβ (*Rattus norvegicus*) from N- to C-terminus and 166 peptides containing symmetric and asymmetric arginine dimethylation, arginine citrullination, lysine mono-, di- and trimethylation and serine, threonine and tyrosine phosphorylation. JPT Peptide Technologies GmbH, a company based in Berlin, Germany, sythesized the designed peptides onto a cellulose membrane using the PepTrack^{TM} technique. The peptide matrices were equilibrated with peptide matrix buffer (20 mM HEPES, pH 8.0, 0.2 mM EDTA, 100 mM KCl, 20 ⁒ Gycerol, 0.5 mM DTT) for 5 minutes on an orbital shaker. Then the peptide membranes were incubated with yeast tRNA (1 mg/ml) dissolved in peptide matrix buffer for 15 min to reduce unspecific peptide-protein binding. Afterwards the peptide matrices were incubated with 8 ml of HeLa nuclear protein extract (5 mg/ml) in HeLa nuclear buffer (20 mM HEPES, pH 7.9, 0.2 mM EDTA, 100 mM KCl, 20 ⁒ Gycerol, 0.5 mM DTT, 0.5 mM PMSF) for 45 minutes. Subsequently, peptide matrices were washed three times for 15 minutes with the peptide matrix buffer to reduce unspecific peptide-protein interaction.

Spots were punched out immediately afterwards with a 2 mm biopsy punch and were placed into 96 well plate wells. The punched out spots were submerged in 20 µl urea buffer (10 mM HEPES, pH 8.0, 6 M urea, 2 M thiourea). The peptide-protein spots were tryptically digested using a PAL HTS-*xt* autosampler custom pipetting robot in-house programmed to perform in-solution digests. The acquired peptides were purified by StageTip and submitted to mass spectrometric analysis on an Orbitrap Velos.

2.10 Preparation of analytical reversed-phase columns

The analytical reversed-phase columns were pulled and packed for direct ionization by electrospray ionization into the Q Exactive, Orbitrap Velos and the QTRAP 5500. For that disposable micropipette tip columns were made out of fused-silica capillary tubing from Polymicro Technologies with an inner diameter of 75 µm and an outer diameter of 360 µm using a laser-based micropipette puller (Ishihama et al., 2002). The Laser Puller P-2000 from Sutter Instrument Co. was set to a heat of 275, a velocity of 6 and to a delay of 255 to pull pairs of 20 cm long micropipette tip columns. The fritless 20 cm long micropipette tip columns were packed with C18 reversed-phase beads with a diameter of 3 µm using a pressure injection cell for column packing. The analytical reversed-phase columns were used for peptide separation in combination with the Proxeon EASY-nLC II and the Eksigent nanoLC-ultra 1D puls.

2.11 LC-MS shotgun proteomics of purified C/EBPs, C/EBPα,β Co-IPs, the C/EBPα-TE3 and C/EBPε peptide pull-downs and the PrISMa peptide spots

A Proxeon easy nLC-II high performance liquid chromatography (HPLC) system was used in order to create a gradient for separating peptides for the liquid chromatography-mass spectrometry (LC-MS) measurements. A 5-50 ٪ (v/v) ACN gradient in 0.1 ٪ (v/v) FA was run to separate peptides due to their hydrophobicity on analytical reversed-phase columns using a flow rate of 250 nl/min. The length of the measurement was selected based on the number of peptides that had to be separated. Purified C/EBPs, C/EBPα,β Co-IPs, the C/EBPα-TE3 and C/EBPε peptide pull-downs were measured in 3-hour runs for PTM discovery and protein interaction screening, whereas the more than 446 measurements for the PrISMa method and the replicate were conducted in an hourly run for each of the peptide spots.

Both the Q Exactive and the Orbitrap Velos were equipped with an Orbitrap electrospray

ion source. On the Q-Exactive the MS2 spectra were acquired with Higher-energy collisional dissociation (HCD), whereas on the Orbitrap Velos the MS2 spectra were generated by collision-induced dissociation (CID) in the linear trap quadrupole. HCD dissociation was conducted at the normalized collision energy of 25, whereas for CID fragmentation the normalized collision energy was set to 35. The isolation window of the mass spectrometric measurements was set to 2.1 Thomson (Th). A mass window of m/z of 300 to 1700 was chosen for the MS1 acquisition with a resolution of 60,000 for the Q-Exactive measurements and a resolution of 70,000 for the Orbitrap Velos measurements. The 10 most abundant m/z values with a charge state greater than one were chosen for MS2 fragmentation using a fill time of 120 ms for the measurement of purified the C/EBPs and the C/EBP Co-IPs and 60 ms for the PrISMa measurements. The dynamic exclusion was set to 30 seconds on both Orbitrap models.

The MaxQuant Software package version 1.2.2.5 was chosen to analyze the mass spectrometric data (Cox et al., 2008). SILAC Co-IPs and pull-downs were quantified using maximal three labeled amino acids per peptide. The heavy lysine^8, medium lysine^4 and light lysine^0 label was selected depending if the experiment was a double or a triple labeled SILAC approach. For the label-free quantification (LFQ) of the C/EBPβ Co-IP from SU-DHL-1 cells the MaxQuant LFQ mode selected with a LFQ minimum ratio count of two. The human database ipi.HUMAN.v3.3.72 was taken to assign the MS1 and the MS2 to the human proteome. The Andromeda search engine compared the detected m/z with the peptide masses verifying the corresponding MS2 spectra for peptide identification. The search included the common contaminant list embedded in MaxQuant 1.2.2.5. For MaxQuant analysis Trypsin/P or Lys-C/P was selected depending on the utilized endoproteinase. Two missed cleavage sites for were permitted per peptide. As a fixed modification carbamidomethylation of cysteines was selected, whereas methionine oxidation and N-acetylation of proteins were selected as variable modifications. The MS1 mass tolerance was 6 parts per million (ppm), whereas the MS2 tolerance was 20 ppm for the measurements on the Q Exactive (HCD) and 0.5 Da for the measurements on the Orbitrap Velos (CID). A false discovery rate of 1 ٪ was set for peptides and proteins. The top 10 MS2 peaks per 100 Da were selected for HCD spectra, whereas the top 6 MS2 peaks per 100 Da were chosen for CID fragmentation. For the identification of C/EBPα or C/EBPβ PTMs acetylated lysines, mono- and dimethylated arginines and lysines and trimethylated lysines were selected as variable

modifications for MaxQuant data computation. For the identification of the chemically modified citrullinated arginine of C/EBPα the modification was established in the Andromeda search engine and was selected as a variable modification for the corresponding measurement. Maximal five PTMs were allowed per peptide. MaxQuant match between runs was selected for the C/EBPβ Co-IPs from SU-DHL-1 and for the PrISMa measurements.

2.12 Synthesis of peptide standards for mass spectrometric analysis

Peptides were synthesized using an automated multiple peptide synthesizer, the ResPep SL. Synthesis was performed using a solid phase synthesis with the fluorenylmethyloxycarbonyl group (Fmoc) as the protection group and 4-alkoxy-2-hydroxybenzaldehyde (AHB) as the solid phase. The peptide synthesis was an iterating cycle during which peptides were synthesized stepwised from their C-terminal amino acid to their last N-terminal amino acid in reaction columns. For the synthesis the Fmoc protected amino acid amino group was deprotected with piperidine. After repeated washing with dimethylformamide (DMF) the coupling of the amino acid took place. The coupling of the Fmoc protected amino acid required the activation with Benzotriazol-1-yl-oxytripyrrolidinophosphonium-hexafluorophosphat (PyBOB) and N-methyl morpholine. Repeated DMF washing steps and a capping step with acetic anhydride followed the coupling step. After further DMF washing steps the cycle was completed and the next amino acid deprotection/coupling cycle started. After the last coupling cycle was complete, the peptide N-terminus was deprotected with piperidine.

The synthesis was followed by the cleavage of the peptides from the AHB resin using a cleavage cocktail (92.5 % TFA, 5 % triisopropylsilane). The cleavage from the resin was completed after 1.5 hours. Then the peptide solution was separated from the resin. To remove all amino acid side chain protection groups the cleavage continued for another 4 hours without the resin. Thereafter, the peptides were precipitated from the cleavage cocktail adding ice-cold tert-butyl-methyl-ether. After the first precipitation the peptide pellet was washed twice with

tert-butyl-methyl-ether to purify the product. The synthesized peptides were used as standards for the development of selected reaction monitoring (SRM) methods.

2.13 SRM of the P300 and the C/EBPβ Co-IPs

For SRM method development either synthesized peptides without isotope labeling or SpikeTides TQL peptides containing C-terminal labeled arginines (arginine^{10}) purchased from JPT Peptide Technologies GmbH were used. These standard peptides were used to determine HPLC gradient retention time, the peptide m/z and the most intense peptide fragmentation ions for each of the targeted peptides. Heavy isotope labeled SpikeTides TQL proteotypic peptides with a cleavable peptide-tag were added to the samples before subjecting them to a tryptic in-solution digest, whereas the in-house synthesized nonisotopically labeled peptides were combined as a master mix. The isotope labeled SpikeTides TQL peptides were used for absolute peptide / protein quantification. The nonisotopically labeled peptide master mix was measured as a separate sample after the experimental samples had been measured to determine the precise peptide retention times for each of the used disposable analytical reversed-phase columns.

An Eksigent nanoLC-ultra 1D plus high performance liquid chromatography (HPLC) system in connection with a PAL 5500 HTC-*xt* auto-sampler was used for sample pick up and for creating a gradient for separating peptides for the SRM measurements. A 10-50 % (v/v) ACN gradient in 0.06 % (v/v) FA was run to separate peptides due to their hydrophobicity on analytical reversed-phase columns using a flow rate of 250 nl/min. The length of the measurement was selected based on the number of peptides that had to be separated. For the P300 Co-IP measurements a 100-minute gradient was chosen, whereas for the C/EBPβ Co-IPs a 150-minute gradient was used.

Samples were measured on a QTRAP 5500 equipped with an AB Sciex Nano Spray II source. SRM measurements were performed using a curtain gas of 35, an ionspray voltage of 2300 V, an ion source gas 1 of 16 and a collision cell exit potential of 9. A consistent declustering potential of 160 and an entrance potential of 10 was selected for the SRM measurements. For

evaluation of the SRM measurments the MultiQuant 1.2 software from AB Sciex, DC, USA was used.

Table 1: SRM method of the P300 Co-IP. The table displays the protein name, the Q1 mass, the Q3 mass, the dwell time, the collision energy (CE) of every targeted transition of the P300 Co-IP SRM method. The peptide identification (ID) lists the amino acid sequences of each targeted peptide, the *m/z* of the peptide and the corresponding fragment ion y-series annotation. SpikeTides TQL peptide transition specifications are marked with ´heavy´in the protein name column, whereas transitions without isotope labeling are marked with ´light´in the protein name column.

Protein	Q1 [Da]	Q3 [Da]	Time [msec]	ID	CE [V]
CEBPβ (heavy)	592.30	1084.53	80	VLELTAENER m/z+2 y9	31
	592.30	971.45	80	VLELTAENER m/z+2 y8	31
	592.30	842.41	80	VLELTAENER m/z+2 y7	31
	592.30	729.32	80	VLELTAENER m/z+2 y6	31
	592.30	628.28	80	VLELTAENER m/z+2 y5	31
CEBPβ (light)	587.30	1074.53	80	VLELTAENER m/z+2 y9	31
	587.30	961.45	80	VLELTAENER m/z+2 y8	31
	587.30	832.41	80	VLELTAENER m/z+2 y7	31
	587.30	719.32	80	VLELTAENER m/z+2 y6	31
	587.30	618.28	80	VLELTAENER m/z+2 y5	31
P300 (heavy)	1227.56	857.38	80	LGLGLDDESNNQQAAATQSPGDSR m/z+2 y8	59
	1227.56	928.42	80	LGLGLDDESNNQQAAATQSPGDSR m/z+2 y9	59
	1227.56	999.46	80	LGLGLDDESNNQQAAATQSPGDSR m/z+2 y10	59
	1227.56	1070.49	80	LGLGLDDESNNQQAAATQSPGDSR m/z+2 y11	59
	818.71	999.46	80	LGLGLDDESNNQQAAATQSPGDSR m/z+3 y10	45
P300 (light)	1222.56	847.38	80	LGLGLDDESNNQQAAATQSPGDSR m/z+2 y8	59
	1222.56	918.42	80	LGLGLDDESNNQQAAATQSPGDSR m/z+2 y9	59
	1222.56	989.46	80	LGLGLDDESNNQQAAATQSPGDSR m/z+2 y10	59
	1222.56	1060.49	80	LGLGLDDESNNQQAAATQSPGDSR m/z+2 y11	59
	815.38	989.46	80	LGLGLDDESNNQQAAATQSPGDSR m/z+3 y10	45

Table 2: SRM method of the C/EBPβ Co-IP. The table on the following page displays the protein name, the Q1 mass, the Q3 mass, the dwell time, the collision energy (CE) of every acquired transition of the P300 Co-IP SRM method. The peptide identification (ID) lists the amino acid sequences of each targeted peptide, the *m/z* of the peptide and the corresponding fragment ion y- or b-series annotation. Synthetic peptides were used for SRM method development and retention time determination.

Protein	Q1 [Da]	Q3 [Da]	Time [msec]	ID	CE [V]
MBD2	817.4	1186.6	40	YLGNTVDLSSFDFR m/z+2 y10	41
	817.4	1085.5	40	YLGNTVDLSSFDFR m/z+2 y9	41
	817.4	986.4	40	YLGNTVDLSSFDFR m/z+2 y8	41
	817.4	871.4	40	YLGNTVDLSSFDFR m/z+2 y7	41
	545.3	671.3	40	YLGNTVDLSSFDFR m/z+3 y5	31
MBD3	809.9	1248.6	40	LSGLNAFDIAEELVK m/z+2 y11	41
	809.9	1134.6	40	LSGLNAFDIAEELVK m/z+2 y10	41
	809.9	1063.6	40	LSGLNAFDIAEELVK m/z+2 y9	41
	809.9	916.5	40	LSGLNAFDIAEELVK m/z+2 y8	41
	540.3	688.4	40	LSGLNAFDIAEELVK m/z+3 y6	31
MEP50	702.4	734.4	40	SDGALLLGASSLSGR m/z+2 y8	36
	702.4	847.5	40	SDGALLLGASSLSGR m/z+2 y9	36
	702.4	960.5	40	SDGALLLGASSLSGR m/z+2 y10	36
	702.4	1073.6	40	SDGALLLGASSLSGR m/z+2 y11	36
	468.6	606.3	40	SDGALLLGASSLSGR m/z+3 y6	27
CHD3	466.3	500.2	40	DDIRLLPSALGVK m/z+3 b4	27
	466.3	613.3	40	DDIRLLPSALGVK m/z+3 b5	27
	466.3	726.4	40	DDIRLLPSALGVK m/z+3 b6	27
	466.3	574.3	40	DDIRLLPSALGVK m/z+3 y6	27
	466.3	671.4	40	DDIRLLPSALGVK m/z+3 y7	27
CHD4	747.3	790.4	40	EGEDSSVIHYDDK m/z+2 y6	38
	498.5	540.2	40	EGEDSSVIHYDDK m/z+3 y4	29
	498.5	677.3	40	EGEDSSVIHYDDK m/z+3 y5	29
	498.5	790.4	40	EGEDSSVIHYDDK m/z+3 y6	29
	498.5	889.4	40	EGEDSSVIHYDDK m/z+3 y7	29
PRMT5	646.3	1128.6	40	YSQYQQAIYK m/z+2 y9	33
	646.3	1041.5	40	YSQYQQAIYK m/z+2 y8	33
	646.3	913.5	40	YSQYQQAIYK m/z+2 y7	33
	646.3	750.4	40	YSQYQQAIYK m/z+2 y6	33
	431.2	670.3	40	YSQYQQAIYK m/z+3 b5	26
BRG	643.3	1156.5	40	EVDYSDSLTEK m/z+2 y10	33
	643.3	1057.5	40	EVDYSDSLTEK m/z+2 y9	33
	643.3	942.4	40	EVDYSDSLTEK m/z+2 y8	33
	643.3	779.4	40	EVDYSDSLTEK m/z+2 y7	33
	643.3	692.3	40	EVDYSDSLTEK m/z+2 y6	33
BRM	736.9	1246.6	40	ILLDPNSEEVSEK m/z+2 y11	37
	736.9	1133.5	40	ILLDPNSEEVSEK m/z+2 y10	37
	736.9	1018.5	40	ILLDPNSEEVSEK m/z+2 y9	37
	736.9	921.4	40	ILLDPNSEEVSEK m/z+2 y8	37
	736.9	807.4	40	ILLDPNSEEVSEK m/z+2 y7	37
RBBP4	564.8	681.3	40	GEFGGFGSVSGK m/z+2 y7	30
	564.8	738.4	40	GEFGGFGSVSGK m/z+2 y8	30
	564.8	795.4	40	GEFGGFGSVSGK m/z+2 y9	30
	564.8	942.5	40	GEFGGFGSVSGK m/z+2 y10	30
	564.8	739.3	40	GEFGGFGSVSGK m/z+2 b8	30
RBBP7	499.7	748.4	40	LHTFESHK m/z+2 y6	27
	333.5	352.2	40	LHTFESHK m/z+3 bm/z+3	21
	333.5	647.3	40	LHTFESHK m/z+3 y5	21
	333.5	500.2	40	LHTFESHK m/z+3 y4	21
	333.5	371.2	40	LHTFESHK m/z+3 ym/z+3	21
CBP	640.8	873.5	100	DEYYHLLAEK m/z+2 y7	33
	640.8	710.4	100	DEYYHLLAEK m/z+2 y6	33
	427.5	710.4	100	DEYYHLLAEK m/z+3 y6	25
	427.5	573.4	100	DEYYHLLAEK m/z+3 y5	25
	427.5	460.3	100	DEYYHLLAEK m/z+3 y4	25
P300	618.8	873.5	100	AEYYHLLAEK m/z+2 y7	32
	618.8	710.4	100	AEYYHLLAEK m/z+2 y6	32
	412.9	710.4	100	AEYYHLLAEK m/z+3 y6	25
	412.9	573.4	100	AEYYHLLAEK m/z+3 y5	25
	412.9	460.3	100	AEYYHLLAEK m/z+3 y4	25
C/EBPβ	587.3	1074.5	40	VLELTAENER m/z+2 y9	29
	587.3	961.5	40	VLELTAENER m/z+2 y8	25
	587.3	832.4	40	VLELTAENER m/z+2 y7	29
	587.3	719.3	40	VLELTAENER m/z+2 y6	29
	587.3	618.3	40	VLELTAENER m/z+2 y5	29

2.14 Bioinformatic analysis and data presentation

The SRM method development was aided by comparing the PeptideAtlas database peptide entries (Deutsch et al., 2008) with an in-house compiled database derived and extracted from all the shotgun proteomics measurements conducted by the the Mass Spectrometry Core Unit, MDC (Dr. Gunnar Dittmar) providing the best proteotypic peptides their corresponding m/z and most favorable transitions. Data analyis and protein network analysis was performed using the Universal Protein Resource (UniProt) (The UniProt Consortium, 2013), the Munich Information Center for Protein Sequence (MIPS) Complete Dataset versus Core Set (CORUM) database (Ruepp et al., 2009), the Search Tool for Retrieval of Interactin Genes/Proteins (STRING) (Szklarczyk et al., 2010), the Human Integrated Protein-Protein Interaction rEference (HIPPIE) (Schaefer et al., 2012) and the Database for Annotation, Visualization and Integrated Discovery (DAVID) (Huang et al., 2009).

For data visualization and network annotation the Cytoscape Software (Cline et al., 2007) with the BisoGenet plugin (Martin et al., 2010) was used. Furthermore, the R Project for Statistical Computing software was employed for data analysis and presentation in combination with a vector graphics editor software (Adobe Illustrator CS6).

2.15 Cell culture and C/EBPα,β overexpression, C/EBPα-TE-3 sumoylation, Co-IP and pull-down experiments

Elisabeth Kowenz-Leutz, Maria Knoblich, Julia W. Böhm and Qingbin Liu performed cell culture and C/EBPα,β overexpression, C/EBPα-TE-3 sumoylation, Co-IP and pull-down experiments. Briefly: All human cell lines were cultured at 37 °C and 5 % CO_2 using 1 % penecillin / streptomycin. HEK293T cells were grown in Dulbecco´s modified Eagle medium (DMEM) and 10 % fetal bovine serum (FBS). SU-DHL-1 cells were grown in RPMI 1640 and 10 % FBS. HEK293T SILAC was performed using SILAC DMEM and 10 % SILAC fetal bovine serum dialyzed, whereas HL60

SILAC was grown in SILAC RPMI 1640 and 10 % SILAC fetal bovine serum dialyzed. Cells were labeled with the ´medium label´ L-Lysine-D_4 hydrochloride (48 mg/L in SILAC DMEM) and the ´heavy label´ L-Lysine-$^{1}3C_6$,$^{1}5N_2$ hydrochloride (48 mg/L in SILAC DMEM and 40 mg/L in SILAC RPMI 1640). Cells were transiently transfected using a calcium-phosphate method. Nuclear enrichment for the C/EBPβ Co-IPs from SU-DHL-1 and the C/EBPε peptide pull-downs from HL60 was performed as described in Schreiber et al., 1989. Sumoylation of the C/EBPα-TE-3 was performed as described by Mencía et al., 2004.

RESULTS

3.1 C/EBPα is post-translationally modified by arginine citrullination, arginine and lysine methylation and lysine acetylation

C/EBPα is an extensively post-translationally modified protein (Figure 2). Up until now no sites of lysine or arginine methylation, arginine citrullination and lysine acetylation have been published for C/EBPα. C/EBPβ has been shown to be extensively modified by arginine and lysine methylation and lysines acetylation (Figure 2) (Leutz et al., 2011). None of the C/EBPs have been published to be modified by protein-arginine deiminases (PADIs) as the detection of citrullinated arginines is still a challenge even with state of the art high mass accuracy mass spectrometers. However, a lab intern research conducted by Qingbin Liu (AG Leutz, MDC) on the deimination of C/EBPα and C/EBPα interaction with PADIs demonstrated that C/EBPα interacts with PADI4 via the basic region of the b-ZIP domain and that C/EBPα-TE-3 is deiminated in vitro by PADI4 (Qingbin Liu, dissertation, 2012).

For detecting the PTM pattern of C/EBPα the p42-isoform (*Rattus norvegicus*) with a HIS-tag was expressed in HEK293T cells. (The survey of the PTM pattern of C/EBPα was done together with Maria Knoblich (AG Leutz, MDC) who performed the C/EBPα expression in HEK293T cells and the purification of C/EBPα by protein liquid chromatography.) C/EBPα was highly purified by nickel-column and reversed-phased fractionation (Figure 3A,C). The C/EBPα fraction was directly subjected to an in-solution digest in urea buffer. C/EBPα was digested into peptides with the endopeptidase trypsin and the Lysyl endopeptidase (Lys-C) or exclusively by Lys-C. The peptides were measured on a Q Exaktive screening for methylation and acetylation patterns during data computation.

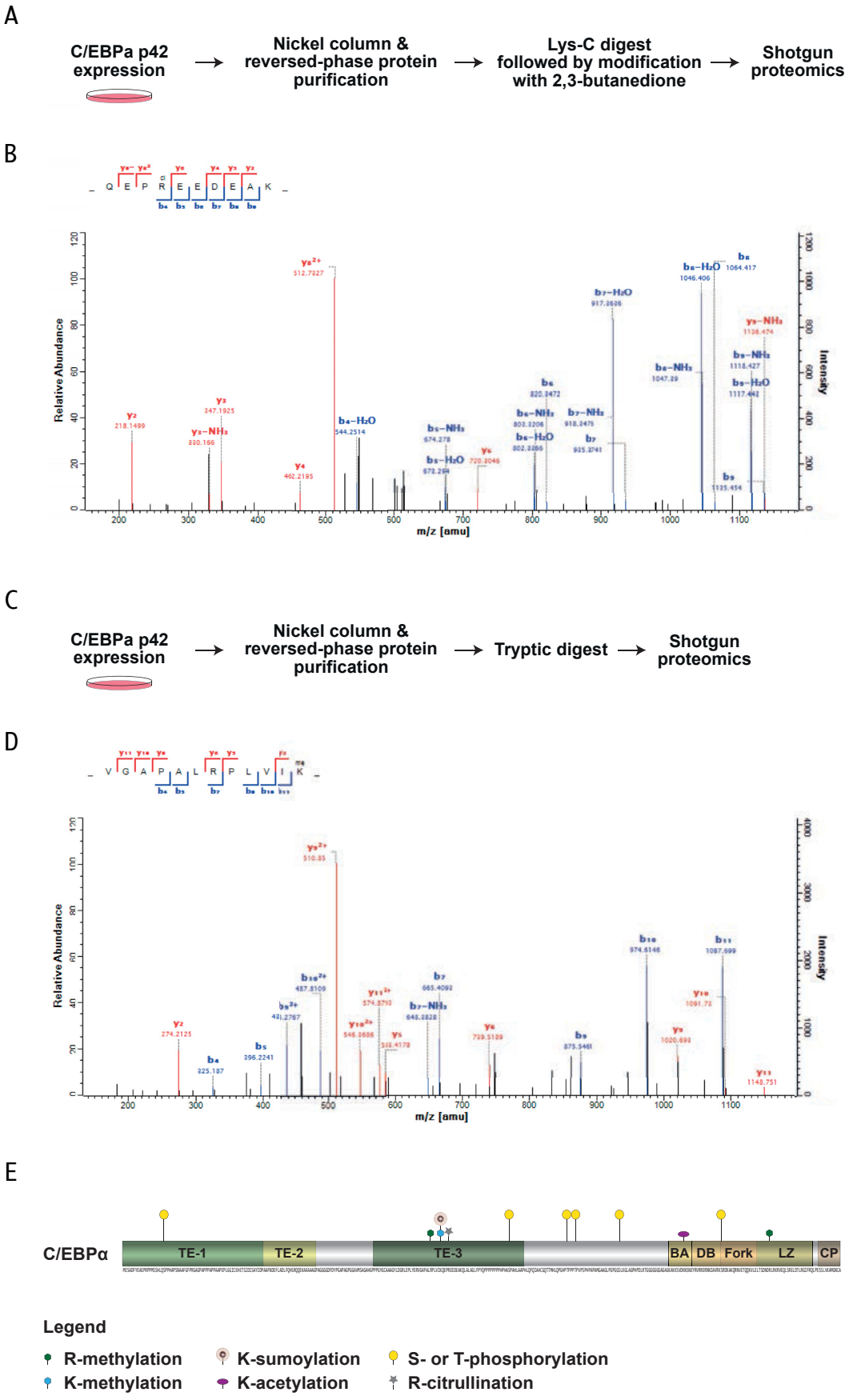
A
C/EBPa p42 expression
Nickel column & reversed-phase protein purification
Lys-C digest followed by modification with 2,3-butanedione
Shotgun proteomics
B
Relative Abundance
Intensity
m/z [amu]
C
C/EBPa p42 expression
Nickel column & reversed-phase protein purification
Tryptic digest
Shotgun proteomics
D
Relative Abundance
Intensity
m/z [amu]
E
C/EBPα
TE-1
TE-2
TE-3
BA
DB
Fork
LZ
CP
Legend
R-methylation
K-methylation
K-sumoylation
K-acetylation
S- or T-phosphorylation
R-citrullination

Figure 3: C/EBPα is revealed to be deiminated, methylated and acetylated using tandem mass spectrometry. A) Scheme of the C/EBPα expression, purification and protein Lys-C digestion followed by the chemical modification of citrullinated argines with 2,3-butadione for the detection by mass spectrometry. B) Tandem mass spectrum of a C/EBPα R163 citrullination. Indicated are the y- and b-series of the Lys-C cleaved and 2-3-butanedione modified peptide. A mass shift of 50 Da is market with ´cl´for the modification/citrullination at position R163. C) Scheme of the C/EBPα expression, purification and tryptic protein digestion followed by mass spectrometry for lysine methylation detection. D) Tandem mass spectrum of a C/EBPα R159 monomethylation. Indicated are the y- and b-series of the tryptically cleaved peptide. A mass shift of 14 Da is marked with ´me´for the modification at position K159. E) Schematic presentation of C/EBPα modification pattern revealing published phosphorylation sites, the sumoylation site and novel citrullination, methylation and acetylation sites. C/EBPα is the first member of the C/EBP family proven to be deiminated by tandem mass spectrometry. The C/EBPα R163 citrullination is located in the TE-3 adjacent to the novel K159 and R154 methylation sites. The K159 is C/EBPα sumoylation site as well. The C/EBPα bZIP is modified by K280 acetylation and R323 methylation. Figure 3E is adapted from Tsukada et al., 2011 and Johnson et al., 2005 and is extended by novel PTM sites detected during this study.

Deamidation of the guanidinium group of arginines is a common artifact during peptide ionization. It is impossible to distinguish between an enzymatically citrullinated arginine and a deamidated arginine measured by a mass spectrometer using electrospray ionization. Thus, the deiminated arginines of C/EBPα were chemically modified using 2,3-butanedione leading to a mass shift of an additional 50 Dalton (De Ceuleneer et al., 2011). For the chemical modification of the citrullinated arginines only peptides were used that had been acquired by an in-solution digest merely using Lys-C (Figure 3A). After the chemical modification of the citrullinated arginines the once more StageTip purified peptides were measured on a Q Exactive. By using the 2,3-butanedione modification C/EBPα R163 was revealed to be citrullinated (Figure 3B). C/EBPα is the first C/EBP family member shown to be modified by deimination using mass spectrometry.

As C/EBPα R163 is in close proximity to the C/EBPα sumoylation site, the K159 was probed for PTMs as well. To expose the K159 modification pattern the purified C/EBPα was tryptically digested and examined for methylation and acetylation patterns (Figure 3C). The experiment revealed that C/EBPα is modified at the sumoylation site K159 by monomethylation (Figure 3D). By detecting this monomethylation on C/EBPα K159 a PTM is identified that might function as a molecular switch to prevent C/EBPα sumoylation. Apart from the R163 citrullination and the K159 methylation, C/EBPα was further detected to be monomethylated at R154 and R323 and acetylated at K280 (Suppl. figure 1A-C).

The PTM survey of the C/EBPα p42 isoform revealed that C/EBPα is highly modified by methylation and acetylation. The acquired tandem mass spectrum of the citrullinated R163 demonstrates that C/EBPα is a protein modified by deiminases.

3.2 C/EBPα R163 is an important amino acid for determining protein interaction patterns

The transactivation element 3 (TE-3) is the C/EBPα protein domain that comprises the R154 methylation, K159 methylation and the R163 citrullination (Figure 3E). The TE-3 is important for the binding of the chromatin-remodeling complex SWI/SNF and for the binding of TBP and TF2B (Pedersen et al., 2001).

As PTMs putatively lead to changes in protein-protein interaction an experiment was devised to examine how the modification of the novel citrullination impacts C/EBPα protein interactome. (This experiment was conducted together with Qingbin Liu (AG Leutz, MDC) who performed the C/EBPα R163 site-directed mutagenesis, the HEK293T stable isotope labeling by amino acids in cell culture (SILAC) and the C/EBPα Co-IPs.) As it is not possible to express a solely R163 citrullinated C/EBPα, the R163 was amino acid substituted with R163Q. Glutamine has an amine as the functional group of its amino acid side-chain intendet to mimic a charge-less deiminated arginine. For detecting R163 site-specific protein-protein interaction SILAC was used. C/EBPα was expressed in the light labeled ($Lysine^0$) HEK293T cells, whereas the C/EBPα mutant R163Q was expressed in heavy labeled ($Lysine^8$) HEK293T cells (Figure 4A). Both the C/EBPα and the R163Q mutant were immunoprecipitated. The Co-IPs were eluted from the magnetic beads and methanol-choloroform precipitated. The Co-IPs were combined and digested with Lys-C. Subsequently, the purified peptides were measurement on a Q Exactive.

The comparison of the wild type C/EBPα with the R163Q mutant Co-IP revealed that STAG1 binds eight times more ($\log_2$ fold change > 3) to the R163Q mutant than to wild type C/EBPα (Figure 4B). The non-mutated C/EBPα preferentially interacts with WDR18,

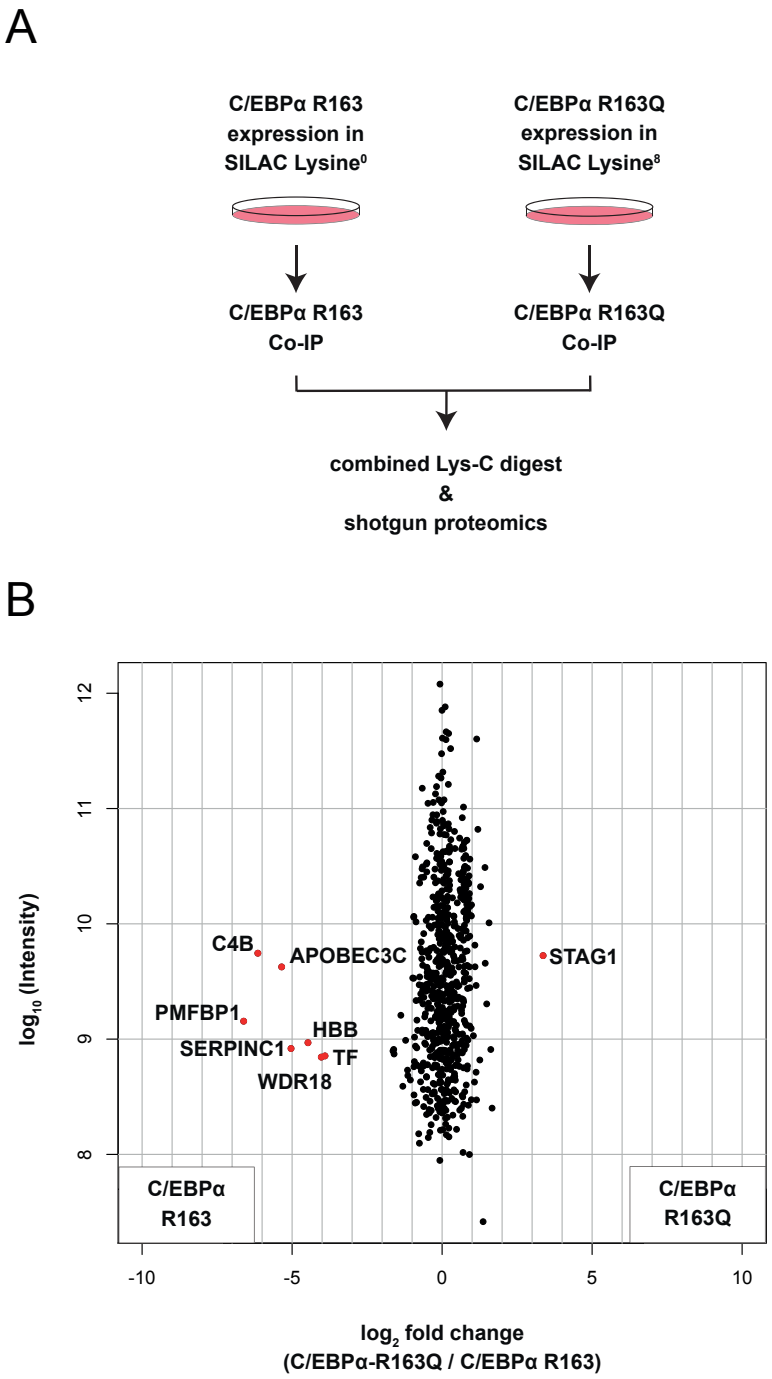

Figure 4: R163 is an important amino acid determining protein interaction pattern of C/EBPα. A) Scheme of the expression of wild type C/EBPα and the C/EBPα R163Q mutant in heavy and light SILAC media followed by Co-immunoprecipitation (Co-IP) of C/EBPα and the R163Q mutant. Combined Co-IPs were digested with the endoproteinase Lys-C and measured by shotgun proteomics. B) Scatterplot of the protein interaction pattern of C/EBPα compared to C/EBPα R163Q mutant. Proteins with a significant SILAC $\log_2$ fold change of (< -2.5 or > 2.5) are labeled with their protein name and are colored in red. Unspecific C/EBPα R163 interactors and bead background binding proteins are colored in black. The legend at the bottom of the scatterplot identifies the right plot side for protein interactions preferentially with the wild type C/EBPα (C/EBPα R163) and the left plot side for the protein interations preferentially with the mutated C/EBPα (C/EBPα R163Q).

APOBEC3C, CA4, HBB, PMFBP1, TF and SERPINC1 with $\log_2$ fold changes ranging from $\approx$ -3 to $<$ -6.5. Of the published C/EBPα TE-3 protein interaction partners the SWI/SNF ATP-dependent helicase BRG1 and the transcription initiation factor TF2B were detected each with a single SILAC peptide pair. To determine a valid SILAC ratio a protein had to be detected with at least two peptide pairs. This is the reason for the absence of BRG1 and TF2B from the analysis.

STAG1 is part of the SNF2h-cohesin-NuRD complex, which plays an important role during chromosome segregation (Hakimi et al., 2002). STAG1 is a known interaction partner of C/EBPβ as well (Steinberg et al., 2012). Of the seven significant C/EBPα R163 interactors the most important are WDR18 and APOBEC3C. WDR18 is part of the Five friends of methylated Chtop complex (5FMC). 5FMC is a complex that functionally combines arginine methylation with desumoylation (Fanis et al., 2012). ABOBEC3C is a DNA cytidine deaminase with RNA editing functions and prevents the replication of viruses and transposons (Refsland et al., 2010). The other proteins preferentially binding to the wild type C/EBPα are secreted proteins.

The mutational analysis of C/EBPα R163 displays how the protein-protein interaction pattern is altered only by the swap of a single amino acid. The usage of mass spectrometry facilitated the detection of novel C/EBPα protein interactors, which might depend on the modification status of C/EBPα R163.

3.3 C/EBPα-TE-3 sumoylation attracts novel protein interaction partners

C/EBPα K159 monomethylation might be one of the molecular switches to abrogate sumoylation. This is intriguing, as terminal cell differentiation has been associated with a declined availability of sumoylated C/EBPα and an increased presence of non-sumoylated C/EBPα (Khanna-Gupta et al., 2008). Sumoylation of C/EBPα was shown to work in an inhibitory manner on C/EBPα transactivation capacities by disturbing the C/EBPα interaction with the SWI/SNF ATP-dependent helicase BRG1 (Geletu et al., 2007; Sato et al., 2006). Sumoylation of C/EBPα is a

process of enzymatic steps, which starts with the activation of small ubiquitin-related modifier (SUMO-1) by the E1 ligases SAE2/SAE1 (Subramanian et al., 2003). Subsequently, SUMO-1 is passed to UBC9, the E2 conjugating enzyme, and E3-like activity has been demonstrated for PIAS4 increasing the sumoylation of C/EBPα. The E3-like activity is not essential for the sumoylation to take place. The knowledge of the importance of C/EBPα R163 for the WDR18 binding, which itself is part of the desumoylating complex 5FMC, raised the question of what impact SUMO-1 has on the protein interaction pattern of C/EBPα.

To gain a better insight into how the covalent attachment of SUMO-1 impacts C/EBPα protein interaction pattern a pull-down was devised, in which the non-sumoylated and sumoylated C/EBPα TE-3 were used as baits. (This experiment was done together with Maria Knoblich (AG Leutz, MDC) who performed the bacterial expression of C/EBPα-TE-3 and C/EBPα-TE-3-SUMO-1, the purification of both the sumoylated and the non-sumoylated C/EBPα-TE-3, the HEK293T SILAC and the pull-down experiment.) The non-sumoylated C/EBPα-TE-3 was expressed containing a C-terminal polyhistidine-tag (HIS-tag), whereas to obtain a sumoylated C/EBPα-TE-3 the same HIS tagged C/EBPα-TE-3 was co-transfected with AOS1, UBC9, UBA2, and SUMO-1-GST (Figure 5A) (Mencía et al., 2004). All these proteins were bacterially expressed in *Escherichia coli*. The C/EBPα-TE-3 was purified via the HIS-tag and the C/EBPα-TE-3-SUMO-1 was purified via the Glutathione S-transferase-tag (GST-tag) of SUMO-1. For the pull-down experiment a SILAC setup was chosen employing light and heavy lysine isotopes. SILAC lysates from fully labeled HEK293T cells were used for the pull-downs (Figure 5B). After the pull-downs were completed they were combined and subjected to a Lys-C digest followed by shotgun proteomics on a Q Exactive.

The C/EBPα-TE-3-SUMO-1 revealed elevated binding ($\log_2$ fold change < -2.5) to PML, SENP1, NUP358 and ARIP4 (Figure 5C). Moreover, there were elevated levels for C/EBPα and SUMO-1 on the C/EBPα-TE-3-SUMO1 side. These elevated levels are artifacts resulting from the bacterially expression of C/EBPα-TE-3 and SUMO-1 in light bacterial media. There were no proteins identified binding preferentially to the non-sumoylated C/EBPα-TE-3. BRG1 was not detected binding to the non-sumoylated C/EBPα-TE-3 either falling below the detection threshold of the mass spectrometric shotgun measurement or requiring a second binding site for protein interaction not included in the TE-3.

The novel protein partners PML, SENP1, NUP358 and ARIP4 of the sumoylated C/EBPα-TE-3 are closely connected with SUMO-1. PML is a non-covalent interaction partner of SUMO-1 as it contains a SUMO binding motif and is covalently modified by SUMO-1 as well (Shen et al., 2006). The interaction via the SUMO binding motif and the sumoylation of PML are crucial requirements for the formation of PML nuclear bodies. These nuclear bodies are located in the nucleoplasm and facilitate efficient interaction of substrates and their corresponding enzymes (Dundr et al., 2012). The C/EBPα-TE-3-SUMO1 interaction partner SENP1 is a nuclear deconjugation enzyme that cleaves SUMO-1 from modified proteins (Gong et al., 2000). The sumoylation specific C/EBPα-TE-3 interactor NUP358, also called RANBP2, is an E3-type SUMO-1 ligase (Pichler et al., 2002). NUP358 functions in a complex with sumoylated RANGAP1 and UBC9 linking sumoylation to the cellular transport machinery (Flotho et al., 2012). Besides that, NUP358 is also part of the nuclear pore complex during interphase (Tran et al., 2006). The SNF2 chromatin-remodeling factor ARIP4, which precipitated preferentially with C/EBPα-TE-3-SUMO1, is a DNA helicase that comprises two SUMO-interaction motifs (Rouleau et al., 2002; Ogawa et al., 2009). ARIP4 binds to sumoylated nuclear receptors via its SUMO-interaction motifs. Summed up, the analysis of the interaction pattern of the C/EBPα-TE-3 revealed that multiple published SUMO-1 protein interaction partners bind to the sumoylated C/EBPα TE-3 domain.

Figure 5: Sumoylated C/EBPα-TE-3 attracts novel interaction partners. A) Scheme (on the following page) of the bacterial C/EBPα-TE-3-HIS expression with and without the co-transfection of SUMO-1-GST, AOS1, UBC9 and UBA2. Followed by the purification of C/EBPα-TE-3 using a HIS-tag and C/EBPα-TE-3-SUMO-1 via a GST-tag. B) Scheme of the pull-down of C/EBPα-TE-3-SUMO- 1 and C/EBPα-TE-3 using light and heavy SILAC lysates. Combined pull-downs were digested with Lys-C and measured by shotgun proteomics. C) Scatterplot of protein interaction pattern of the C/EBPα-TE-3-SUMO-1 pull-down compared to C/EBPα-TE-3 pull-down. Proteins with a significant SILAC $\log_2$ fold change (< -2.5 or > 2.5) are labeled with the protein name and are colored in red. Mutual C/EBPα-TE-3 binders and bead binding proteins are colored in black. The legend at the bottom of the scatterplot identifies the right plot side for the protein interactions preferentially with the sumoylated C/EBPα-TE-3 (C/EBPα-TE-3-SUMO-1) and the left plot side for the protein interactions preferentially with the non-sumoylated C/EBPα-TE-3 (C/EBPα-TE-3).

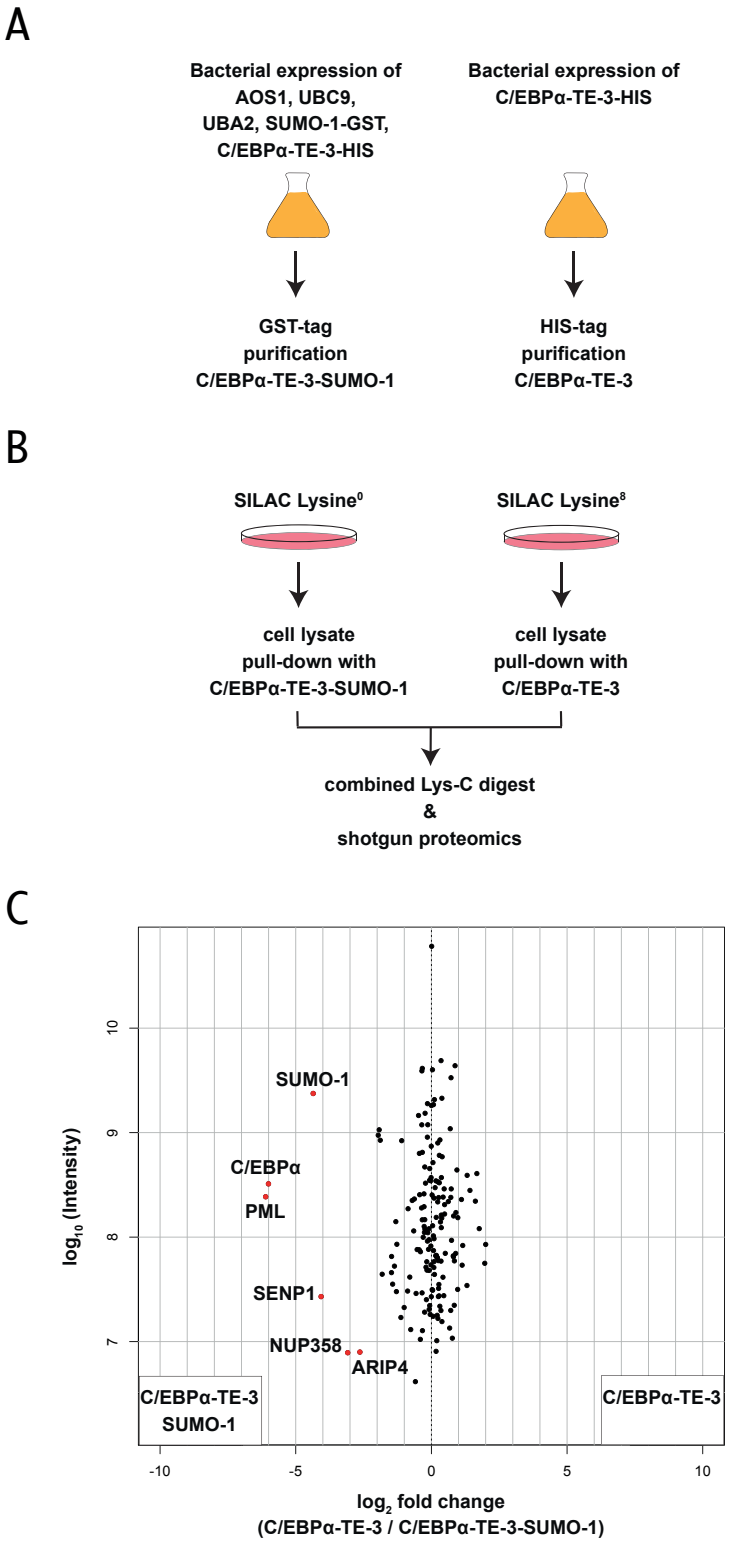
A
Bacterial expression of AOS1, UBC9, UBA2, SUMO-1-GST, C/EBPα-TE-3-HIS
Bacterial expression of C/EBPα-TE-3-HIS
GST-tag purification C/EBPα-TE-3-SUMO-1
HIS-tag purification C/EBPα-TE-3
B
SILAC Lysine0
SILAC Lysine8
cell lysate pull-down with C/EBPα-TE-3-SUMO-1
cell lysate pull-down with C/EBPα-TE-3
combined Lys-C digest & shotgun proteomics
C
SUMO-1
C/EBPα
PML
SENP1
NUP358
ARIP4
C/EBPα-TE-3 SUMO-1
C/EBPα-TE-3
log10 (Intensity)
log2 fold change (C/EBPα-TE-3 / C/EBPα-TE-3-SUMO-1)

3.4 PrISMa, a new method for detecting C/EBPβ PTM dependent interaction patterns

C/EBPβ is a highly modified protein but little is known about how protein-protein interaction is regulated by its PTMs. When C/EBPβ is purified from cells the yield is always the sum of the expressed C/EBPβ isoforms as well as the sum of differentially post-translationally modified C/EBPβ molecules. Due to the lack of antibodies for most of the C/EBPβ PTMs, the influence of C/EBPβ site-specific arginine and lysine methylation and lysine acetylation patterns on protein-protein interactions cannot be elucidated by common immunoprecipitation methods. Moreover, the mapping of C/EBPβ methylation patterns revealed that many of the arginine and lysine methylation sites are separated only by a few amino acids or are adjacent to each other (Leutz et al., 2011). Therefore this survey intended to unravel, how C/EBPβ PTMs, some in close vicinity to each other, affect C/EBPβ protein interaction patterns. Up until now, C/EBPβ has been published to interact with more than 400 proteins, many of which perform pivotal functions in protein complexes. However, there is little known about which conserved regions or amino acid sequences of C/EBPβ mediate these interactions.

Short 14-mere long C/EBPβ amino acid sequences were synthesized using a membrane as a matrix. These spotted peptides were designed in such a way that the C/EBPβ amino acid sequences were presented in a tiled manner to unravel C/EBPβ peptide-protein interactions in a PTM dependent fashion (Figure 6). The tiled C/EBPβ peptides were interspersed with duplicate peptides that contained the most important lysine monomethylations, lysine dimethylations, lysine trimethylations, lysine acetylations, symmetric arginine dimethylations, asymmetric arginine dimethylations, arginine citrullinations and serine, threonine and tyrosine phosphorylations. For many of these C/EBPβ peptides two or even three modifications per sequence were chosen for the synthesis process.

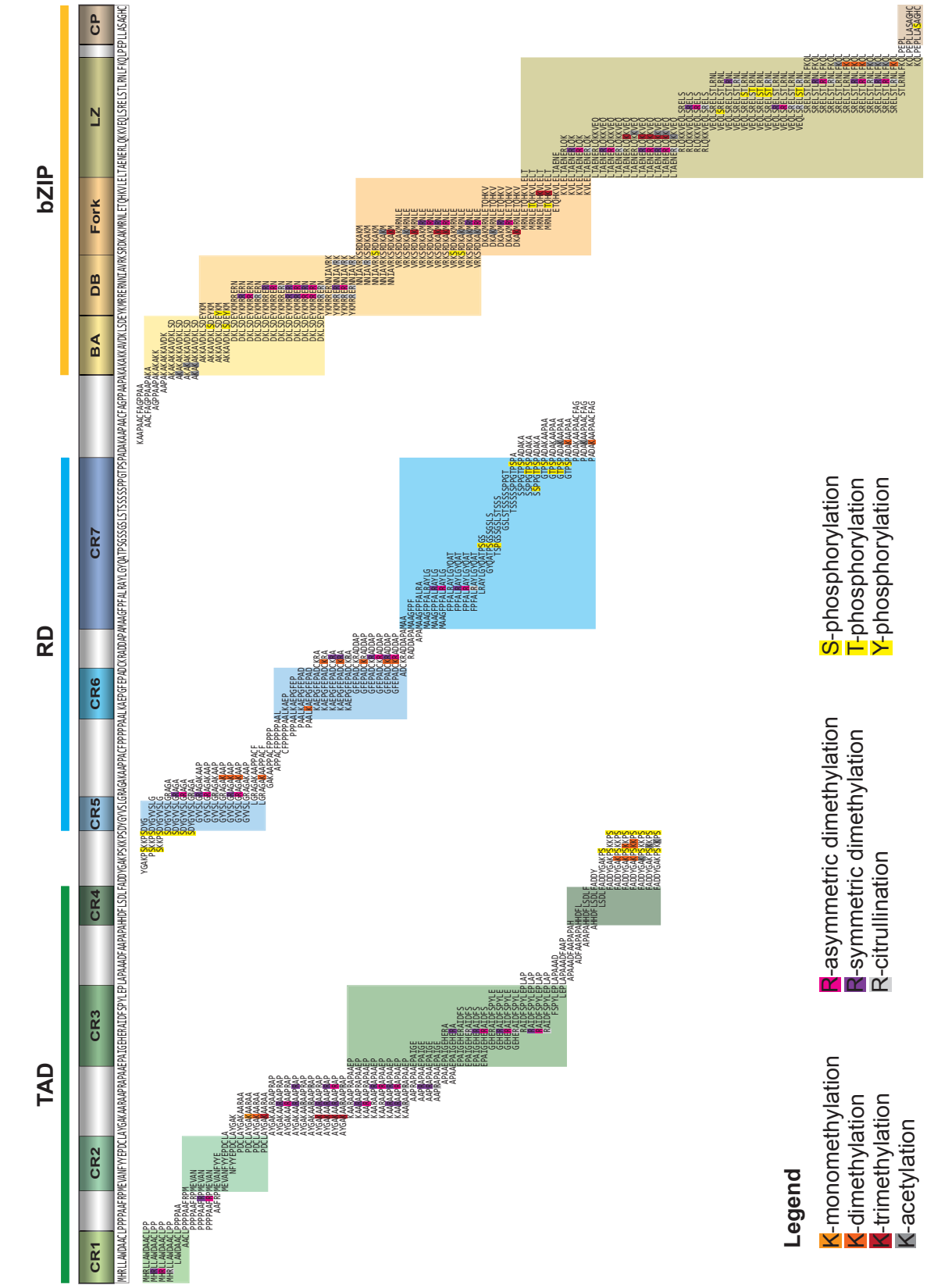
TAD
RD
bZIP
CR1
CR2
CR3
CR4
CR5
CR6
CR7
BA
DB
Fork
LZ
CP
Legend
K-monomethylation
K-dimethylation
K-trimethylation
K-acetylation
R-asymmetric dimethylation
R-symmetric dimethylation
R-citrullination
S-phosphorylation
T-phosphorylation
Y-phosphorylation

Figure 6: PrISMa, a method for detecting C/EBPβ protein interaction partners in a PTM dependent manner. The Protein Interaction Screen on peptide Matrices (PrISMa) is method for detecting C/EBPβ peptide-protein interaction partners. The 14-mere long C/EBPβ amino acid sequences were designed in a tiled manner from C/EBPβ N- to the C-terminus. The matrix is interspersed with peptide replicates containing the most prominent PTMs. The PTMs included are lysine monomethylation (yellow), lysine dimethylation (orange), lysine trimethylation (red), lysine acetylation (darkgrey), asymmetric arginine dimethylation (pink), symmetric arginine dimethylation (purple), arginine citrullination (light grey) and serine, threonine and tyrosine phosphorylation (yellow). As depicted in the legend the modified amino acids are indicated with the color of the PTM in the peptide amino acid sequence annotation. Furthermore, C/EBPβ is sub-divided into the TAD (green), the RD (blue) and the bZIP (golden yellow). The TAD contains four CRs (light to dark green), the RD contains three CRs (light to dark blue) and the bZIP consists out of five subdomains (light golden to bronze). The C/EBPβ CRs and subdomains are indicated with their color in the peptide amino acid sequence annotation.

These peptide sequences and their modified counterparts were synthesized onto a cellulose membrane in cooperation with JPT Peptide Technologies GmbH, a company based in Berlin, Germany. By means of the peptide matrices a new semi-automated workflow was devised. This workflow was termed Protein Interaction Screen on peptide Matrices (PrISMa). For the PrISMa approach the C/EBPβ peptide matrices were incubated with HeLa nuclear extract (Figure 7). The peptide-protein interaction spots were punched out with a biopsy puncher. Then the spots were subjected to a tryptical in-solution digest on an in-house programmed PAL HTS-*xt* autosampler. Subsequently, the obtained peptides were purified by StageTip. The peptides of every single spot were submitted to a separate shotgun proteomics measurement on an Orbitrap Velos. The resulting raw-data files were analyzed using the MaxQuant software package utilizing the label-free quantification (LFQ) option for comparing the normalized peptide-protein binding intensities for all spots of the matrices (for further details vide the material and methods section). The PrISMa workflow was performed in a joint effort together with Daniel Perez Hernandez (Mass Spectrometry Core Unit, MDC).

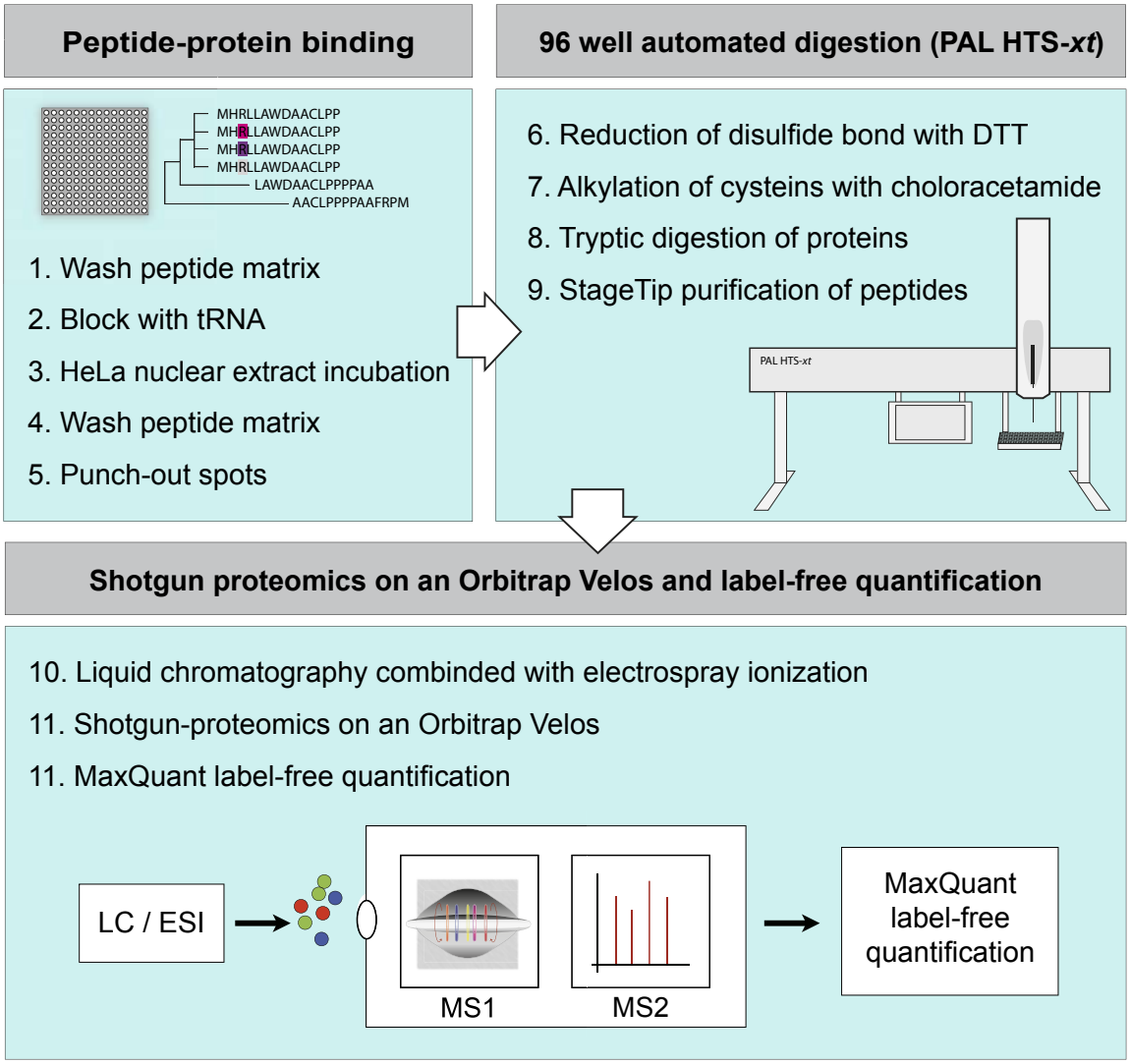

Figure 7: Scheme of the PrISMa workflow. The peptide matrix was incubated with a HeLa nuclear extract in a step-by-step procedure. The procedure including washing steps, the incubation with t-RNA to block the membrane against unspecific binding of proteins and the incubation of the matrix with the HeLa nuclear extract. The spots were punched out and proteins binding to the peptides were tryptically digested in a semi-automated procedure on a PAL HTS-*xt* autosampler. The obtained peptides were purified via StageTip. The samples were separated by liquid-chomatography (LC) and ionized by electrospray ionization (ESI). The peptides were measured by shotgun proteomics on an Orbitrap Velos in a tandem mass spectrometry mode acquiring peptide mass-to-charge ratio scans (MS1) and the peptide fragmentation spectra (MS2) for peptide validation. The raw-data files were analyzed using the MaxQuant software selecting the label-free quantification mode.

The PrISMa technique was performed twice using two of the C/EBPβ peptide matrices. For computational reasons the PrISMa raw-data files were analyzed with MaxQuant separately for each matrix. The datasets were merged with the free software programming language R. In total 2459 proteins were detected to bind to the synthetic peptide sequences of C/EBPβ. Of these

1435 proteins were detected to interact with both peptide matrices, whereas 575 proteins were detected exclusively with the first matrix and 449 proteins were detected only during the analysis of the second matrix (Figure 8A). For the presentation of the data the maximas of the LFQ intensities of the detected proteins were normalized to 100. The normalization was performed for each of the proteins binding to the 213 C/EBPβ peptide sequences of the matrix. By this the presented data emphasizes the C/EBPβ peptide sequence specific protein interaction pattern not the protein abundance intensities potentially only reflecting the interaction availability of a protein during HeLa nuclear extract incubation (Figure 7). The intensities of proteins that were detected twice were added up before they were normalized. When clustered in a heatmap all 2459 proteins revealed interaction patterns aligning to single or multiple C/EBPβ peptide sequences, overlapping peptide sequences or to whole protein regions in a PTM dependent manner (Suppl. figure 2).

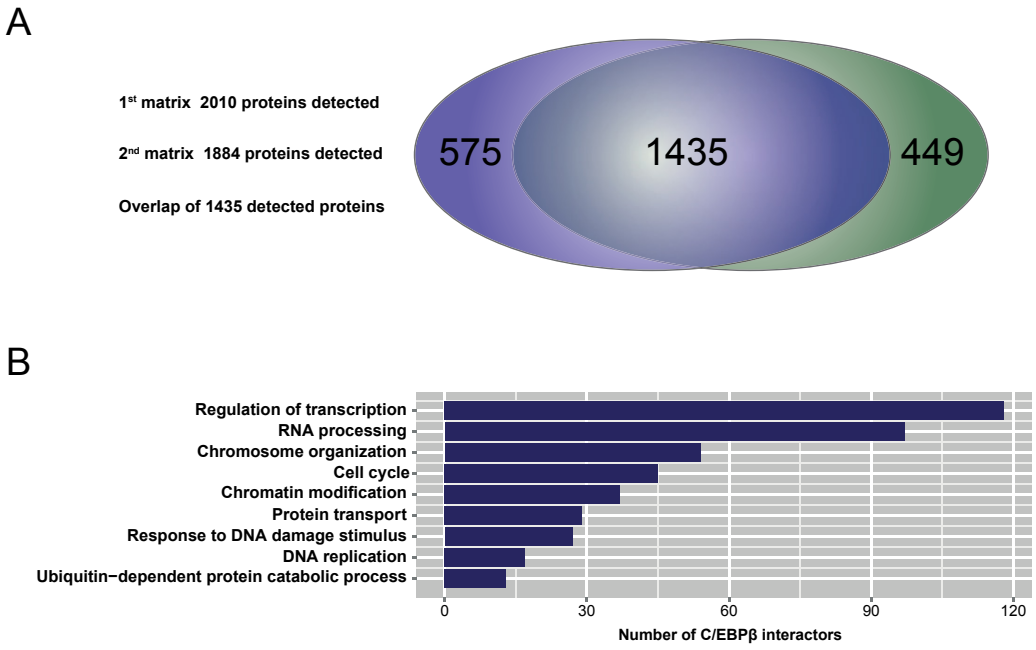

Figure 8: PrISMa is a highly reproducible method for detecting published C/EBPβ interaction partners. A) PrISMa is a highly reproducible method having an overlap of 1435 detected proteins in the measurement of the first and the second matrix. 575 proteins were detected exclusively with the first matrix, whereas 449 proteins were detected only with the second matrix. B) GO:terms of previously reported C/EBPβ interactors that were detected by PrISMa (analyzed by the NIH DAVID tool with GOTERM_BP_FAT: cut-off Benjamini Hochberg 0.05) revealed ´regulation of transcription´ and ´RNA processing´ as the most enriched GO:terms.

Of the 2459 proteins detected using PrISMa 372 proteins are published C/EBPβ interaction partners (Suppl. table 1; Suppl. figures 3-10) verified by literature research, by HIPPIE database queries and by published mass spectrometric protein-protein interaction screenings (Schaefer et al., 2012; Steinberg et al., 2012; Siersbæk et al., 2014). 18 of these published C/EBPβ partners that were detected by PrSIMa were discovered with two of their protein isoforms, distinguishable by mass spectrometry (Suppl. figure 3-10). Gene ontology (GO) analysis of the PrISMa detected C/EBPβ interacton partners using the DAVID tool (GOTERM_BP_FAT: cut-off Benjamini Hochberg 0.05) revealed that the ´regulation of transcription´ is the prime ranking GO:term followed by ´RNA processing´ and ´chromosome organization´ (Figure 8B). Additionally, the GO:terms are enriched for ´cell cylce´, ´chromatin modification´, ´protein transport´, ´response to DNA damage stimulus´ and ´DNA replication´.

3.5 CBP and P300 bind to anticipated C/EBPβ peptides

C/EBPβ binds to promoters and interacts with the diverse parts of the transcription machinery, such as the histone acetyltransferases (HATs) CBP and P300. CBP and P300 are important for the acetylation of the histones H2A, H2B, H3 and H4 causing the decompression of chromatin and by this vitally impacting on transcription (Kouzarides et al, 2007).

With the PrISMa approach we could show that P300 and CBP bind to C/EBPβ peptides of the TAD, which comprises the conserved regions CR1 to CR4 (Figure 9A-B). Both of these HATs bind with a maximum intensity to the CR4 peptide with the amino acid sequence AHHDFLS-DLFADDY and to the foregoing peptide APAPAHHDFLSDLF. Apart from the CR4, the CR3 revealed a second binding region of these HATs for the overlapping peptides GEHERAIDFSPYLE and RAIDFSPYLEPLAP. PrISMa shows a third noteworthy binding of P300 and CBP to the C/EBPβ CR2 as well. CBP also was detected binding to the C/EBPβ CR1. Noteworthy is, that the secondary interaction between C/EBPβ CR3 and the two HATs was more intense when the C/EBPβ GEHERAIDFSPYLE peptide contained a citrullinated arginine (C/EBPβ R59). This finding reveales that these HATs preferentially bind to the chargeless guanidinium group in a

PTM specific manner.

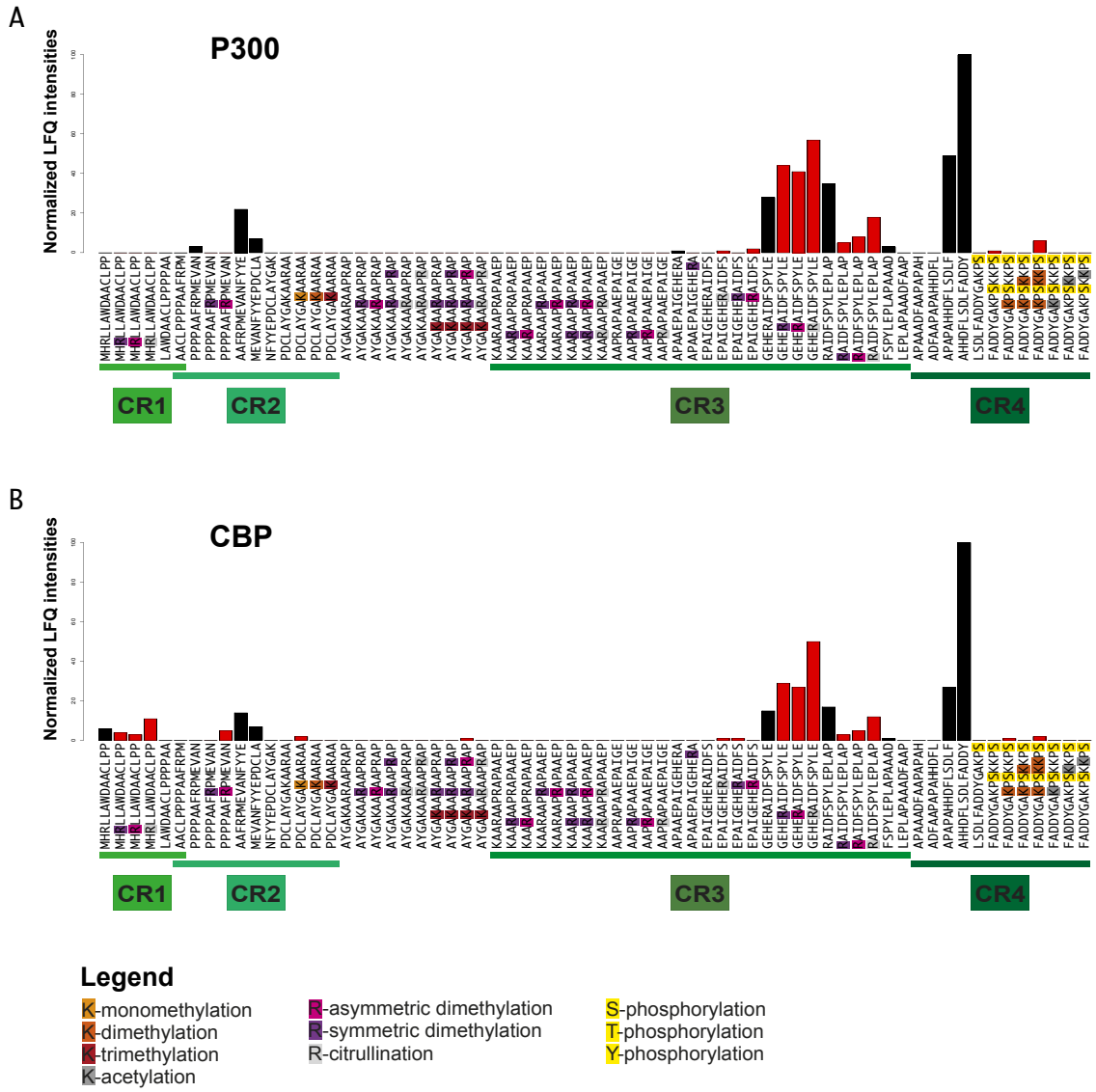

Figure 9: PrISMa reveals that P300 and CBP bind in a similar way to C/EBPβ peptides. A) P300 binds to three CRs of C/EBPβ TAD in a PTM specific manner revealing a maximal binding intensity for the CR4. B) CBP binds to four CRs of C/EBPβ TAD in a PTM specific manner with a maximal binding intensity for the CR4. The bar graphs show the normalized LFQ intensities for the two HATs P300 and CBP. The bars of the graph are color-coded. Black bars depict the binding intensities to peptide sequences without PTMs, whereas red bars represent the binding intensities to peptides that contain one or multiple PTMs. The bar graphs x-axes are annotated with the presented C/EBPβ peptide amino acid sequences. The legend at the bottom of the figure accounts for the color code of the PTMs highlighted in x-axes texts. The CRs of C/EBPβ TAD are labeled and underlined in the previously introduced TAD color code (compare Figure 1).

The interaction of P300 and CBP with the amino acid sequences of C/EBPβ CR3 and CR4 is in accord with two published amino acid binding motives of the C/EBP family (Nerlov et al., 1995). These motives are known to be important for the binding of the transcriptional activators TBP and TF2B and for the binding of P300 with C/EBPδ (Kovács et al., 2003). The PrISMa results verify the published C/EBP amino acid sequences to be the main and secondary interaction motives for P300 and CBP.

3.6 Dimethylation of C/EBPβ R42 and R46 abrogates P300 / CBP binding

The C/EBPβ TAD is heavily modified by arginine methylation in vivo (Figure 2) (Leutz et al., 2011). PrISMa revealed that the modification of C/EBPβ R59 impacts the interaction between C/EBPβ and the two HATs, P300 and CBP (Figure 9A-B). C/EBPβ is putatively methylated at arginine R42 (Leutz et al., 2011). Furthermore, in this study an extended PTM screening of C/EBPβ (*Rattus norvegicus*) revealed a novel C/EBPβ R46 methylation (Suppl.Figure 11C) by tandem mass spectrometry (Suppl.Figure 11B). The PTM survey revealing the C/EBPβ R46 monomethylation was conducted in the same way as the PTM survey of the C/EBPα modification pattern had been conducted (vide material and method section). For detecting the C/EBPβ PTM the C/EBPβ LAP* isoform (*Rattus norvegicus*) with a HIS-tag was expressed in HEK293T cells. (This survey was done together with Maria Knoblich (AG Leutz, MDC) who performed the C/EBPβ expression in HEK293T cells and the purification of C/EBPβ by protein liquid chromatography.) C/EBPβ was highly purified by nickel-column and reversed-phase fractionation (Suppl.Figure 11A). The C/EBPβ fraction was directly subjected to an in-solution digest in urea buffer. C/EBPβ was digested into peptides with the Lysyl endopeptidase (Lys-C) and the endopeptidase trypsin. The peptides were measured on a Q Exaktive screening for methylation patterns during data computation.

As PrISMa is based on the interaction of relatively short peptides with proteins, not all of the indirect effects of the known C/EBPβ PTMs on C/EBPβ protein interaction pattern

could be elucidated using this methodical approach, such as C/EBPβ protein folding due to PTMs. This especially applies for the effects of the R42 methylation and R46 methylation on the C/EBPβ interplay with P300 and CBP. The R42 and R46 are located in a low complexity region (LCR) of C/EBPβ in close proximity to the secondary C/EBPβ P300/CBP interaction motive in C/EBPβ CR3 (Suppl.Figure 11C; Figure 9). Mutational analysis of these two C/EBPβ arginines to alanines revealed an increase in the expression of the myeloid C/EBPβ target gene mim-1 (also referred to as *LECT2*) compared to the low transactivation capability of the non-mutated C/EBPβ (Leutz et al., 2011). The research of Leutz et al. suggests that the modification of the R42 and R46 plays a decisive part in the regulation of C/EBPβ transactivation. Both of these C/EBPβ arginines are conserved in the C/EBPε N-terminal transactivation domain (TAD) as well. C/EBPβ and C/EBPε have homologous regions in their TADs, such as the CR2, CR3 and CR4. However, the C/EBPε TAD is shorter, as its TAD CRs are interspersed with shorter LCRs. The C/EBPβ TAD has a length of approximately 92 amino acids depending on the species, whereas the C/EBPε TAD is approximately 55 amino acids long.

To investigate the influence of the transcriptional effects of C/EBPβ R42 and R46 methylation on the C/EBPβ interplay with P300 and CBP an experiment was devised. Due to the limited length of synthetic peptides the short C/EBPε TAD was chosen for the experiment setup. C/EBPε TAD peptides containing a C-terminal biotin-tag with and without the asymmetrically dimethylated arginines were used for pull-downs (Figure 10A). (This experiment was done together with Elisabeth Kowenz-Leutz (AG Leutz, MDC) and Maria Knoblich (AG Leutz, MDC) who performed the HL60 SILAC and the C/EBPε nuclear extract peptide pull-downs.) A triple SILAC approach was chosen for the quantification strategy of the experiment. By using a triple SILAC approach not only the specific interaction partners of the two different peptides could be investigated but also the mutual interaction partners protruded from the bead control. HL60 cells labeled with lysine isotopes were used for the pull-downs. The light lysine^{0} label was used for the bead control pull-down, whereas the medium lysine^{4} label was used for wild type C/EBPε peptide pull-down. The cells labeled with heavy lysine^{8} were used for the pull-down with the C/EBPε peptide containing the two asymmetrically dimethylated arginines (C/EBPε-Rme2as).

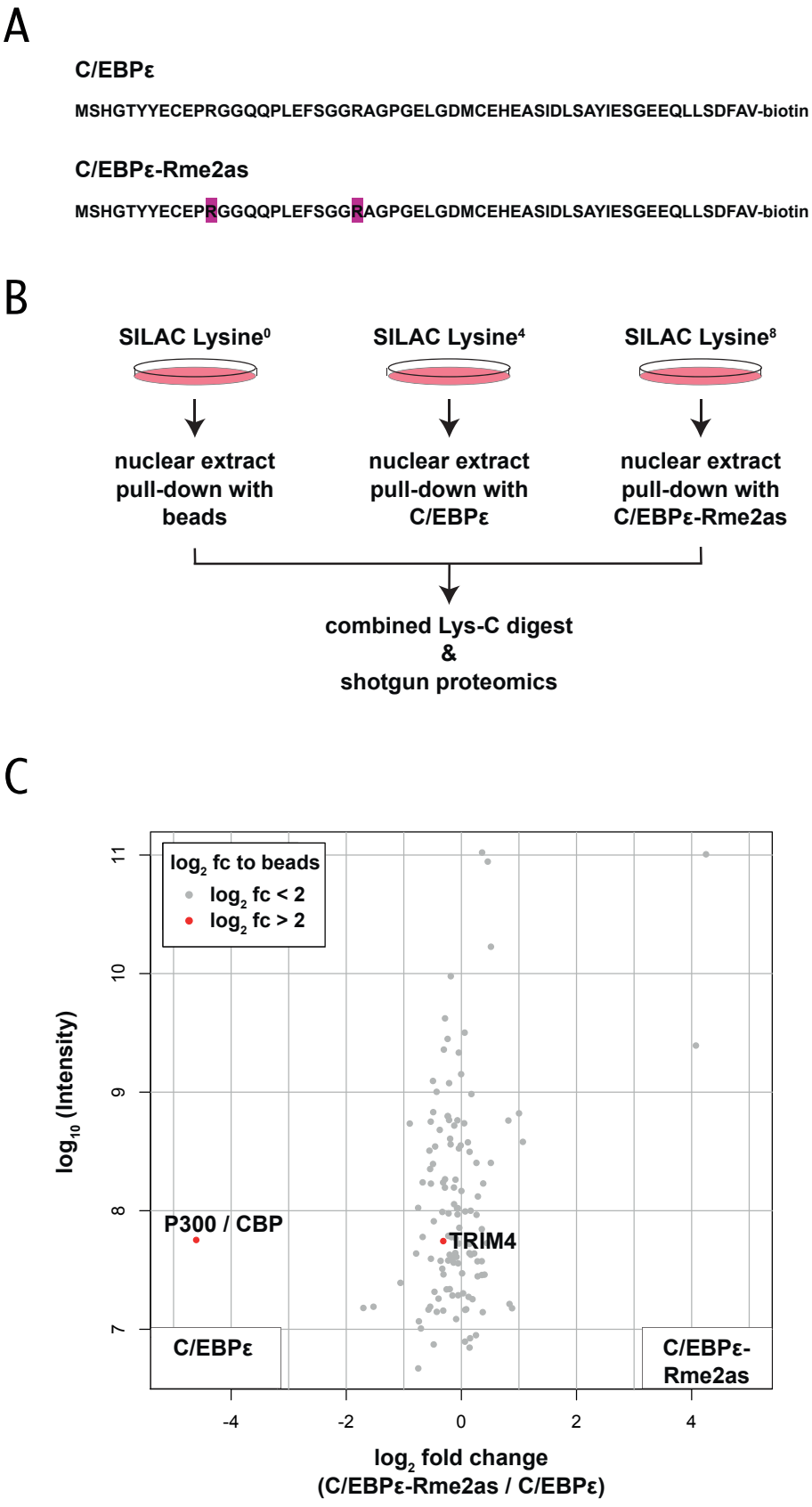
A
C/EBPε
MSHGTYYECEPRGGQQPLEFSGGRAGPGELGDMCEHEASIDLSAYIESGEEQLLSDFAV-biotin
C/EBPε-Rme2as
MSHGTYYECEPRGGQQPLEFSGGRAGPGELGDMCEHEASIDLSAYIESGEEQLLSDFAV-biotin
B
SILAC Lysine0
SILAC Lysine4
SILAC Lysine8
nuclear extract pull-down with beads
nuclear extract pull-down with C/EBPε
nuclear extract pull-down with C/EBPε-Rme2as
combined Lys-C digest & shotgun proteomics
C
log2 fc to beads
log2 fc < 2
log2 fc > 2
P300 / CBP
TRIM4
C/EBPε
C/EBPε-Rme2as
log10 (Intensity)
log2 fold change (C/EBPε-Rme2as / C/EBPε)

Figure 10: Asymmetric dimethylation of two arginines diminish the P300 / CBP interaction with the C/EBPε TAD significantly. A) C/EBPε peptide sequence with (C/EBPε-Rme2as) and without (C/EBPε) asymmetrically dimethylated arginines. The dimethylated arginines are marked with underlying purple color. B) Scheme of C/EBPε TAD peptide pull-downs using a triple SILAC approach. Combined pull-downs were digested with the endoproteinase Lys-C and measured by shotgun proteomics. C) Scatterplot of the protein-peptide interaction pattern of C/EBPε and C/EBPε-Rme2as. Proteins with a significant SILAC fold change (fc) towards the beads ($\log_2$ fc > 2) are labeled with their protein names and are colored in red. Bead background binding proteins are colored in grey. Scatterplot is labeled with the upper legend depicting the $\log_2$ fc of the C/EBPε peptides towards the bead. The two legends at the bottom of the scatterplot identify the right plot side for the preferential protein interactions with C/EBPε peptide (C/EBPε) and the left plot side for the preferential protein interactions with C/EBPε peptide containing dimethylated arginines (C/EBPε-Rme2as).

The pull-downs were conducted with nuclear extracts from the isotopically labeled cells. The combined pull-downs were digested with Lys-C and measured on a Q Exactive.

With this triple SILAC experiment 191 proteins were detected binding to the beads, the C/EBPε peptide and the C/EBPε-Rme2as peptide. The HATs P300 / CBP were detected with shared peptide sequences IQQQLVLLLHAHK and VQAIFPTPDPAALK binding predominantly to the non-modified C/EBPε peptide (Figure 10C). TRIM4 was detected to bind to both C/EBPε peptides equally. Both the P300 / CBP and TRIM4 were detected with a significant $\log_2$ fold change towards the bead control ($\log_2$ fold change > 2).

The TRIM4 binding to C/EBPε TAD is not influenced by the dimethylated arginines. The P300 / CBP interaction was more than 24 times higher ($\log_2$ fold change of - 4.6) with the non-modified C/EBPε TAD than with the C/EBPε TAD harboring dimethylated arginines. These results reveal that the arginine methylations profoundly influence the interaction of the transcriptionally activating HATs with the C/EBP family member C/EBPε.

Given that the dimethylation of the C/EBPε arginines had shown such a significant reduction in the interaction with P300/CBP, a further experiment was devised with the aim to investigate, if these two arginines have a similar effect regarding the interaction pattern for the full-length C/EBPβ. (This experiment was done together with Elisabeth Kowenz-Leutz (AG Leutz, MDC) who performed the molecular cloning of C/EBPβ R43L/R48L mutant, carried out the HEK293T cell culture, the C/EBPβ overexpression and the P300 Co-IPs.) For this experiment the C/EBPβ from *Gallus gallus* with a 58.8 % amino acid sequence homology to the C/EBPβ from *Rattus norvegicus* underwent site directed mutagenesis. The C/EBPβ R42 and

R46 from rat are homologous in chicken to the R43 and R48. These two arginines were mutated to leucines. Leucines were chosen with the intention to mimick aliphatic dimethylated arginines, as leucines posses an aliphatic amino acid side chain. The C/EBPβ R43L/R48L mutant and the non-mutated wild type C/EBPβ were used for a P300 Co-IP experiments. C/EBPβ and the C/EBPβ R43L/R48L mutant were overexpressed separately followed by the immunoprecipitation of the endogenous P300 from the transfected cells (Figure 11A). Absolutely quantified isotopically labeled peptide standards with an endopeptidase cleavable C-terminal tag were added in order to quantify the C/EBPβ amounts co-immunoprecipitated with P300. The proteotypic peptides with the amino acid sequences VLELTAENER (C/EBPβ) and LGLGLDDESNNQQAAATQSPGDSR (P300) were chosen for the measurements (vide Table 1 in the material and methods section). Selected reaction monitoring (SRM), a targeted mass spectrometrical method was used to absolutely quantify the P300 and C/EBPβ amounts using a QTRAP 5500 mass spectrometer.

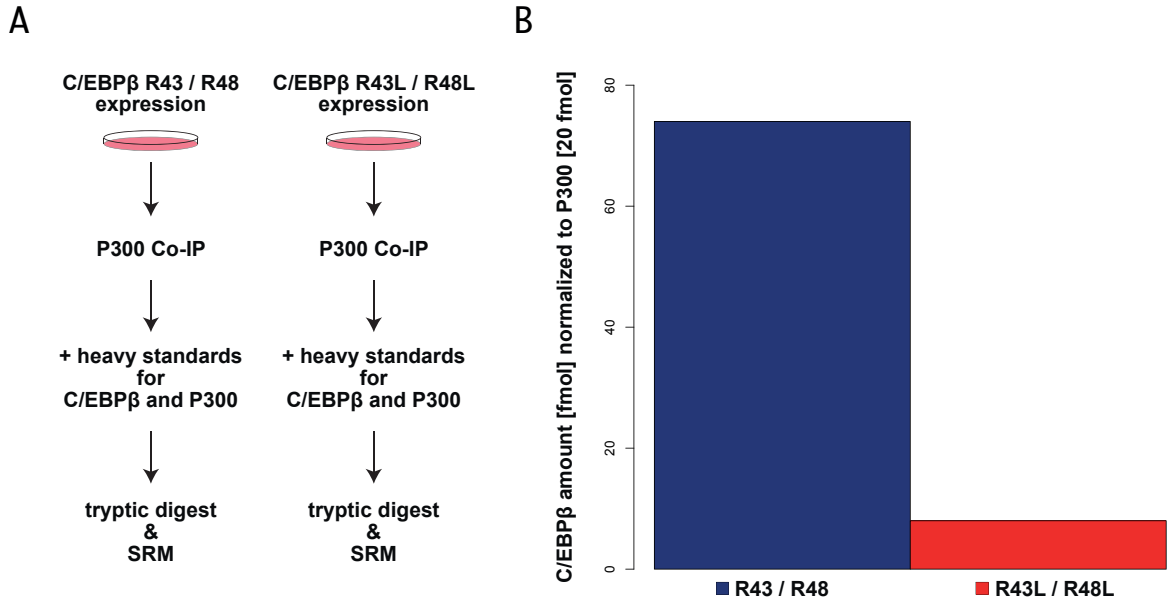

Figure 11: C/EBPβ R43 and R48 are decisive arginines for the P300 C/EBPβ interaction. A) Scheme of P300 Co-IPs targeting C/EBPβ and P300. Heavy isotope standards for P300 and C/EBPβ were added to Co-IPs followed by digestion of proteins with trypsin. Samples were measured by Selected reaction monitoring (SRM). B) The bar graph of normalized C/EBPβ amount detected by immunoprecipitating P300. The blue bar depicts the amount of wild type C/EBPβ (R43/R48) detected in the P300 Co-IP, whereas the red bar depicts the amount of the C/EBPβ mutant (R43L/R48L) detected in the P300 Co-IP.

C/EBPβ was co-immunoprecipitated with P300. 20 femtomol (fmol) of endogenous im-

munoprecipitated P300 yielded 74 fmol of non-mutated C/EBPβ, whereas 8 fmol C/EBPβ R43L/R48L was co-immunoprecipitated with 20 fmol of P300, respectively (Figure 11B). The wild type C/EBPβ interacted 9-times more with P300 than the C/EBPβ R43L/R48L mutant revealing that the aliphatic leucine mimicking the dimethylated arginine was sufficient to abrogate the P300 C/EBPβ interaction considerably.

The results of the P300 Co-IPs of the wild type C/EBPβ and the R43L/R48L mutant (Figure 11B) demonstrate that the probed conserved C/EBP arginines impact the interaction with the transcriptional activators P300 and CBP significantly when modified to leucines. Moreover, by comparing the P300 Co-IPs with the pull-down experiments conducted with the C/EBPε peptides (Figure 10B-C) the relevance of the methylation pattern of the conserved arginines for the P300/CBP C/EBP interaction becomes apparant. This is intriguing, as C/EBPβ R43 and R48 are located in a LCR between C/EBPβ CR2 and CR3 (Suppl. figure 11C) where no C/EBPβ P300/CBP interaction was detected using PrISMa (Figure 9A-B).

3.7 The mediator complex interacts with C/EBPβ peptides

The mediator complex interacts with the general transcription machinery and the RNA POL II to regulate transcription (Carlsten et al., 2013). MED23 and MED26 are two components of the mediator complex known to be C/EBPβ interaction partners (Mo et al., 2004). Depending on the composition, the mediator complex acts in an activating or in a repressive manner on C/EBPβ gene regulatory functions (Eastburn et al., 2004). A recent mass spectrometrical study by the Mandrup lab revealed multiple members of the mediator complex (vide Suppl. table 1) interacting with C/EBPβ (Siersbæk et al., 2014).

Using PrISMa 25 components of the mediator complex were detected binding to C/EBPβ amino acid sequences (Figure 12). The by PrISMa detected mediator complex components are MED1, MED4, MED7, MED8, MED10, MED12, MED13, MED13L, MED14, MED15, MED16,

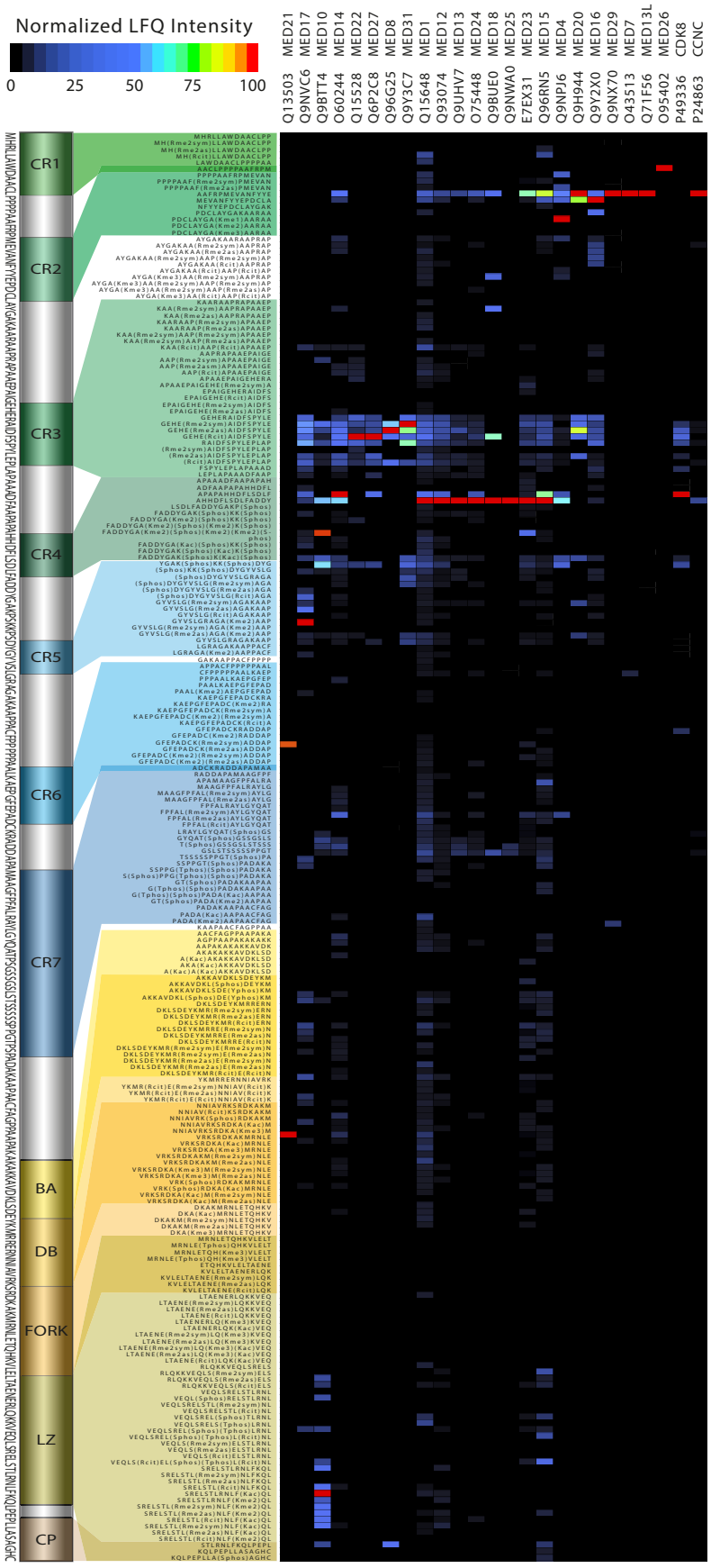
Normalized LFQ Intensity
0
25
50
75
100
Q13503 MED21
Q9NVC6 MED17
Q9BTT4 MED10
O60244 MED14
Q15528 MED22
Q6P2C8 MED27
Q96G25 MED8
Q9Y3C7 MED31
Q15648 MED1
Q93074 MED12
Q9UHV7 MED13
O75448 MED24
Q9BUE0 MED18
Q9NWA0 MED25
E7EX31 MED23
Q96RN5 MED15
Q9NPJ6 MED4
Q9H944 MED20
Q9Y2X0 MED16
Q9NX70 MED29
O43513 MED7
Q71F56 MED13L
O95402 MED26
P49336 CDK8
P24863 CCNC
CR1
CR2
CR3
CR4
CR5
CR6
CR7
BA
DB
FORK
LZ
CP

Figure 12: Heatmap of the mediator complex components binding to C/EBPβ peptides discovered using PrISMa. Heatmap of the normalized LFQ intensities of all detected mediator complex components revealing increased binding affinity to C/EBPβ peptides of the CR2, CR3 and CR4. On the top left the color key for the normalized LFQ values ranging from black to red (black, blue, green, yellow, red) is depicted. On top of the heatmap the UniProt accession numbers and the matching protein names one for each of the columns of the heatmap are specified. On the left next to the heatmap the C/EBPβ peptide amino acid sequences corresponding to each row of the heatmap are annotated containing abbreviations for the PTMs. The PTMs accounted for are symmetric arginine dimethylation (Rme2sym), asymmetric arginine dimethylation (Rme2as), arginine citrullination (Rcit), lysine monomethylation (Kme), lysine dimethylation (Kme2), lysine trimethylation (Kme3), lysine acetylation (Kac), serine phosphorylation (Sphos), threonine phosphorylation (Tphos) and tyrosine phosphorylation (Yphos). On the left next to the heatmap a schematic representation of C/EBPβ LAP* isoform depicts the CRs and bZIP domain in a color code. On the far left the C/EBPβ amino acid sequence for the complete LAP* isoform is annotated.

MED17, MED18, MED20, MED21, MED22, MED23, MED24, MED25, MED26, MED27, MED29, MED31, CDK8 and CCNC. Most of the mediator components bind with a maximum LFQ intensity to the C/EBPβ TAD. MED20, MED16, MED29, MED7, MED13L, CDK8 and CCNC bind with a maximum to the overlapping C/EBPβ peptide sequences AAFRPMEVANFYYE and MEVANFYYEPDCLA of the C/EBPβ CR2, whereas MED1, MED12, MED13, MED24, MED18, MED25, MED23, MED14 and MED15 bind with a maximum LFQ intensity to the C/EBPβ CR4 peptide AHHDFLSDLFADDY and the overlapping peptide APAPAHHDFLSDLF. MED22, MED27, MED8 and MED31 bind with a maximum to the C/EBPβ CR3 peptide sequence GEHERAIDFSPYLE in a PTM specific manner.

The PrISMa results are in accord with published findings identifying that the mediator complex preferentially interacts with the C/EBPβ TAD (Mo et al., 2004). Apart from verifying this TAD interaction, PrISMa provides insight into which members of the mediator preferentially interact either with the C/EBPβ CR2, CR3 or CR4. Intriguingly, some mediator complex members preferentially bind to the C/EBPβ RD or bZIP or have a secondary binding motive in these domains of C/EBPβ as well.

The mediator complex is a good example of how PrISMa not only reveals PTM specific interaction but also pinpoints the exact amino acid sequences necessary for the binding of proteins to C/EBPβ. When depicted without the PTM containing peptides the PrISMa results disclose peptide-protein interaction motives (Figure 13). Many of the mediator complex interactions with

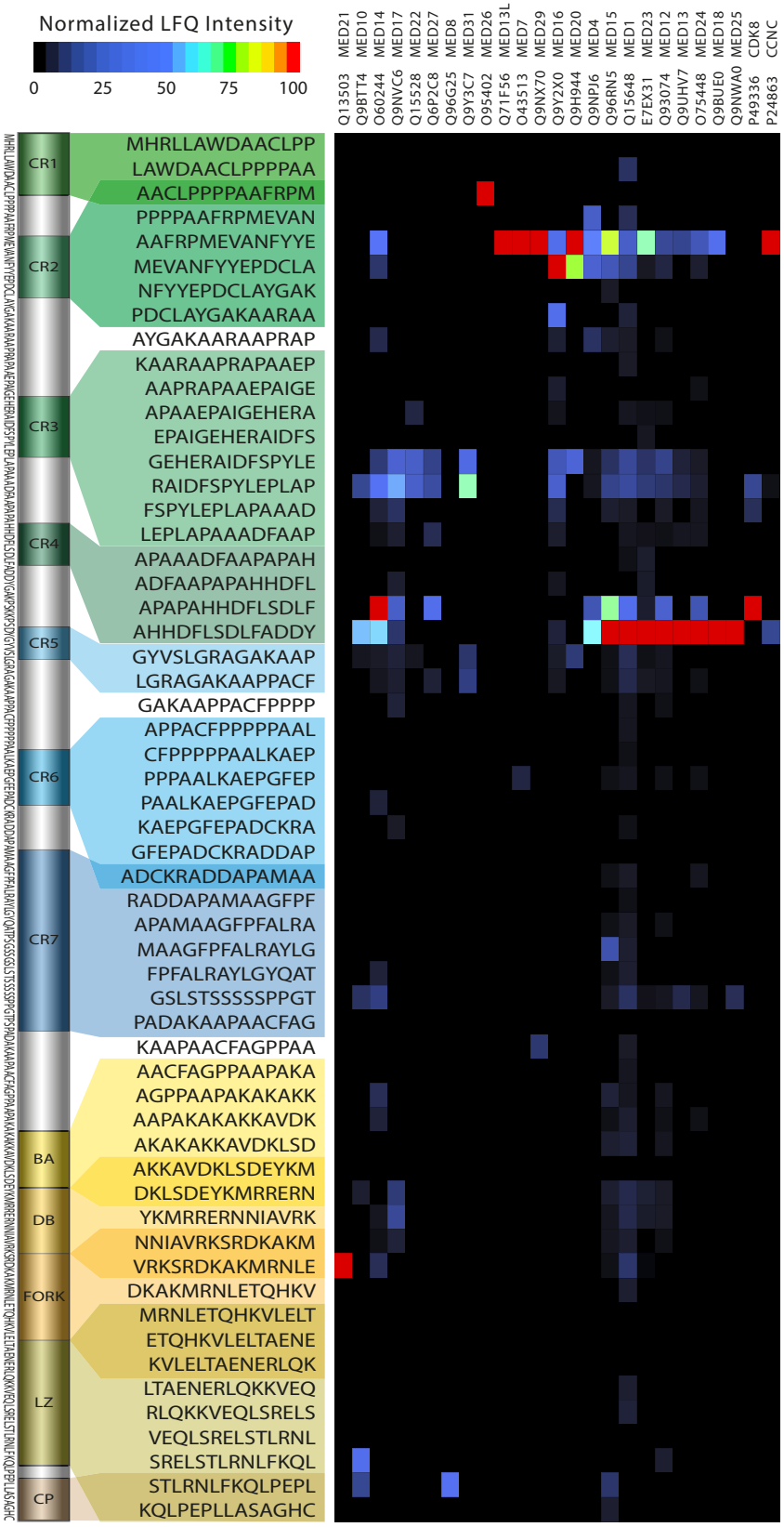
Normalized LFQ Intensity
0
25
50
75
100
Q13503 MED21
Q9BTT4 MED10
O60244 MED14
Q9NVC6 MED17
Q15528 MED22
Q6P2C8 MED27
Q96G25 MED8
Q9Y3C7 MED31
O95402 MED26
Q71F56 MED13L
O43513 MED7
Q9NX70 MED29
Q9Y2X0 MED16
Q9H944 MED20
Q9NPJ6 MED4
Q96RN5 MED15
Q15648 MED1
E7EX31 MED23
Q93074 MED12
Q9UHV7 MED13
O75448 MED24
Q9BUE0 MED18
Q9NWA0 MED25
P49336 CDK8
P24863 CCNC
CR1
CR2
CR3
CR4
CR5
CR6
CR7
BA
DB
FORK
LZ
CP
MHRLLAWDAACLPP
LAWDAACLPPPPAA
AACLPPPPAAFRPM
PPPPAAFRPMEVAN
AAFRPMEVANFYYE
MEVANFYYEPDCLA
NFYYEPDCLAYGAK
PDCLAYGAKAARAA
AYGAKAARAAPRAP
KAARAAPRAPAAEP
AAPRAPAAEPAIGE
APAAEPAIGEHERA
EPAIGEHERAIDFS
GEHERAIDFSPYLE
RAIDFSPYLEPLAP
FSPYLEPLAPAAAD
LEPLAPAAADFAAP
APAAADFAAPAPAH
ADFAAPAPAHHDFL
APAPAHHDFLSDLF
AHHDFLSDLFADDY
GYVSLGRAGAKAAP
LGRAGAKAAPPACF
GAKAAPPACFPPPP
APPACFPPPPPAAL
CFPPPPPAALKAEP
PPPAALKAEPGFEP
PAALKAEPGFEPAD
KAEPGFEPADCKRA
GFEPADCKRADDAP
ADCKRADDAPAMAA
RADDAPAMAAGFPF
APAMAAGFPFALRA
MAAGFPFALRAYLG
FPFALRAYLGYQAT
GSLSTSSSSSPPGT
PADAKAAPAACFAG
KAAPAACFAGPPAA
AACFAGPPAAPAKA
AGPPAAPAKAKAKK
AAPAKAKAKKAVDK
AKAKAKKAVDKLSD
AKKAVDKLSDEYKM
DKLSDEYKMRRERN
YKMRRERNNIAVRK
NNIAVRKSRDKAKM
VRKSRDKAKMRNLE
DKAKMRNLETQHKV
MRNLETQHKVLELT
ETQHKVLELTAENE
KVLELTAENERLQK
LTAENERLQKKVEQ
RLQKKVEQLSRELS
VEQLSRELSTLRNL
SRELSTLRNLFKQL
STLRNLFKQLPEPL
KQLPEPLLASAGHC

Figure 13: Heatmap of the mediator complex binding to C/EBPβ peptides containing no PTMs. Heatmap of the normalized LFQ intensities of all detected mediator complex components revealing increased binding affinity to C/EBPβ peptides of the CR2, CR3 and CR4. The tiled properties of the peptide matrix make it possible to pinpoint the amino acid sequences necessary for protein binding. On the top left the color key for the normalized LFQ values ranging from black to red (black, blue, green, yellow, red) is depicted. On top of the heatmap the UniProt accession numbers and the matching protein names one for each of the columns of the heatmap are specified. On the left next to the heatmap the C/EBPβ peptide amino acid sequences corresponding to each row of the heatmap are annotated. On the left next to the heatmap a schematic representation of C/EBPβ LAP* isoform depicts the CRs and bZIP domain in a color code. On the far left the C/EBPβ amino acid sequence for the complete LAP* isoform is annotated.

C/EBPβ peptide sequences can be narrowed down to a few amino acids. For example, nearly two thirds of the mediator complex members were detected to bind to the CR4 peptide sequences AHHDFLSDLFADDY and the overlapping peptide APAPAHHDFLSDLF. Interestingly, MED4, MED15, MED1, MED12 and MED24 were detected interacting more with AHHDFLSDLFADDY peptide than with the APAPAHHDFLSDLF peptide sequence. Hence, the APAPAHHDFLSDLF peptide includes more of the amino acids of the C/EBPβ squence motif required for the interaction with these mediator complex components.

3.8 PrISMa elucidates C/EBPβ interplay with proteins involved in the nucleoplasmic transport

The nucleoplasmic transport is important for every protein that carries out duties in the nucleus. Proteins get imported and exported from the nucleus (Katta et al. 2013). To facilitate this specific transition from the cytoplasm to the nucleus many proteins destined for the nucleus possess a nuclear localization signal (NLS) crucial for recruitment of the nuclear import machinery (Freitas et al., 2009). On the contrary to the NLS, the leucine-rich nuclear export signal (NES) enables the export of a protein from the nucleus by exportins.

C/EBPβ NLS is located in the in C/EBPβ bZIP (Williams et al., 1997). C/EBPβ NLS motif is embedded in C/EBPβ DB and FORK comprising the amino acids 216 to 245 of the LAP* isoform (*Rattus norvegicus*). During the nuclear import of proteins sumoylation plays a important role (Seeler et al., 2003). C/EBPβ is sumoylated at K134 in the CR6 (Kim et al.,

2002). The sumoylation of proteins requires two enzymatic steps. One of these steps involves the SUMO E2 tansfer enzyme UBC9, a known interaction partner of the two long C/EBPβ isoforms LAP* and LAP (Steinberg et al., 2012). C/EBPβ export is regulated via its NES, which is stated to be located in C/EBPβ LZ comprising the amino acids 272 to 282 (*Rattus norvegicus*) of the LAP* isoform (Buck et al., 2001b). C/EBPβ has been shown to interact with XPO1. This exportin plays an important role in the nucleoplasmic transport and was shown to interact with the LAP* and LAP isoform as well (Steinberg et al., 2012). A recent mass spectrometrical study uncovered multiple proteins involved in the nucleoplasmic transport (Suppl. table 1) interacting with C/EBPβ (Siersbæk et al., 2014).

Using PrISMa numerous components of the nucleoplasmic transport were detected binding preferentially to C/EBPβ CR7 and the LZ (Figure 14). IPO4, IPO5, IPO7, KPNB1, KPNB2, KPNA1, KPNA2, KPNA3 and KPNA4 sum up the nine importins detected by PrISMa. Apart from showing the mentioned binding affinity to C/EBPβ CR7 and LZ, KPNB1, KPNB2 and KPNA1-KPNA4 reveal further interaction with C/EBPβ peptides of the C/EBPβ TAD. This interaction occurs primarily in a low complexity region (LCR) between the CR2 and CR3. Intriguingly, KPAN1-KPNA4 interacts with C/EBPβ peptides of the DB as well. This is where the C/EBPβ NLS is located.

UBC9, sumoylated RANGAP1 and NUP358 are protein-protein interaction partners that bind to each other even during mitosis when the nuclear membrane is dissolved (Swaminathan et al., 2004). It is not possible to distinguish between a sumoylated and a non-sumoylated protein, such as the sumoylated RANGAP1, under the conditions used for PrISMa. Nonetheless, PrISMa revealed that RANGAP1, SUMO-1, UBC9 and NUP358 bind to the same C/EBPβ CR7 peptide with the amino acid sequence FPFALRAYLGYQAT (Figure 14). RANGAP1, SUMO-1 and NUP358 bind preferentially to this PrISMa peptide when the C/EBPβ R162 is symmetrically methylated. Apart from the interaction with the CR7 peptide, all four of these proteins bind to peptides of the C/EBPβ DB as well. This is interesting, as these C/EBPβ peptides of the DB harbor the C/EBPβ NLS. A third PrISMa peptide sequence interaction pattern of UBC9, RANGAP1 and NUP358 was detected for a C/EBPβ peptide of the CR4 with the amino acid

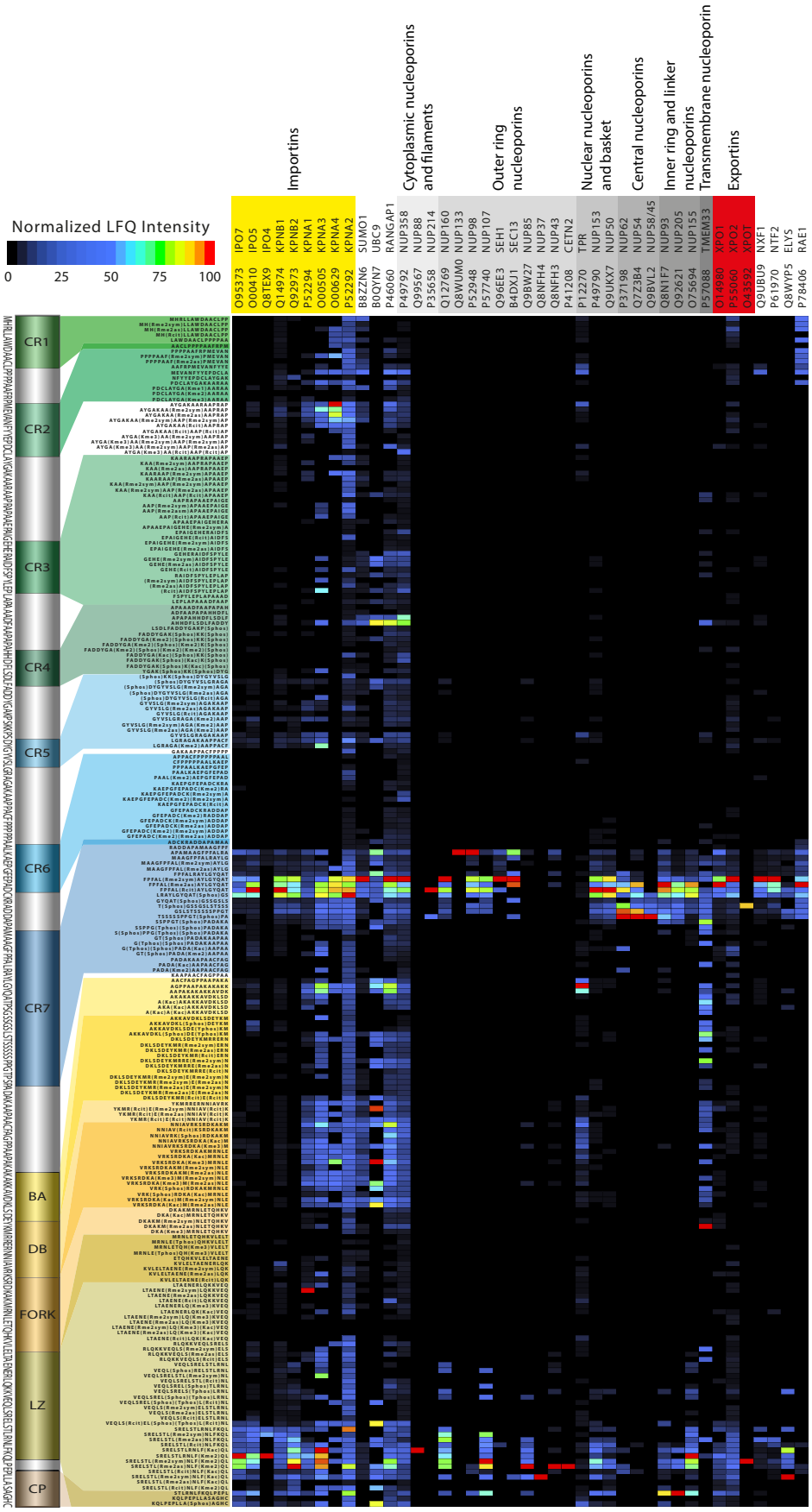
Normalized LFQ Intensity
0
25
50
75
100
Importins
Cytoplasmic nucleoporins and filaments
Outer ring nucleoporins
Nuclear nucleoporins and basket
Central nucleoporins
Inner ring and linker nucleoporins
Transmembrane nucleoporin
Exportins
IPO7
IPO5
IPO4
KPNB1
KPNB2
KPNA1
KPNA3
KPNA4
KPNA2
SUMO1
UBC9
RANGAP1
NUP358
NUP88
NUP214
NUP160
NUP133
NUP98
NUP107
SEH1
SEC13
NUP85
NUP37
NUP43
CETN2
TPR
NUP153
NUP50
NUP62
NUP54
NUP58/45
NUP93
NUP205
NUP155
TMEM33
XPO1
XPO2
XPOT
NXF1
NTF2
ELYS
RAE1
O95373
O00410
Q8TEX9
Q14974
Q92973
P52294
O00505
O00629
P52292
B8ZZN6
B0QYN7
P46060
P49792
Q99567
P35658
Q12769
Q8WUM0
P52948
P57740
Q96EE3
B4DXJ1
Q9BW27
Q8NFH4
Q8NFH3
P41208
P12270
P49790
Q9UKX7
P37198
Q7Z3B4
Q9BVL2
Q8N1F7
Q92621
O75694
P57088
Q14980
P55060
O43592
Q9UBU9
P61970
Q8WYP5
P78406
CR1
CR2
CR3
CR4
CR5
CR6
CR7
BA
DB
FORK
LZ
CP

Figure 14: Heatmap of proteins important for the nucleoplasmic transport discovered binding to C/EBPβ peptides using PrISMa. Heatmap of normalized LFQ intensities of importins, the nuclear pore complex members, exportins and nucleoplasmic transport associated proteins. Most of the components that are engaged in the nucleoplasmic transport reveal a high affinity to C/EBPβ peptides of the CR7 or LZ. On the top left is the color key for the normalized LFQ values ranging from black to red (black, blue, green, yellow, red). On top of the heatmap the UniProt accession numbers and the matching protein names one for each of the columns of the heatmap are specified. These names and accession numbers are marked with a color code and a descriptive text on top identifying if these proteins belong to the group of importins or exportins or which part of the nuclear pore complex they are associated with. On the left next to the heatmap the C/EBPβ peptide amino acid sequences corresponding to each row of the heatmap are annotated containing abbreviations for the PTMs. The PTMs accounted for are symmetric arginine dimethylation (Rme2sym), asymmetric arginine dimethylation (Rme2as), arginine citrullination (Rcit), lysine monomethylation (Kme), lysine dimethylation (Kme2), lysine trimethylation (Kme3), lysine acetylation (Kac), serine phosphorylation (Sphos), threonine phosphorylation (Tphos) and tyrosine phosphorylation (Yphos). On the left next to the heatmap a schematic representation of C/EBPβ LAP* isoform depicts the CRs and bZIP domain in a color code. On the far left the C/EBPβ amino acid sequence for the complete LAP* isoform is annotated.

sequence AHHDFLSDLFADDY revealing that the C/EBPβ TAD is involved in the interactions with these proteins as well.

The nuclear pore complex (NPC) is a highly organized transmembrane protein complex 125 MDa in size, through which proteins shuttle on their way into and out of the nucleus (Mattaj et al., 1998; Katta et al., 2013). The cytosolic side of the NPC is made up of cytoplasmic nucleoporins and filaments of which NUP358, NUP88 and NUP214 were detected using PrISMa (Figure 14). Of the outer ring of nucleoporins PrISMa detected NUP160, NUP133, NUP98, NUP107, SEH1, SEC13, NUP85, NUP37, NUP43 and CETN2. Of the nuclear nucleoporins and the basket NUP153, NUP50 and TPR were detected with PrISMa. PrISMa revealed NUP62, NUP54 and NUP58/45 of the central nucleoporins binding to C/EBPβ peptide sequences as well. Moreover, with PrISMa the inner ring and linker nucleoporins NUP93, NUP205 and NUP155 were detected. The transmembrane nucleoporine TMEM33 was discovered as well. All of these different subunits of the NPC reveal a similarity by maximal binding of most of their components to C/EBPβ peptides of the CR7 or the LZ. The exeption of this binding affinity is TPR and TMEM33, that interact preferentially either with the C/EBPβ BA or the C/EBPβ FORK.

Three exportins were detected using PrISMa (Figure 14). XPO1, XPO2 and XPOT also match in their binding affinity to C/EBPβ peptides of the CR7 or the LZ. The same binding preferences to C/EBPβ peptides of the CR7 and the LZ apply also to NXF1, a protein involved

in nuclear mRNA export and binding of the NPC (Zolotukhin et al. 2001), and to NTF2, a protein that binds to the NPC and to Ran making the transition of RanGDP to nuclear side of the NPC possible (Ribbeck et al., 1998). The preference for the CR7 and the LZ applies also to ELYS, a transcription factor important for the stability of the NPC (Rasala et al., 2006), and to RAE1, a protein that interacts with NUP98 during mitosis (Jeganathan et al., 2006). Many of these by PrISMa detected nucleoplasmic transport proteins that align with their maximal intensity to the same regions of C/EBPβ fulfill alternative functions during mitosis when the nuclear envelope disassembles (Katta et al., 2013).

3.9 C/EBPβ and chromatin remodelers

Chromatin remodeling is a crucial part of transcription. How dense the chromatin is packed is regulated by means of histone modifications and ATP-dependent chromatin remodeling (Swygert et al., 2014). In addition, transcription is regulated by histone variants, non-allelic forms of histones generally found in nucleosomes (Biterge et al., 2014). C/EBPβ has been published to interact with members of the INO80 complex, TIP60 complex, STAGA complex and the Mi2/NuRD complex (Suppl. table 1) (Steinberg et al., 2012). The INO80 complex is important for replacing histone variants of the nucleosomal dimers H2A.Z/H2B with free H2A/H2B dimers (Papamichos-Chronakis et al., 2011). The TIP60 complex is a histone acetylase complex important for cell maintenance and differentiation (Ikura et al., 2000; Yamada et al., 2014). GCN5 is part of the human STAGA complex (Martinez et al., 2001). The histone acetyltransferase GCN5 is a published C/EBPβ interaction partner and is known for acetylating C/EBPβ at K99, K102 and K103 (Wiper-Bergeron et al., 2007). C/EBPβ GNC5 dependent acetylation is essential for the glucocorticoid-stimulated preadipocyte differentiation. The Mi2/NuRD complex is a complex, which consists of two distinct subcomplexes, the MBD2/NuRD and the MBD3/NuRD (Le Guezennec et al., 2006). Due to two of its components, the histone deacetylases HDAC1 and HDAC2, these subcomplexes are generally regarded as a transcriptional repressive (Gao et al., 2009).

Employing PrISMa multiple members of the INO80 complex, the TIP60 complex, the STAGA complex and the Mi2/NuRD complex were detected (Figure 15). The detected members of the INO80 complex are MCRS1, C18orf37, INO80G, INOC1, INO80N, RUVBL1, RUVBL2 and BAF53. RUVBL1, RUVBL2 and BAF53 are members of the TIP60 complex as well and bind with a maximum to C/EBPβ peptides of the LZ. RUVBL2 binds maximal to a peptide harboring a symmetrically dimethylated arginine, whereas RUVBL1 binds maximal to a peptide with a symmetrically dimethylated arginine and an acetylated lysine. BAF53 binds with a maximum to a C/EBPβ peptide containing a dimethylated lysine. The other four identified components of the INO80 complex C18orf37, INO80G, INOC1 and INO80N bind maximal to two C/EBPβ peptides of the CR3 with the amino acid sequence GEHERAIDFSPYLE either containing a symmetrically or an asymmetrically dimethylated arginine. MCRS1 was detected interacting with a maximum to a C/EBPβ peptide of the CR5 containing a dimethylated lysine. Summed up, all components of the INO80 complex were detected to preferentially interact with C/EBPβ peptides carrying a methylation. Moreover, half of the detected INO80 complex members bind maximal to C/EBPβ peptides of the CR3.

RUVBL1, RUVBL2, BAF53, MORF4L1, MORF4L2, YEATS4, EP400, DMAP1, MRGBP, BRD8, ING3, EPC1 and PAF400 are members of the TIP60 complex and were detected binding to C/EBPβ peptide sequences (Figure 15). MORF4L1 binds with a maximum to a C/EBPβ peptide sequence of the CR2, whereas MORF4L2, YEATS4, EP400, DMAP1, MRGBP and BRD8 bind with a maximum to the overlapping amino acid sequences GEHERAIDFSPYLE and RAIDFSPYLEPLAP of C/EBPβ CR3 in a PTM dependent manner. Similar to the INO80 complex member MCRS1, the TIP60 complex members ING3 and EPC1 bind maximal to C/EBPβ peptides of the CR5 as well. PAF400 is a component of the TIP60 complex and a member of the STAGA complex as well.

PAF400, TADA1, GCN5, PAF65A, TAF10, FAF2G, TADA3 and AK6 are members of the STAGA complex. These components of the STAGA complex were detected binding to C/EBPβ peptide sequences (Figure 15). The STAGA complex members PAF400, TADA1, GCN5 and PAF65A were detected binding with a maximum to a C/EBPβ peptide of the CR4 with the amino acid sequence AHHDFLSDLFADDY. This C/EBPβ peptide sequence comprising the

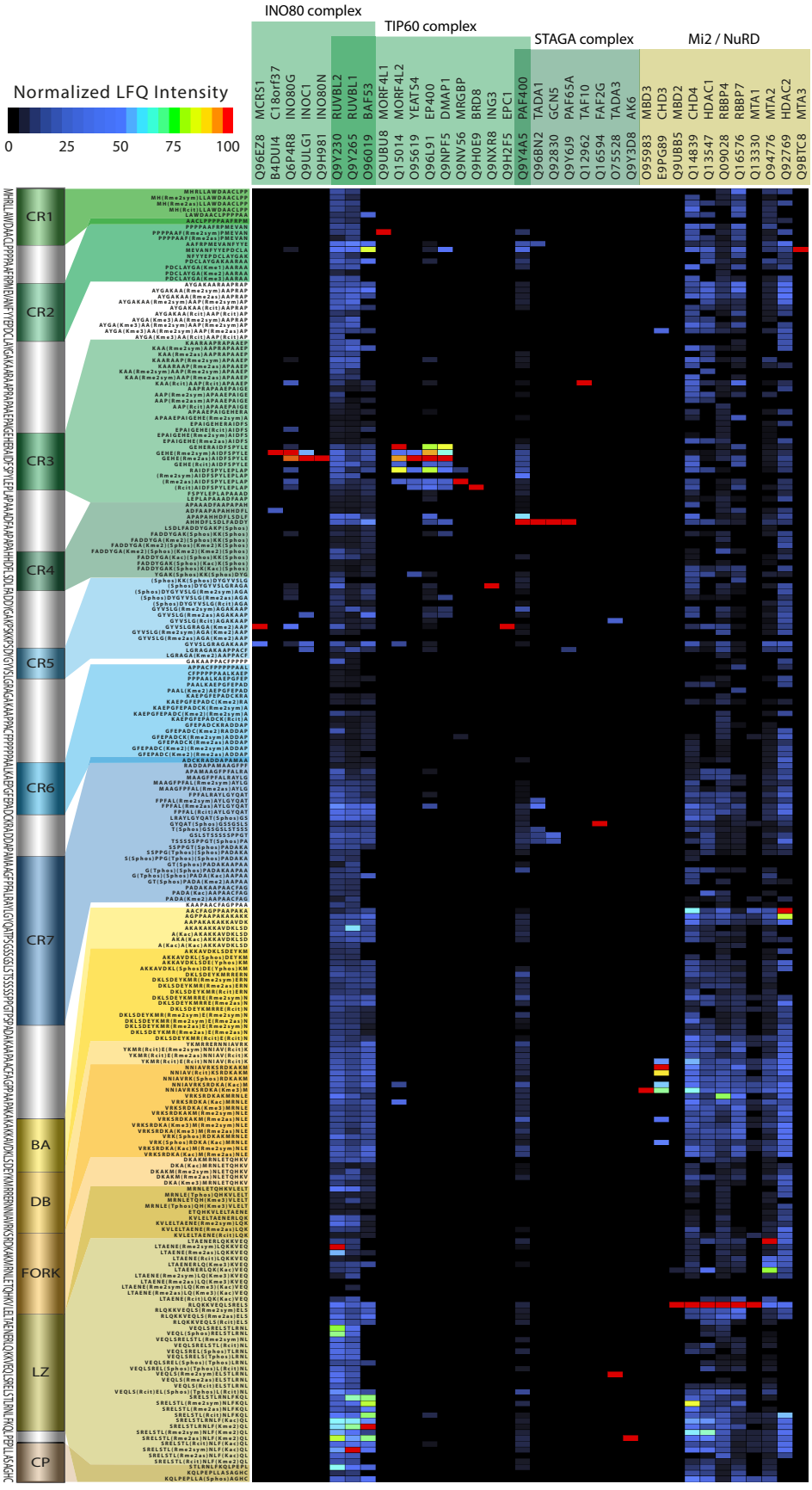
INO80 complex
TIP60 complex
STAGA complex
Mi2 / NuRD
Normalized LFQ Intensity
0
25
50
75
100
Q96EZ8 MCRS1
B4DUI4 C18orf37
Q6P4R8 INO80G
Q9ULG1 INOC1
Q9H9B1 INO80N
Q9Y230 RUVBL2
Q9Y265 RUVBL1
Q96G19 BAF53
Q9UBU8 MORF4L1
Q15014 MORF4L2
O95619 YEATS4
Q96L91 EP400
Q9NPF5 DMAP1
Q9NV56 MRGBP
Q9H0E9 BRD8
Q9NXR8 ING3
Q9H2F5 EPC1
Q9Y4A5 PAF400
Q96BN2 TADA1
Q92830 GCN5
Q9Y6J9 PAF65A
Q12962 TAF10
Q16594 FAF2G
O75528 TADA3
Q9Y3D8 AK6
O95983 MBD3
E9PG89 CHD3
Q9UBB5 MBD2
Q14839 CHD4
Q13547 HDAC1
Q09028 RBBP4
Q16576 RBBP7
Q13330 MTA1
O94776 MTA2
Q92769 HDAC2
Q9BTC8 MTA3
CR1
CR2
CR3
CR4
CR5
CR6
CR7
BA
DB
FORK
LZ
CP

Figure 15: Heatmap of the chromatin-remodeling complexes discovered binding to C/EBPβ peptides using PrISMa. Heatmap of normalized LFQ intensities of proteins belonging to the chromatin-remodeling and chromating-modifying complexes INO80, TIP60, STAGA or Mi2/NuRD. On the top left is the color key for the normalized LFQ values ranging from black to red (black, blue, green, yellow, red). On top of the heatmap the UniProt accession numbers and the matching protein names one for each of the columns of the heatmap are specified. These protein names and accession numbers are marked with a color code and a descriptive text identifying to which of the chromatin-remodeling complexes they belong. On the left next to the heatmap the C/EBPβ peptide amino acid sequences corresponding to each row of the heatmap are annotated containing abbreviations for the PTMs. The PTMs accounted for are symmetric arginine dimethylation (Rme2sym), asymmetric arginine dimethylation (Rme2as), arginine citrullination (Rcit), lysine monomethylation (Kme), lysine dimethylation (Kme2), lysine trimethylation (Kme3), lysine acetylation (Kac), serine phosphorylation (Sphos), threonine phosphorylation (Tphos) and tyrosine phosphorylation (Yphos). On the left next to the heatmap a schematic representation of C/EBPβ LAP* isoform depicts the CRs and bZIP domain in a color code. On the far left the C/EBPβ amino acid sequence for the complete LAP* isoform is annotated.

amino acids 83 to 96 of C/EBPβ (LAP* isoform) is interesting, as GCN5 is known to acetylate C/EBPβ K99, K102 and K103 right adjacent to this C/EBPβ amino acid sequence. Furthermore, this C/EBPβ peptide sequence is noteworthy as it is the maximal binding sequence of the two HATs P300 and CBP as well (Figure 9A-B).

Of the Mi2/NuRD complex the complex members MBD3, MBD2, CHD3, CHD4, HDAC1, HDAC2, RBBP4, RBBP7, MTA1, MTA2 and MTA3 were detected using PrISMa (Figure 15). With the exception of MTA3, all Mi2/NuRD complex components bind with a maximum to C/EBPβ peptides of the bZIP. MDB2, CHD4, HDAC1, RBBP4, RBBP7, MTA1 and MTA2 bind with a maximum to the same C/EBPβ amino acid sequence, RLQKKVEQLSRELS of the LZ. MBD3 and CHD3 bind maximal to C/EBPβ peptide sequences of the DB / FORK region, whereas HDAC2 binds maximal to a C/EBPβ peptide of the BA region. MTA3 binds maximal to a C/EBPβ CR2 peptide sequence. Summed up, the components Mi2/NuRD complex are mapped by PrISMa with their prime interaction sequence to C/EBPβ bZIP domain, a domain that has been up to date associated with DNA binding and dimerization.

3.10 The Mi2/NuRD cooperation with C/EBPβ is CR1 and RD dependent

The Mi2/NuRD complex is a transcriptional repressive complex that, with the help of PrISMa, could be revealed to bind primarily to C/EBPβ peptides of the LZ. Of the by PrISMa detected chromatin-remodeling complexes the Mi2/NuRD complex plays a pivotal role, as it has been suggested to be the antagonist of the SWI/SNF complex (Gao et al., 2009). The SWI/SNF complex facilitates the expression of a subgroup of myeloid genes by C/EBPβ (Kowenz-Leutz et al., 1999). The SWI/SNF complex is known to interact with the C/EBPβ TAD, in particular with the CR1 (Kowenz-Leutz et al., 2010). Interestingly, PrISMa revealed a lot of secondary interaction patterns of the Mi2/NuRD complex members to C/EBPβ peptides of the peptide matrix (Figure 15). The members of the Mi2/NuRD have been detected to interact with C/EBPβ in a mass spectrometric screening done by Steinberg et al. (Steinberg et al., 2012). For this screening the three C/EBPβ isoforms, LAP*, LAP and LIP were used for Co-IPs. The results of Steinberg et al. showed that all three C/EBPβ isoforms interact with the members of the Mi2/NuRD complex. But the results of the screening lacked important information on the effects of the C/EBPβ RD on the interaction with these proteins.

To elucidate the C/EBPβ CRs and domains important for the binding of the members of the Mi2/NuRD complex to the C/EBPβ protein an experiment was devised using the two long C/EBPβ isoforms (*Gallus gallus*) and two C/EBPβ deletion mutants (*Gallus gallus*) for co-immunoprecipitating, amongst others, the components of the Mi2/NuRD complex. (This experiment was done together with Elisabeth Kowenz-Leutz (AG Leutz, MDC) who performed the molecular cloning of the C/EBPβ ΔCR5-7 and the C/EBPβ ΔCR1,5-7 mutants, the HEK293T cell culture and the C/EBPβ Co-IPs.) For this C/EBPβ interaction screening of the two long C/EBPβ isoforms LAP* and LAP as well as two C/EBPβ deletion mutants, C/EBPβ ΔCR5-7 lacking the whole RD and C/EBPβ ΔCR1,5-7 lacking the whole RD and the CR1, were chosen. The C/EBPβ isoforms and the C/EBPβ deletion mutants were overexpressed in HEK293T cells (Figure 16A). Then these C/EBPβ isoforms and mutants were immunoprecipitated. The samples were tryptically digested and measured using targeted proteomics. The proteins that were

targeted by selected reaction monitoring (SRM) were the Mi2/NuRD complex members MBD2, MBD3, CHD3, CHD4, RBBP4, RBBP7, MTA1, MTA2 and MTA3. Apart from the Mi2/NuRD complex components, other proteins were targeted as well, such as the two HATs P300 and CBP, the SWI/SNF complex members BRG1, SMARCA2 (hBRM) and MeCP2 and PRMT5 and MEP50. PRMT5 and MEP50 were included as they form a complex, termed the PRMT5:MEP50 complex, known to methylate numerous chromatin-remodeling complexes, such as Mi2/NuRD complex and the SWI/SNF complex (Antonysamy et al., 2012). For developing the SRM method peptides were synthesized with an automated multiple peptide synthesizer. One peptide for each targeted protein was synthesized (vide Table 2 in the material and methods section). These peptides were used to obtain the best mass-to-charge ratios (m/z) of each peptide and their corresponding most convenient peptide fragmentation ions. In addition, these peptides were used as master mix. This master mix was measured after all the actual samples to obtain the accurate retention time for each of the peptides on the employed analytical column. The samples were measured in a non-scheduled SRM mode on a QTRAP 5500 mass spectrometer.

Of all the targeted proteins C/EBPβ, MBD3, RBBP4, RBBP7, MTA1, MTA2, PRMT5 and MEP50 were detected using SRM (Figure 16B). The detected area counts of the protein-protein interaction partners were normalized to the area counts of the bait, C/EBPβ. First fold changes of the normalized area counts of the four Co-IPs were calculated and subsequently the C/EBPβ isoform LAP was set as the reference point (100 %) for the presentation of the data (Figure 16B). The results of the seven-detectected C/EBPβ protein partners are almost consistent for all four measurements. Interestingly, the C/EBPβ LAP* isoform harboring the CR1 shows an increase of binding to all of the detected components of the Mi2/NuRD complex in comparison to the LAP isoform. This increase in binding affinity to the LAP* isoform compared to the LAP isoform is also consistent for the targeted proteins PRMT5 and MEP50. The C/EBPβ ΔCR5-7 mutant lacking C/EBPβ RD exhibits an increase of binding for all the detected C/EBPβ protein-protein interaction partners compared to the LAP and the LAP* isoform, with the exception of RBBP4 that binds less abundantly to the C/EBPβ ΔCR5-7 mutant than to the two long C/EBPβ isoforms. The C/EBPβ ΔCR1,5-7 mutant that lacks the RD and the CR1 displays a significant loss of protein-protein interaction compared to the LAP and the LAP isoform.

A

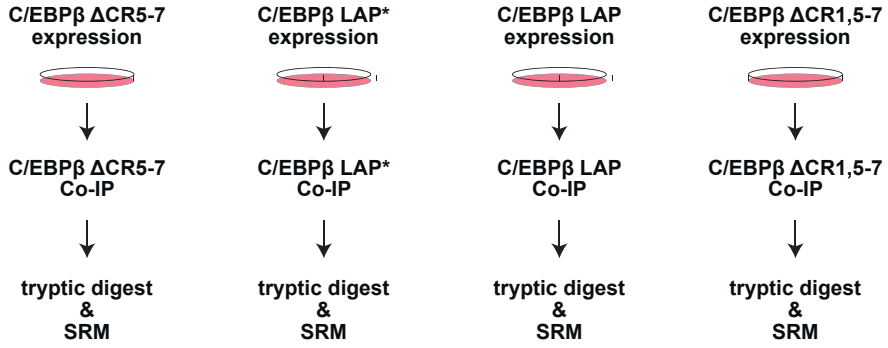
C/EBPβ ΔCR5-7 expression
C/EBPβ LAP* expression
C/EBPβ LAP expression
C/EBPβ ΔCR1,5-7 expression
C/EBPβ ΔCR5-7 Co-IP
C/EBPβ LAP* Co-IP
C/EBPβ LAP Co-IP
C/EBPβ ΔCR1,5-7 Co-IP
tryptic digest & SRM
tryptic digest & SRM
tryptic digest & SRM
tryptic digest & SRM

B

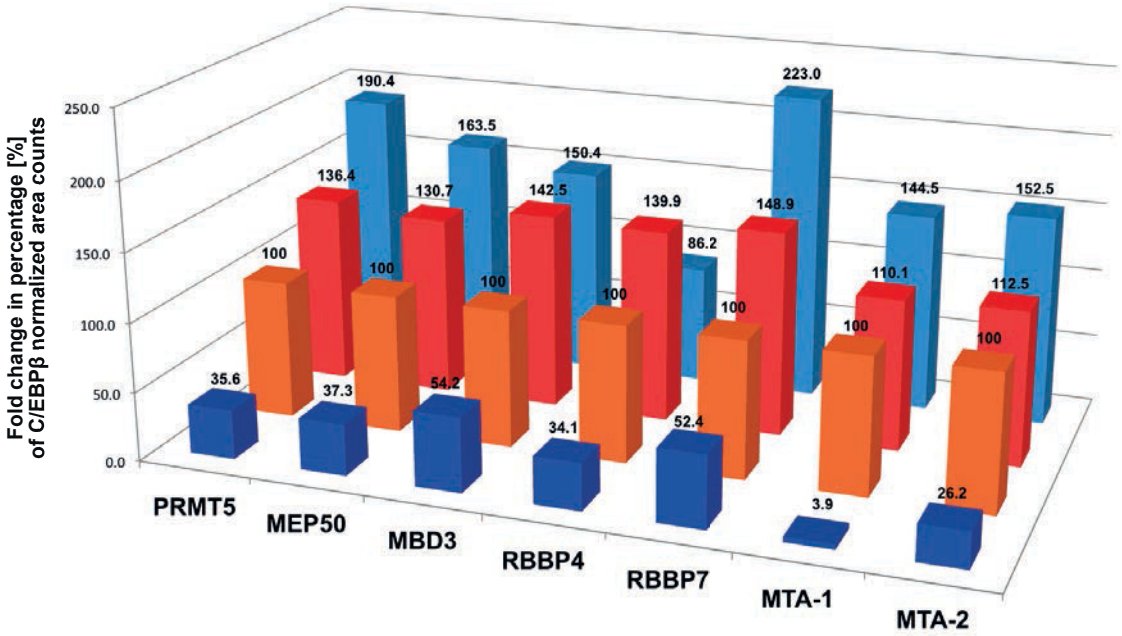
Fold change in percentage [%] of C/EBPβ normalized area counts
250.0
200.0
150.0
100.0
50.0
0.0
PRMT5
MEP50
MBD3
RBBP4
RBBP7
MTA-1
MTA-2
190.4
136.4
100
35.6
163.5
130.7
100
37.3
150.4
142.5
100
54.2
139.9
86.2
100
34.1
223.0
148.9
100
52.4
144.5
110.1
100
3.9
152.5
112.5
100
26.2

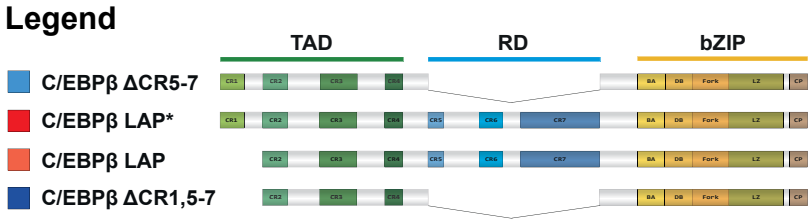
Legend
TAD
RD
bZIP
C/EBPβ ΔCR5-7
C/EBPβ LAP*
C/EBPβ LAP
C/EBPβ ΔCR1,5-7

Figure 16: C/EBPβ CR1 and RD play an important role in the protein-protein interaction of C/EBPβ with the components of the Mi2/NuRD and the PRMT5/MEP50 complex. A) Scheme of C/EBPβ isoform and C/EBPβ mutant Co-IPs. Samples are tryptically digested and measured using selected reaction monitoring (SRM). B) Bar plot of the protein-protein interaction area count fold change of the C/EBPβ normalized area counts. The C/EBPβ isoform LAP was set as the reference point (100 %) for the presentation of the data. The C/EBPβ ΔCR5-7 mutant binds increased to most of the targeted proteins, with the exception for RBBP4, in comparison to the LAP* and LAP isoforms. The C/EBPβ isoform LAP reveals decreased interaction with the targeted proteins compared to the LAP* isoform. The C/EBPβ ΔCR1,5-7 mutant displays a significant drop in the interaction with the targeted proteins compared to the LAP* and LAP isoform. The legend depicts the C/EBPβ LAP* (red) and LAP (orange) isoform, the C/EBPβ ΔCR5-7 mutant (light blue) and the C/EBPβ ΔCR1,5-7 mutant (darkblue).

By assessing these results it can be concluded that C/EBPβ RD is important for repelling the components of the Mi2/NuRD and the PRMT5/MEP50 complex, whereas the C/EBPβ CR1 is crucial for stabilizing these C/EBPβ interactions, as demonstrated by the LAP* isoform and the C/EBPβ ΔCR1,5-7 mutant. Of the targeted members of the Mi2/NuRD complex the two ATP-dependent helicases CHD3 and CHD4 were not detected during the SRM runs. This is surprising, as a stoichiometric investigation of the MBD3/NuRD complex by Smits et al. showed that the MBD3/NuRD complex is composed of one molecule of MBD3 and one molecule of CHD3/CHD4 per complex, whereas six molecules of RBBP4/RBBP7 and three molecules of MTA1/2/3 are contained in the MBD3/NuRD complex (Smits et al., 2012). Why the other targeted proteins, such as the Mi2/NuRD complex members CHD3, CHD4, MBD2 and MTA3, were not detected in any of the SRM measurements conducted (Figure 16B) can have various reasons. Either the co-immunoprecipitated proteins were not interacting with C/EBPβ under these experimental conditions or a set of different peptides with better ionization properties has to be utilized for detecting the targeted proteins. Moreover, the stoichiometric ratio of a complex, such as the MBD3/NuRD complex, can impact the detection of its complex members as well.

3.11 The tudor domain containing protein SPF30 interacts with C/EBPβ symmetrically dimethylated R280

PrISMa was devised in such a manner that it would give insight into how methylation of arginines and lysines influences the interaction pattern of proteins with C/EBPβ. The tudor domain is a protein domain, that binds amino acid sequences of proteins containing a methylated arginine or lysine (Chen et al., 2011).

The methylarginine binding protein SPF30 is a protein essential for the spliceosome assembly (Rappsilber et al., 2001; Jurica et al., 2002). Using PrISMa SPF30 was identified binding to C/EBPβ peptide sequences. Moreover, SPF30 binds to C/EBPβ peptides in a PTM dependent manner (Figure 17A). SPF30 binds with its maximum LFQ intensity to a C/EBPβ peptide sequence of the LZ containing the symmetrically dimethylated R280. The preference of SPF30 for symmetrically dimethylated arginines is in accordance with published data, which demonstrated that, the tudor domain of SPF30 binds to this type of arginine methylation (Côté et al., 2005).

SPF30 is part of one of the subunits of the spliceosome termed the 17S U2 snRNP complex (Will et al., 2002). By employing PrISMa 32 members of the 17S U2 snRNP complex were detected (Suppl. figure 12). Of these, eleven were observed to bind with a maximum to the C/EBPβ peptide sequence SRELSTLRNLFKQL containing C/EBPβ R280 (Figure 17B). Apart from SPF30, also U2AF2, SF3B14, SNRPD3, DHX15, U2AF1, PUF60 and SF3B1 revealed their maximal binding to the C/EBPβ peptide containing the symmetrically dimethylated R280. SNRPG binds maximal to the C/EBPβ peptide containing an asymmetrically dimethylated R280 and SNRPE and CHERP revealed their maximal protein-peptide interaction to the same C/EBPβ peptide sequence not containing any PTM at all.

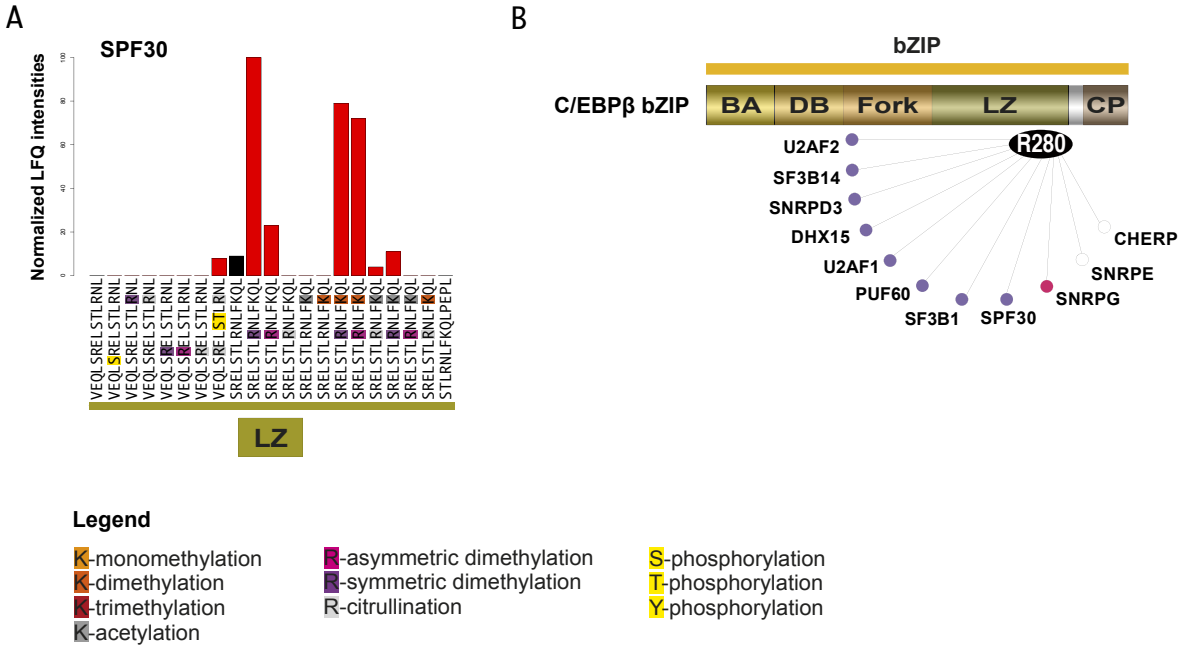

Figure 17: Members of the 17S U2 snRNP complex preferentially bind to C/EBPβ peptide sequences of the LZ in a PTM dependent manner. A) SPF30 binds preferentially to C/EBPβ peptide sequences of the LZ containing a symmetrically dimethylated arginine. The bar graphs show the normalized LFQ intensity for SPF30. Black bars depict the binding intensities to peptide sequences without PTMs, whereas red bars represent the binding intensities to peptides that contain one or multiple PTMs. The bar graph x-axis is annotated with the presented C/EBPβ peptide amino acid sequences. The legend at the bottom of the figure accounts for the color code of PTMs highlighted in the x-axis text. B) Many members of the spliceosomal subcomplex 17S U2 snRNP are detected to preferentially bind to C/EBPβ peptides containing the C/EBPβ R280 in a PTM dependent manner. C/EBPβ bZIP is depicted in the previously introduced bZIP color code (compare Figure 1). The legend at the bottom accounts for the PTM color code of the points representing the members of the 17S U2 snRNP complex.

3.12 C/EBPβ interactome of the anaplastic large cell lymphoma cell line SU-DHL-1

C/EBPβ is highly expressed ALK-positive anaplastic large cell lymphomas (ALK+ALCL) (Quintanilla-Martinez et al., 2006). The SU-DHL-1 cell line is a human derived ALK+ALCL cell line that harbors the oncogenic NPM-ALK fusion gene. Cell proliferation of SU-DHL-1 cells is abrogated by the knockdown of C/EBPβ (Anastasov et al., 2010). The expression of the C/EBPβ mRNA in SU-DHL-1 cells is dependent on the NPM-ALK kinase activity and its downstream target STAT3. Published gene expression profiling studies have concluded that

C/EBPβ is significantly involved in gene regulation leading to cell growth and cell survival of SU-DHL-1 cells (Bonzheim et al., 2013).

Due to the fundamental role of C/EBPβ in the SU-DHL-1 cell proliferation a Co-IP experiment was devised to elucidate the C/EBPβ interactome in this ALK+ALCL cell line. (This experiment was done together with Julia W. Böhm (AG Leutz, MDC) who performed the SU-DHL-1 cell culture and Co-IPs from nuclear enriched lysates.) The Co-IP experiment was done using a label-free quantification (LFQ) approach (Figure 18A). For enrichment purposes of C/EBPβ the Co-IPs were performed from nuclear enriched cell extracts. The six Co-IPs were tryptically digested and measured via shotgun proteomics on a Q Exactive. The data files were analyzed using MaxQuant with the LFQ mode selected. For the multiple hypothesis testing only proteins were selected that were detected at least two times either in the bead control group or in the C/EBPβ immunoprecipitation group. Missing values were imputated. A false discovery rate (FDR) of ≤ 0.05 was preconditioned as the significance cut-off to determine specific C/EBPβ protein interaction partners.

With the LFQ approach from the Co-IPs of SU-DHL-1 cells 472 proteins were detected at least twice either for the bead triplicate or the C/EBPβ triplicate (Figure 18B). 162 of these detected proteins are significant C/EBPβ protein-protein interaction partners with a FDR of $\leq$ 5 ٪ (Table 3). Intriguingly, of these significant C/EBPβ interaction partners in SU-DHL-1 133 proteins were also detected with the PrISMa method (Suppl. figure 13-14; marked in Table 3).

C/EBPβ interacts with STAT3 and ALK in SU-DHL-1. ALK and NPM were detected as separate proteins due to the identification with the human protein database even though these proteins are at least partially expressed as a fusion protein in SU-DHL-1 cells. Hence, STAT3 and NPM-ALK are not only crucial for the transcription of C/EBPβ mRNA but these proteins are C/EBPβ protein-protein interaction partners as well. STAT3 was also detected with the PrISMa method binding preferentially to C/EBPβ CR7 and to a far lesser extent to C/EBPβ LZ peptides (Suppl. figure 13).

GO analysis of the significant C/EBPβ interactors detected in the ALK+ALCL cell line SU-DHL-1 uncovered an enrichment for the GO:terms ´Regulation of transcription´, ´RNA processing´, ´protein transport´ and ´chromosome organization´ (Suppl. figure 15). A database search of the Comprehensive Resource of Mammalian protein complex (CORUM) yielded that

the protein-protein interaction partners of C/EBPβ in SU-DHL-1 are members of various protein complexes with multiple functions, such as splicing, DNA repair, ribosome biogenesis, mitotic cell cycle and transcription activation (Table 3).

Many of C/EBPβ interaction partners in SU-DHL-1 are members of chromatin-remodeling complexes. CHD4, MTA2, SMARCA5 and SMC1 were uncovered to interact with C/EBPβ in SU-DHL-1. These interaction partners are components of the Mi2/NuRD complex or the SNF2h-cohesin-NuRD complex. Moreover, many components of the Mi2/NuRD complex were detected binding to C/EBPβ peptide sequences of C/EBPβ LZ using PrISMa as well (Figure 15; Suppl. figure 13-14). BRG1, SMARCC1 and MeCP2, components of the SWI/SNF complex and the BRG1-based SWI/SNF complex, were detected interacting with C/EBPβ in SU-DHL-1 (Figure 18B; Table 3) and by PrISMa (Suppl. figure 13-14). The SWI/SNF complex is a published C/EBPβ interacting complex (Kowenz-Leutz et al., 1999). The SWI/SNF complex is well known for its transactivation effect on C/EBPβ.

C/EBPβ interacts with KDM3B in SU-DHL-1 (Figure 18B; Table 3). KDM3B is a lysine demethylase that demethylates lysine 9 of histone 3, a repressive histone modification (Brauchle et al., 2013). TOP1 and TOP2 are topoisomerases that interact with C/EBPβ in SU-DHL-1 cells. These two topoisomerases play a pivotal role in removing torsional tension of DNA supercoils, induce conformational changes at promoter sites and above that bridge protein-protein interactions relevant for regulating transcription (Baranello et al., 2013). Both of these topoisomerases were also detected using PrISMa revealing that these proteins bind preferentially to C/EBPβ peptide sequences of C/EBPβ bZIP domain (Suppl. figure 13).

C/EBPβ interacts with all components of the DNA-PK-Ku complex in SU-DHL-1 cells (Figure 18B; Table 3). XRCC5, XRCC6 and PRKDC are components of the DNA-PK-Ku complex, a complex important for sensing DNA damage and the non-homologous end joining of DNA (Spagnolo et al., 2006). These three PK-Ku complex components were detected interacting mainly with C/EBPβ TAD and bZIP peptide sequences employing the PrISMa method (Suppl. figure 13-14).

C/EBPβ interacts with CREB1 and RUNX2 in SU-DHL-1 (Figure 18B; Table 3). These transcription factors are known to work synergistically together with C/EBPβ to regulate transcription (Chen et al., 2002; Gutierrez et al., 2002). Moreover, C/EBPβ interacts with ATF3

in the ALK+ALCL cell line SU-DHL-1. The protein-protein interaction of ATF3 and C/EBPβ is stated to enhance C/EBPβ DNA-binding potential (Lee et al., 2010a).

Proteins important for the nucleoplasmic transport were detected to interact with C/EBPβ in SU-DHL-1 cells (Figure 18B; Table 3), such as KPNB1, KPNB2, NUP358, NUP50, NUP210, TPR and XPO1. All of these proteins associated with the nucleoplasmic transport, with the exception of NUP210, were also detected using PrISMa primarily binding to C/EBPβ peptides of the CR7 and the LZ (Figure 14; Suppl. figure 13-14). These C/EBPβ protein partners in SU-DHL-1 cells are essential for protein shuttling and mitotic processes leading to chromosome segregation.

Proteins involved in RNA splicing were co-immunoprecipitated with C/EBPβ from SU-DHL-1 cells, too (Figure 18B; Table 3). C/EBPβ significantly interacts in SU-DHL-1 cells with SF3A1, SF3B1, SRFS3, TAF2S, SNRPA1, CDC5L, DDX48, DDX5, DDX9, DDX3X, DDX46, DDX17, RBMX, RALY, PRPF8, PRPF6, SKIV2L2, HNRNPC, HNRNPA1, HNRPH1, HNRNPA3, HNRNPM, HNRNPK, SNRNP200, SNRNP70, PRPF40A, HSPD1 and HNRNPU. All of these proteins important for RNA splicing, with the exception of HNRNPCL2, were also detected binding to C/EBPβ peptide sequences using PrISMa (Suppl. figure 13-14). Most of these C/EBPβ interaction partners in SU-DHL-1 are members of RNA processing complexes, such as the spliceosome, the C complex spliceosome or the 17S U2 snRNP complex (Zhou et al., 2002; Jurica et al., 2002; Will et al., 2002).

Figure 18: C/EBPβ interacts with proteins of different cellular functions in the ALK+ALCL cell line SU-DHL-1. A) Scheme of C/EBPβ Co-IPs (on the following page) from nuclear enriched extract of SU-DHL-1 cells using a label-free quantification (LFQ) approach. Co-IPs were tryptically digested and measured by mass spectrometry. The data analysis includes LFQ and is evaluated by a two-sample test and multiple hypothesis testing. B) Volcano plot of the C/EBPβ Co-IPs from SU-DHL-1 cells. C/EBPβ significantly interacts with 162 proteins in SU-DHL-1 with a FDR ≤ 0.05. The two legends at the bottom of the volcano plot identify the left plot side for protein interactions with the bead control (bead) and the right plot side for protein interactions with C/EBPβ (C/EBPβ). Significant C/EBPβ interactors are labeled with numbers as numerated in table 3. Red points are proteins with a FDR ≤ 0.05 and grey points are proteins with a FDR > 0.05.

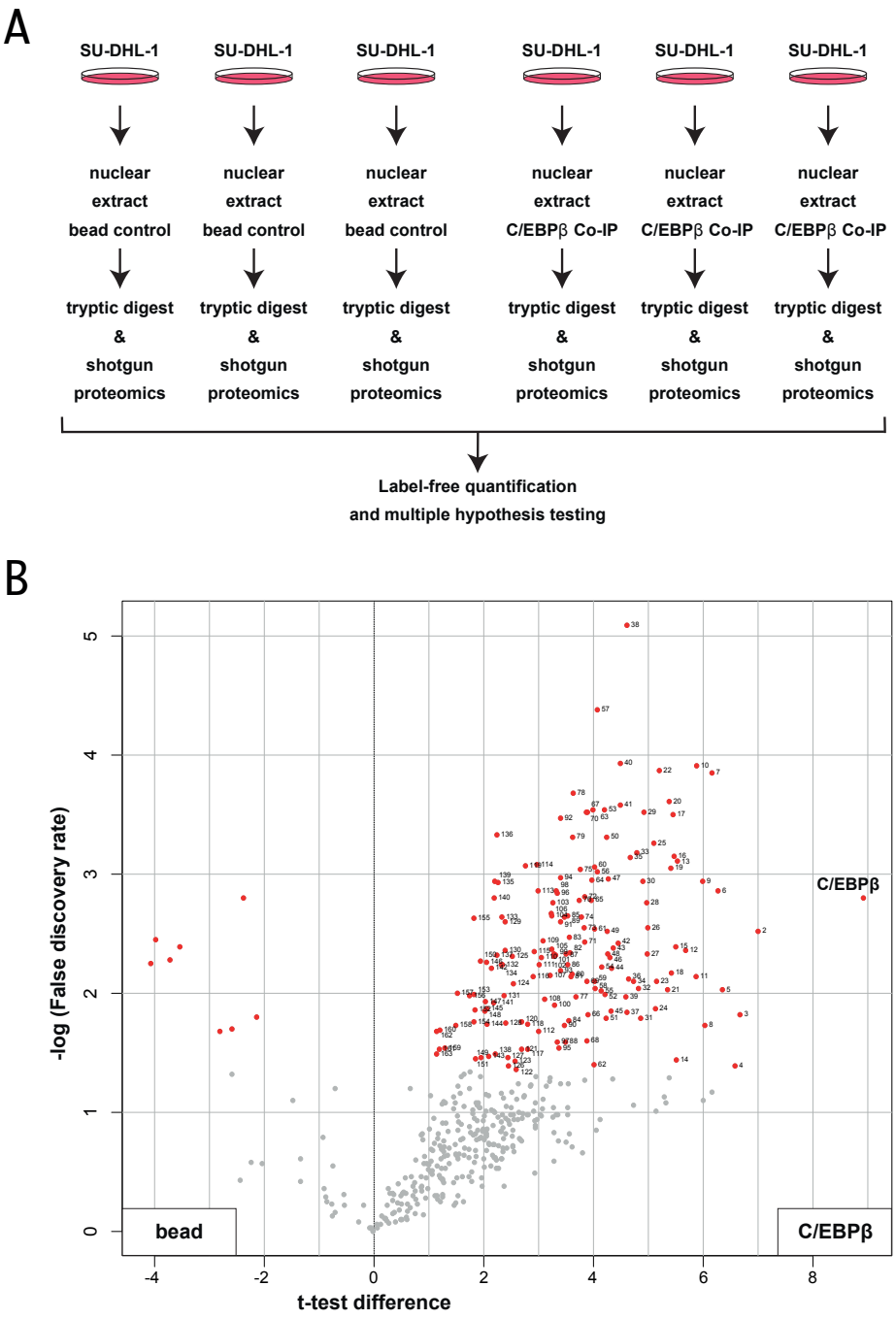

Table 3: Table of C/EBPβ protein-protein interaction partners from SU-DHL-1 cells. Table contains the Uniprot accession numbers, protein names and alternative protein names of the C/EBPβ interaction partners from SU-DHL-1 cells. C/EBPβ protein interaction partners are assigned to protein complexes and their corresponding functional category from the Complete Dataset versus Core Set (CORUM) database. Rows highlighted in lightblue and typed in bold itemize proteins that were detected in the PrISMa dataset as well (Suppl. figure 13-14).

No.	Uniprot	Name	Alternative Name	Corum Complex	Functional Catagory
2.	P12956	XRCC6		DNA-PK-Ku antigen complex	mRNA synthesis
3.	P78527	PRKDC	HYRC	DNA-PK-Ku antigen complex	mRNA synthesis
4.	Q00839	HNRNPU		C complex spliceosome	splicing
5.	E9PRY8	EEF1D			
6.	P26641	EEF1G		SNW1 complex	transcription activation
7.	Q99623	PHB2	BAP		
8.	P07910	HNRNPC		C complex spliceosome	splicing
9.	Q16666	IFI16			
10.	P09874	PARP1	ADPRT	Condensin I-PARP-1-XRCC1 complex	DNA repair
11.	Q9H0C8	ILKAP			
12.	P42166	TMPO	LAP2		
13.	P05141	SLC25A5	ANT2	Nop56p-associated pre-rRNA complex	ribosome biogenesis
14.	P09651	HNRNPA1		C complex spliceosome	ribosome biogenesis
15.	P21796	VDAC1	VDAC	CAV1-VDAC1-ESR1 complex	ion channels
16.	O14980	XPO1	CRM1	CRM1-Survivin mitotic complex	mitotic cell cycle
17.	P45880	VDAC2			
18.	P13010	XRCC5		DNA-PK-Ku antigen complex	mRNA synthesis
19.	Q14974	KPNB1		RANBP1-RAN-KPNB1 complex	protein transport
20.	P49792	NUP358	RANBP2	Nuclear pore complex	protein transport
21.	P17844	DDX5		C complex spliceosome; Spliceosome	splicing
22.	B0UZ83	C4A			
23.	P52272	HNRNPM		C complex spliceosome	splicing
24.	Q92841	DDX17		Spliceosome	splicing
25.	P11142	HSPA8	HSC70	HMGB1-HMGB2-HSC70-ERP60-GAPDH complex	DNA repair
26.	P35637	FUS			
27.	P11021	HSPA5	GRP78	SNW1 complex	transcription activation
28.	P60842	EIF4A1	DDX2A	MNK1-eIF4F complex	translation initiation
29.	P38919	EIF4A3	DDX48	C spliceosome complex; Spliceosome	splicing
30.	Q15365	PCBP1			
31.	P13639	EEF2		Nop56p-associated pre-rRNA complex	ribosome biogenesis
32.	P14866	HNRNPL		Emerin complex 52	RNA processing
33.	P14625	HSP90B1	GRP94		
34.	A8MXP9	MATR3		SNW1 complex	transcription activation
35.	Q9NR30	DDX21		Nop56p-associated pre-rRNA complex	ribosome biogenesis
36.	P38646	HSPA9	GRP75	Frataxin complex	protein binding
37.	P11387	TOP1		Nop56p-associated pre-rRNA complex	ribosome biogenesis
38.	P11388	TOP2		Toposome	DNA topology
39.	P62987	UBA52		60S ribosomal subunit, cytoplasmic	protein sythesis
40.	O43823	AKAP8			
41.	Q99459	CDC5L		C complex spliceosome; Spliceosome	splicing
42.	P35659	DEK		Splicing-associated factors complex	splicing
43.	P38159	RBMX	HNRPG	C complex spliceosome	
44.	Q08211	DDX9		Spliceosome	splicing
45.	P31943	HNRNPH1		C complex spliceosome	splicing
46.	P20700	LMNB1		Emerin complex 52	RNA processing
47.	P84103	SFRS3		Spliceosome	splicing
48.	P35232	PHB			
49.	P12268	IMPD2			
50.	P04843	RPN1		Oligosaccharyltransferase OSTC-I	N-directed glycosylation
51.	P18754	RCC1	CHC1		
52.	P35579	MYH9		WIP-WASp-actin-myosin-IIa complex	adaptive cell mediated response (T-cell)
53.	O75643	SNRNP200	ASCC3L1	C complex spliceosome; Spliceosome	splicing
54.	Q8N1F7	NUP93		Nuclear pore complex	protein transport
55.	J9JID7	LMN2		Emerin complex 52	RNA processing
56.	O00567	NOP56		Nop56p-associated pre-rRNA complex	ribosome biogenesis
57.	Q9UKM9	RALY	HNRPCL2	C complex spliceosome	splicing
58.	P49368	CCT3		CCT micro-complex	protein folding and stabilization
59.	O43175	PGDH3	PHGDH		
60.	P17987	TCP1		CCT micro-complex	protein folding and stabilization
61.	P42704	LRPPRC	LRP130	TNF-alpha/NF-kappa B signaling complex 5	NIK-I-kappaB/NF-kappaB cascade
62.	P61978	HNRNPK		C complex spliceosome	splicing
63.	Q14204	DYNC1H1	DHC1	CDC5L complex	splicing
64.	O75475	PSIP1	DFS70		
65.	Q8TEM1	NUP210		Nuclear pore complex	protein transport
66.	P78371	CCT2		CCT micro-complex	protein folding and stabilization
67.	Q16649	NFIL3	E4BP4		
68.	B0V043	VARS			
69.	Q6P2Q9	PRPF8	PRPC8	C complex spliceosome; Spliceosome	splicing
70.	Q14839	CHD4		Mi2/NuRD complex	DNA conformation modification
71.	Q92733	PRCC			
72.	P11586	MTHFD1	MTHFC		
73.	P07814	EPRS		GAIT complex	translational control
74.	P60468	SEC61B		Sec61-Sec62-Sec63 complex	protein transport
75.	Q9HBD4	BRG1		BRG1-based SWI/SNF chromatin-remodeling complex	DNA conformation modification
76.	Q92945	KHSRP	FUBP2		
77.	P06576	ATP5B		F1F0-ATP synthase	phosphate metabolism
78.	P40939	HADHA	HADH		
79.	Q9UM73	ALK	ALK		
80.	P51991	HNRNPA3		C complex spliceosome	splicing
81.	Q13200	TRAP2		PA700 complex	proteasomal degradation
82.	Q13151	HNRNPA0			
83.	O14776	TAF2S		Spliceosome	splicing
84.	P21333	FLNA	FLN		

No.	Uniprot	Name	Alternative Name	Corum Complex	Functional Catagory
85.	Q16891	IMMT	HMP		
86.	Q9H3N1	TMX1	PSEC0085		
87.	P62263	RPS14		Nop56p-associated pre-rRNA complex	ribosome biogenesis
88.	O00571	DDX3X	DBX	Spliceosome	splicing
89.	O00299	CLIC1			
90.	P27635	RPL10		Nop56p-associated pre-rRNA complex	ribosome biogenesis
91.	E7ENR4	HK1			
92.	Q13950	RUNX2			
93.	P51148	RAB5C			
94.	Q00610	CLTC	CLH17	Profilin 1 complex	assembly of protein complexes
95.	P18847	ATF3			
96.	O94776	MTA2		Mi2/NuRD complex	DNA conformation modification
97.	P62081	RPS7		Nop56p-associated pre-rRNA complex	ribosome biogenesis
98.	Q92922	SMARCC1		BRG1-based SWI/SNF chromatin-remodeling complex	DNA conformation modification
99.	Q7LBC6	KDM3B	JHDM2B		
100.	P42167	TMPO	LAP2B		
101.	P05114	HMGN1	HMG14		
102.	Q9Y2X3	NOP58		Nop56p-associated pre-rRNA complex	ribosome biogenesis
103.	P22695	UQCRC2			
104.	P02786	TFRC		SNX complex	protein transport
105.	P19338	NCL		Nop56p-associated pre-rRNA complex	ribosome biogenesis
106.	Q9UJZ1	STOML2	HSPC108		
107.	P50990	CCT8		CCT micro-complex	protein folding and stabilization
108.	P24539	ATP5F1		F1F0-ATP synthase	phosphate metabolism
109.	P08621	SNRNP70		Spliceosome	splicing
110.	P31939	ATIC			
111.	P32189	GK			
112.	P46782	RPS5			
113.	O43684	BUB3		Mitotic checkpoint complex	cell cycle checkpoint
114.	O75533	SF3B1	SAP155	Spliceosome; 17S U2 snRNP	splicing
115.	P33176	KIF5B		PLEKHM2-KIF5B complex	cell motility
116.	P09429	HMGB1		HMGB1-HMGB2-HSC70-ERP60-GAPDH complex	DNA repair
117.	P27708	CAD			
118.	P10809	HSPD1	HSP60	17S U2 snRNP	splicing
119.	P40763	STAT3		VEGF transcriptional complex	transcriptional control
120.	P50991	CCT4		CCT micro-complex	protein folding and stabilization
121.	Q13423	NNT			
122.	P08107	HSPA1A	HSPA1	Polycomb repressive complex 1	DNA conformation modification
123.	P62195	PSMC5		PA700 complex	proteasomal degradation
124.	O94906	PRPF6		C complex spliceosome; Spliceosome	splicing
125.	Q9UBE0	SAE1	AOS1	SUMO1-SUA1-UBA2 complex	modification by ubiquitination
126.	P51572	BCAP31	BAP31		
127.	O60264	SMARCA5		SNF2h-cohesin-NuRD complex	DNA conformation modification
128.	O75400	PRPF40A	FBP11	Spliceosome	splicing
129.	P61981	YWHAG		BRAF-RAF1-14-3-3 complex	MAPKKK cascade
130.	Q8N163	CCAR2	DBC1	IKBKB-CDC37-KIAA1967-HSP90AB1 complex	NIK-I-kappaB/NF-kappaB cascade
131.	Q14683	SMC1A		SNF2h-cohesin-NuRD complex	DNA conformation modification
132.	P30153	PPP2R1A		RFC2-RIalpha complex	protein binding
133.	Q7L014	DDX46		Spliceosome; 17S U2 snRNP	splicing
134.	Q9BQG0	MYBBP1A		Nop56p-associated pre-rRNA complex	ribosome biogenesis
135.	P30101	PDIA3	ERP57	HMGB1-HMGB2-HSC70-ERP60-GAPDH complex	DNA repair
136.	P48643	CCT5		CCT micro-complex	protein folding and stabilization
137.	Q9Y5B9	SUPT16H	FACT140	Cen complex	mitotic cell cycle
138.	P16220	CREB1		FHL2-CREB complex	transcription activation
139.	P49959	MRE11A	HNGS1	MRN complex (MRE11-RAD50-NBN complex)	DNA degradation
140.	Q15149	PLEC	PLEC1	PLEKHM2-KIF5B complex	cell motility
141.	P46013	MKI67			
142.	Q15459	SF3A1	SAP114	C complex spliceosome; Spliceosome; 17S U2 snRNP	splicing
143.	Q9UKX7	NUP50		Nuclear pore complex	protein transport
144.	P51608	MECP2		SWI/SNF chromatin-remodeling complex	transcription repression
145.	P61221	ABCE1			
146.	P23193	GTF2S			
147.	P05455	SSB		Emerin complex 25	RNA processing
148.	Q92522	H1FX		Nop56p-associated pre-rRNA complex	ribosome biogenesis
149.	P39687	ANP32A			
150.	P22102	GART			
151.	D6RCF4	CISD2	CDGSH2		
152.	Q9NQ29	LUC7L2	LUC7L	Nop56p-associated pre-rRNA complex	ribosome biogenesis
153.	O95347	SMC2		Condensin I-PARP-1-XRCC1 complex	DNA repair
154.	P09661	SNRPA1		C complex spliceosome; Spliceosome; 17S U2 snRNP	splicing
155.	Q5UIP0	RIF1			
156.	Q01780	EXOSC10		Exosome	RNA degradation
157.	P12270	TPR		Nuclear pore complex	protein transport
158.	P35251	RFC1		RFC complex	phosphate metabolism
159.	P42285	SKIV2L2		C complex spliceosome; Spliceosome	splicing
160.	Q92973	KPNB2			
161.	Q14152	EIF3A		EIF3 complex	translational initiation
162.	P30626	SRI		SRI homodimer complex	protein binding
163.	J3KQ73	FKBP38		HSP90-FKBP38-CAM-Ca(2+) complex	regulation of apoptosis

3.13 C/EBPβ interacts with a network of proteins in a PTM specific manner

With the PrISMa method 372 published protein interaction partners of C/EBPβ (Suppl. table 1) were detected binding to C/EBPβ peptide sequences (Suppl. fig. 3-10). Furthermore, PrISMa revealed components of the mediator complex (Figure 12), proteins involved in the nucleoplasmic transport (Figure 14), chromatin-remodeling complexes (Figure 15) and the RNA processing complex 17S U2 snRNP (Figure 17; Suppl. figure 12) to mutually bind to specific C/EBPβ peptide sequences. Moreover, the investigation of C/EBPβ interactome in SU-DHL-1 cells uncovered the protein-protein interaction partners necessary for C/EBPβ oncogenic impact on an ALK+ALCL cell line (Figure 18B; Table 3). A large proportion of these published and novel C/EBPβ protein partners in SU-DHL-1 are also detected with the PrISMa approach preferentially interacting with specific C/EBPβ peptide sequences (Suppl. figure 13-14; Table 3).

A part of the C/EBPβ interaction network revealed by literature research (Suppl. table 1; Suppl. figure 3-10), by PrISMa data analysis (Figure 12, 14, 15, 17; Suppl. figure 12) and by the C/EBPβ Co-IPs from SU-DHL-1 (Table 3) is outlined in Figure 19. C/EBPβ peptides harboring C/EBPβ R3, R20, K39, R42, R46, R59, R162, R264, R274 and R280 were selected to represent the potential of PrISMa to elucidate PTM specific protein interaction networks. The proteins shown in Figure 19 interact with their maximum LFQ intensity to one of the C/EBPβ peptides containing one of the selected arginines or the lysine. The network is depicted as connecting lines between the proteins. These lines represent published protein-protein interactions retrieved from the databases BIOGRID, INTACT, MINT, HPRD, BIND and DIP using the Cytoscape plugin Bisogenet.

The C/EBPβ peptide-protein interactors detected using PrISMa belong to a tightly interwoven network of protein-protein interaction partners (Figure 19). For example, C/EBPβ peptide sequences containing the C/EBPβ R3 bind TPI1, TRX1 and CCND1 with the non-modified

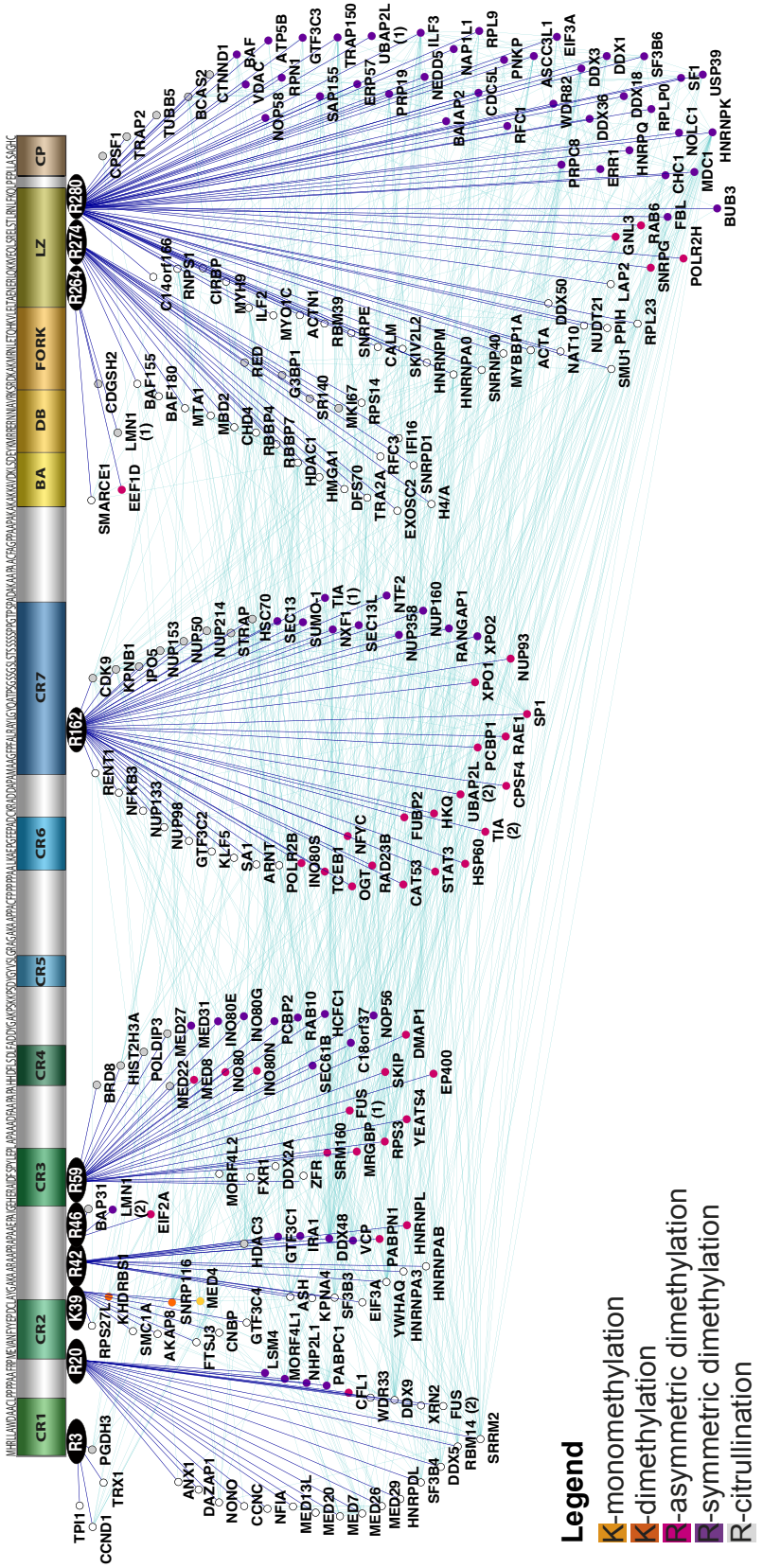
CR1
CR2
CR3
CR4
CR5
CR6
CR7
BA
DB
FORK
LZ
CP
R3
R20
K39
R42
R46
R59
R162
R264
R274
R280
Legend
K-monomethylation
K-dimethylation
R-asymmetric dimethylation
R-symmetric dimethylation
R-citrullination

Figure 19: C/EBPβ interacts with a tighly interwoven network proteins in a PTM dependent manner. Proteins binding to C/EBPβ peptides containing C/EBPβ R3, R20, K39, R42, R46, R59, R162, R262, R274 and R280 were selected to demonstrate that C/EBPβ interacts with a closely connected network of proteins. On top of the figure is a schematic representation of C/EBPβ structure depicting the CRs and domain structures with a previously introduced color code (vide Figure 1). The nine selected arginine and the selected lysine modification are depicted as black ovals annotated with their corresponding arginine or lysine position. Blue lines connect proteins to one of the selected arginines or the lysine. These proteins were detected with their maximum LFQ intensity binding to the C/EBPβ peptide sequences harboring one of the selected arginines or the lysine. The points representing C/EBPβ peptide-protein interaction partners are depicted with a PTM color code accounted for in the legend at the bottom. The PTM color code legend depicts proteins interacting with peptide sequences containing a monomethylated lysine (yellow), a dimethylated lysine (orange), an asymmetrically dimethylated arginine (pink), a symmetrically dimethylated arginine (violet) or a citrullinated arginine (gray). The turquoise lines connecting the depicted proteins represent protein-protein interactions retrieved from the databases BIOGRID, INTACT, MINT, HPRD, BIND and DIP.

C/EBPβ R3 peptide sequence MHRLLAWDAACLPP, whereas PGDH3 preferentially interacts with the same C/EBPβ sequence containing a citrullinated R3. These proteins detected with their maximal LFQ intensities binding to a C/EBPβ peptide containing the R3 are published C/EBPβ protein interaction partners (Suppl. table 1) or C/EBPβ protein interaction partners immunoprecipitated from SU-DHL-1 cells (Table 3). Interestingly, the C/EBPβ CR1 peptide harboring the R3 (Figure 6) is only present in the long C/EBPβ LAP* isoform (Figure 1). Thus, these protein interactions with C/EBPβ R3 amino acid sequence (Figure 19) potentially depend on the expression of LAP* in a cellular context. C/EBPβ peptides containing C/EBPβ R20, K39 and R42 interact with proteins belonging to the mediator complex and RNA processing proteins (Figure 19). The PrISMa peptides of the C/EBPβ isoforms LAP* and LAP containing the R46 or R59 attract proteins that regulate transcription, organize chromatin and process RNA. Proteins associated with nucleoplasmic transport, transcription and RNA localization are associated with C/EBPβ peptides containing the R162. The C/EBPβ peptides containing the R264, R274 or R280 are enriched for proteins important for RNA processing, regulation of transcription, cell cycle and chromatin organization.

In summary, PrISMa is not only a novel tool to map protein interaction but it also reveals the protein interaction pattern in a PTM dependent manner. Moreover, PrISMa enables a comprehensive overview of protein interactions belonging to protein networks making PrISMa a tool of choice for protein interaction surveys.

DISCUSSION

4.1 C/EBPα PTMs and the impact on protein interaction patterns

C/EBPα is a transcription factor that plays a crucial role in cell proliferation arrest, terminal differentiation and posses oncogenic functions in AML patients. Up to date C/EBPα has been published to be modified in a signal dependent manner by kinases that phosphorylate C/EBPα TE-1, TE-3, FORK region and the amino acid stretch between the TE-3 and the BA (Figure 2). In this study novel PTMs sites of C/EBPα were verified with a tandem mass spectrum for C/EBPα R154, K159, R163, K280 and R323 (Figure 3; Suppl. figure 1) demonstrating that methylation, acetylation and even deimination are a part of C/EBPα signal dependent PTM pattern.

The R163 citrullination (Figure 3B) is a momentous novel C/EBP-PTM, as this type of enzymatic modification has not been published for the C/EBP family up until now. A multistep procedure involving the modifycation of citrullinated arginines by 2,3-butanedione (Ceuleneer et al., 2011) was used to reveal the deimination site by mass spectrometry. Proteins are citrullinated by enzymes belonging to the family of peptidylarginine deiminases (PADIs) (Wang et al., 2013). PADIs antagonize protein arginine methyltransferases (PRMTs) and additionally diminish the charge of the non-modified arginine guanidinium group as well. PADI4 is one of the five family members of the PADIs. PADI4 is predominantly expressed in granulocytes and has been associated with inflammation (Mowen et al., 2014). Furthermore, PADI4 is known for playing a part in chromatin decondensation, transcriptional regulation and tumorigenesis (Wang et al., 2013). Lab internal research conducted by Qingbin Liu (AG Leutz, MDC) demonstrated that PADI4 interacts with the C/EBPα bZIP domain and deiminates C/EBPα-TE-3 in vitro (Qingbin Liu, dissertation, 2012). Interestingly, C/EBPα is a key transcription factor for the formation of

granulocytes (Zhang et al., 1997), the same type of blood cells where PADI4 is predominantly expressed (Mowen et al., 2014). Based on the results of Qingbin Liu and the cellular expression pattern, PADI4 turns out to be a potential candidate for citrullinating C/EBPα at R163.

This study revealed that the R163 is essential for the interaction of C/EBPα with WDR18 (Figure 4). WDR18 is a member of the Five friends of methylated Chtop complex (5FMC) (Fanis et al., 2012). The 5FMC complex regulates the transactivation potential of transcription factors by affecting their sumoylation status through desumoylation of SUMO-2 and SUMO-3. Additionally, WDR18 is associated with DNA damage checkpoint signaling critical for the cell cycle arrest during DNA damage repair (Yan et al., 2013). The C/EBPα R163Q mutant mimicking a charge-less citrullinated arginine interacted preferentially with STAG1. STAG1 is part of the SNF2h-cohesin-NuRD complex and the Cohesin-SA1 complex (Hakimi et al., 2002; Kong et al., 2014). Both of these complexes are putative regulators of the segregation of chromosomes during cell division. STAG1 is a known interaction partner of C/EBPβ as well (Steinberg et al., 2012). Summed up, C/EBPα R163 may function as a significant transition point for proteins involved in desumoylation, DNA damage repair and the regulation of chromosome segregation. This is intriguing, as C/EBPα belongs to the proteins that remain bound to DNA during mitosis, a function termed as mitotic bookmarking (Kadauke et al., 2013). Mitotic bookmarking is the combination of the mitotic stable histone marks, stable DNA methylation patterns and the retention of transcription factors to DNA during mitosis guaranteeing the lineage fidelity of cells during cell division.

4.2 Sumoylated C/EBPα-TE-3 reveals novel protein-protein interplay

The C/EBPα citrullination site is adjacent to C/EBPα sumoylation site K159. C/EBPα sumoylation disrupts the interaction of C/EBPα with the SWI/SNF complex member BRG1 diminishing C/EBPα transactivation properties (Sato et al., 2006). It was shown that throughout the course of cell differentiation of the fetal liver and neutrophil granulocyte maturation C/EBPα sumoylation

status declines leading to terminal cell differentiation (Khanna-Gupta et al., 2008). Lysines are targets of multiple posttranslational modifications including sumoylation, ubiquitination, acetylation and three different states of methylation. In this study C/EBPα K159 was uncovered to be a multimodification site. As K159 methylation possibly prevents C/EBPα from being sumoylated, it was of interest, how C/EBPα protein interaction network is altered by SUMO-1. In the course of this study it was revealed that the sumoylated C/EBPα-TE-3 preferentially interacts with the proteins PML, SENP1, NUP358 and ARIP4 (Figure 5C).

The PML protein is the main component of PML (promyelocytic leukemia) nuclear bodies. These subcellular structures have been suggested to be storage sites for transcription factors, the location of transcription and RNA buildup sites (Boisvert et al., 2000). Additionally, these PML nuclear bodies are known to aid efficient interaction between enzymes and their matching substrates (Dundr et al., 2012). The PML protein contains a non-covalent sumo interaction motif (SIM) and is covalently modified with SUMO-1, too (Shen et al., 2006). The formation of mature PML nuclear bodies is induced by the covalent modification of the PML protein by SUMO-1 (Lallemand-Breitenbach et al., 2010). The proteins destined for the PML nuclear bodies either contain a SIM or are sumoylated themselves. PML protein knock-out mice display impaired myeloid differentiation (Wang et al., 1998). The PML protein is an interaction partner of PU.1, a key transcription factor for regulating myeloid and lymphoid cell differentiation (Yoshida et al., 2007; Iwasaki et al., 2005). The gene expression of the C/EBP family member C/EBPε is regulated by PU.1. C/EBPε is a published protein-protein interaction partner of the PML protein as well (Tagata et al., 2008). The interaction of PU.1 and C/EBPε with the phosphorylated PML protein accelerates granulocyte differentiation and stimulates PU.1 dependent transcription. The interaction of sumoylated C/EBPα-TE-3 with the PML protein in the here presented study (Figure 5C) is intriguing, considering that C/EBPα is a part of a myeloid transcription cascade. C/EBPα is known to activate PU.1 gene transcription (Friedman et al., 2007; Fiedler et al., 2012). The PML protein interplay with the sumoylated C/EBPα-TE-3, PU.1 and C/EBPε and the given gene regulatory cascade from C/EBPα to PU.1 to C/EBPε are likely to be regarded in coherence to each other. Future research will have to clarify if the acceleration of granulocyte differentiation by means of the PML protein interaction with PU.1 and C/EBPε involves the interplay of the PML protein with the sumoylated C/EBPα as well.

A subtype of Acute myeloid leukemia (AML) is Acute promyeloid leukemia (APL). The main oncogenic characteristic of APL is the fusion protein PML-RARα (Puccetti et al., 2004). An effective treatment of APL is the administration of all trans retinoic acid (t-RA). C/EBPα colocalizes with PML-RARα in PML nuclear bodies in APL (Tenen et al., 2001). C/EBPα is generally not mutated in APL patients. Applying t-RA disrupts C/EBPα and PML-RARα colocalization. The interaction between PML-RARα and C/EBPα blocks C/EBPα induced granulopoiesis and can be reverted by C/EBPα expression suppressing cell proliferation and leading to partial cell differentiation (Truong et al., 2002). This is interesting, as increased presence of the non-sumoylated C/EBPα and decreased availability of sumoylated C/EBPα has been associated with terminal cell differentiation as well (Khanna-Gupta et al., 2008). The preferential binding of the PML protein to C/EBPα-TE3 via SUMO-1 (Figure 5C) suggests that the interaction of C/EBPα and PML-RARα may rely on SUMO-1 in APL as well.

The androgen receptor (AR) is a transcription factor that after interacting with its ligand testosterone binds to DNA at the androgen response element (Shaffer et al., 2004). ARIP4 is an ATP dependent DNA helicase that interacts with the AR (Rouleau et al., 2002). ARIP4 contains a SIM by which it interacts with a variety of sumoylated transcription factors (Ogawa et al., 2009). The recruitment of ARIP4 by sumoylated transcription factors has been suggested to coincide with transcriptional repression. ARIP4 interacts with the sumoylated C/EBPα-TE-3 (Figure 5C). Interestingly, C/EBPα plays a key role in repressing the AR transactivation, when AR is bound to its ligand (Chattopadhyay et al., 2006). C/EBPα does this by competing with AR coactivators for the binding to AR, while the AR binds to the androgen response element. C/EBPα competes with the AR coactivators ARA70, SRC-1, P300 and GRIP1 for AR binding. Moreover, the DNA-bound C/EBPα was stated to recruit the ligand independent AR in a transcriptionally activating manner to the C/EBP DNA-binding motif, too (Zhang et al., 2010). Yeast two-hybrid reporter experiments conducted by Zhang et al. showed that a C/EBPα R154A mutation diminishes the AR supported C/EBPα promotor activation. Interestingly, the survey of C/EBPα PTM pattern conducted in the here presented study revealed that C/EBPα R154 is monomethylated in vivo (Suppl. figure 1A; Figure 3E) suggesting that this arginine methylation may influence the AR dependent C/EBPα transactivation as well. The ARIP4 interplay with the sumoylated C/EBPα-TE-3 is intriguing, as it indicates that C/EBPα and AR may have

the common protein-protein interaction partner ARIP4 in a cellular context. Furthermore, the sumoylation dependent interaction of C/EBPα and the DNA helicase ARIP4 may affect C/EBPα transcriptsactivation capability as well, as shown for the interplay of ARIP4 with other transcription factors.

SENP1 and NUP358, the two other proteins detected to preferentially interact with the sumoylated C/EBPα-TE-3 have noteworthy enzymatic functions. SENP1 is a nuclear deconjugation enzyme that prepares the SUMO-1 precursor for conjugation and cleaves SUMO-1 from its sumoylated targets (Gong et al., 2000). SENP1 conducts its function in the nucleus and is detectable in PML nuclear bodies. SENP1 and SENP2 are cruicial for the localization of nucleoporins resulting in the formation of the nuclear pore complex (NPC) (Chow et al., 2013). NUP358, also known as RANBP2, is part of the NPC (Yokoyama et al., 1995). Apart from being a component of the cytoplasmic filament of the NPC, NUP358 is a SUMO-1 E3-ligase as well (Pichler et al., 2002). NUP358 contains a SIM essential for the binding of sumoylated RanGAP1 (Song et al., 2004). Moreover, NUP358 is part of a complex comprising the sumoylated RanGAP1 and UBC9 (Flotho et al., 2012). This complex is required for efficient nuclear import of protein cargo in collaboration with importins (Hutten et al., 2008). During mitosis this complex regulates the kinetochore assembly and the attachment of microtubules to kinetochores (Bukata et al., 2013). The sumoylation status of C/EBPα has been suggested to impact neutrophil development by affecting C/EBPα gene regulatory functions, such as the repression of the lactoferrin gene, a hallmark of immature neutrophils (Hankey et al., 2011). C/EBPα sumoylation status decreases during neutrophil maturation resulting in the increased expression of the lactorferrin gene. With the detection of SENP1 as a protein interaction partner of the sumoylated C/EBPα-TE-3 in this study (Figure 5C) an interesting relationship is disclosed. SENP1 is likely to be involved in C/EBPα functional status through desumoylation. The in this survey reported preferential binding of NUP358 to the sumoylated C/EBPα-TE-3 and not to non-sumoylated C/EBPα-TE-3 indicates that this protein-protein interplay is most likely not linked to the SUMO-1 E3-ligase activity of NUP358. In all likelihood, this sumoylation-governed interaction links C/EBPα either with the NUP358 mediated nucleoplasmic transport or the NUP358 guided mitotic activity. Both of these functions are feasible, as C/EBPα has to be shuttled into the nucleus to execute its gene regulatory functions and as C/EBPα belongs to the proteins known for their mitotic

bookmarking properties as well (Kadauke et al., 2013).

Summed up, the interaction pattern of the C/EBPα-TE-3 with the PML protein, ARIP4, SENP1 and NUP358 (Figure 5C) revealed the interaction of a sumoylated part of C/EBPα with published interation partners of SUMO-1 that are covalently modified by SUMO-1 themselves, harbor a SIM or are involved in sumoylation and desumoylation processes. Additional investigation is required to validate these interactions not only with a sumoylated C/EBPα-TE-3 but also with the fully expressed sumoylated C/EBPα to further strenghten the results of the here presented study. Furthermore, a non-covalently bound SUMO-1 control should be used as a control to distinguish the interaction pattern of the free SUMO-1 compared to the covalently to C/EBPα bound SUMO-1.

4.3 PrISMA a novel method to reveal PTM dependent interaction

PrISMa is a novel method to map C/EBPβ protein interaction network in a PTM dependent manner. By using PrISMa 372 published C/EBPβ interaction partners were mapped interacting with C/EBPβ peptide sequences (Suppl. figure 3-10; Suppl. table 1). The majority of these C/EBPβ protein interaction partners had not been mapped to C/EBPβ CRs and domains up until now. Moreover, PrISMa not only discloses the prime interaction site of these C/EBPβ protein interaction partners or protein complexes but also quantitatively reveals further C/EBPβ interaction motifs as well. By this PrISMa demonstrates that many of the published C/EBPβ proteins partners bind to multiple C/EBPβ amino acid sequences distributed amongst C/EBPβ CRs and domains. This is noteworthy, as the three C/EBPβ isoform (Figure 1) vary in length and have been shown to play different roles during cell proliferation, cell differentiation and in cancerous cell lines (Wethmar et al., 2010b).

With the PrISMa method a new method is presented. Peptide pull-downs in combination with shotgun proteomics have been used for detecting PTM dependent interactions. By using peptide pull-downs numerous histone mark readers were uncovered in recent years (Vermeulen

et al., 2010; Eberl et al., 2013). By introducing PrISMa a large scale high-throughput method is introduced that reveals mutliple-binding sites of proteins to specific amino acid motifs in a PTM dependent and quantitative manner using a peptide matrix. By selecting a label-free quantification (LFQ) approach and making use of MaxQuant a new method is presented in this study. Further advantages of PrISMa are the easy handling and that the incubation of single peptide matrix comes along with reduced handling variation during expermental procedures.

4.4 C/EBPβ and the interaction with the HATs P300 and CBP

The two HATs P300 and CBP are key enzymes recognized to play a decisive role in chromatin decondensation contributing to gene activation by disrupting nucleosome-nucleosome interaction by means of acetylation (Szerlong et al., 2010). P300 and CBP are conserved among species and share a high amino acid sequence overlap (Yuan et al., 2002). C/EBPβ and P300 are putative functional collaborators and protein-protein interaction partners (Mink et al., 1997). The P300 interaction with C/EBPβ is mediated via the P300 E1A binding region. The interaction of C/EBPβ and P300 prompts a transcriptionally activating phosphorylation of P300 (Schwartz et al., 2003).

With the aid of PrISMa C/EBPβ CR4 and CR3 were validated as the main and secondary C/EBP interaction motives for P300/CBP and further binding of these two HATs was detected for C/EBPβ peptides of C/EBPβ CR2 (P300/CBP) and CR1 (CBP) (Figure 9A-B). The C/EBPβ CR4 and CR3 amino acid sequences are published interaction motifs of C/EBPs cruicial for the cooperation with TBP, TF2B and P300/CBP (Nerlov et al., 1995; Kovács et al., 2003). Using PrISMa the citrullinated C/EBPβ R59 was identified to intensify the C/EBPβ interaction with P300 and CBP (Figure 9A-B). A mutational investigation of C/EBPβ arginine methylation sites conducted by the Leutz lab revealed that the chicken C/EBPβ R60A mutant (in rat C/EBPβ R59) exhibits an increased expression pattern of the *mim-1* gene (also referred to as *LECT2*) compared to non-mutated wild type C/EBPβ (Leutz et al., 2011). The *mim-1* gene is a granulocyte lineage specific gene induced by C/EBPβ transcription (Burk et al., 1993). The C/EBPβ R59 arginine

to alanine mutant (R59A) used by Leutz et al. was chosen as it does not have a positive charge in the amino acid side-chain and it cannot be methylated by PRMTs during gene expression experiments (Leutz et a., 2011). To address the transcriptional effects of the C/EBPβ R59 citrullination an arginine to glutamine mutation (R59Q) would be prefereable as glutamine in comparison to alanine has an amine in its side-chain, which is better suited in mimicking a charge-less deiminated arginine.

The same transcriptionally activating effect of the C/EBPβ R59A mutant on the *mim-1* gene expression is also observable with a chicken C/EBPβ R43A/R48A mutant (in rat C/EBPβ R42 and R46) (Leutz et al., 2011) suggesting an involvement of arginine methylation in the regulation of gene expression for these two arginines as well. As the chicken C/EBPβ R43 is a published target of methylation (Leutz et al., 2011) and the rat C/EBPβ R46 was detected to be methylated by this survey (Suppl. figure 11B) the modification of these two arginines was scrutinized for the involvement in the C/EBPβ P300 interaction. Pull-down experiments conducted with the C/EBPε peptides (Figure 10C) and the P300 Co-IPs of the wild type C/EBPβ and the R43L/R48L mutant (Figure 11B) demonstrate that the probed conserved C/EBP arginines impact the interaction with the transcriptional coactivators P300 and CBP significantly when modified.

Taken together, this study elucidated the methylation sensitivity of the C/EBPβ interaction with P300 and CBP indicating that the surveyed PTM pattern controls C/EBPβ transactivation capacity. Interestingly, C/EBPβ R43 and R48 are located in a LCR between C/EBPβ CR2 and CR3 (Suppl. figure 11C) where no C/EBPβ P300/CBP interaction was detected using PrISMa (Figure 9A-B). This is intriguing, as C/EBPβ is classified as an intrinsically disordered protein (Miller et al., 2009). Intrinsically disordered transcription factors have been suggested to rely on their structural convertibility to form transient but highly specific interactions with transcriptional cofactors. The stuctural convertibility of C/EBPβ has been associated with PTM dependent charge repulsion mechanisms (Lee et al., 2010c). These mechanisms interfere with C/EBPβ intraprotein interactions of the TAD and RD, which are managed by short α-helical sequences. The research of Lee et al. demonstrated that the C/EBPβ LAP-isoform N-terminus (amino acid 22-104) is auto-inhibited and is activated by phosphorylation via the Ras signaling pathway (Lee et al., 2010b). The C/EBPβ R43 and R48 methylation, examined in the here

presented study (Figure 10; Figure 11), may potentially lead to structural changes of C/EBPβ that abrogate the C/EBPβ P300/CBP interaction, which is predominatly mediated by the C/EBPβ CR4 and CR3 (Figure 9A-B). These two arginine methylations might possibly alter the transcriptionally activating effects of the C/EBPβ phosphorylation via the oncogenic Ras signaling pathway.

4.5 The mediator complex tightly connects C/EBPβ with the transcription machinery

The mediator complex is a multi-protein complex crucial for the transcription of RNA POL II complex regulated genes (Sato et al., 2004). C/EBPβ is linked to the RNA POL II complex and general transcription factors by interacting with the mediator complex (Mo et al., 2004). This interaction is either transcriptionally activating or repressive depending on the composition of the mediator complex (Eastburn et al., 2004). With the PrISMa approach it was possible to narrow down the specific amino acid sequences pivotal for the interaction with C/EBPβ (Figure 13). The twenty-five mediator complex components detected interacted mainly with peptides of C/EBPβ CR2, CR3 or CR4 (Figure 12). Among these twenty-five detected proteins, is the transcriptionally activating complex member MED26 and the transcriptionally repressive complex member CDK8. Moreover, by using PrISMa MED23 and MED1 were mapped to C/EBPβ peptide sequences as well. These two mediator complex members are published interaction partners of C/EBPβ (Mo et al., 2004; Li et al., 2008). A recent mass spectrometrical survey revealed fifteen members of the mediator complex (vide Suppl. table 1) interacting with C/EBPβ (Siersbæk et al., 2014). All of these fifteen mediator complex members were detected using PrISMa as well.

A remarkable feature of PrISMa is revealed by the detection of the mediator complex, that is that the mediator complex has several C/EBPβ amino acid sequences mainly distributed among the TAD CRs important for its binding. This suggests that more than one binding site is necessary for a stable complex interaction pattern. The mediator predominantly binds to C/EBPβ peptides of the TAD and only demonstrates marginal interaction with C/EBPβ RD

and bZIP domain. This is noteworthy, as only the two long C/EBPβ isoforms LAP* and LAP contain C/EBPβ TAD, CR5 and CR6, whereas the short C/EBPβ isoforms LIP is deprived of these domains (Figure 1). LIP is the putative transcriptionally repressive C/EBPβ isoform not only known to be the antagonist of the LAP* and LAP but also a prevalent isoform detected in a variety of cancer types (Wethmar et al., 2010b). The results of PrISMa suggest, that one of the reasons why LIP is the transcriptionally repressive C/EBPβ isoform is the lack of its interaction with the mediator complex.

4.6 C/EBPβ a partner of chromatin-remodeler and chromatin-modifier

Chromatin remodeling and chromatin PTMs are key requirements for the transcriptionally active transformation of the densely organized chromatin. The modification of chromatin is viewed as a sequential process during which specific transcription factors recruit chromatin-remodeling complexes to their recognition sites increasing nucleosome mobility leading to the recruitment of further transcription factors and pivotal histone modifying enzymes (Müller et al., 2001). C/EBPβ is an interaction platform for chromatin-remodeling and chromatin-modifying complexes. In a mass spectrometric survey, conducted by the lab of Gutiérrez, complex members of the INO80 complex, the TIP60 complex, the STAGA complex and the Mi2/NuRD complex were detected to interact with the C/EBPβ isoforms (Steinberg et al., 2012). Using the PrISMa method numerous members of these four complexes were detected binding to C/EBPβ peptides (Figure 15).

The members of the INO80 complex, the TIP60 complex and the STAGA complex were detected to interact preferentially with C/EBPβ peptides of the TAD, in particular covering the C/EBPβ CR3 and CR4 (Figure 15). The INO80 and TIP60 complex members RUVBL1, RUVBL2 and BAF53 vary in their C/EBPβ peptide interaction pattern. The maximal binding of RUVBL1, RUVBL2 and BAF53 to C/EBPβ peptides was detected in the LZ region. These three proteins are not only members of the INO80 complex and the TIP60 complex but are also

components of numerous other protein complexes (Jha et al., 2009; Park et al., 2002).

The INO80 complex is a highly conserved chromatin-remodeling complex important for the replacement of the histone dimers H2A-H2B with the histone dimers H2A.Z-H2B in nucleosomes (Jin et al., 2005). The INO80 complex is involved in transcriptional regulation and has been associated with DNA repair and checkpoint regulation (Vassileva et al., 2014; Bao et al., 2011). Intriguingly, all the by PrISMa detected members of the INO80 complex bind with a maximum to C/EBPβ peptides that contain a methylated arginine or a methylated lysine. Half of the detected INO80 members preferentially interacted with C/EBPβ peptides containing a methylated R59. A similar methylation dependency was uncovered by this survey for the interactions of the TIP60 complex members with C/EBPβ peptide sequences.

The TIP60 complex is a complex conserved from yeast to human associated with histone acetylation, regulation of transcription and DNA repair (Doyon et al., 2004). Apart from histone acetylation, the TIP60 complex is involved in the histone dimer exchange H2AZ-H2B as well (Auger et al., 2008).

The third complex detected with its members binding to C/EBPβ TAD is the STAGA complex. The STAGA complex is associated with chromatin modification, transcriptional regulation and DNA repair (Martinez et al., 2001). The STAGA complex member GCN5 is a histone acetyltransferase. GCN5 acetylates C/EBPβ at K99, K102 and K103 (Wiper-Bergeron et al., 2007). This acetylation is important for the glucocorticoid-stimulated differentiation of preadipocytes. Remarkably, with the help of PrISMa it was possible to reveal that GCN5 and half of the by PrISMa detected STAGA complex members bind to a C/EBPβ peptide sequence of the CR4 adjacent to the C/EBPβ lysines that GCN5 acetylates.

The members of the INO80 complex, TIP60 complex and STAGA complex mostly interact with C/EBPβ peptides of the TAD, whereas the members of the Mi2-NuRD complex preferentially interact with C/EBPβ peptide sequences of the bZIP (Figure 15). The Mi2-NuRD complex is putatively subdivided into the two subcomplexes, the MBD2/NuRD and the MBD3/NuRD subcomplex (Le Guezennec et al., 2006). The MBD2 protein contains a methyl cytosine-phosphate-guanine (mCpG) binding domain and is known to interact with mCpG islands, whereas the MBD3 protein has a non-functional mCpG-binding domain (Saito et al., 2002). The MBD2/NuRD bound promoters are in general transcriptionally inactive, whereas MBD3/NuRD bound promoters

are associated with transcriptional activation (Günther et al., 2013). One of the ways in that the Mi2/NuRD complex carries out its gene regulatory tasks, is by histone deacetylation via its complex members HDAC1 and HDAC2 (Bowen et al., 2004). The detection of the the MBD2/NuRD complex members with the PrISMA approach is intriguing, as the members of this repessive chromatin-remodeling and chromatin-modification complex interact with C/EBPβ LZ adjacent to C/EBPβ DNA binding domain. This C/EBPβ bZIP domain interaction suggests a close proximity of MBD2 to DNA in connection with C/EBPβ and potentially to mCpG islands as well. To further understand, how C/EBPβ interaction with the Mi2/NuRD complex is influenced by C/EBPβ structure, C/EBPβ Co-IPs were performed (Figure 16A-B). The experiments revealed that C/EBPβ RD is significantly involved in abrogating the interaction with the MBD3/NuRD complex, whereas C/EBPβ CR1 probably plays a decisive role in stabilizing the interaction of C/EBPβ with the MBD3/NuRD complex. Interestingly, the loss of C/EBPβ CR1 together with RD leads to a significant loss of C/EBPβ MBD3/NuRD interaction. These results are in agreement with mass spectrometric interaction screening performed by the Gutiérrez lab, which demonstrated that many of the Mi2/NuRD complex members show an increased interaction with the C/EBPβ LAP* isoform in comparison to the LAP isoform, whereas the LIP isoform comprising only the CR7 and the bZIP domain showed the least binding capacity to the Mi2/NuRD complex members (Steinberg et al., 2012).

The protein network C/EBPβ interacts with in the ALK+ALCL cell line SU-DHL-1 contained the chromatin-remodeling complex members CHD4 and MTA2 belonging to the Mi2/NuRD complex. Moreover, BRG1, SMARCC1, and MeCP2 members of the SWI/SNF chromatin-remodeling complex or the BRG1-based SWI/SNF chromatin-remodeling complex were identified as C/EBPβ interaction partners in SU-DHL-1. The SWI/SNF complex is a C/EBPβ interacting chromatin-remodeling complex pivotal for the activation of myeloid genes (Kowenz-Leutz et al., 1999). The Mi2/NuRD complex and the SWI/SNF complex are putatively recruited together during the inflammatory response of macrophages resulting in a delayed gene activation by the SWI/SNF complex due to the Mi2/NuRD complex influence (Ramirez-Carrozzi et al., 2006). C/EBPβ transactivation plays a part in the lymphoid transformation of the ALK+ALCL cell line SU-DHL-1 contributing to the transcription of genes associated with the Gene Ontology terms ´inflammatory response´, ´immune system response´ and ´cell

proliferation´ (Bonzheim et al., 2013).

4.7 C/EBPβ shuttling to and fro the nucleus

All proteins destined for the nucleus are subject of the nucleoplasmic transport. The nucleoplasmic traffic is a bidirectional transit through the nuclear pore complex (NPC) (Terry et al., 2007). Apart from the numerous NPC members, the import and export of the cargo to and fro the nucleus is highly regulated by importins, exportins and multiple co-factors. Sumoylation and desumoylation are processes that at least partly take place at the NPC closely connecting this modification with the nucleoplasmic transport (Zhang et al., 2002). The NUP358-RANGAP1*SUMO1-UBC9 complex is a sumoylation complex located at the NPC filaments (Flotho et al., 2012). By containing NUP358 this sumoylation complex contains a NPC member as well.

C/EBPβ functional duties are primarily located in the nucleus. C/EBPβ has a nuclear localization signal (NLS) and a nuclear export signal (NES) for efficiently being transported in and out of the nucleus (Williams et al., 1997, Buck et al., 2001b). With the PrISMa approach it was possible to map the NPC members, importins, exportins, the NUP358-RANGAP1*SUMO1-UBC9 complex and nucleoplasmic transport associated co-factors primarily to amino acid sequences of C/EBPβ CR7 and the LZ (Figure 14). This plethora of interaction is in more than one way formidable, as many of these mapped interactors have various cellular functions diverging from being an orifice or a nucleoplamic shuttle.

The importins interacting with C/EBPβ peptides can be separated into two groups either binding to PrISMa peptides of the C/EBPβ BA and DB or not binding to them (Figure 14). KPNA1, KPNA2, KPNA3 and KPNA4 belong to the C/EBPβ BA and DB interacting group. The C/EBPβ NLS is embedded in C/EBPβ BA and DB closely connecting these PrISMa interactions with C/EBPβ nuclear import. Moreover, of the proteins detected by PrISMA and classified as nucleoplasmic transport proteins only the members of the NUP358-RANGAP1*SUMO1-UBC9 complex show the same PrISMa interaction pattern to the C/EBPβ BA and DB like KPNA1-KPNA4. This is interesting, as NUP358-RANGAP1*SUMO1-UBC9 complex is required for the

efficient nuclear import of proteins by means of importins (Hutten et al., 2008).

The nuclear pore complex is a supramolecular structure that controls the traffic of mRNAs, nuclear proteins, ribosomal proteins, small nuclear ribonuleic proteins (snRNPs), transfer RNAs (tRNAs) and small nuclear RNAs (snRNAs) (Bagley et al., 2000). The basket like structure of the NPC is sectionalized into cytoplasmic nucleoporins and filaments, the outer ring nucleoporins, nuclear nucleoporins and basket, the central nucleoporins, the inner ring and linker nucleoporins and the transmembrane nucleoporins (Katta et al., 2013). By employing PrISMa members of all NPC sections were mapped to C/EBPβ amino acid sequences. Of the cytoplasmic nucleoporins and the filaments the already mentioned NUP358 is a NPC with diverse functions. In addition to the importance for effective protein import, the NUP358-RANGAP1*SUMO1-UBC9 complex plays a significant role in the kinetochore assembly during mitosis and depletion of NUP358 leads to mitotic cells with unaligned chromosomes (Joseph et al., 2004). Mutational alterations of NUP153, NUP88, ELYS, SEH1 and TPR are linked to defects in cytokinesis and in the appearance of multinucleated cells (Bukata et al., 2013). The kinetochore interaction of these NPC members is intriguing, as C/EBPβ is known to localize at the centromeres during mitotic clonal expansion of adipocytes leading to terminal cell differentiation (Tang et al., 1999). The nuclear pore complex promotes transcription by interacting with DNA gene recruitment sequences resulting in the alteration of the chromatin structure (Sood et al., 2014). Activated genes are drawn to the NPC where the interaction with transcription machinery takes place (Akhtar et al., 2007). Apart from the RNA POL II, chromatin-remodeling complexes interact with components of the NPC as well, for example the yeast homologue of the STAGA complex (Luthra et al., 2007). This is noteworthy, as the NUP358, RANGAP1 and UBC9 also significantly interact with the same the PrISMa C/EBPβ peptide of the CR4 that the members of the STAGA complex predominantly bind to (Figure 14; Figure 15).

KPNB1, KPNB2, NUP358, NUP93, NUP50, TPR, and XPO1 are significant C/EBPβ interaction partners in the SU-DHL-1 cell line. This abundance of proteins essential for the nucleoplasmic transport associated with C/EBPβ in SU-DHL-1 cells is remarkable. C/EBPβ expression is indispensable for the proliferation of the ALK+ALCL cell line SU-DHL-1 (Anastasov et al., 2010) suggesting that these identified C/EBPβ protein interaction partners might regulate mitotic events in SU-DHL-1 as well.

4.8 C/EBPβ and RNA processing proteins

Transactivation by means of transcription factors results in the production of mRNAs. Many of these mRNAs contain introns and are subjects of splicing or alternative splicing (Matera et al., 2014). A recent study conducted by the Mandrup lab elucidated that C/EBPβ interacts with RNA processing proteins belonging to the spliceosome and the 17S U2 snRNP complex (Siersbæk et al., 2014). By using PrISMa it was possible to map numerous members of RNA processing complexes to C/EBPβ peptide sequences (Suppl. figure 12; Suppl. figure 3-10). Apart from providing valuable insight into where these RNA processing proteins bind C/EBPβ, the PrISMa approach also broadens the understanding of the PTM dependency of these interactions. The family of tudor domain comprising proteins interacts with proteins modified by arginine or lysine methylation (Chen et al., 2011). SPF30 is a tudor domain containing protein that recognizes symmetrically dimethylated arginines (Côté et al., 2005). In this survey the 17S U2 snRNP complex member SPF30 interacted primarily with C/EBPβ peptides that contained the symmetrically dimethylated R280 (Figure 17A). Apart from SFP30, multiple other components of the 17S U2 snRNP complex interacted preferentially with C/EBPβ R280 when modified by methylation (Figure 17B).

This is intriguing, as the C/EBPβ protein interaction network in the ALK+ALCL cell line SU-DHL-1 revealed multiple C/EBPβ interaction partners belonging to the spliceosome, the C complex spliceosome and the 17S U2 snRNP complex. Especially, a large number of heterogeneous nuclear ribonucleoproteins (hnRNPs) were among the C/EBPβ protein interaction network in SU-DHL-1 cells. The hnRNPs contain RNA recognition motives and are essential components of splicing complexes (He et al., 2008). Furthermore, hnRNPs bind to DNA and regulate transcription as well. The SU-DHL-1 C/EBPβ interaction partner HNRNPK is a published C/EBPβ interactor known to repress C/EBPβ transactivation functions (Miau et al., 1998). The PrISMa survey and the C/EBPβ lymphomic protein interaction pattern in SU-DHL-1 closely connect C/EBPβ transactivation capacity with RNA processing in a PTM dependent

manner.

4.9 Concluding remarks and future directions

C/EBPα and C/EBPβ are two essential transcription factors important for the proliferation and differentiation of multiple tissue types. Murine studies have shown the lethal C/EBPα knockout can be rescued by expressing C/EBPβ from the *CEBPA* gene locus (Jones et al, 2002). This makes the results of this survey riveting, as the detected citrullination discovered by mass spectrometry for C/EBPα will doubtless not be an isolated case of a deiminase post-translationally modifying a C/EBP family member. Advances in cutting edge mass spectrometric technologies and more efficient ways to chemically modify citrullinated arginines for mass spectrometric analysis will substantiate the research on this transient modification. The protein-protein interaction pattern of the sumoylated C/EBPα with the PML protein is most interesting indicating a potential sojourn of the sumoylated C/EBPα in the PML nuclear bodies. Further studies on the C/EBPα subnuclear localization are necessary to elucidate this issue.

With the, in this study newly developed, PrISMa approach a new tool was applied not only to detect the interaction of complete protein networks with a transcription factor but also to perform this interaction screening in a PTM dependent fashion. This is a great advance in comparison to previous techniques, as the C/EBPβ peptide matrix comprises the complete C/EBPβ amino acid sequence in a tiled manner and numerous PTMs as well. The same rigor is applied to all the analysed peptide-protein interaction. Furthermore, the data evaluation by label-free quantification (LFQ) harnesses the computational power to quantify these peptide-protein interactions without having to introduce time-consuming and expensive mass spectrometric labeling techniques. The mapping of the 372 published C/EBPβ protein interaction partners, such as members of the mediator complex, chromatin-remodeling complexes, proteins involved in the nucleoplasmic transport and RNA processing proteins, to specific C/EBPβ amino acid sequences, opens up opportunities for further studies. Future studies can use the mapping of this survey to elucidate what effects this C/EBPβ protein interaction network has on C/EBPβ transactivation and cell proliferation.

The C/EBPα PTM sites discovered and verified by tandem mass spectrums and the PTM dependent interaction patterns of C/EBPα and C/EBPβ revealed by this study testifies that the protein interaction networks are significantly influenced by protein methytransferases and deiminases. Future studies will unravel how this C/EBPa and C/EBPβ fine-tuning by PTMs emerges in tissues and cancers. Lysine methyltransferase inhibitors have been used for preclinical and clinical trials for treating various cancer types (Copeland et al., 2013). Follow-up research could link the here reported C/EBPα PTMs with the quest for effective methyltransferase inhibitors. Furthermore, this study demonstrated that the arginine methylation of C/EBPβ TAD affects the interaction with the transcriptional coactivators P300/CBP. Future studies could also address PTM related questions by using cross-linking in combination with mass spectrometry to capture structural changes of the intrinsically disordered C/EBPβ. With the help of cross-linkers and mass spectrometry three-dimensional structural analysis of proteins and protein complexes has been performed (Chen et al., 2010). Future research could apply cross-linking in combination with mass spectrometry to reveal C/EBPβ intra- and intermolecular protein interactions to elucidate their involvement in the regulation of C/EBPβ transactivation properties.

This study shed light on C/EBPβ protein interaction network in the ALK+ALCL cell line SU-DHL-1 revealing many novel and published protein-protein interaction patners of C/EBPβ. Many of these significant C/EBPβ interactors were detected with PrISMa as well. In SU-DHL-1 cells C/EBPβ transactivation has been shown to be important for the proliferation of this cancer cell line (Bonzheim et al., 2013). A further survey could uncover how C/EBPβ protein interaction network influences the oncogenic character of C/EBPβ in this ALK+ALCL leading to a better understanding of how to target C/EBPβ by therapeutically manipulating its protein interaction network.

C/EBPα is a prominent oncogene in AML. The same PrISMa approach performed with a C/EBPβ peptide matrix is applicable for C/EBPα as well. Mapping C/EBPα interaction partners to specific C/EBPα amino acid sequences would elucidate how this AML oncogene is embedded into its own protein interaction network. Ten percent of all AML patients carry a mutation in the C/EBPα gene often-even biallelic mutations. This makes the mapping of C/EBPα protein interaction partners in a PTM dependent manner a pressing matter.

REFERENCES

Aebersold, R., & Mann, M. (2003). Mass spectrometry-based proteomics. *Nature*, *422*(6928), 198–207.

Akasaka, T., Balasas, T., Russell, L., Sugimoto, K., Majid, A., Walewska, R., et al. (2007). Five members of the CEBP transcription factor family are targeted by recurrent IGH translocations in B-cell precursor acute lymphoblastic leukemia (BCP-ALL). *Blood*, *109*(8), 3451.

Akhtar, A., & Gasser, S. M. (2007). The nuclear envelope and transcriptional control. *Nature Reviews Genetics*, *8*(7), 507–517.

Anastasov, N., Bonzheim, I., Rudelius, M., Klier, M., Dau, T., Angermeier, D., et al. (2010). C/EBP expression in ALK-positive anaplastic large cell lymphomas is required for cell proliferation and is induced by the STAT3 signaling pathway. *Haematologica*, *95*(5), 760–767.

Antonysamy, S., Bonday, Z., Campbell, R. M., Doyle, B., Druzina, Z., Gheyi, T., et al. (2012). Crystal structure of the human PRMT5:MEP50 complex. *Proceedings of the National Academy of Sciences*, *109*(44), 17960–17965.

Atwood, A. A., Jerrell, R., & Sealy, L. (2011). Negative regulation of C/EBPbeta1 by sumoylation in breast cancer cells. *PloS One*, *6*(9), e25205.

Auger, A., Galarneau, L., Altaf, M., Nourani, A., Doyon, Y., Utley, R. T., et al. (2008). Eaf1 Is the Platform for NuA4 Molecular Assembly That Evolutionarily Links Chromatin Acetylation to ATP - Dependent Exchange of Histone H2A Variants. *Molecular and Cellular Biology*, *28*(7), 2257–2270.

Baek, S. H. (2011). When Signaling Kinases Meet Histones and Histone Modifiers in the Nucleus. *Molecular Cell*, *42*(3), 274–284.

Bagley, S., Goldberg, M. W., Cronshaw, J. M., Rutherford, S., & Allen, T. D. (2000). The nuclear pore complex. *Journal of Cell Science*, *113 (Pt 22)*, 3885–3886.

Bantscheff, M., Schirle, M., Sweetman, G., Rick, J., & Kuster, B. (2007). Quantitative mass spectrometry in proteomics: a critical review. *Analytical and Bioanalytical Chemistry*, *389*(4), 1017–1031.

Bao, Y., & Shen, X. (2011). SnapShot: Chromatin Remodeling: INO80 and SWR1. *Cell*, *144*(1), 158–158.e2.

Baranello, L., Kouzine, F., & Levens, D. (2013). DNA Topoisomerases: Beyond the standard role. *Transcription*, *4*(5), 232–237.

Basu, S. K., Malik, R., Huggins, C. J., Lee, S., Sebastian, T., Sakchaisri, K., et al. (2011). 3′UTR elements inhibit Ras-induced C/EBPβ post-translational activation and senescence in tumour cells. *The EMBO Journal*, *30*(18), 3714–3728.

Bégay, V., Smink, J., & Leutz, A. (2004). Essential Requirement of CCAAT/Enhancer Binding Proteins in Embryogenesis. *Molecular and Cellular Biology*, *24*(22), 9744–9751.

Bégay, V., Smink, J., Loddenkemper, C., Zimmermann, K., Rudolph, C., Scheller, M., et al. (2015). Deregulation of the endogenous C/EBPβ LIP isoform predisposes to tumorigenesis. *Journal of Molecular Medicine (Berlin, Germany)*, *93*(1), 39–49.

Behre, G., Singh, S. M., Liu, H., Bortolin, L. T., Christopeit, M., Radomska, H. S., et al. (2002). Ras Signaling Enhances the Activity of C/EBPalpha to Induce Granulocytic Differentiation by Phosphorylation of Serine 248. *Journal of Biological Chemistry*, *277*(29), 26293–26299.

Bergalet, J., Fawal, M., Lopez, C., Desjobert, C., Lamant, L., Delsol, G., et al. (2011). HuR-Mediated Control of C/EBP mRNA Stability and Translation in ALK-Positive Anaplastic Large Cell Lymphomas. *Molecular Cancer Research*, *9*(4), 485–496.

Biterge, B., & Schneider, R. (2014). Histone variants: key players of chromatin. *Cell and Tissue Research*, *356*(3), 457–466.

Black, J. C., Van Rechem, C., & Whetstine, J. R. (2012). Histone Lysine Methylation Dynamics: Establishment, Regulation, and Biological Impact. *Molecular Cell*, *48*(4), 491–507.

Boisvert, F-M., Hendzel, M. J., & Bazett-Jones, D. P. (2000). Promyelocytic Leukemia (PML) Nuclear Bodies Are Protein Structuresthat Do Not Accumulate RNA. *The Journal of Cell Biology*, *148*, 283–292.

Bonzheim, I., Irmler, M., Klier-Richter, M., Steinhilber, J., Anastasov, N., Schäfer, S., et al. (2013). Identification of C/EBPβ Target Genes in ALK+ Anaplastic Large Cell Lymphoma (ALCL) by Gene Expression Profiling and Chromatin Immunoprecipitation. *PloS One*, *8*(5), e64544.

Bowen, N. J., Fujita, N., Kajita, M., & Wade, P. A. (2004). Mi-2/NuRD: multiple complexes for many purposes. *Biochimica Et Biophysica Acta*, *1677*(1-3), 52–57.

Brauchle, M., Yao, Z., Arora, R., Thigale, S., Clay, I., Inverardi, B., et al. (2013). Protein Complex Interactor Analysis and Differential Activity of KDM3 Subfamily Members Towards H3K9 Methylation. *PloS One*, *8*(4), e60549.

Buck, M., Poli, V., Chojkier, M., Mario Chojkier, A. T. H., & van der Geer, P. (1999). Phosphorylation of Rat Serine 105or Mouse Threonine 217 in C/EBP Is Required for Hepatocyte Proliferation Induced by TGF. *Molecular Cell*, 1–6.

Buck, M., Poli, V., Hunter, T., & Chojkier, M. (2001a). C/EBPbeta phosphorylation by RSK creates a functional XEXD caspase inhibitory box critical for cell survival. *Molecular Cell*, *8*(4), 807–816.

Buck, M., Zhang, L., Halasz, N., & Hunter, T. (2001b). Nuclear export of phosphorylated C/EBPβ mediatesthe inhibition of albumin expression by TNF. *EMBO Journal*, 1–12.

Bukata, L., Parker, S. L., & D'Angelo, M. A. (2013). Nuclear pore complexes in the maintenance of genome integrity. *Current Opinion in Cell Biology*, *25*(3), 378–386.

Burk, O., Mink, S., Ringwald, M., & Klempnauer, K. H. (1993). Synergistic activation of the chicken mim-1 gene by v-myb and C/EBP transcription factors. *EMBO Journal*, *12*(5), 2027–2038.

Calkhoven, C. F., Müller, C., & Leutz, A. (2000). Translational control of C/EBPalpha and C/EBPbeta isoform expression. *Genes & Development*, *14*(15), 1920–1932.

Cao, Z., Umek, R. M., & McKnight, S. L. (1991). Regulated expression of three C/EBP lsoforms during adipose conversion of 3T3-L1 cells. *Genes & Development*, *5*, 1538–1552.

Cesena, T. I., Cardinaux, J. R., Kwok, R., & Schwartz, J. (2007). CCAAT/Enhancer-binding Protein (C/EBP) β Is Acetylated at Multiple Lysines. *Journal of Biological Chemistry*, *282*(2), 956–967.

Chait, B. T. (2006). Chemistry. Mass spectrometry: bottom-up or top-down? *Science*, *314*(5796), 65–66.

Chang, C. J., Chen, Y. L., & Lee, S. C. (1998). Coactivator TIF1β interacts with transcription factor C/EBPβ and glucocorticoid receptor to induce α1-acid glycoprotein gene expression. *Molecular and Cellular Biology*, *18*(10), 5880–5887.

Chattopadhyay, S., Gong, E.-Y., Hwang, M., Park, E., Lee, H. J., Hong, C. Y., et al. (2006). The CCAAT Enhancer-Binding Protein-α Negatively Regulates the Transactivation of Androgen Receptor in Prostate Cancer Cells. *Molecular Endocrinology*, *20*(5), 984–995.

Chen, C., Nott, T. J., Jin, J., & Pawson, T. (2011). Deciphering arginine methylation: Tudor tells the tale. *Nature Reviews Molecular Cell Biology*, *12*(10), 629–642.

Chen, S.-S., Chen, J.-F., Johnson, P. F., Muppala, V., & Lee, H.-Y. (2000). C/EBPβ, When Expressed from the *C/ebp*α Gene Locus, Can Functionally Replace C/EBPα in Liver but Not in Adipose Tissue. *Molecular and Cellular Biology*, *20*(19), 7292–7299.

Chen, Z. A., Jawhari, A., Fischer, L., Buchen, C., Tahir, S., Kamenski, T., Rasmussen, M., Lariviere, L., Bukowski-Wills, J.C., Nilges, M. Cramer, P., & Rappsilber, J. (2010). Architecture of the RNA polymerase II-TFIIF complex revealed by cross-linking and mass spectrometry. *The EMBO Journal*, *29*(4), 717–726.

Choi, Y., Asada, S., & Uesugi, M. (2000). Divergent hTAFII31-binding Motifs Hidden in Activation Domains. *Journal of Biological Chemistry*, *275*(21), 15912–15916.

Chow, K. H., Elgort, S., Dasso, M., Powers, M. A., & Ullman, K. S. (2013). The SUMO proteases SENP1 and SENP2 play a critical role in nucleoporin homeostasis and nuclear pore complex function. *Molecular Biology of the Cell*, *25*(1), 160–168.

Cline, M. S., Smoot, M., Cerami, E., Kuchinsky, A., Landys, N., Workman, C., et al. (2007). Integration of biological networks and gene expression data using Cytoscape. *Nature Protocols*, *2*(10), 2366–2382.

Copeland, R. A. (2013). Molecular Pathways: Protein Methyltransferases in Cancer. *Clinical Cancer Research*, *19*(23), 6344–6350.

Côté, J., & Richard, S. (2005). Tudor Domains Bind Symmetrical Dimethylated Arginines. *Journal of Biological Chemistry*, *280*(31), 28476–28483.

Cox, J., Hein, M. Y., Luber, C. A., Paron, I., Nagaraj, N., & Mann, M. (2014). Accurate proteome-wide label-free quantification by delayed normalization and maximal peptide ratio extraction, termed MaxLFQ. *Molecular & Cellular Proteomics*, *13*(9), 2513–2526.

Cox, J., & Mann, M. (2008). MaxQuant enables high peptide identification rates, individualized ppb-range mass accuracies and proteome-wide protein quantification. *Nature Biotechnology*, *26*(12), 1367–1372.

De Ceuleneer, M., De Wit, V., Van Steendam, K., Van Nieuwerburgh, F., Tilleman, K., & Deforce, D. (2011). Modification of citrulline residues with 2, 3 butanedione facilitates their detection by liquid chromatography/mass spectrometry. *Rapid Communications in Mass Spectrometry : RCM*, *25*(11), 1536–1542.

Del Rizzo, P. A., & Trievel, R. C. (2014). Molecular basis for substrate recognition by lysine methyltransferases and demethylases. *BBA - Gene Regulatory Mechanisms*, 1–12.

De Ruijter, A. J. M., van Gennip, A. H., Caron, H. N., Kemp, S., & van Kuilenburg, A. B. P. (2003). Histone deacetylases (HDACs): characterization of the classical HDAC family. *The Biochemical Journal*, *370*(Pt 3), 737–749.

Descombes, P., & Schibler, U. (1991). A liver-enriched transcriptional activator protein, LAP, and a transcriptional inhibitory protein, LIP, are translated from the same mRNA. *Cell*, *67*(3), 569–579.

Deutsch, E. W., Lam, H., & Aebersold, R. (2008). PeptideAtlas: a resource for target selection for emerging targeted proteomics workflows. *EMBO Reports*, *9*(5), 429–434.

Dintilhac, A. (2001). HMGB1 Interacts with Many Apparently Unrelated Proteins by Recognizing Short Amino Acid Sequences. *Journal of Biological Chemistry*, *277*(9), 7021–7028.

Doyon, Y., & Côté, J. (2004). The highly conserved and multifunctional NuA4 HAT complex. *Current Opinion in Genetics & Development*, *14*(2), 147–154.

Dundr, M. (2012). Nuclear bodies: multifunctional companions of the genome. *Current Opinion in Cell Biology*, *24*(3), 415–422.

Eastburn, D., & Han, M. (2004). When Ras signaling reaches the mediator. *Developmental Cell*, *6*(2), 158–159.

Eaton, E. M., & Sealy, L. (2003). Modification of CCAAT/Enhancer-binding Protein-β by the Small Ubiquitin-like Modifier (SUMO) Family Members, SUMO-2 and SUMO-3. *Journal of Biological Chemistry*, *278*(35), 33416–33421.

Eberl, H. C., Spruijt, C. G., Kelstrup, C. D., Vermeulen, M., & Mann, M. (2013). A Map of General and Specialized Chromatin Readers in Mouse Tissues Generated by Label-free Interaction Proteomics. *Molecular Cell*, *49*(2), 368–378.

Fanis, P., Gillemans, N., Aghajanirefah, A., Pourfarzad, F., Demmers, J., Esteghamat, F., et al. (2012). Five Friends of Methylated Chromatin Target of Protein-Arginine-Methyltransferase[Prmt]-1 (Chtop), a Complex Linking Arginine Methylation to Desumoylation. *Molecular & Cellular Proteomics*, *11*(11), 1263–1273.

Fiedler, K., & Brunner, C. (2012). The role of transcription factors in the guidance of granulopoiesis. *American Journal of Blood Research*, *2*(1), 57–65.

Filippakopoulos, P., & Knapp, S. (2012). The bromodomain interaction module. *FEBS Letters*, *586*(17), 2692–2704.

Flotho, A., & Werner, A. (2012). The RanBP2/RanGAP1*SUMO1/Ubc9 complex: A multisubunit E3 ligase at the intersection of sumoylation and the RanGTPase cycle. *Nucleus*, *3*(5), 429–432.

Foti, D., Iuliano, R., Chiefari, E., & Brunetti, A. (2003). A Nucleoprotein Complex Containing Sp1, C/EBPβ, and HMGI-Y Controls Human Insulin Receptor Gene Transcription. *Molecular and Cellular Biology*, *23*(8), 2720–2732.

Freitas, N., & Cunha, C. (2009). Mechanisms and signals for the nuclear import of proteins. *Current Genomics*, *10*(8), 550–557.

Friedman, A. D. (2007). C/EBPalpha induces PU.1 and interacts with AP-1 and NF-kappaB to regulate myeloid development. *Blood Cells, Molecules, and Diseases*, *39*(3), 340–343.

Gaidzik, V., & Döhner, K. (2008). Prognostic implications of gene mutations in acute myeloid leukemia with normal cytogenetics. *Seminars in Oncology*, *35*(4), 346–355.

Gao, H., Lukin, K., Ramírez, J., Fields, S., Lopez, D., & Hagman, J. (2009). Opposing effects of SWI/SNF and Mi-2/NuRD chromatin remodeling complexes on epigenetic reprogramming by EBF and Pax5. *Proceedings of the National Academy of Sciences of the United States of America*, *106*(27), 11258–11263.

Gayatri, S., & Bedford, M. T. (2014). Readers of histone methylarginine marks. *BBA - Gene Regulatory Mechanisms*, *1839*(8), 702–710.

Geletu, M., Balkhi, M. Y., Peer Zada, A. A., Christopeit, M., Pulikkan, J. A., Trivedi, A. K., et al. (2007). Target proteins of C/EBP p30 in AML: C/EBP p30 enhances sumoylation of C/EBP p42 via up-regulation of Ubc9. *Blood*, *110*(9), 3301–3309.

Gevaert, K., Impens, F., Ghesquière, B., Van Damme, P., Lambrechts, A., & Vandekerckhove, J. (2008). Stable isotopic labeling in proteomics. *Proteomics*, *8*(23-24), 4873–4885.

Giambruno, R., Grebien, F., Stukalov, A., Knoll, C., Planyavsky, M., Rudashevskaya, E. L., et al. (2013). Affinity Purification Strategies for Proteomic Analysis of Transcription Factor Complexes. *Journal of Proteome Research*, *12*(9), 4018–4027.

Golebiowski, F., Matic, I., Tatham, M. H., Cole, C., Yin, Y., Nakamura, A., et al. (2009). System-Wide Changes to SUMO Modifications in Response to Heat Shock. *Science Signaling*, *2*(72), 1–12.

Gong, L. (2000). Differential Regulation of Sentrinized Proteins by a Novel Sentrin-specific Protease. *Journal of Biological Chemistry*, *275*(5), 3355–3359.

Graf, T., & Enver, T. (2009). Forcing cells to change lineages. *Nature*, *462*(7273), 587–594.

Gregoretti, I., Lee, Y.-M., & Goodson, H. V. (2004). Molecular Evolution of the Histone Deacetylase Family: Functional Implications of Phylogenetic Analysis. *Journal of Molecular Biology*, *338*(1), 17–31.

Günther, K., Rust, M., Leers, J., Boettger, T., Scharfe, M., Jarek, M., et al. (2013). Differential roles for MBD2 and MBD3 at methylated CpG islands, active promoters and binding to exon sequences. *Nucleic Acids Research*, *41*(5), 3010–3021.

Gutierrez, S., Javed, A., Tennant, D. K., van Rees, M., Montecino, M., Stein, G. S., et al. (2002). CCAAT/Enhancer-binding Proteins (C/EBP) and Activate Osteocalcin Gene Transcription and Synergize with Runx2 at the C/EBP Element to Regulate Bone-specific Expression. *Journal of Biological Chemistry*, *277*(2), 1316–1323.

Hakimi, M.-A., Bochar, D. A., Schmiesing, J. A., Dong, Y., Barak, O. G., Speicher, D. W., et al. (2002). A chromatin remodelling complex that loads cohesin onto human chromosomes. *Nature*, *418*(6901), 994–998.

Hankey, W., Silver, M., Sun, B. S. H., Zibello, T., Berliner, N., & Khanna-Gupta, A. (2011). Differential effects of sumoylation on the activities of CCAAT enhancer binding protein alpha (C/EBPα) p42 versus p30 may contribute in part, to aberrant C/EBPα activity in acute leukemias. *Hematology Reports (Formerly Hematology Reviews)*, *3*(1), e5.

Hasserjian, R. P. (2013). Acute myeloid leukemia: advances in diagnosis and classification. *International Journal of Laboratory Hematology*, *35*(3), 358–366.

He, Y., & Smith, R. (2008). Nuclear functions of heterogeneous nuclear ribonucleoproteins A/B. *Cellular and Molecular Life Sciences : CMLS*, *66*(7), 1239–1256.

Huang, D. W., Sherman, B. T., & Lempicki, R. A. (2008). Systematic and integrative analysis of large gene lists using DAVID bioinformatics resources. *Nature Protocols*, *4*(1), 44–57.

Hubner, N., & Mann, M. (2011). Extracting gene function from protein-protein interactions using Quantitative BAC InteraCtomics (QUBIC). *Methods*, *53*, 453–459.

Hutten, S., Flotho, A., Melchior, F., & Kehlenbach, R. H. (2008). The Nup358-RanGAP Complex Is Required for Efficient Importin α/β -dependent Nuclear Import. *Molecular Biology of the Cell*, *19*(5), 2300–2310.

Ikura, T., Ogryzko, V. V., Grigoriev, M., Groisman, R., Wang, J., Horikoshi, M., et al. (2000). Involvement of the TIP60 histone acetylase complex in DNA repair and apoptosis. *Cell*, *102*(4), 463–473.

Ishihama, Y., Rappsilber, J., Andersen, J., & Mann, M. (2002). Microcolumns with self-assembled particle frits for proteomics. *Journal of Chromatography A*, *979*(1-2), 233–239.

Iwasaki, H., Somoza, C., Shigematsu, H., Duprez, E. A., Iwasaki-Arai, J., Mizuno, S.-I., et al. (2005). Distinctive and indispensable roles of PU.1 in maintenance of hematopoietic stem cells and their differentiation. *Blood*, *106*(5), 1590–1600.

Jeganathan, K. B., Baker, D., & van Deursen, J. M. (2006). Securin Associates with APC*Cdh1 in Promethaphase but its Destruction is Delayed by Rae1 and Nup 98 until the Metaphase/Anaphase Transititon. *Cell Cycle, 5*(4), 366–370.

Jha, S., & Dutta, A. (2009). RVB1/RVB2: Running Rings around Molecular Biology. *Molecular Cell*, *34*(5), 521–533.

Jiang, K., Hein, N., Eckert, K., Luscher-Firzlaff, J., & Luscher, B. (2008). Regulation of the MAD1 promoter by G-CSF. *Nucleic Acids Research*, *36*(5), 1517–1531.

Jin, J., Cai, Y., Yao, T., Gottschalk, A. J., FLORENS, L., Swanson, S. K., et al. (2005). A Mammalian Chromatin Remodeling Complex with Similarities to the Yeast INO80 Complex. *Journal of Biological Chemistry*, *280*(50), 41207–41212.

Johnson, P. F. (2005). Molecular stop signs: regulation of cell-cycle arrest by C/EBP transcription factors. *Journal of Cell Science*, *118*(12), 2545–2555.

Johnson, P. F., & McKnight, S. L. (1989). Eukaryotic transcriptional regulatory proteins. *Annual Review of Biochemistry*, *58*, 799–839.

Jones, H., Carver, M., & Pekala, P. H. (2007). HuR binds to a single site on the C/EBPbeta mRNA of 3T3-L1 adipocytes. *Biochemical and Biophysical Research Communications*, *355*(1), 217–220.

Jones, L. C., Lin, M.-L., Chen, S.-S., Krug, U., Hofmann, W.-K., Lee, S., et al. (2002). Expression of C/EBPbeta from the C/ebpalpha gene locus is sufficient for normal hematopoiesis in vivo. *Blood*, *99*(6), 2032–2036.

Joseph, J., Liu, S.-T., Jablonski, S. A., Yen, T. J., & Dasso, M. (2004). The RanGAP1-RanBP2 Complex Is Essential for Microtubule-Kinetochore Interactions In Vivo. *Current Biology*, *14*(7), 611–617.

Jurica, M. S., Licklider, L. J., Gygi, S. R., Grigorieff, N., & Moore, M. J. (2002). Purification and characterization of native spliceosomes suitable for three-dimensional structural analysis. *RNA (New York, NY)*, *8*(4), 426–439.

Katta, S. S., Smoyer, C. J., & Jaspersen, S. L. (2013). Destination: inner nuclear membrane. *Trends in Cell Biology*, 1–9.

Kadauke, S., & Blobel, G. A. (2013). Mitotic bookmarking by transcription factors. *Epigenetics & Chromatin*, *6*(1), 1–1.

Khanna-Gupta, A. (2008). Sumoylation and the function of CCAAT enhancer binding protein alpha (C/EBP [alpha]). *Blood Cells, Molecules, and Diseases*, *41*(1), 77–81.

Ki, S. H., Cho, I. J., Choi, D. W., & Kim, S. G. (2005). Glucocorticoid receptor (GR)-associated SMRT binding to C/EBPβ TAD and Nrf2 Neh4/5: role of SMRT recruited to GR in GSTA2 gene repression. *Molecular and Cellular Biology*, *25*(10), 4150–4165.

Kim, J., Cantwell, C., Johnson, P., Pfarr, C., & Williams, S. (2002). Transcriptional activity of CCAAT/enhancer-binding proteins is controlled by a conserved inhibitory domain that is a target for sumoylation. *Journal of Biological Chemistry*, *277*(41), 38037.

Klose, R. J., & Zhang, Y. (2007). Regulation of histone methylation by demethylimination and demethylation. *Nature Reviews Molecular Cell Biology*, *8*(4), 307–318.

Kong, X., Ball, A. R., Pham, H. X., Zeng, W., Chen, H. Y., Schmiesing, J. A., et al. (2014). Distinct Functions of Human Cohesin-SA1 and Cohesin-SA2 in Double-Strand Break Repair. *Molecular and Cellular Biology*, *34*(4), 685–698.

Kouzarides, T. (2007). Chromatin Modifications and Their Function. *Cell*, *128*(4), 693–705.

Kovacs, K. A. (2003). CCAAT/Enhancer-binding Protein Family Members Recruit the Coactivator CREB-binding Protein and Trigger Its Phosphorylation. *Journal of Biological Chemistry*, *278*(38), 36959–36965.

Kowenz-Leutz, E., & Leutz, A. (1999). A C/EBP beta isoform recruits the SWI/SNF complex to activate myeloid genes. *Molecular Cell*, *4*(5), 735–743.

Kowenz-Leutz, E., Pless, O., Dittmar, G., Knoblich, M., & Leutz, A. (2010). Crosstalk between C/EBP. *The EMBO Journal*, *29*(6), 1105–1115.

Kowenz-Leutz, E., Twamley, G., Ansieau, S., & Leutz, A. (1994). Novel mechanism of C/EBP beta (NF-M) transcriptional control: activation through derepression. *Genes & Development*, *8*(22), 2781–2791.

Laiosa, C. V., Stadtfeld, M., & Graf, T. (2006). DETERMINANTS OF LYMPHOID-MYELOID LINEAGE DIVERSIFICATION. *Annual Review of Immunology*, *24*(1), 705–738.

Lallemand-Breitenbach, V., & de The, H. (2010). PML Nuclear Bodies. *Cold Spring Harbor Perspectives in Biology*, *2*(5), a000661–a000661.

Lamb, J., Ramaswamy, S., Ford, H. L., Contreras, B., Martinez, R. V., Kittrell, F. S., et al. (2003). A mechanism of cyclin D1 action encoded in the patterns of gene expression in human cancer. *Cell*, *114*(3), 323–334.

Lange, V., Picotti, P., Domon, B., & Aebersold, R. (2008). Selected reaction monitoring for quantitative proteomics: a tutorial. *Molecular Systems Biology*, *4*, 222.

Le Guezennec, X., Vermeulen, M., Brinkman, A. B., Hoeijmakers, W. A. M., Cohen, A., Lasonder, E., & Stunnenberg, H. G. (2006). MBD2/NuRD and MBD3/NuRD, two distinct complexes with different biochemical and functional properties. *Molecular and Cellular Biology*, *26*(3), 843–851.

Lee, K. K., & Workman, J. L. (2007). Histone acetyltransferase complexes: one size doesn't fit all. *Nature Reviews Molecular Cell Biology*, *8*(4), 284–295.

Lee, S. H., Krisanapun, C., & Baek, S. J. (2010a). NSAID-activated gene-1 as a molecular target for capsaicin-induced apoptosis through a novel molecular mechanism involving GSK3 , C/EBP and ATF3. *Carcinogenesis*, *31*(4), 719–728.

Lee, S., Miller, M., Shuman, J. D., & Johnson, P. F. (2010b). CCAAT/Enhancer-binding protein beta DNA binding is auto-inhibited by multiple elements that also mediate association with p300/CREB-binding protein (CBP). *Journal of Biological Chemistry*, *285*(28), 21399–21410.

Lee, S., Shuman, J. D., Guszczynski, T., Sakchaisri, K., Sebastian, T., Copeland, T. D., et al. (2010c). RSK-Mediated Phosphorylation in the C/EBP Leucine Zipper Regulates DNA Binding, Dimerization, and Growth Arrest Activity. *Molecular and Cellular Biology*, *30*(11), 2621–2635.

Leutz, A., Pless, O., Lappe, M., Dittmar, G., & Kowenz-Leutz, E. (2011). Crosstalk between phosphorylation and multi-site arginine/lysine methylation in C/EBPs. *Transcription*, *2*(1), 3–8.

Li, H., Gade, P., Nallar, S. C., Raha, A., Roy, S. K., Karra, S., et al. (2008). The Med1 Subunit of Transcriptional Mediator Plays a Central Role in Regulating CCAAT/Enhancer-binding Protein- -driven Transcription in Response to Interferon. *Journal of Biological Chemistry*, *283*(19), 13077–13086.

Lin, F., MacDougald, O., Diehl, A., & Lane, M. (1993). A 30-kDa alternative translation product of the CCAAT/enhancer binding protein alpha message: transcriptional activator lacking antimitotic activity. *Proceedings of the National Academy of Sciences of the United States of America*, *90*(20), 9606.

Lincoln, A. J., Monczak, Y., Williams, S. C., & Johnson, P. F. (1998). Inhibition of CCAAT/Enhancer-binding Protein α and β Translation by Upstream Open Reading Frames. *Journal of Biological Chemistry*, *273*(16), 9552–9560.

Liu, H.-K., Perrier, S., Lipina, C., Finlay, D., McLauchlan, H., Hastie, C. J., et al. (2006). Functional characterisation of the regulation of CAAT enhancer binding protein alpha by GSK-3 phosphorylation of Threonines 222/226. *BMC Molecular Biology*, *7*(1), 14.

Liu, Qingbin (2012). Post-Translational Modification on Arginine and Function of CCAAT/Enhancer Binding Protein α. Dissertation Humboldt-Universität zu Berlin, *http://edoc.hu-berlin.de/dissertationen/liu-qingbin-2012-06-05/PDF/liu.pdf*.

Lopez, R. G., Garcia-Silva, S., Moore, S. J., Bereshchenko, O., Martinez-Cruz, A. B., Ermakova, O., et al. (2009). C/EBPα and β couple interfollicular keratinocyte proliferation arrest to commitment and terminal differentiation. *Nature Cell Biology*, *11*(10), 1181–1190.

Mahoney, C. W., Shuman, J. D., McKnight, S. L., Chen, H.-C., & Huang, K.-P. (1992). Phosphorylation of CCAAT-enhancer Binding Protein by Protein Kinase C Attenuates Site-selective DNA Binding. *Journal of Biological Chemistry*, 1–8.

Mann, M. (2006). Functional and quantitative proteomics using SILAC. *Nature Reviews Molecular Cell Biology*, *7*(12), 952–958.

Martin, A., Ochagavia, M. E., Rabasa, L. C., Miranda, J., Fernandez-de-Cossio, J., & Bringas, R. (2010). BisoGenet: a new tool for gene network building, visualization and analysis. *BMC Bioinformatics*, *11*(1), 91.

Martinez, E., Palhan, V. B., Tjernberg, A., Lymar, E. S., Gamper, A. M., Kundu, T. K., et al. (2001). Human STAGA Complex Is a Chromatin-Acetylating Transcription Coactivator That Interacts with Pre-mRNA Splicing and DNA Damage-Binding Factors In Vivo. *Molecular and Cellular Biology*, *21*(20), 6782–6795.

Marx, V. (2013). Targeted proteomics. *Nature Methods*, *10*(1), 19–22.

Matera, A. G., & Wang, Z. (2014). A day in the life of the spliceosome. *Nature Reviews Molecular Cell Biology*, *15*(2), 108–121.

Mattaj, I. W., & Englmeier, L. (1998). Nucleocytoplasmic transport: the soluble phase. *Annual Review of Biochemistry*, *67*, 265–306.

Maytin, V. E., & Habener, J. F. (1998). Transcription Factors C/EBPα, C/EBPβ, and CHOP (Gadd153) Expressed During the Differentiation Program of Keratinocytes In Vitro and In Vivo. *The Journal of Investigative Dermatology*, *110*, 238–246.

Mencía, M., & de Lorenzo, V. (2004). Functional transplantation of the sumoylation machinery into Escherichia coli. *Protein Expression and Purification*, *37*(2), 409–418.

Miau, L. H., Chang, C. J., Shen, B. J., Tsai, W. H., & Lee, S. C. (1998). Identification of Heterogeneous Nuclear Ribonucleoprotein K (hnRNP K) as a Repressor of C/EBPβ-mediated Gene Activation. *Journal of Biological Chemistry*, *273*(17), 10784–10791.

Miau, L. H., Chang, C. J., Tsai, W. H., & Lee, S. C. (1997). Identification and characterization of a nucleolar phosphoprotein, Nopp140, as a transcription factor. *Molecular and Cellular Biology*, *17*(1), 230–239.

Michalopoulos, G. (2014). Terminating hepatocyte proliferation during liver regeneration: The roles of two members of the same family (C/EBP α and β) with opposing actions. *Hepatology*, Accepted Article.

Miller, M., Shuman, J., Sebastian, T., Dauter, Z., & Johnson, P. (2003). Structural basis for DNA recognition by the basic region leucine zipper transcription factor CCAAT/enhancer-binding protein α. *Journal of Biological Chemistry*, *278*(17), 15178.

Miller, M. (2009). The importance of being flexible: the case of basic region leucine zipper transcriptional regulators. *Current Protein & Peptide Science*, *10*(3), 244–269.

Mink, S., Haenig, B., & Klempnauer, K. H. (1997). Interaction and functional collaboration of p300 and C/EBPβ. *Molecular and Cellular Biology*, *17*(11), 6609–6617.

Mo, X., Kowenz-Leutz, E., Xu, H., & Leutz, A. (2004). Ras induces mediator complex exchange on C/EBP beta. *Molecular Cell*, *13*(2), 241–250.

Mohanan, S., Cherrington, B. D., Horibata, S., McElwee, J. L., Thompson, P. R., & Coonrod, S. A. (2012). Potential Role of Peptidylarginine Deiminase Enzymes and Protein Citrullination in Cancer Pathogenesis. *Biochemistry Research International*, *2012*(5), 1–11.

Mowen, K. A., & David, M. (2014). Unconventional post-translational modifications in immunological signaling. *Nature Immunology*, *15*(6), 512–520.

Müller, C., Bremer, A., Schreiber, S., Eichwald, S., & Calkhoven, C. F. (2010). Nucleolar retention of a translational C/EBPα isoform stimulates rDNA transcription and cell size. *The EMBO Journal*, *29*(5), 897–909.

Müller, C., Calkhoven, C. F., Sha, X., & Leutz, A. (2004). The CCAAT enhancer-binding protein alpha (C/EBPalpha) requires a SWI/SNF complex for proliferation arrest. *The Journal of Biological Chemistry*, *279*(8), 7353–7358.

Müller, C., & Leutz, A. (2001). Chromatin remodeling in development and differentiation. *Current Opinion in Genetics & Development*, *11*(2), 167–174.

Nakajima, T., Kinoshita, S., Sasagawa, T., Sasaki, K., Naruto, M., Kishimoto, T., & Akira, S. (1993). Phosphorylation at threonine-235 by a ras-dependent mitogen-activated protein kinase cascade is essential for transcription factor NF-IL6. *Proceedings of the National Academy of Sciences of the United States of America*, *90*(6), 2207–2211.

Nerlov, C., & Ziff, E. (1994). Three levels of functional interaction determine the activity of CCAAT/enhancer binding protein-α on the serum albumin promoter. *Genes & Development*, *8*, 350–362.

Nerlov, C., & Ziff, E. (1995). CCAAT/enhancer binding protein-alpha amino acid motifs with dual TBP and TFIIB binding ability co-operate to activate transcription in both yeast and mammalian cells. *EMBO Journal*, *14*(17), 4318–4328.

Nilsson, T., Mann, M., Aebersold, R., Yates, J. R., Bairoch, A., & Bergeron, J. J. M. (2010). Mass spectrometry in high-throughput proteomics: ready for the big time. *Nature Methods*, *7*(9), 681–685.

Ogawa, H., Komatsu, T., Hiraoka, Y., & Morohashi, K.-I. (2009). Transcriptional Suppression by Transient Recruitment of ARIP4 to Sumoylated nuclear receptor Ad4BP/SF-1. *Molecular Biology of the Cell*, *20*(19), 4235–4245.

Ossipow, V., Descombes, P., & Schibler, U. (1993). CCAAT/enhancer-binding protein mRNA is translated into multiple proteins with different transcription activation potentials. *Proceedings of the National Academy of Sciences of the United States of America*, *90*(17), 8219–8223.

Pal, S., & Sif, S. (2007). Interplay between chromatin remodelers and protein arginine methyltransferases. *Journal of Cellular Physiology*, *213*(2), 306–315.

Papamichos-Chronakis, M., Watanabe, S., Rando, O. J., & Peterson, C. L. (2011). Global Regulation of H2A.Z Localization by the INO80 Chromatin-Remodeling Enzyme Is Essential for Genome Integrity. *Cell*, *144*(2), 200–213.

Park, J., Wood, M. A., & Cole, M. D. (2002). BAF53 Forms Distinct Nuclear Complexes and Functions as a Critical c-Myc-Interacting Nuclear Cofactor for Oncogenic Transformation. *Molecular and Cellular Biology*, *22*(5), 1307–1316.

Paz-Priel, I., & Friedman, A. (2011). C/EBPα dysregulation in AML and ALL. *Critical Reviews in Oncogenesis*, *16*(1-2), 93–102.

Pedersen, T. A., Bereshchenko, O., Garcia-Silva, S., Ermakova, O., Kurz, E., Mandrup, S., et al. (2007). Distinct C/EBPalpha motifs regulate lipogenic and gluconeogenic gene expression in vivo. *EMBO Journal*, *26*(4), 1081–1093.

Pedersen, T. A., Kowenz-Leutz, E., Leutz, A., & Nerlov, C. (2001). Cooperation between C/EBPalpha TBP/TFIIB and SWI/SNF recruiting domains is required for adipocyte differentiation. *Genes & Development*, *15*(23), 3208–3216.

Pek, J. W., Anand, A., & Kai, T. (2012). Tudor domain proteins in development. *Development*, *139*(13), 2255–2266.

Pichler, A., Gast, A., Seeler, J.-S., Dejean, A., & Melchior, F. (2002). The nucleoporin RanBP2 has SUMO1 E3 ligase activity. *Cell*, *108*(1), 109–120.

Picotti, P., & Aebersold, R. (2012). Selected reaction monitoring–based proteomics: workflows, potential, pitfalls and future directions. *Nature Methods*, *9*(6), 555–566.

Picotti, P., Rinner, O., Stallmach, R., Dautel, F., Farrah, T., Domon, B., et al. (2010). High-throughput generation of selected reaction-monitoring assays for proteins and proteomes. *Nature Methods*, *7*(1), 43–46.

Piwien-Pilipuk, G., Van Mater, D., Ross, S. E., MacDougald, O. A., & Schwartz, J. (2001). Growth hormone regulates phosphorylation and function of CCAAT/enhancer-binding protein beta by modulating Akt and glycogen synthase kinase-3. *The Journal of Biological Chemistry*, *276*(22), 19664–19671.

Pless, O., Kowenz-Leutz, E., Knoblich, M., Lausen, J., Beyermann, M., Walsh, M. J., & Leutz, A. (2008). G9a-mediated lysine methylation alters the function of CCAAT/enhancer-binding protein-beta. *The Journal of Biological Chemistry*, *283*(39), 26357–26363.

Porse, B. T., Pedersen, T. A., Xu, X., Lindberg, B., Wewer, U. M., Fritis-Hansen, L., & Nerlov, C. (2001). E2F Repression by C/EBPα Is Required for Adipogenesis and Granulopoiesis In Vivo. *Cell*, 1–12.

Poss, Z. C., Ebmeier, C. C., & Taatjes, D. J. (2013). The Mediator complex and transcription regulation. *Critical Reviews in Biochemistry and Molecular Biology*, *48*(6), 575–608.

Puccetti, E., & Ruthardt, M. (2004). Acute promyelocytic leukemia: PML/RARα and the leukemic stem cell. *Leukemia*, *18*(7), 1169–1175.

Puchades, M., Westman, A., Blennow, K., & Davidsson, P. (1999). Removal of sodium dodecyl sulfate from protein samples prior to matrix-assisted laser desorption/ionization mass spectrometry. *Rapid Communications in Mass Spectrometry : RCM*, *13*(5), 344–349.

Quintanilla-Martinez, L., Pittaluga, S., Miething, C., Klier, M., Rudelius, M., Davies-Hill, T., et al. (2006). NPM-ALK-dependent expression of the transcription factor CCAAT/enhancer binding protein beta in ALK-positive anaplastic large cell lymphoma. *Blood*, *108*(6), 2029–2036.

Radomska, H. S., Bassères, D. S., Zheng, R., Zhang, P., Dayaram, T., Yamamoto, Y., et al. (2006). Block of C/EBP alpha function by phosphorylation in acute myeloid leukemia with FLT3 activating mutations. *The Journal of Experimental Medicine*, *203*(2), 371–381.

Ramirez-Carrozzi, V. R., Nzarian, A. A., Li, C. C., Gore, S. L., Sridharan, R., Imbalzano, A. N., & Smale, S. T. (2006). Selective and antagonistic functions of SWI/SNF and Mi-2beta nucleosome remodeling complexes during an inflammatory response. *Genes & Development*, *20*(3), 282–296.

Rappsilber, J. (2001). SPF30 Is an Essential Human Splicing Factor Required for Assembly of the U4/U5/U6 Tri-small Nuclear Ribonucleoprotein into the Spliceosome. *Journal of Biological Chemistry*, *276*(33), 31142–31150.

Rappsilber, J., Mann, M., & Ishihama, Y. (2007). Protocol for micro-purification, enrichment, pre-fractionation and storage of peptides for proteomics using StageTips. *Nature Protocols*, *2*(8), 1896–1906.

Rasala, B. A., Orjalo, A. V., Shen, Z., Briggs, S., & Forbes, D. J. (2006). ELYS is a dual nucleoporin/kinetochore protein required for nuclear pore assembly and proper cell division. *Proceedings of the National Academy of Sciences of the United States of America*, *103*(47), 17801–17806.

Rask, K., Thörn, M., Pontén, F., Kraaz, W., Sundfeldt, K., Hedin, L., & Enerbäck, S. (2000). Increased expression of the transcription factors CCAAT-Enhancer Binding Proteins-β (C/EBPβ) and C/EBPζ (CHOP) correlate with invasiveness of human colorectal cancer. *Int. J. Cancer*, *86*, 337–343.

Refsland, E. W., Stenglein, M. D., Shindo, K., Albin, J. S., Brown, W. L., & Harris, R. S. (2010). Quantitative profiling of the full APOBEC3 mRNA repertoire in lymphocytes and tissues: implications for HIV-1 restriction. *Nucleic Acids Research*, *38*(13), 4274–4284.

Ribbeck, K., Lipowsky, G., Kent, H. M., Stewart, M., & Görlich, D. (1998). NTF2 mediates nuclear import of Ran. *EMBO Journal*, *17*(22), 6587–6598.

Rooney, J. W., & Calame, K. L. (2001). TIF1beta functions as a coactivator for C/EBPβ and is required for induced differentiation in the myelomonocytic cell line U937. *Genes & Development*, *15*(22), 3023–3038.

Rothbart, S. B., & Strahl, B. D. (2014). Biochimica et Biophysica Acta. *BBA - Gene Regulatory Mechanisms*, *1839*(8), 627–643.

Rouleau, N., Domans'kyi, A., Reeben, M., Moilanen, A.-M., Havas, K., Kang, Z., et al. (2002). Novel ATPase of SNF2-like protein family interacts with androgen receptor and modulates androgen-dependent transcription. *Molecular Biology of the Cell*, *13*(6), 2106–2119.

Ruepp, A., Waegele, B., Lechner, M., Brauner, B., Dunger-Kaltenbach, I., Fobo, G., et al. (2009). CORUM: the comprehensive resource of mammalian protein complexes--2009. *Nucleic Acids Research*, *38*(Database), D497–D501.

Saito, M., & Ishikawa, F. (2002). The mCpG-binding domain of human MBD3 does not bind to mCpG but interacts with NuRD/Mi2 components HDAC1 and MTA2. *The Journal of Biological Chemistry*, *277*(38), 35434–35439.

Sato, S., Tomomori-Sato, C., Parmely, T. J., Florens, L., Zybailov, B., Swanson, S. K., et al. (2004). A Set of Consensus Mammalian Short Article Mediator Subunits Identified byMultidimensional Protein Identification Technology. *Molecular Cell*, *14*(5), 685–691.

Sato, Y. (2006). Sumoylation of CCAAT/Enhancer-binding Protein and Its Functional Roles in Hepatocyte Differentiation. *Journal of Biological Chemistry*, *281*(31), 21629–21639.

Schaefer, M. H., Fontaine, J.-F., Vinayagam, A., Porras, P., Wanker, E. E., & Andrade-Navarro, M. A. (2012). HIPPIE: Integrating Protein Interaction Networks with Experiment Based Quality Scores. *PloS One*, *7*(2), e31826.

Schmidt, D., Wilson, M. D., Ballester, B., Schwalie, P. C., Brown, G. D., Marshall, A., et al. (2010). Five-Vertebrate ChIP-seq Reveals the Evolutionary Dynamics of Transcription Factor Binding. *Science*, *328*(5981), 1036–1040.

Schnatbaum, K., Zerweck, J., Nehmer, J., Wenschuh, H., Schutkowski, M., & Reimer, U. (2011). Application notes. *Nature Methods*, *8*(3), i–ii.

Schreiber, E., Matthias, P., Müller, M. M., & Schaffner, W. (1989). Rapid detection of octamer bining proteins with "mini-extracts," prepared from a small number of cells. *Nucleic Acids Research*, *17*(15), 6419.

Schwartz, C., Beck, K., Mink, S., Schmolke, M., Budde, B., Wenning, D., & Klempnauer, K.-H. (2003). Recruitment of p300 by C/EBPbeta triggers phosphorylation of p300 and modulates coactivator activity. *EMBO Journal*, *22*(4), 882–892.

Screpanti, I., Romani, L., Musiani, P., Modesti, A., Fattori, E., Lazzaro, D., et al. (1995). Lymphoproliferative disorder and imbalanced T-helper response in C/EBP beta-deficient mice. *The EMBO Journal*, *14*(9), 1932–1941.

Sebastian, T., Malik, R., Thomas, S., Sage, J., & Johnson, P. F. (2005). C/EBPbeta cooperates with RB:E2F to implement Ras(V12)-induced cellular senescence. *EMBO Journal*, *24*(18), 3301–3312.

Seeler, J.-S., & Dejean, A. (2003). Nuclear and unclear functions of SUMO. *Nature Reviews Molecular Cell Biology*, *4*(9), 690–699.

Shaffer, P. L., Jivan, A., Dollins, D. E., Claessens, F., & Gewirth, D. T. (2004). Structural basis of androgen receptor binding to selective androgen response elements. *Proceedings of the National Academy of Sciences of the United States of America*, *101*(14), 4758–4763.

Shen, F., Li, N., Gade, P., Kalvakolanu, D. V., Weibley, T., Doble, B., et al. (2009). IL-17 Receptor Signaling Inhibits C/EBP by Sequential Phosphorylation of the Regulatory 2 Domain. *Science Signaling*, *2*(59), ra8–ra8.

Shen, T. H., Lin, H.-K., Scaglioni, P. P., Yung, T. M., & Pandolfi, P. P. (2006). The mechanisms of PML-nuclear body formation. *Molecular Cell*, *24*(3), 331–339.

Shi, Y. (2007). Histone lysine demethylases: emerging roles in development, physiology and disease. *Nature Reviews Genetics*, *8*(11), 829–833.

Shuman, J. D., Sebastian, T., Kaldis, P., Copeland, T. D., Zhu, S., Smart, R. C., & Johnson, P. F. (2004). Cell cycle-dependent phosphorylation of C/EBPbeta mediates oncogenic cooperativity between C/EBPbeta and H-RasV12. *Molecular and Cellular Biology*, *24*(17), 7380–7391.

Siersbæk, R., Rabiee, A., Nielsen, R., Sidoli, S., Traynor, S., Loft, A., et al. (2014). Transcription Factor Cooperativityin Early Adipogenic Hotspots and Super-Enhancers. *CellReports*, 1–13.

Slamova, L., Starkova, J., Fronkova, E., Zaliova, M., Reznickova, L., van Delft, F. W., et al. (2014). CD2-positive B-cell precursor acute lymphoblastic leukemia with an early switch to the monocytic lineage. *Leukemia*, *28*(3), 609–620.

Slomiany, B. A., D'Arigo, K. L., Kelly, M. M., & Kurtz, D. T. (2000). C/EBPalpha inhibits cell growth via direct repression of E2F-DP-mediated transcription. *Molecular and Cellular Biology*, *20*(16), 5986–5997.

Smits, A. H., Jansen, P. W. T. C., Poser, I., Hyman, A. A., & Vermeulen, M. (2012). Stoichiometry of chromatin-associated protein complexes revealed by label-free quantitative mass spectrometry-based proteomics. *Nucleic Acids Research*, *41*(1), e28–e28.

Song, J., Durrin, L. K., Wilkinson, T. A., Krontiris, T. G., & Chen, Y. (2004). Identification of a SUMO-binding motif that recognizes SUMO-modified proteins. *Proceedings of the National Academy of Sciences of the United States of America*, *101*(40), 14373–14378.

Sood, V., & Brickner, J. H. (2014). ScienceDirectNuclear pore interactions with the genome. *Current Opinion in Genetics & Development*, *25*, 43–49.

Spagnolo, L., Rivera-Calzada, A., Pearl, L. H., & Llorca, O. (2006). Three-Dimensional Structure of the Human DNA-PKcs/Ku70/Ku80 Complex Assembled on DNA and Its Implications for DNA DSB Repair. *Molecular Cell*, *22*(4), 511–519.

Steinberg, X. P., Hepp, M. I., Fernández García, Y., Suganuma, T., Swanson, S. K., Washburn, M., et al. (2012). Human CCAAT/Enhancer-Binding Protein β Interacts with Chromatin Remodeling Complexes of the Imitation Switch Subfamily. *Biochemistry*, *51*(5), 952–962.

Sterneck, E., Tessarollo, L., & Johnson, P. F. (1997). An essential role for C/EBPbeta in female reproduction. *Genes & Development*, *11*(17), 2153–2162.

Stoilova, B., Kowenz-Leutz, E., Scheller, M., & Leutz, A. (2013). Lymphoid to Myeloid Cell Trans-Differentiation Is Determined by C/EBPβ Structure and Post-Translational Modifications. *PloS One*, *8*(6), e65169.

Subramanian, L. (2003). A Synergy Control Motif within the Attenuator Domain of CCAAT/Enhancer-binding Protein alpha Inhibits Transcriptional Synergy through Its PIASy-enhanced Modification by SUMO-1 or SUMO-3. *Journal of Biological Chemistry*, *278*(11), 9134–9141.

Swaminathan, S. (2004). RanGAP1*SUMO1 is phosphorylated at the onset of mitosis and remains associated with RanBP2 upon NPC disassembly. *The Journal of Cell Biology*, *164*(7), 965–971.

Swygert, S. G., & Peterson, C. L. (2014). Biochimica et Biophysica Acta. *BBA - Gene Regulatory Mechanisms*, *1839*(8), 728–736.

Szerlong, H. J., Prenni, J. E., Nyborg, J. K., & Hansen, J. C. (2010). Activator-dependent p300 acetylation of chromatin in vitro: enhancement of transcription by disruption of repressive nucleosome-nucleosome interactions. *The Journal of Biological Chemistry*.

Szklarczyk, D., Franceschini, A., Kuhn, M., Simonovic, M., Roth, A., Minguez, P., et al. (2010). The STRING database in 2011: functional interaction networks of proteins, globally integrated and scored. *Nucleic Acids Research*, *39*(Database), D561–D568.

Tagata, Y., Yoshida, H., Nguyen, L. A., Kato, H., Ichikawa, H., Tashiro, F., & Kitabayashi, I. (2008). Phosphorylation of PML is essential for activation of C/EBP epsilon and PU.1 to accelerate granulocytic differentiation. *Leukemia*, *22*(2), 273–280.

Takayama, K., Kawabata, K., Nagamoto, Y., Inamura, M., Ohashi, K., Okuno, H., et al. (2013). CCAAT/enhancer binding protein-mediated regulation of TGF receptor 2 expression determines the hepatoblast fate decision. *Development*, *141*(1), 91–100.

Tanaka, T., Tanaka, T., Akira, S., Akira, S., Yoshida, K., Yoshida, K., et al. (1995). Targeted disruption of the NF-IL6 gene discloses its essential role in bacteria killing and tumor cytotoxicity by macrophages. *Cell*, *80*(2), 353–361.

Tang, Q.-Q., & Lane, M. D. (1999). Activation and centromeric localization of CCAAT/enhancer-binding proteins during the mitotic clonal expansion of adipocyte differentiation. *Genes & Development*, *13*(17), 2231–2241.

Tang, Q.-Q., & Lane, M. D. (2012). Adipogenesis: From Stem Cell to Adipocyte. *Annual Review of Biochemistry*, *81*(1), 715–736.

Tenen, D. G. (2001). Abnormalities of the CEBP alpha transcription factor: a major target in acute myeloid leukemia. *Leukemia*, *15*(4), 688–689.

Terry, L. J., Shows, E. B., & Wente, S. R. (2007). Crossing the Nuclear Envelope: Hierarchical Regulation of Nucleocytoplasmic Transport. *Science*, *318*(5855), 1412–1416.

The UniProt Consortium. (2013). Activities at the Universal Protein Resource (UniProt). *Nucleic Acids Research*, *42*(D1), D191–D198.

Tran, E. J., & Wente, S. R. (2006). Dynamic Nuclear Pore Complexes: Life on the Edge. *Cell*, *125*(6), 1041–1053.

Trautwein, C., van der Geer, P., Karin, M., Hunter, T., & Chojkier, M. (1994). Protein kinase A and C site-specific phosphorylations of LAP (NF-IL6) modulate its binding affinity to DNA recognition elements. *The Journal of Clinical Investigation*, *93*(6), 2554–2561.

Truong, B. T. H., Lee, Y.-J., Lodie, T. A., Park, D., Perrotti, D., Watanabe, N., et al. (2002). CCAAT/Enhancer binding proteins repress the leukemic phenotype of acute myeloid leukemia. *Blood*, *101*(3), 1141–1148.

Tsukada, J., Yoshida, Y., Kominato, Y., & Auron, P. E. (2011). The CCAAT/enhancer (C/EBP) family of basic-leucine zipper (bZIP) transcription factors is a multifaceted highly-regulated system for gene regulation. *Cytokine*, 1–14.

Varier, R. A., & Timmers, H. T. M. (2011). Histone lysine methylation and demethylation pathways in cancer. *BBA - Reviews on Cancer*, *1815*(1), 75–89.

Vassileva, I., Yanakieva, I., Peycheva, M., Gospodinov, A., & Anachkova, B. (2014). The mammalian INO80 chromatin remodeling complex is required for replication stress recovery. *Nucleic Acids Research*, *42*(14), 9074–9086.

Vermeulen, M., Eberl, H. C., Matarese, F., Marks, H., Denissov, S., Butter, F., et al. (2010). Quantitative interaction proteomics and genome-wide profiling of epigenetic histone marks and their readers. *Cell*, *142*(6), 967–980.

Wang, G. Z., Delva, L., Gaboli, M., Rivi, R., Giorgio, M., Cordon-Cardo, C., et al. (1998). Role of PML in Cell Growth and the Retinoic Acid Pathway. *Science*, *279*(5356), 1547–1551.

Wang, G.-L., Iakova, P., Wilde, M., Awad, S., & Timchenko, N. A. (2004). Liver tumors escape negative control of proliferation via PI3K/Akt-mediated block of C/EBP alpha growth inhibitory activity. *Genes & Development*, *18*(8), 912–925.

Wang, G. L., & Timchenko, N. A. (2005). Dephosphorylated C/EBP Accelerates Cell Proliferation through Sequestering Retinoblastoma Protein. *Molecular and Cellular Biology*, *25*(4), 1325–1338.

Wang, H., Iakova, P., Wilde, M., Welm, A., Roesler, W. J., & Timchenko, N. A. (2001). C/EBPα Arrests Cell Proliferationthrough Direct Inhibition of Cdk2 and Cdk4. *Molecular Cell*, *8*, 817–828.

Wang, N. D., Finegold, M. J., Bradley, A., Ou, C. N., Abdelsayed, S. V., Wilde, M. D., et al. (1995). Impaired energy homeostasis in C/EBP alpha knockout mice. *Science*, *269*(5227), 1108–1112.

Wang, S., & Wang, Y. (2013). Peptidylarginine deiminases in citrullination, gene regulation, health and pathogenesis. *Biochemica Et Biophysica Acta*, *1829*(10), 1126–1135.

Weber, M., Sydlik, C., Quirling, M., Nothdurfter, C., Zwergal, A., Heiss, P., et al. (2003). Transcriptional Inhibition of Interleukin-8 Expression in Tumor Necrosis Factor-tolerant Cells: EVIDENCE FOR INVOLVEMENT OF C/EBPβ. *Journal of Biological Chemistry*, *278*(26), 23586–23593.

Wegner, M., Cao, Z., & Rosenfeld, M. (1992). Calcium-Regulated Phosphorylation within the Leucine Zipper of C/EBP beta. *Science*, *256*, 370–373.

Wessel, D., & Flügge, U. I. (1984). A method for the quantitative recovery of protein in dilute solution in the presence of detergents and lipids. *Analytical Biochemistry*, *138*(1), 141–143.

Wethmar, K., Bégay, V., Smink, J. J., Zaragoza, K., Wiesenthal, V., Dörken, B., et al. (2010a). C/EBPbetaDeltauORF mice--a genetic model for uORF-mediated translational control in mammals. *Genes & Development*, *24*(1), 15–20.

Wethmar, K., Smink, J. J., & Leutz, A. (2010b). Upstream open reading frames: Molecular switches in (patho)physiology. *BioEssays: News and Reviews in Molecular, Cellular and Developmental Biology*, *32*, 885–893.

Will, C. L., Urlaub, H., Acel, T., Gentzel, M., Wilm, M., & Lührmann, R. (2002). Characterization of novel SF3b and 17S U2 snRNP proteins, including a human Prp5p homologue and an SF3b DEAD-box protein. *EMBO Journal*, *21*(18), 4978–4988.

Williams, S. C., Angerer, N. D., & Johnson, P. F. (1997). C/EBP proteins contain nuclear localization signals imbedded in their basic regions. *Gene Expression*, *6*(6), 371–385.

Wiper-Bergeron, N., Salem, H. A., Tomlinson, J. J., Wu, D., & Haché, R. J. G. (2007). Glucocorticoid-stimulated preadipocyte differentiation is mediated through acetylation of C/EBPbeta by GCN5. *Proceedings of the National Academy of Sciences of the United States of America*, *104*(8), 2703–2708.

Wozniak, G. G., & Strahl, B. D. (2014). Biochimica et Biophysica Acta. *BBA - Gene Regulatory Mechanisms*, 1–9.

Xia, C., Cheshire, J., Patel, H., & Woo, P. (1997). Cross-talk Between Transcription Factors NF-KB and C/EBP in the Transcriptional Regulation of Genes, 1–15.

Xie, H., Ye, M., Feng, R., & Graf, T. (2004). Stepwise reprogramming of B cells into macrophages. *Cell*, *117*(5), 663–676.

Xu, M., Nie, L., Kim, S.-H., & Sun, X.-H. (2003). STAT5-induced Id-1 transcription involvesrecruitment of HDAC1 and deacetylation of C/EBPβ. *The EMBO Journal*, *22*(4), 893–904.

Yamada, H. Y. (2014). Human Tip60 (NuA4) Complex and Cancer. *Intechopen*, 1–25.

Yan, S., & Willis, J. (2013). WD40-repeat protein WDR18 collaborates with TopBP1 to facilitate DNA damage checkpoint signaling. *Biochemical and Biophysical Research Communications*, *431*(3), 466–471.

Yokoyama, N., Hayashi, N., Seki, T., Panté, N., Ohba, T., Nishii, K., et al. (1995). A giant nucleopore protein that binds Ran/TC4. *Nature*, *376*(6536), 184–188.

Yoshida, H., Ichikawa, H., Tagata, Y., Katsumoto, T., Ohnishi, K., Akao, Y., et al. (2007). PML-Retinoic Acid Receptor α Inhibits PML IV Enhancement of PU.1-Induced C/EBPε Expression in Myeloid Differentiation. *Molecular and Cellular Biology*, *27*(16), 5819–5834.

Yuan, L. W., & Giordano, A. (2002). Acetyltransferase machinery conserved in p300/CBP-family proteins. *Oncogene*, *21*(14), 2253–2260.

Zahnow, C. A. (2002). CCAAT/enhancer binding proteins in normal mammary development and breast cancer. *Breast Cancer Research*, *4*(3), 113–121.

Zahnow, C. A. (2009). CCAAT/enhancer-binding protein β: its role in breast cancer and associations with receptor tyrosine kinases. *Expert Reviews in Molecular Medicine*, *11*, e12.

Zeng, L., & Zhou, M. M. (2002). Bromodomain: an acetyl-lysine binding domain. *FEBS Letters*, *513*(1), 124–128.

Zhang, D. E., Zhang, P., Wang, N. D., Hetherington, C. J., Darlington, G. J., & Tenen, D. G. (1997). Absence of granulocyte colony-stimulating factor signaling and neutrophil development in CCAAT enhancer binding protein alpha-deficient mice. *Proceedings of the National Academy of Sciences of the United States of America*, *94*(2), 569–574.

Zhang, H., Saitoh, H., & Matunis, M. J. (2002). Enzymes of the SUMO Modification Pathway Localize to Filaments of the Nuclear Pore Complex. *Molecular and Cellular Biology*, *22*(18), 6498–6508.

Zhang, J., Gonit, M., Salazar, M. D., Shatnawi, A., Shemshedini, L., Trumbly, R., & Ratnam, M. (2010). C/EBPα redirects androgen receptor signaling through a unique bimodal interaction. *Oncogene*, *29*(5), 723–738.

Zhou, Z., Licklider, L. J., Gygi, S. P., & Reed, R. (2002). Comprehensive proteomic analysis of the human spliceosome. *Nature*, *419*(6903), 182–185.

Zolotukhin, A. S. (2001). U2AF Participates in the Binding of TAP (NXF1) to mRNA. *Journal of Biological Chemistry*, *277*(6), 3935–3942.

Zubarev, R. A., & Makarov, A. (2013). Orbitrap Mass Spectrometry. *Analytical Chemistry*, *85*(11), 5288–5296.

Zwergal, A., Quirling, M., Saugel, B., Huth, K. C., Sydlik, C., Poli, V., et al. (2006). C/EBPβ blocks p65 phosphorylation and thereby NF-κB-mediated transcription in TNF-tolerant cells. *Journal of Immunology, 177*(1), 665–672.

ABBREVIATIONS

5FMC	Five friends of methylated Chtop complex
ABC	Ammoniumbicarbonate
ACN	Acetonitrile
AHB	4-alkoxy-2-hydroxybenzaldehyde
ALK+ALCL	ALK positive Anaplastic Large Cell Lymphoma
ALCL	Anaplastic Large Cell Lymphoma
AML	Acute myeloid leukemia
APL	Acute promyeloid leukemia
AR	Androgen receptor
a-Ra	All trans retinoic acid
AU-rich	Adenylate-uridylate-rich
BA	Pre-bZip basic/acidic region
bZIP	Basic leucine zipper
CE	Collision energy
C/EBP	CCAAT/enhancer-binding protein
C/EBPα Ext	C/EBPα extended isoform
C/EBPε-Rme2as	C/EBPε TAD containing two asymmetrically dimethylated arginines
Co-IP	Co-immunoprecipitation
CP	C-terminal peptide
CR	Conserved regions
Da	Dalton
DB	DNA binding region

DMEM	Dulbecco´s modified Eagle medium
DMF	Dimethylformamide
DNA	Deoxyribonucleic acid
DTT	Dithiothreitol
ESI	Electrospray ionization
FA	Formic acid
fc	Fold change
FDR	False discovery rate
FBS	Fetal bovine serum
Fmoc	Fluorenylmethyloxycarbonyl
fmol	Femtomol
FORK	Fork region
GO	Gene ontology
HAT	Histone acetyltransferase
HCD	Higher-energy collisional dissociation
HDAC	Histone deacetylase
HPLC	High performance liquid chromatography
ID	Peptide identification
KMT	Lysine methyltransferase
LC	Liquid chromatography
LC-MS	Liquid chromatographyÐmass spectrometry
LCR	Low complexity region
LFQ	Label-free quantification
Lys-C	Lysyl endopeptidase
LZ	Leucine zipper
M	Molar
mCpG	Methyl cytosine-phosphate-guanine

min	Minute
mM	Millimolar
mRNA	Messenger ribonucleic acid
MS1	Peptide mass-to-charge ratio scan
MS2	Peptide fragmention spectra
msec	Milliseconds
m/z	Mass-to-charge ratio
NES	Nuclear export signal
nl	Nanoliters
NLS	Nuclear localization signal
NPC	Nuclear pore complex
PADI	Protein-arginine deiminase
pH	Power of hydrogen
PML	Promyelocytic leukemia
ppm	Parts per million
PrISMa	Protein Interaction Screen on peptide Matrices
PRMT	Protein arginine methyltransferase
PTM	Posttranslational modification
PyBOB	Benzotriazol-1-yl-oxytripyrrolidinophosphonium-hexafluorophosphat
Q1	First quadrupole
Q2	Second quadrupole
Q3	Third quadrupole
QQQ	Triple quadrupole mass spectrometer
RD	Regulatory domain
RNA	Ribonucleic acid
rpm	Revolutions per minute

SDS	Sodium dodecyl sulfate
SILAC	Stable isotope labeling by amino acids in cell culture
SIM	Sumo interaction motif
snRNA	Small nuclear ribonucleic acid
snRNP	Small nuclear ribonuleic protein
SRM	Selected reaction monitoring
StageTip	Stop-and-go-extraction tip
SUMO-1	Small ubiquitin-related modifier 1
TAD	Transactivation domain
TE-1	Transactivation domain 1
TE-2	Transactivation domain 2
TE-3	Transactivation domain 3
TFA	Trifluoroacetic acid
Th	Thomson
TRIS	Tris-(hydroxymethyl)-aminomethan
tRNA	Transfer ribonucleic acid
uORF	Upstream open reading frame
UTR	Untranslated region
V	Volt

List of Figures

List of Tables

SUPPLEMENT

Supplemental figure 1: C/EBPα is modified in vivo by arginine methylation and lysine acetylation. A) Tandem mass spectrum of a C/EBPα R154 monomethylation. Indicated are the y- and b-series of the triptically cleaved peptide. A mass shift of 14 Da is marked with ´me´ for the modification at position R154. B) Tandem mass spectrum of a C/EBPα R323 monomethylation. Indicated are the y- and b-series of the tryptically cleaved peptide. A mass shift of 14 Da is marked with ´me´ for the modification at position R323. C) Tandem mass spectrum of a C/EBPα K280 methylation. Indicated are the y- and b-series of the tryptically cleaved peptide. A mass shift of 42 Da is marked with ´ac´ for the modification at position K280.

A

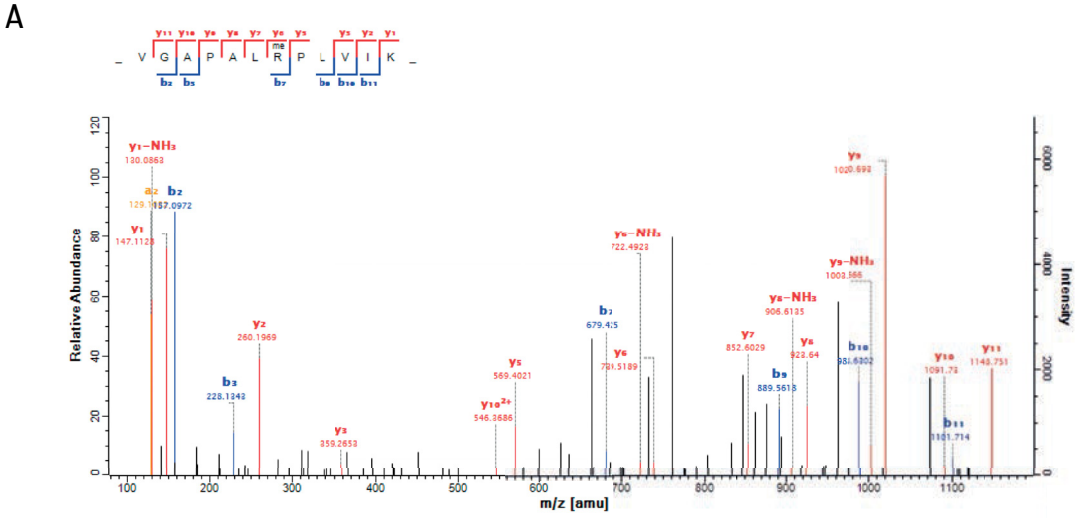
_ V G A P A L R P L V I K _
Relative Abundance
m/z [amu]
Intensity

B

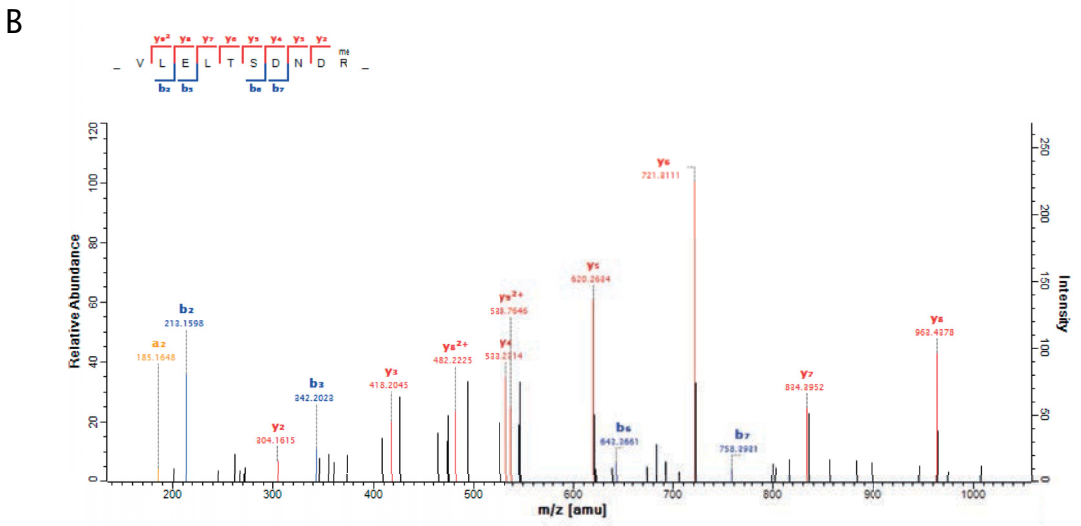
_ V L E L T S D N D R _
Relative Abundance
m/z [amu]
Intensity

C

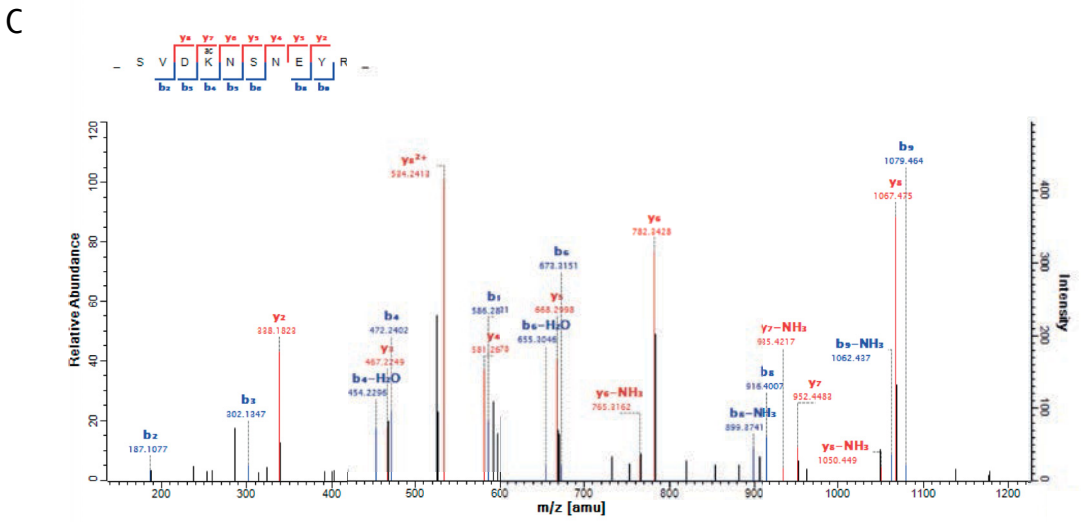
_ S V D K N S N E Y R _
Relative Abundance
m/z [amu]
Intensity

Supplemental figure 2: Heatmap of all 2459 proteins detected using PrISMa sorted by hierarchical clustering. Heatmap of normalized LFQ intensities of all 2459 proteins detected binding to C/EBPβ peptide sequences clustered with a Euclidian clustering algorithm. On the top left is the color key for the normalized LFQ values ranging from black to red (black, blue, green, yellow, red). On top of the heatmap the clustering dendrogram is depicted. On the left next to the heatmap the C/EBPβ peptide amino acid sequences corresponding to each row of the heatmap are annotated containing abbreviations for the PTMs. The PTMs accounted for are symmetric arginine dimethylation (Rme2sym), asymmetric arginine dimethylation (Rme2as), arginine citrullination (Rcit), lysine monomethylation (Kme), lysine dimethylation (Kme2), lysine trimethylation (Kme3), lysine acetylation (Kac), serine phosphorylation (Sphos), threonine phosphorylation (Tphos) and tyrosine phosphorylation (Yphos). On the left next to the heatmap a schematic representation of C/EBPβ LAP* isoform depicts the CRs and bZIP domain in a color code. On the far left the C/EBPβ amino acid sequence for the complete LAP* isoform is annotated.

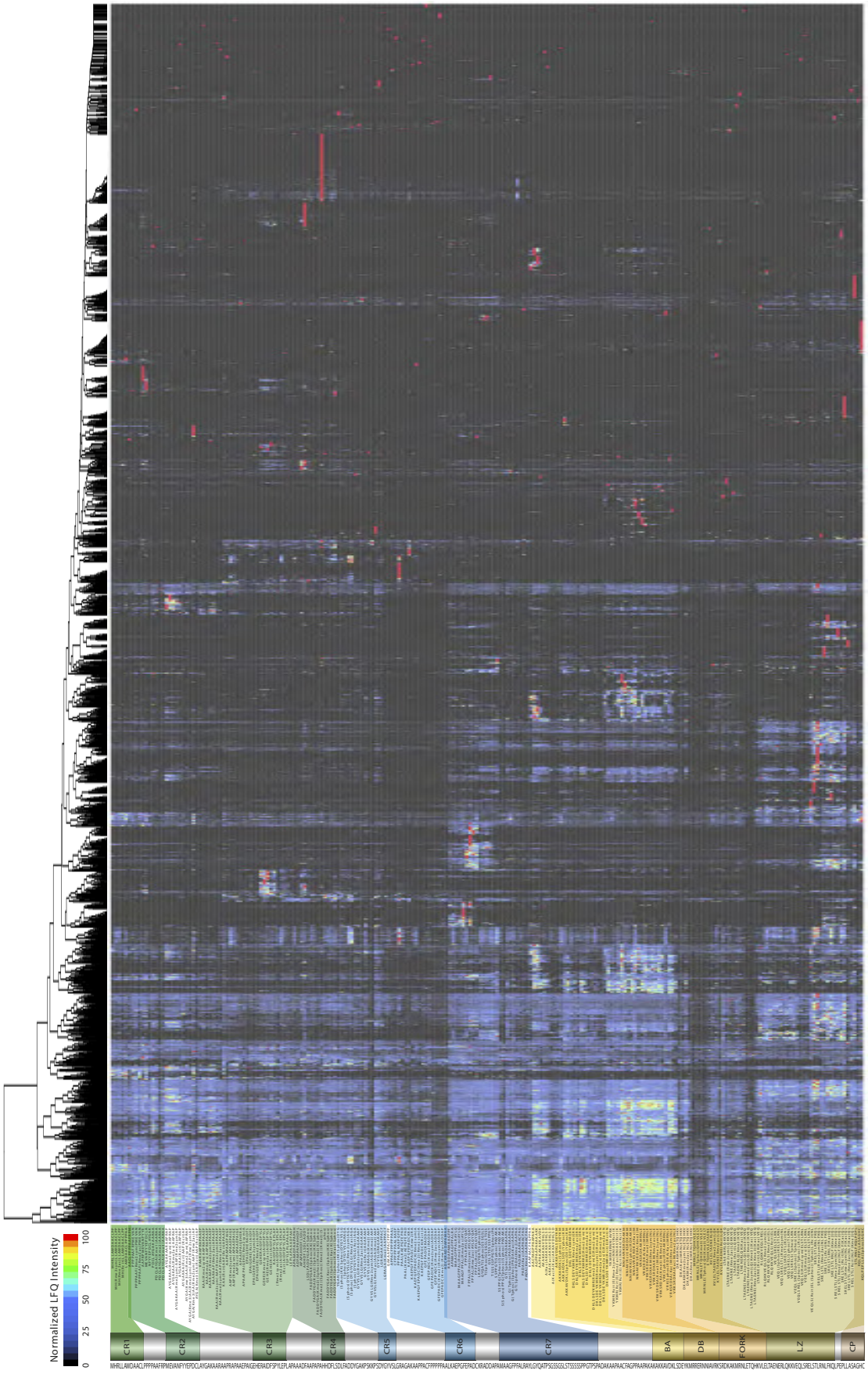
Normalized LFQ Intensity
0
25
50
75
100
CR1
CR2
CR3
CR4
CR5
CR6
CR7
BA
DB
FORK
LZ
CP

Supplemental figures 3 - 10: Heatmap of all published C/EBPβ protein interaction partners discovered by PrISMa binding to C/EBPβ peptides. Heatmap of normalized LFQ intensities of all published C/EBPβ protein interaction partners detected binding to C/EBPβ peptide sequences clustered with a Euclidian clustering algorithm and split into eight separate figures for better readability. On the top left the color key for the normalized LFQ values ranging from black to red (black, blue, green, yellow, red) is depicted. On top of the heatmap the UniProt accession numbers and the matching protein names one for each of the columns of the heatmap are specified. Distinguishable protein isoforms are marked after the Uniprot accession number by using a dash and the corresponding protein isoform number. On the left next to the heatmap the C/EBPβ peptide amino acid sequences corresponding to each row of the heatmap are annotated containing abbreviations for the PTMs. The PTMs accounted for are symmetric arginine dimethylation (Rme2sym), asymmetric arginine dimethylation (Rme2as), arginine citrullination (Rcit), lysine monomethylation (Kme), lysine dimethylation (Kme2), lysine trimethylation (Kme3), lysine acetylation (Kac), serine phosphorylation (Sphos), threonine phosphorylation (Tphos) and tyrosine phosphorylation (Yphos). On the left next to the heatmap a schematic representation of C/EBPβ LAP* isoform depicts the CRs and bZIP domain in a color code. On the far left the C/EBPβ amino acid sequence for the complete LAP* isoform is annotated.

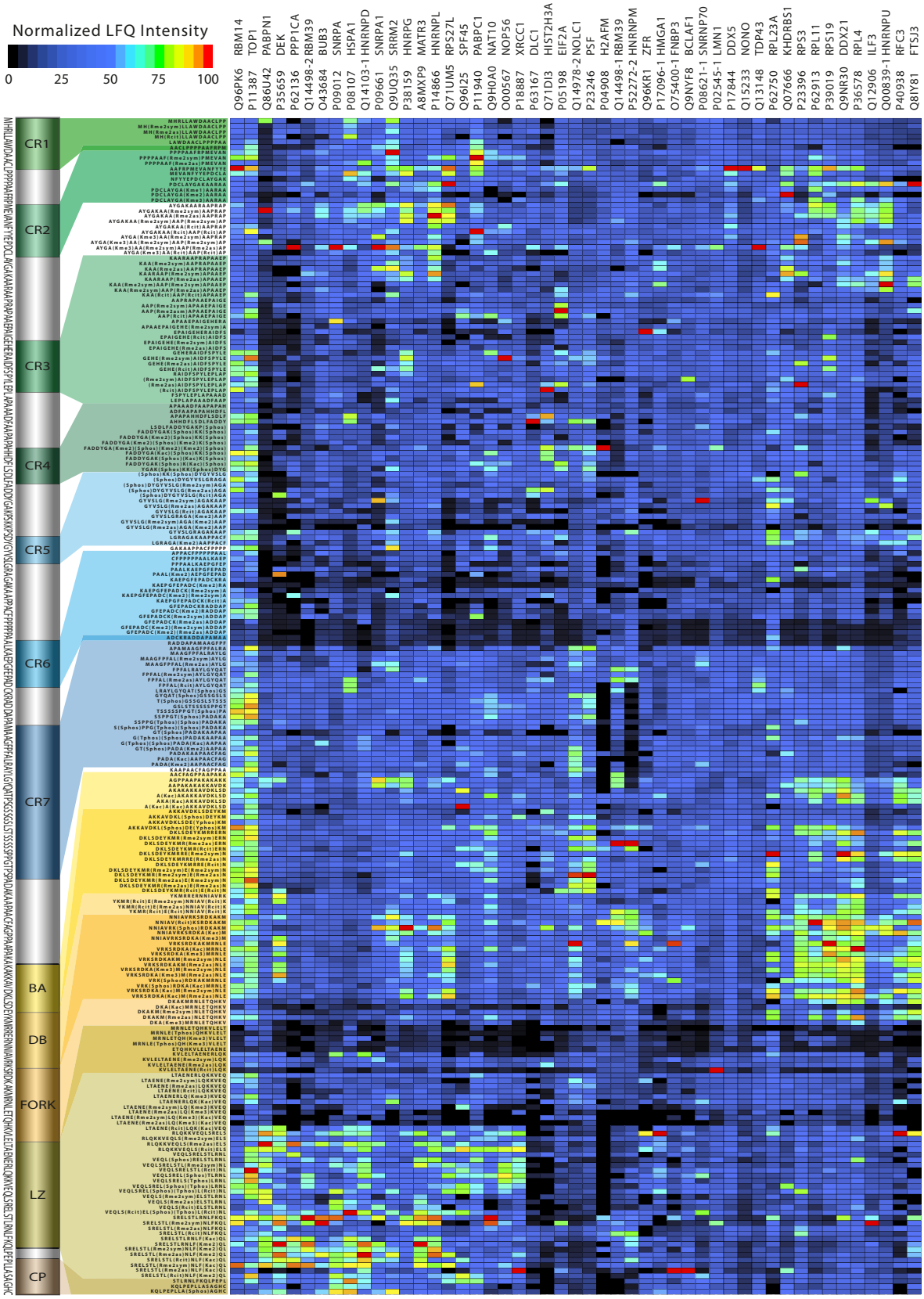
Normalized LFQ Intensity
0
25
50
75
100
Q96PK6 RBM14
P11387 TOP1
Q86U42 PABPN1
P35659 DEK
P62136 PPP1CA
Q14498-2 RBM39
O43684 BUB3
P09012 SNRPA
P08107 HSPA1
Q14103-1 HNRNPD
P09661 SNRPA1
Q9UQ35 SRRM2
P38159 HNRPG
A8MXP9 MATR3
P14866 HNRNPL
Q71UM5 RPS27L
Q96I25 SPF45
P11940 PABPC1
Q9H0A0 NAT10
O00567 NOP56
P18887 XRCC1
P63167 DLC1
Q71DI3 HIST2H3A
P05198 EIF2A
Q14978-2 NOLC1
P23246 PSF
P04908 H2AFM
Q14498-1 RBM39
P52272-2 HNRNPM
Q96KR1 ZFR
P17096-1 HMGA1
O75400-1 FNBP3
Q9NYF8 BCLAF1
P08621-1 SNRNP70
P02545-1 LMN1
P17844 DDX5
Q15233 NONO
Q13148 TDP43
P62750 RPL23A
Q07666 KHDRBS1
P23396 RPS3
P62913 RPL11
P39019 RPS19
Q9NR30 DDX21
P36578 RPL4
Q12906 ILF3
Q00839-1 HNRNPU
P40938 RFC3
Q8IY81 FTSJ3
CR1
CR2
CR3
CR4
CR5
CR6
CR7
BA
DB
FORK
LZ
CP

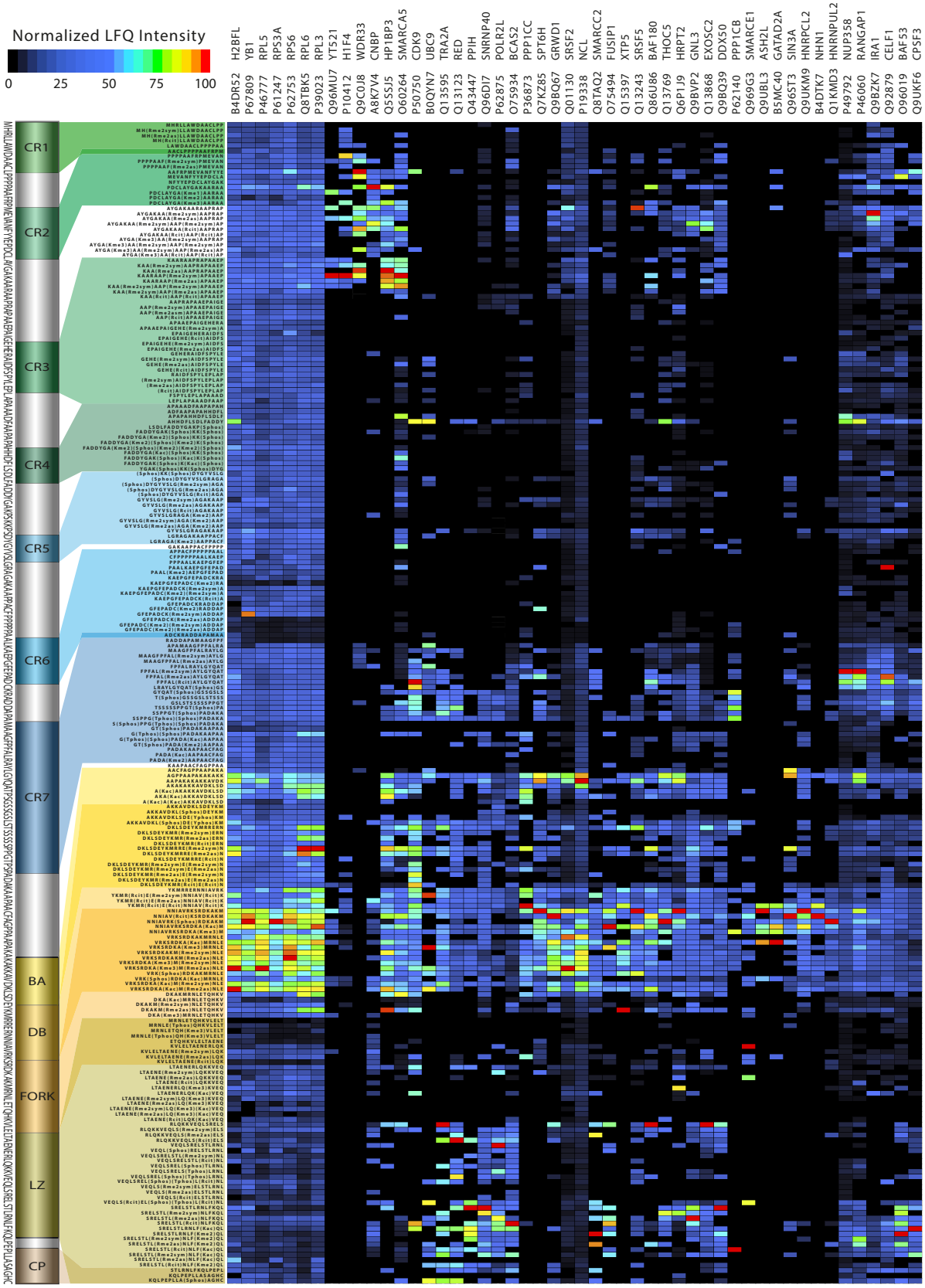
Normalized LFQ Intensity
0
25
50
75
100
B4DR52 H2BFL
P67809 YB1
P46777 RPL5
P61247 RPS3A
P62753 RPS6
Q8TBK5 RPL6
P39023 RPL3
Q96MU7 YT521
P10412 H1F4
Q9C0J8 WDR33
A8K7V4 CNBP
Q5SSJ5 HP1BP3
O60264 SMARCA5
P50750 CDK9
B0QYN7 UBC9
Q13595 TRA2A
Q13123 RED
O43447 PPIH
Q96DI7 SNRNP40
P62875 POLR2L
O75934 BCAS2
P36873 PPP1CC
Q7KZ85 SPT6H
Q9BQ67 GRWD1
Q01130 SRSF2
P19338 NCL
Q8TAQ2 SMARCC2
O75494 FUSIP1
Q15397 XTP5
Q13243 SRSF5
Q86U86 BAF180
Q13769 THOC5
Q6P1J9 HRPT2
Q9BVP2 GNL3
Q13868 EXOSC2
Q9BQ39 DDX50
P62140 PPP1CB
Q969G3 SMARCE1
Q9UBL3 ASH2L
B5MC40 GATAD2A
Q96ST3 SIN3A
Q9UKM9 HNRPCL2
B4DTK7 NHN1
Q1KMD3 HNRNPUL2
P49792 NUP358
P46060 RANGAP1
Q9BZK7 IRA1
Q92879 CELF1
O96019 BAF53
Q9UKF6 CPSF3
CR1
CR2
CR3
CR4
CR5
CR6
CR7
BA
DB
FORK
LZ
CP

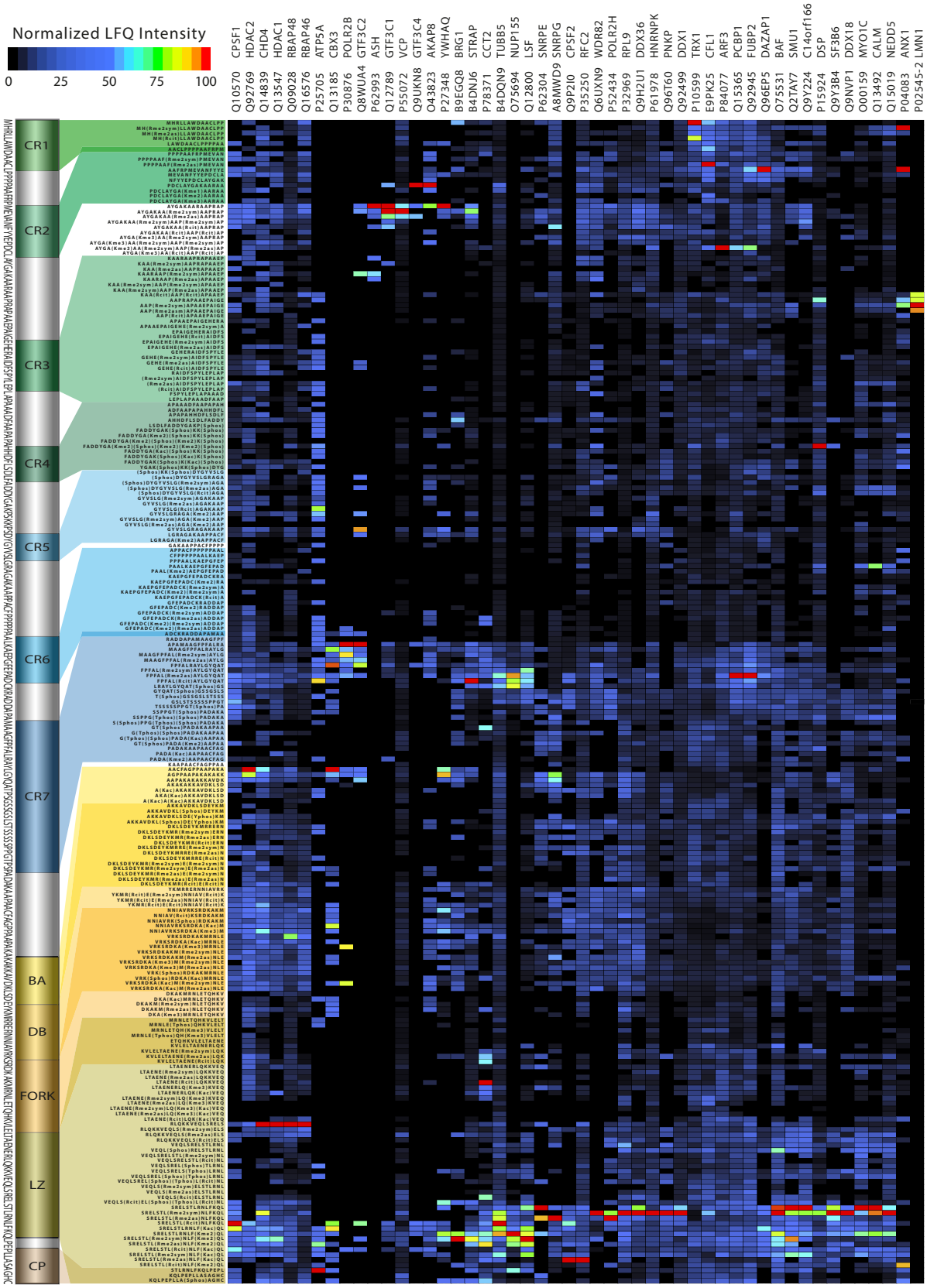
Normalized LFQ Intensity
0
25
50
75
100
Q10570 CPSF1
Q92769 HDAC2
Q14839 CHD4
Q13547 HDAC1
Q09028 RBAP48
Q16576 RBAP46
P25705 ATP5A
Q13185 CBX3
P30876 POLR2B
Q8WUA4 GTF3C2
P62993 ASH
Q12789 GTF3C1
P55072 VCP
Q9UKN8 GTF3C4
O43823 AKAP8
P27348 YWHAQ
B9EGQ8 BRG1
B4DNJ6 STRAP
P78371 CCT2
B4DQN9 TUBB5
O75694 NUP155
Q12800 LSF
P62304 SNRPE
A8MWD9 SNRPG
Q9P2I0 CPSF2
P35250 RFC2
Q6UXN9 WDR82
P52434 POLR2H
P32969 RPL9
Q9H2U1 DDX36
P61978 HNRNPK
Q96T60 PNKP
Q92499 DDX1
P10599 TRX1
E9PK25 CFL1
P84077 ARF3
Q15365 PCBP1
Q92945 FUBP2
Q96EP5 DAZAP1
O75531 BAF
Q2TAY7 SMU1
Q9Y224 C14orf166
P15924 DSP
Q9Y3B4 SF3B6
Q9NVP1 DDX18
O00159 MYO1C
Q13492 CALM
Q15019 NEDD5
P04083 ANX1
P02545-2 LMN1
CR1
CR2
CR3
CR4
CR5
CR6
CR7
BA
DB
FORK
LZ
CP

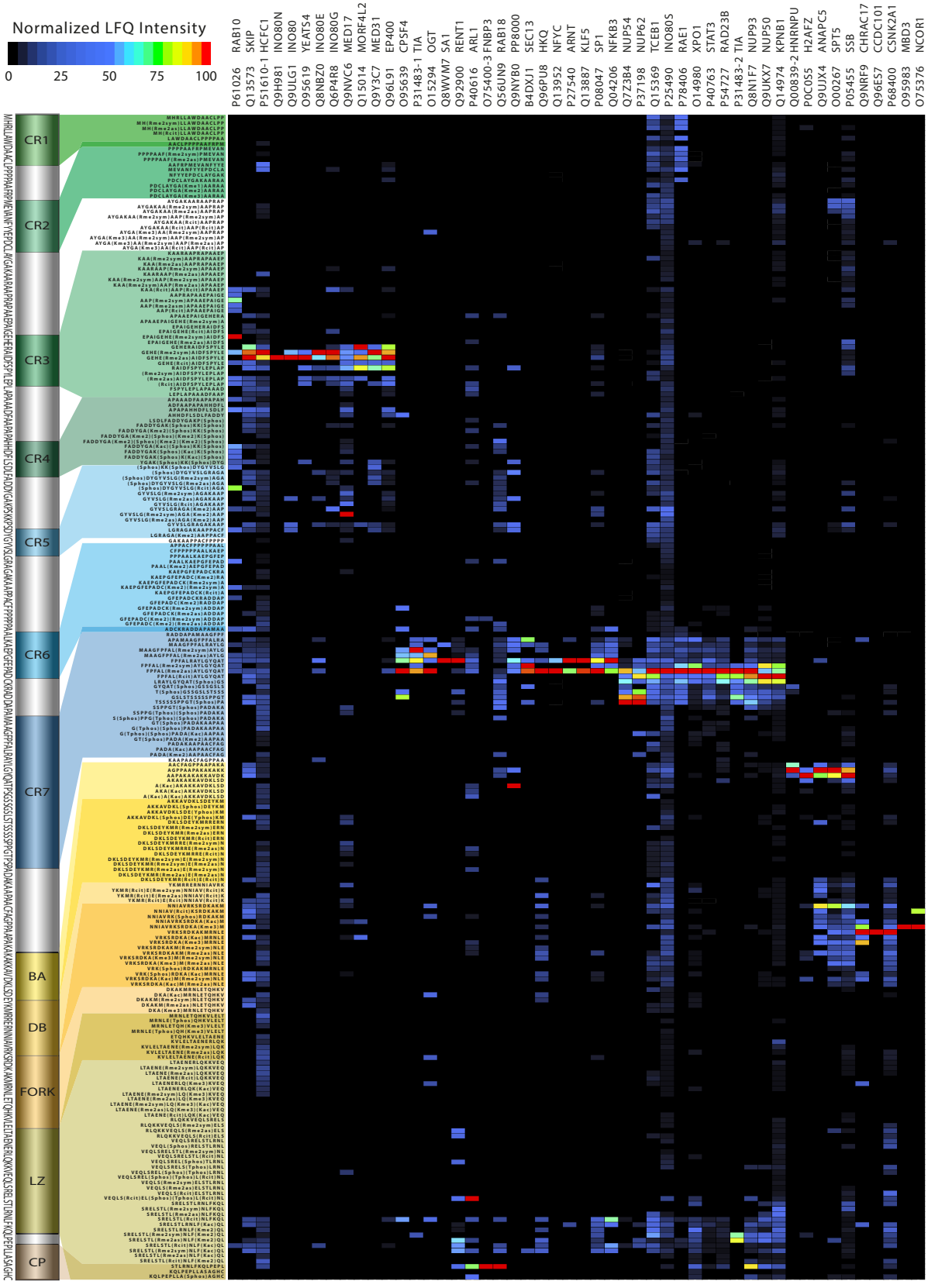
Normalized LFQ Intensity
0
25
50
75
100
P61026 RAB10
Q13573 SKIP
P51610-1 HCFC1
Q9H981 INO80N
Q9ULG1 INO80
O95619 YEATS4
Q8NBZ0 INO80E
Q6P4R8 INO80G
Q9NVC6 MED17
Q15014 MORF4L2
Q9Y3C7 MED31
Q96L91 EP400
O95639 CPSF4
P31483-1 TIA
O15294 OGT
Q8WVM7 SA1
Q92900 RENT1
P40616 ARL1
O75400-3 FNBP3
Q56UN9 RAB18
Q9NYB0 PP8000
B4DXJ1 SEC13
Q96PU8 HKQ
Q13952 NFYC
P27540 ARNT
Q13887 KLF5
P08047 SP1
Q04206 NFKB3
Q7Z3B4 NUP54
P37198 NUP62
Q15369 TCEB1
P25490 INO80S
P78406 RAE1
O14980 XPO1
P40763 STAT3
P54727 RAD23B
P31483-2 TIA
Q8N1F7 NUP93
Q9UKX7 NUP50
Q14974 KPNB1
Q00839-2 HNRNPU
P0C0S5 H2AFZ
Q9UJX4 ANAPC5
O00267 SPT5
P05455 SSB
Q9NRF9 CHRAC17
Q96E57 CCDC101
P68400 CSNK2A1
O95983 MBD3
O75376 NCOR1
CR1
CR2
CR3
CR4
CR5
CR6
CR7
BA
DB
FORK
LZ
CP

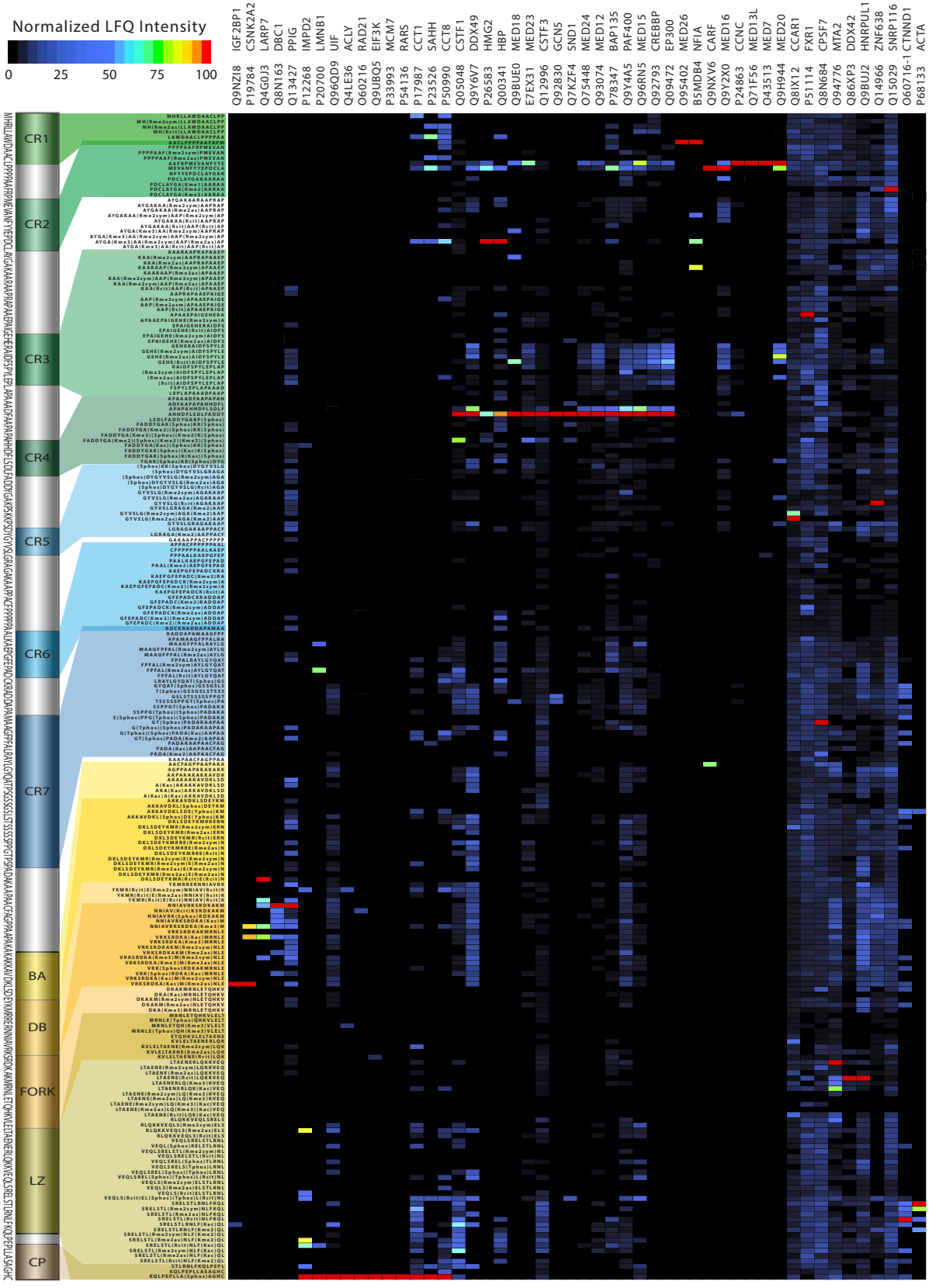
Normalized LFQ Intensity
0
25
50
75
100
Q9NZI8 IGF2BP1
P19784 CSNK2A2
Q4G0J3 LARP7
Q8N163 DBC1
Q13427 PPIG
P12268 IMPD2
P20700 LMNB1
Q96QD9 UIF
Q4LE36 ACLY
O60216 RAD21
Q9UBQ5 EIF3K
P33993 MCM7
P54136 RARS
P17987 CCT1
P23526 SAHH
P50990 CCT8
Q05048 CSTF1
Q9Y6V7 DDX49
P26583 HMG2
Q00341 HBP
Q9BUE0 MED18
E7EX31 MED23
Q12996 CSTF3
Q92830 GCN5
Q7KZF4 SND1
O75448 MED24
Q93074 MED12
P78347 BAP135
Q9Y4A5 PAF400
Q96RN5 MED15
Q92793 CREBBP
Q09472 EP300
O95402 MED26
B5MDB4 NFIA
Q9NXV6 CARF
Q9Y2X0 MED16
P24863 CCNC
Q71F56 MED13L
O43513 MED7
Q9H944 MED20
Q8IX12 CCAR1
P51114 FXR1
Q8N684 CPSF7
O94776 MTA2
Q86XP3 DDX42
Q9BUJ2 HNRPUL1
Q14966 ZNF638
Q15029 SNRP116
O60716-1 CTNND1
P68133 ACTA
CR1
CR2
CR3
CR4
CR5
CR6
CR7
BA
DB
FORK
LZ
CP

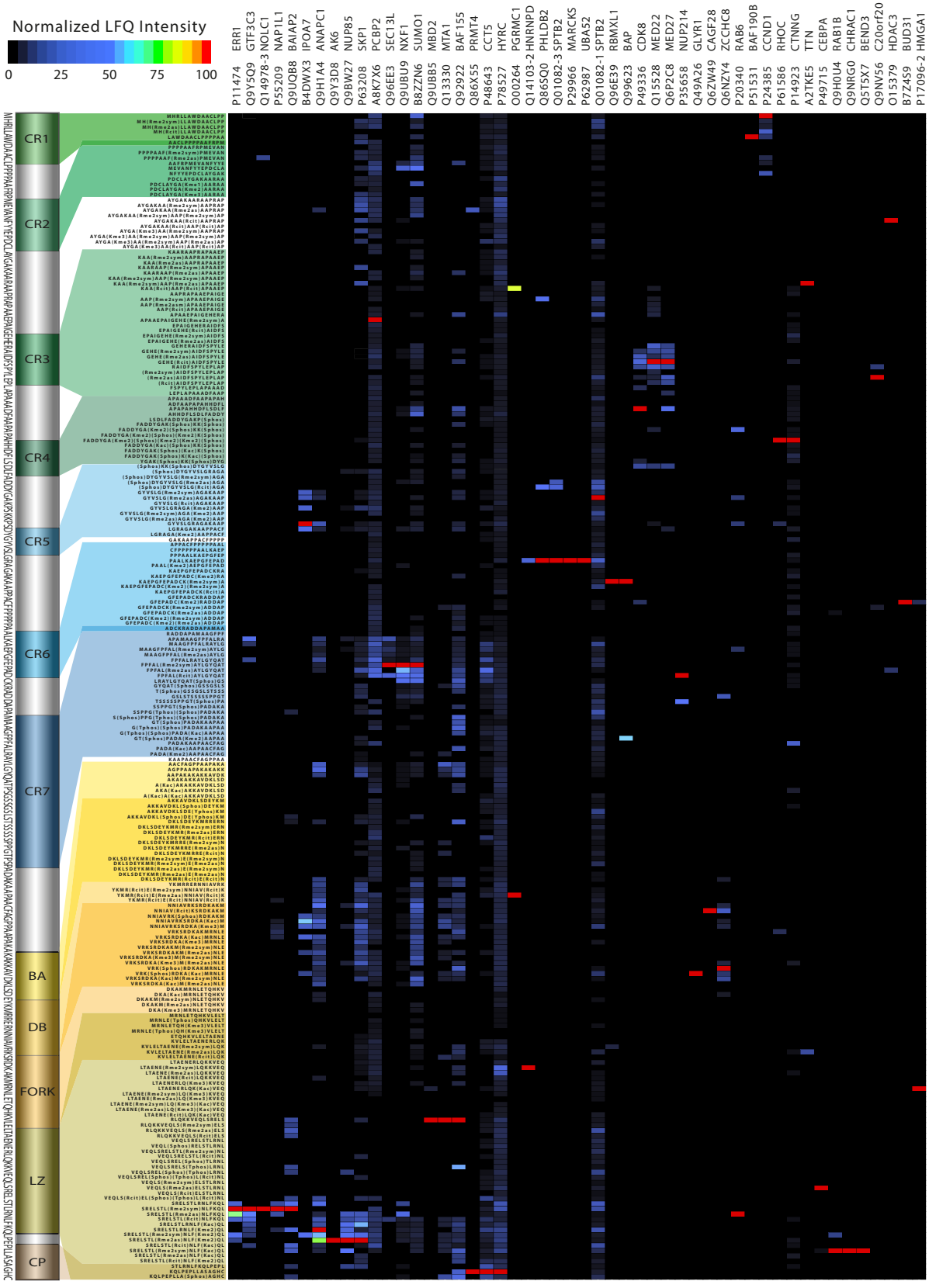
Normalized LFQ Intensity
0
25
50
75
100
P11474 ERR1
Q9Y5Q9 GTF3C3
Q14978-3 NOLC1
P55209 NAP1L1
Q9UQB8 BAIAP2
B4DWX3 IPOA7
Q9H1A4 ANAPC1
Q9Y3D8 AK6
Q9BW27 NUP85
P63208 SKP1
A8K7X6 PCBP2
Q96EE3 SEC13L
Q9UBU9 NXF1
B8ZZN6 SUMO1
Q9UBB5 MBD2
Q13330 MTA1
Q92922 BAF155
Q86X55 PRMT4
P48643 CCT5
P78527 HYRC
O00264 PGRMC1
Q14103-2 HNRNPD
Q86SQ0 PHLDB2
Q01082-3 SPTB2
P29966 MARCKS
P62987 UBA52
Q01082-1 SPTB2
Q96E39 RBMXL1
Q99623 BAP
P49336 CDK8
Q15528 MED22
Q6P2C8 MED27
P35658 NUP214
Q49A26 GLYR1
Q6ZW49 CAGF28
Q6NZY4 ZCCHC8
P20340 RAB6
P51531 BAF190B
P24385 CCND1
P61586 RHOC
P14923 CTNNG
A2TKE5 TTN
P49715 CEBPA
Q9H0U4 RAB1B
Q9NRG0 CHRAC1
Q5T5X7 BEND3
Q9NV56 C20orf20
O15379 HDAC3
B7Z459 BUD31
P17096-2 HMGA1
CR1
CR2
CR3
CR4
CR5
CR6
CR7
BA
DB
FORK
LZ
CP

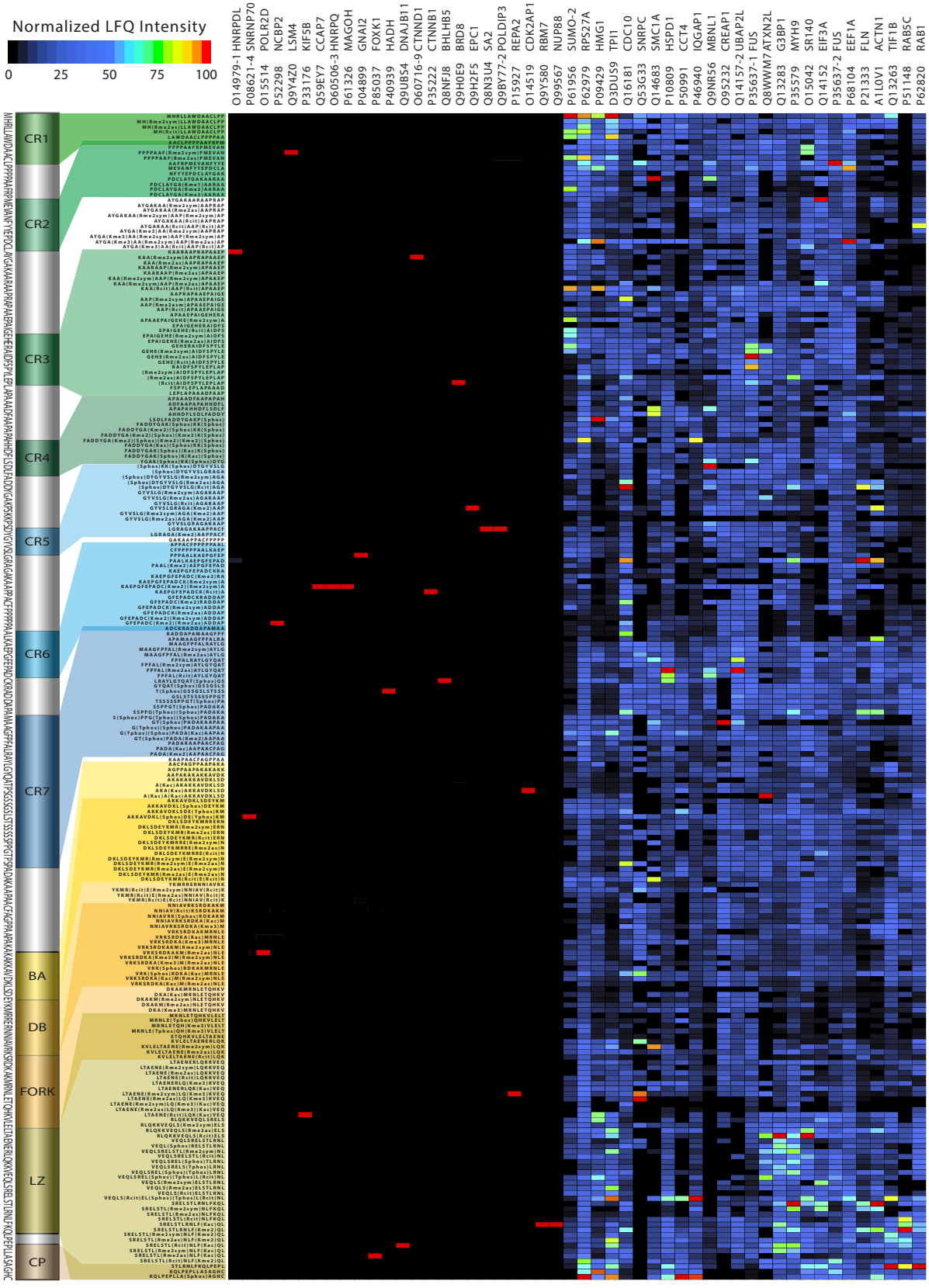
Normalized LFQ Intensity
0
25
50
75
100
O14979-1 HNRPDL
P08621-4 SNRNP70
O15514 POLR2D
P52298 NCBP2
Q9Y4Z0 LSM4
P33176 KIF5B
Q59EY7 CCAP7
O60506-3 HNRPQ
P61326 MAGOH
P04899 GNAI2
P85037 FOXK1
P40939 HADH
Q9UBS4 DNAJB11
O60716-9 CTNND1
P35222 CTNNB1
Q8NFJ8 BHLHB5
Q9H0E9 BRD8
Q9H2F5 EPC1
Q8N3U4 SA2
Q9BY77-2 POLDIP3
P15927 REPA2
O14519 CDK2AP1
Q9Y580 RBM7
Q99567 NUP88
P61956 SUMO-2
P62979 RPS27A
P09429 HMG1
D3DUS9 TPI1
Q16181 CDC10
Q53G33 SNRPC
Q14683 SMC1A
P10809 HSPD1
P50991 CCT4
P46940 IQGAP1
Q9NR56 MBNL1
O95232 CREAP1
Q14157-2 UBAP2L
P35637-1 FUS
Q8WWM7 ATXN2L
Q13283 G3BP1
P35579 MYH9
O15042 SR140
Q14152 EIF3A
P35637-2 FUS
P68104 EEF1A
P21333 FLN
A1L0V1 ACTN1
Q13263 TIF1B
P51148 RAB5C
P62820 RAB1
CR1
CR2
CR3
CR4
CR5
CR6
CR7
BA
DB
FORK
LZ
CP

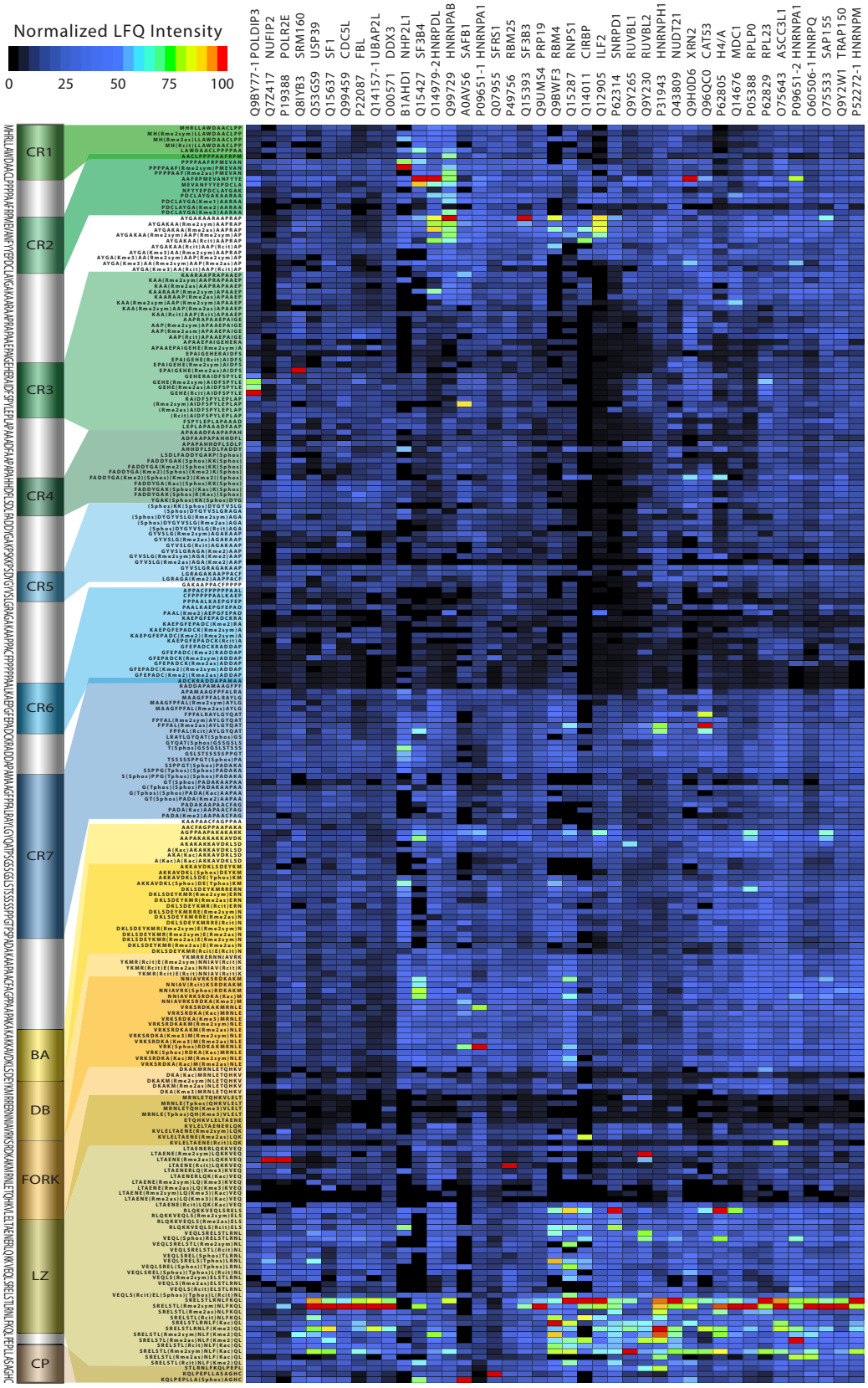
Normalized LFQ Intensity
0
25
50
75
100
Q9BY77-1 POLDIP3
Q7Z417 NUFIP2
P19388 POLR2E
Q8IYB3 SRM160
Q53GS9 USP39
Q15637 SF1
Q99459 CDC5L
P22087 FBL
Q14157-1 UBAP2L
O00571 DDX3
B1AHD1 NHP2L1
Q15427 SF3B4
O14979-2 HNRPDL
Q99729 HNRNPAB
A0AV56 SAFB1
P09651-1 HNRNPA1
Q07955 SFRS1
P49756 RBM25
Q15393 SF3B3
Q9UMS4 PRP19
Q9BWF3 RBM4
Q15287 RNPS1
Q14011 CIRBP
Q12905 ILF2
P62314 SNRPD1
Q9Y265 RUVBL1
Q9Y230 RUVBL2
P31943 HNRNPH1
O43809 NUDT21
Q9H0D6 XRN2
Q96QC0 CAT53
P62805 H4/A
Q14676 MDC1
P05388 RPLP0
P62829 RPL23
O75643 ASCC3L1
P09651-2 HNRNPA1
O60506-1 HNRPQ
O75533 SAP155
Q9Y2W1 TRAP150
P52272-1 HNRNPM
CR1
CR2
CR3
CR4
CR5
CR6
CR7
BA
DB
FORK
LZ
CP

Supplemental figure 11: C/EBPβ is modified in vivo by arginine methylation. A) Scheme of C/EBPβ expression, purification and tryptic protein digestion followed by mass spectrometry for arginine methylation detection. B) Tandem mass spectrum of a C/EBPβ R46 monomethylation. Indicated are the y- and b-series of the triptically cleaved peptide. A mass shift of 14 Da is marked with ´me´ for the modification at position R46. C) C/EBPβ is modified by methylation on R46 PTMs. Schematic presentation C/EBPβ (*Rattus norvegicus*) PTMs including the R46 monomethylation. All parts of C/EBPβ are thoroughly modified by serine and threonine phosphorylation, arginine and lysine methylation and lysine acetylation. C/EBPβ CR6 is modified by SUMO-1, SUMO-2 and SUMO-3 (vide legend at the bottom). The figure is adapted from Tsukada et al., 2011 and Leutz et al., 2011.

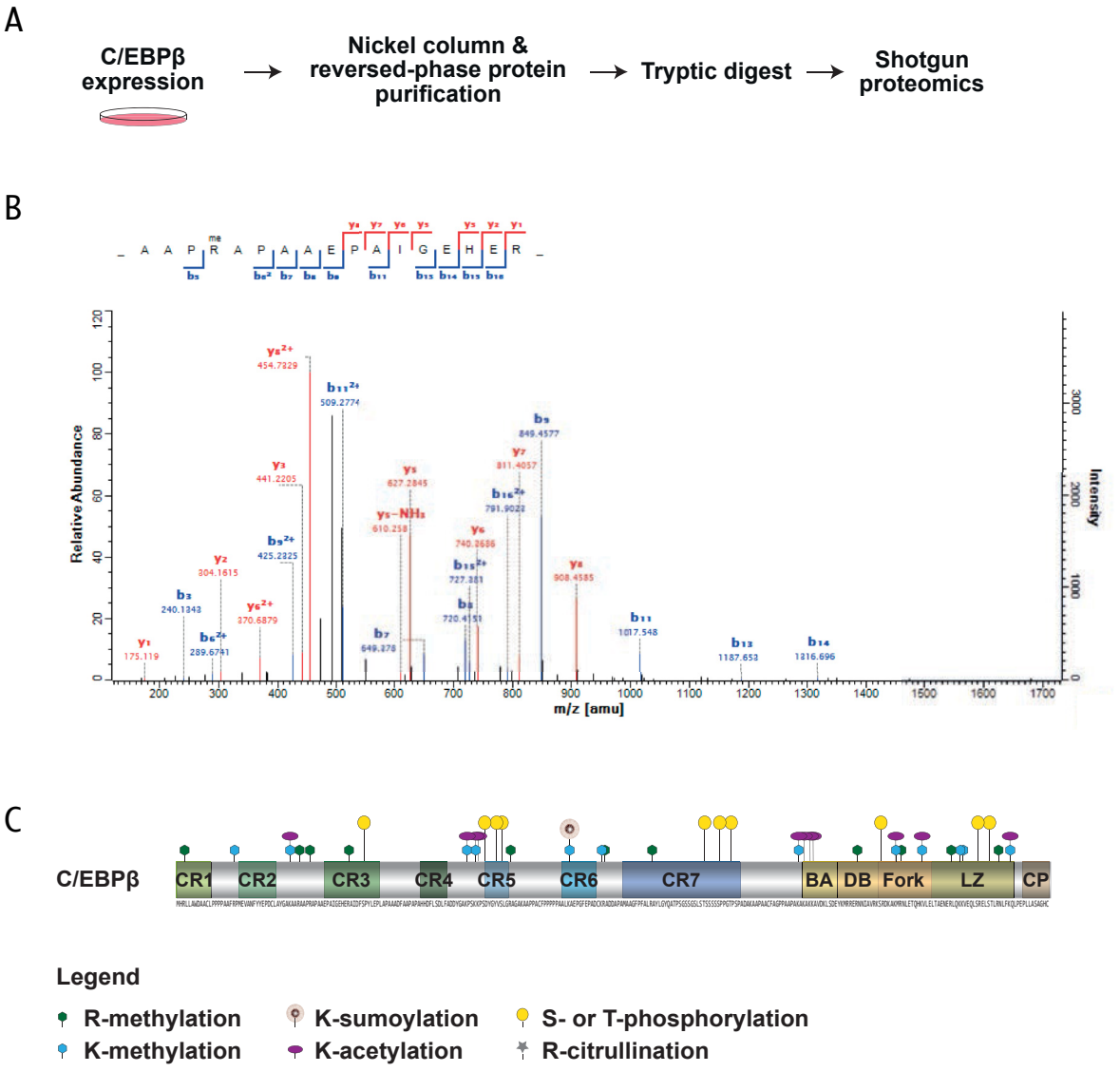

Supplemental figure 12: Heatmap of all 17S U2 snRNP complex members discovered by PrISMa binding to C/EBPβ peptides. Heatmap of normalized LFQ intensities of all 17S U2 snRNP complex members detected binding to C/EBPβ peptide sequences. On the top left the color key for the normalized LFQ values ranging from black to red (black, blue, green, yellow, red) is depicted. On top of the heatmap the UniProt accession numbers and the matching protein names one for each of the columns of the heatmap are specified. On the left next to the heatmap the C/EBPβ peptide amino acid sequences corresponding to each row of the heatmap are annotated containing abbreviations for the PTMs. The PTMs accounted for are symmetric arginine dimethylation (Rme2sym), asymmetric arginine dimethylation (Rme2as), arginine citrullination (Rcit), lysine monomethylation (Kme), lysine dimethylation (Kme2), lysine trimethylation (Kme3), lysine acetylation (Kac), serine phosphorylation (Sphos), threonine phosphorylation (Tphos) and tyrosine phosphorylation (Yphos). On the left next to the heatmap a schematic representation of C/EBPβ LAP* isoform depicts the CRs and bZIP domain in a color code. On the far left the C/EBPβ amino acid sequence for the complete LAP* isoform is annotated.

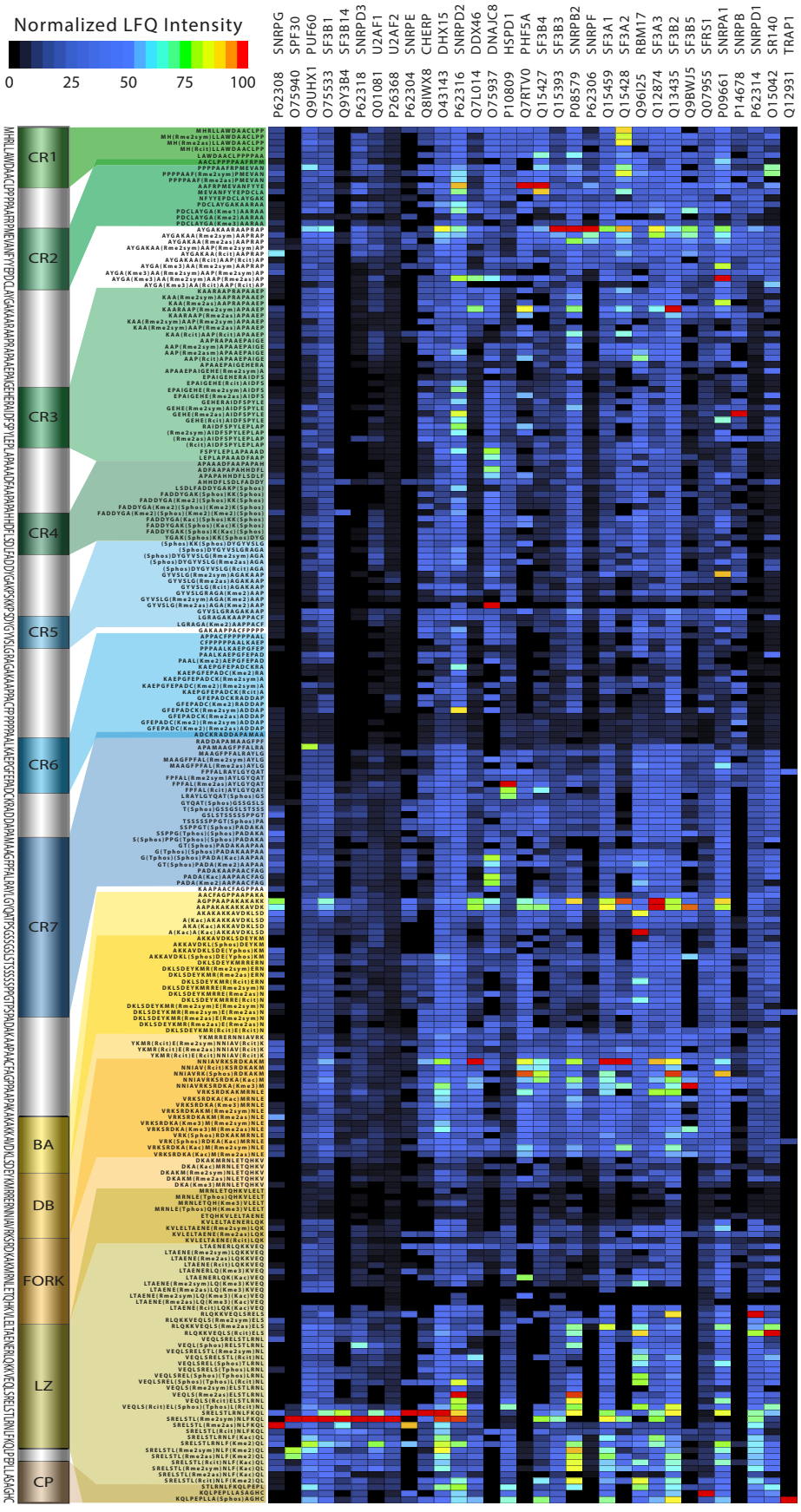
Normalized LFQ Intensity
0
25
50
75
100
P62308 SNRPG
O75940 SPF30
Q9UHX1 PUF60
O75533 SF3B1
Q9Y3B4 SF3B14
P62318 SNRPD3
Q01081 U2AF1
P26368 U2AF2
P62304 SNRPE
Q8IWX8 CHERP
O43143 DHX15
P62316 SNRPD2
Q7L014 DDX46
O75937 DNAJC8
P10809 HSPD1
Q7RTV0 PHF5A
Q15427 SF3B4
Q15393 SF3B3
P08579 SNRPB2
P62306 SNRPF
Q15459 SF3A1
Q15428 SF3A2
Q96I25 RBM17
Q12874 SF3A3
Q13435 SF3B2
Q9BWJ5 SF3B5
Q07955 SFRS1
P09661 SNRPA1
P14678 SNRPB
P62314 SNRPD1
O15042 SR140
Q12931 TRAP1
CR1
CR2
CR3
CR4
CR5
CR6
CR7
BA
DB
FORK
LZ
CP

Supplemental figures 13 - 14: Heatmap of all significant C/EBPβ interaction partners from the SU-DHL-1 cell line discovered by PrISMa binding to C/EBPβ peptides as well. Heatmap of normalized LFQ intensities of all significant C/EBPβ interaction partners from the ALK+ALCL SU-DHL-1 cell line binding to C/EBPβ peptide sequences clustered with a Euclidian clustering algorithmand and split into two separate figures for better readability. On the top left the color key for the normalized LFQ values ranging from black to red (black, blue, green, yellow, red) is depicted. On top of the heatmap the UniProt accession numbers and the matching protein names one for each of the columns of the heatmap are specified. Furthermore, the numeration as presented in table 3 (vide results section) is annotated as well. On the left next to the heatmap the C/EBPβ peptide amino acid sequences corresponding to each row of the heatmap are annotated containing abbreviations for the PTMs. The PTMs accounted for are symmetric arginine dimethylation (Rme2sym), asymmetric arginine dimethylation (Rme2as), arginine citrullination (Rcit), lysine monomethylation (Kme), lysine dimethylation (Kme2), lysine trimethylation (Kme3), lysine acetylation (Kac), serine phosphorylation (Sphos), threonine phosphorylation (Tphos) and tyrosine phosphorylation (Yphos). On the left next to the heatmap a schematic representation of C/EBPβ LAP* isoform depicts the CRs and bZIP domain in a color code. On the far left the C/EBPβ amino acid sequence for the complete LAP* isoform is annotated.

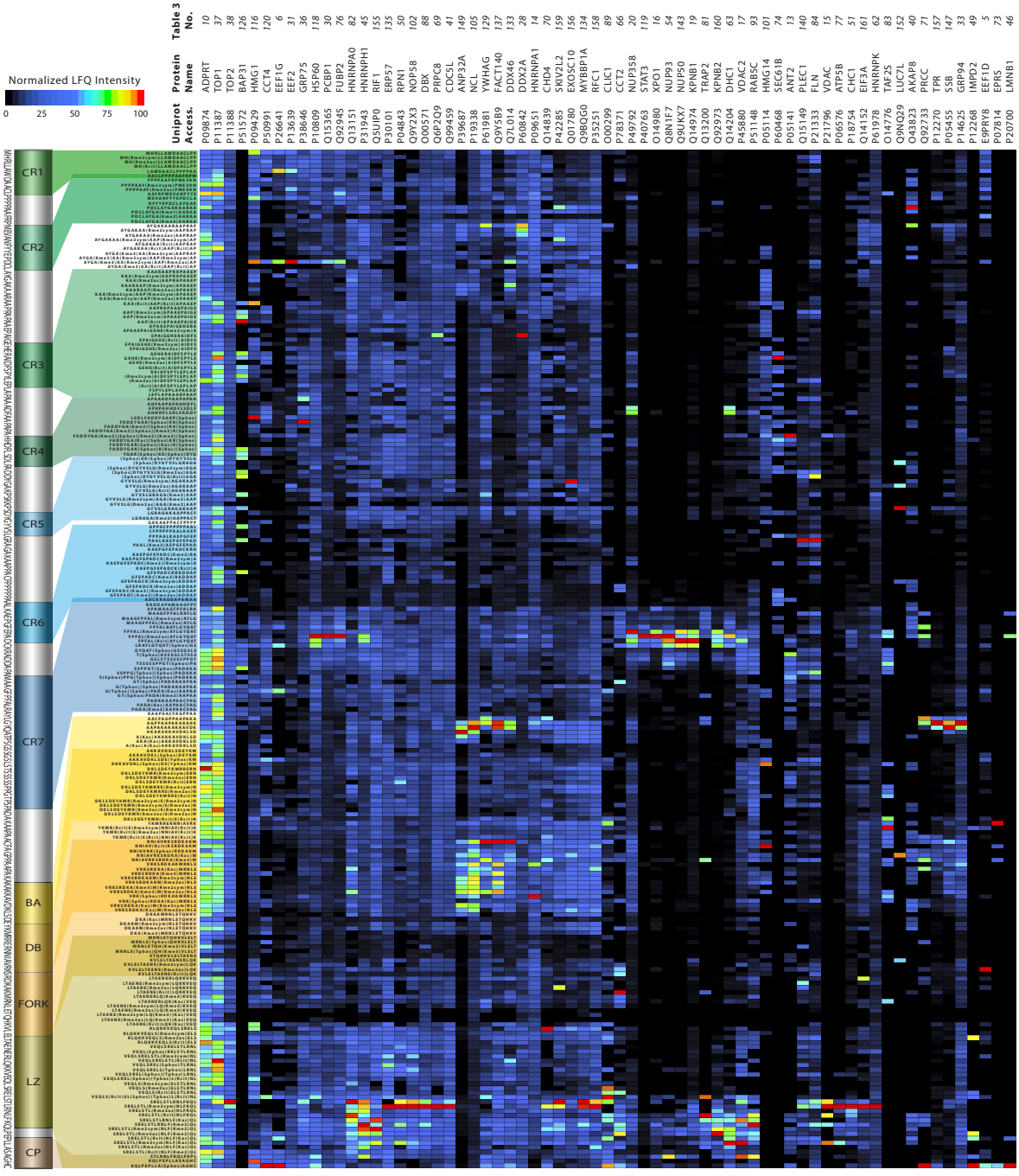
Normalized LFQ Intensity
0
25
50
75
100
Uniprot Access.
Protein Name
Table 3 No.
CR1
CR2
CR3
CR4
CR5
CR6
CR7
BA
DB
FORK
LZ
CP

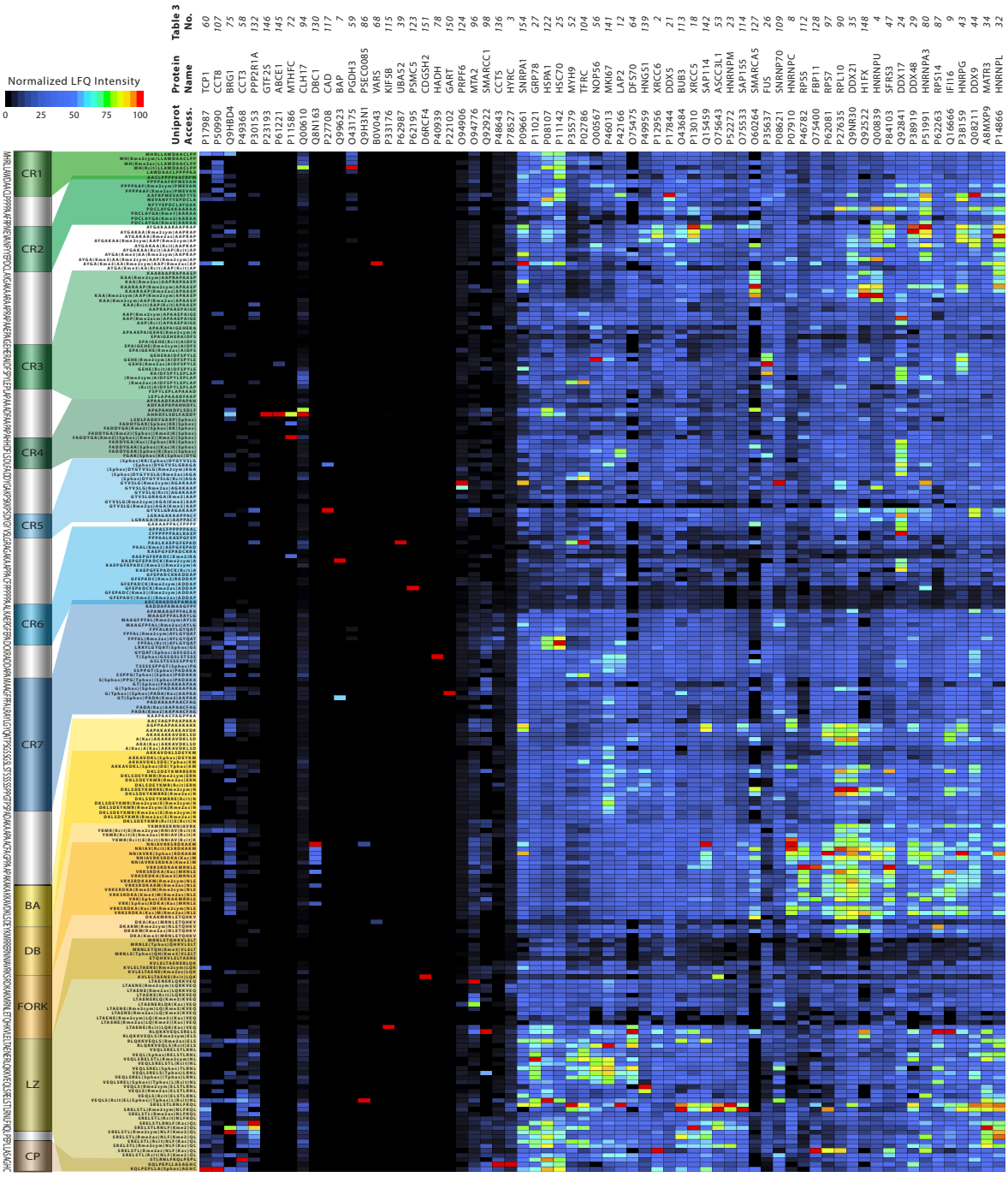
Normalized LFQ Intensity
0
25
50
75
100
Uniprot Access.
Protein Name
Table 3 No.
CR1
CR2
CR3
CR4
CR5
CR6
CR7
BA
DB
FORK
LZ
CP

Supplemental figure 15: Gene ontology enrichment analysis of the C/EBPβ interaction network in SU-DHL-1 cells. GO:terms of C/EBPβ interactors in the ALK+ALCL cell line SU-DHL-1 (analyzed by the NIH DAVID tool with GOTERM_BP_FAT: cut-off Benjamini Hochberg 0.05) revealed ´regulation of transcription´ and ´RNA processing´ as the most enriched GO:terms.

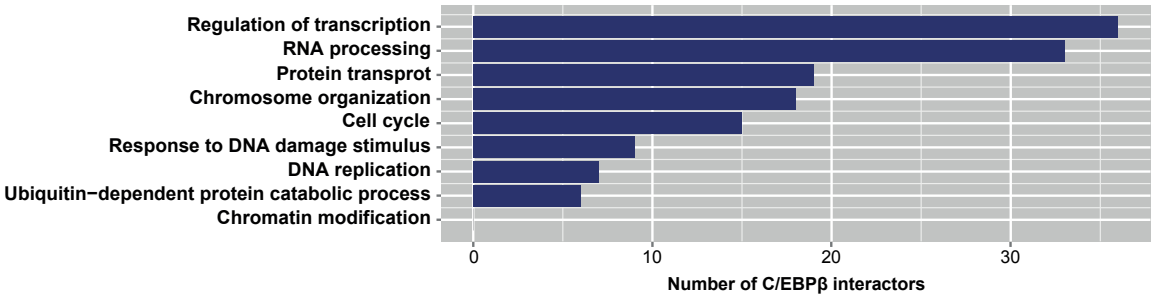

Supplemental table 1: Table of published C/EBPβ interacting proteins that were detected by PrISMa, too. The table presents 372 of the published C/EBPβ interaction partners detected by PrISMa binding to C/EBPβ peptide sequences as well. 18 of these 372 proteins were detected with two by mass spectrometry distinguishable protein isoforms. The table displays the Uniprot accession numbers, the protein name and the publication references linking C/EBPβ with the particular protein interaction partner. The protein isoforms are annotated in the Uniprot accession number column by using a dash and the corresponding protein isoform number. All the by this table presented published C/EBPβ interaction partners detected by PrISMa are depicted in the heatmaps of the Supplemental figures 3 - 10.

Uniprot	Name	C/EBPβ publication
Q96PK6	RBM14	Siersbæk et al., 2014
P11387	TOP1	Siersbæk et al., 2014
Q86U42	PABPN1	Siersbæk et al., 2014
P35659	DEK	Steinberg et al., 2012
P62136	PPP1CA	Steinberg et al., 2012
Q14498-2	RBM39	Siersbæk et al., 2014
O43684	BUB3	Siersbæk et al., 2014
P09012	SNRPA	Siersbæk et al., 2014
P08107	HSPA1	Siersbæk et al., 2014
Q14103-1	HNRNPD	Siersbæk et al., 2014
P09661	SNRPA1	Siersbæk et al., 2014
Q9UQ35	SRRM2	Siersbæk et al., 2014
P38159	HNRPG	Siersbæk et al., 2014
A8MXP9	MATR3	Siersbæk et al., 2014
P14866	HNRNPL	Siersbæk et al., 2014
Q71UM5	RPS27L	Siersbæk et al., 2014
Q96I25	SPF45	Siersbæk et al., 2014
P11940	PABPC1	Siersbæk et al., 2014
Q9H0A0	NAT10	Siersbæk et al., 2014
O00567	NOP56	Siersbæk et al., 2014
P18887	XRCC1	Steinberg et al., 2012
P63167	DLC1	Siersbæk et al., 2014
Q71DI3	HIST2H3A	Siersbæk et al., 2014
P05198	EIF2A	Siersbæk et al., 2014
Q14978-2	NOLC1	Miau et al., 1997; Miau et al., 1998
P23246	PSF	Siersbæk et al., 2014
P04908	H2AFM	Siersbæk et al., 2014
Q14498-1	RBM39	Siersbæk et al., 2014
P52272-2	HNRNPM	Siersbæk et al., 2014
Q96KR1	ZFR	Siersbæk et al., 2014
P17096-1	HMGA1	Steinberg et al., 2012
O75400-1	FNBP3	Siersbæk et al., 2014
Q9NYF8	BCLAF1	Siersbæk et al., 2014
P08621-1	SNRNP70	Siersbæk et al., 2014
P02545-1	LMN1	Siersbæk et al., 2014
P17844	DDX5	Siersbæk et al., 2014
Q15233	NONO	Siersbæk et al., 2014
Q13148	TDP43	Siersbæk et al., 2014
P62750	RPL23A	Siersbæk et al., 2014
Q07666	KHDRBS1	Siersbæk et al., 2014
P23396	RPS3	Siersbæk et al., 2014
P62913	RPL11	Siersbæk et al., 2014
P39019	RPS19	Siersbæk et al., 2014
Q9NR30	DDX21	Siersbæk et al., 2014
P36578	RPL4	Siersbæk et al., 2014
Q12906	ILF3	Siersbæk et al., 2014
Q00839-1	HNRNPU	Siersbæk et al., 2014
P40938	RFC3	Steinberg et al., 2012
Q8IY81	FTSJ3	Siersbæk et al., 2014
B4DR52	H2BFL	Siersbæk et al., 2014
P67809	YB1	Siersbæk et al., 2014
P46777	RPL5	Siersbæk et al., 2014
P61247	RPS3A	Siersbæk et al., 2014

Uniprot	Name	C/EBPβ publication
Q96ES7	CCDC101	Steinberg et al., 2012
P68400	CSNK2A1	Siersbæk et al., 2014
O95983	MBD3	Steinberg et al., 2012
O75376	NCOR1	Ki et al., 2005; Siersbæk et al., 2014
Q9NZI8	IGF2BP1	Siersbæk et al., 2014
P19784	CSNK2A2	Siersbæk et al., 2014
Q4G0J3	LARP7	Siersbæk et al., 2014
Q8N163	DBC1	Siersbæk et al., 2014
Q13427	PPIG	Siersbæk et al., 2014
P12268	IMPD2	Siersbæk et al., 2014
P20700	LMNB1	Siersbæk et al., 2014
Q96QD9	UIF	Siersbæk et al., 2014
Q4LE36	ACLY	Siersbæk et al., 2014
O60216	RAD21	Steinberg et al., 2012
Q9UBQ5	EIF3K	Siersbæk et al., 2014
P33993	MCM7	Siersbæk et al., 2014
P54136	RARS	Siersbæk et al., 2014
P17987	CCT1	Siersbæk et al., 2014
P23526	SAHH	Siersbæk et al., 2014
P50990	CCT8	Siersbæk et al., 2014
Q05048	CSTF1	Siersbæk et al., 2014
Q9Y6V7	DDX49	Steinberg et al., 2012
P26583	HMG2	Steinberg et al., 2012
Q00341	HBP	Siersbæk et al., 2014
Q9BUE0	MED18	Siersbæk et al., 2014
E7EX31	MED23	Mo et al., 2004; Siersbæk et al., 2014
Q12996	CSTF3	Siersbæk et al., 2014
Q92830	GCN5	Wiper-Bergeron et al., 2007
Q7KZF4	SND1	Siersbæk et al., 2014
O75448	MED24	Siersbæk et al., 2014
Q93074	MED12	Siersbæk et al., 2014
P78347	BAP135	Siersbæk et al., 2014
Q9Y4A5	PAF400	Steinberg et al., 2012
Q96RN5	MED15	Siersbæk et al., 2014
Q92793	CREBBP	Kovács et al., 2003; Siersbæk et al., 2014
Q09472	EP300	Mink et al., 1997; Siersbæk et al., 2014
O95402	MED26	Mo et al., 2004
B5MDB4	NFIA	Siersbæk et al., 2014
Q9NXV6	CARF	Siersbæk et al., 2014
Q9Y2X0	MED16	Siersbæk et al., 2014
P24863	CCNC	Siersbæk et al., 2014
Q71F56	MED13L	Siersbæk et al., 2014
O43513	MED7	Siersbæk et al., 2014
Q9H944	MED20	Siersbæk et al., 2014
Q8IX12	CCAR1	Siersbæk et al., 2014
P51114	FXR1	Siersbæk et al., 2014
Q8N684	CPSF7	Siersbæk et al., 2014
O94776	MTA2	Steinberg et al., 2012; Siersbæk et al., 2014
Q86XP3	DDX42	Siersbæk et al., 2014
Q9BUJ2	HNRPUL1	Siersbæk et al., 2014
Q14966	ZNF638	Siersbæk et al., 2014
Q15029	SNRP116	Siersbæk et al., 2014
O60716-1	CTNND1	Siersbæk et al., 2014

Uniprot	Name	C/EBPβ publication
P62753	RPS6	Siersbæk et al., 2014
Q8TBK5	RPL6	Siersbæk et al., 2014
P39023	RPL3	Siersbæk et al., 2014
Q96MU7	YT521	Siersbæk et al., 2014
P10412	H1F4	Siersbæk et al., 2014
Q9C0J8	WDR33	Siersbæk et al., 2014
A8K7V4	CNBP	Siersbæk et al., 2014
Q5SSJ5	HP1BP3	Siersbæk et al., 2014
O60264	SMARCA5	Steinberg et al., 2012; Siersbæk et al., 2014
P50750	CDK9	Siersbæk et al., 2014
B0QYN7	UBC9	Steinberg et al., 2012
Q13595	TRA2A	Siersbæk et al., 2014
Q13123	RED	Siersbæk et al., 2014
O43447	PPIH	Siersbæk et al., 2014
Q96DI7	SNRNP40	Siersbæk et al., 2014
P62875	POLR2L	Steinberg et al., 2012
O75934	BCAS2	Siersbæk et al., 2014
P36873	PPP1CC	Siersbæk et al., 2014
Q7KZ85	SPT6H	Siersbæk et al., 2014
Q9BQ67	GRWD1	Siersbæk et al., 2014
Q01130	SRSF2	Siersbæk et al., 2014
P19338	NCL	Siersbæk et al., 2014
Q8TAQ2	SMARCC2	Steinberg et al., 2012; Siersbæk et al., 2014
O75494	FUSIP1	Siersbæk et al., 2014
Q15397	XTP5	Siersbæk et al., 2014
Q13243	SRSF5	Siersbæk et al., 2014
Q86U86	BAF180	Steinberg et al., 2012
Q13769	THOC5	Siersbæk et al., 2014
Q6P1J9	HRPT2	Siersbæk et al., 2014
Q9BVP2	GNL3	Siersbæk et al., 2014
Q13868	EXOSC2	Siersbæk et al., 2014
Q9BQ39	DDX50	Siersbæk et al., 2014
P62140	PPP1CB	Siersbæk et al., 2014
Q969G3	SMARCE1	Steinberg et al., 2012; Siersbæk et al., 2014
Q9UBL3	ASH2L	Siersbæk et al., 2014
B5MC40	GATAD2A	Siersbæk et al., 2014
Q96ST3	SIN3A	Steinberg et al., 2012
Q9UKM9	HNRPCL2	Siersbæk et al., 2014
B4DTK7	NHN1	Siersbæk et al., 2014
Q1KMD3	HNRNPUL2	Siersbæk et al., 2014
P49792	NUP358	Siersbæk et al., 2014
P46060	RANGAP1	Siersbæk et al., 2014
Q9BZK7	IRA1	Siersbæk et al., 2014
Q92879	CELF1	Siersbæk et al., 2014
O96019	BAF53	Steinberg et al., 2012; Siersbæk et al., 2014
Q9UKF6	CPSF3	Siersbæk et al., 2014
Q10570	CPSF1	Siersbæk et al., 2014
Q92769	HDAC2	Steinberg et al., 2012; Siersbæk et al., 2014

Uniprot	Name	C/EBPβ publication
P68133	ACTA	Steinberg et al., 2012
P11474	ERR1	Steinberg et al., 2012
Q9Y5Q9	GTF3C3	Steinberg et al., 2012
Q14978-3	NOLC1	Miau et al., 1997; Miau et al., 1998
P55209	NAP1L1	Steinberg et al., 2012
Q9UQB8	BAIAP2	Siersbæk et al., 2014
B4DWX3	IPOA7	Siersbæk et al., 2014
Q9H1A4	ANAPC1	Siersbæk et al., 2014
Q9Y3D8	AK6	Choi et al., 2000
Q9BW27	NUP85	Siersbæk et al., 2014
P63208	SKP1	Steinberg et al., 2012; Siersbæk et al., 2014
A8K7X6	PCBP2	Siersbæk et al., 2014
Q96EE3	SEC13L	Siersbæk et al., 2014
Q9UBU9	NXF1	Siersbæk et al., 2014
B8ZZN6	SUMO-1	Kim et al., 2002
Q9UBB5	MBD2	Steinberg et al., 2012; Siersbæk et al., 2014
Q13330	MTA1	Steinberg et al., 2012
Q92922	BAF155	Kowenz-Leutz et al., 1999; Steinberg et al., 2012
Q86X55	PRMT4	Kowenz-Leutz et al., 2010; Siersbæk et al., 2014
P48643	CCT5	Siersbæk et al., 2014
P78527	HYRC	Steinberg et al., 2012
O00264	PGRMC1	Siersbæk et al., 2014
Q14103-2	HNRNPD	Siersbæk et al., 2014
Q86SQ0	PHLDB2	Siersbæk et al., 2014
Q01082-3	SPTB2	Siersbæk et al., 2014
P29966	MARCKS	Siersbæk et al., 2014
P62987	UBA52	Siersbæk et al., 2014
Q01082-1	SPTB2	Siersbæk et al., 2014
Q96E39	RBMXL1	Siersbæk et al., 2014
Q99623	BAP	Siersbæk et al., 2014
P49336	CDK8	Mo et al., 2004
Q15528	MED22	Siersbæk et al., 2014
Q6P2C8	MED27	Siersbæk et al., 2014
P35658	NUP214	Siersbæk et al., 2014
Q49A26	GLYR1	Siersbæk et al., 2014
Q6ZW49	CAGF28	Steinberg et al., 2012
Q6NZY4	ZCCHC8	Siersbæk et al., 2014
P20340	RAB6	Siersbæk et al., 2014
P51531	BAF190B	Kowenz-Leutz et al., 1999; Steinberg et al., 2012; Siersbæk et al., 2014
P24385	CCND1	Lamb et al., 2003
P61586	RHOC	Steinberg et al., 2012
P14923	CTNNG	Siersbæk et al., 2014
A2TKE5	TTN	Siersbæk et al., 2014
P49715	CEBPA	Cao et al., 1991
Q9H0U4	RAB1B	Siersbæk et al., 2014
Q9NRG0	CHRAC1	Steinberg et al., 2012
Q5T5X7	BEND3	Steinberg et al., 2012
Q9NV56	C20orf20	Steinberg et al., 2012

Uniprot	Name	C/EBPβ publication
Q14839	CHD4	Steinberg et al., 2012; Siersbæk et al., 2014
Q13547	HDAC1	Steinberg et al., 2012; Siersbæk et al., 2014
Q09028	RBAP48	Steinberg et al., 2012; Siersbæk et al., 2014
Q16576	RBAP46	Steinberg et al., 2012; Siersbæk et al., 2014
P25705	ATP5A	Siersbæk et al., 2014
Q13185	CBX3	Siersbæk et al., 2014
P30876	POLR2B	Siersbæk et al., 2014
Q8WUA4	GTF3C2	Siersbæk et al., 2014
P62993	ASH	Siersbæk et al., 2014
Q12789	GTF3C1	Steinberg et al., 2012
P55072	VCP	Siersbæk et al., 2014
Q9UKN8	GTF3C4	Steinberg et al., 2012
O43823	AKAP8	Siersbæk et al., 2014
P27348	YWHAQ	Siersbæk et al., 2014
B9EGQ8	BRG1	Kowenz-Leutz et al., 1999; Steinberg et al., 2012; Siersbæk et al., 2014
B4DNJ6	STRAP	Siersbæk et al., 2014
P78371	CCT2	Siersbæk et al., 2014
B4DQN9	TUBB5	Siersbæk et al., 2014
O75694	NUP155	Siersbæk et al., 2014
Q12800	LSF	Steinberg et al., 2012
P62304	SNRPE	Siersbæk et al., 2014
A8MWD9	SNRPG	Siersbæk et al., 2014
Q9P2I0	CPSF2	Siersbæk et al., 2014
P35250	RFC2	Siersbæk et al., 2014
Q6UXN9	WDR82	Siersbæk et al., 2014
P52434	POLR2H	Siersbæk et al., 2014
P32969	RPL9	Siersbæk et al., 2014
Q9H2U1	DDX36	Siersbæk et al., 2014
P61978	HNRNPK	Miau et al., 1998; Siersbæk et al., 2014
Q96T60	PNKP	Steinberg et al., 2012
Q92499	DDX1	Siersbæk et al., 2014
P10599	TRX1	Siersbæk et al., 2014
E9PK25	CFL1	Siersbæk et al., 2014
P84077	ARF3	Siersbæk et al., 2014
Q15365	PCBP1	Siersbæk et al., 2014
Q92945	FUBP2	Siersbæk et al., 2014
Q96EP5	DAZAP1	Siersbæk et al., 2014
O75531	BAF	Siersbæk et al., 2014
Q2TAY7	SMU1	Siersbæk et al., 2014
Q9Y224	C14orf166	Siersbæk et al., 2014
P15924	DSP	Siersbæk et al., 2014
Q9Y3B4	SF3B6	Siersbæk et al., 2014
Q9NVP1	DDX18	Siersbæk et al., 2014
O00159	MYO1C	Siersbæk et al., 2014
Q13492	CALM	Siersbæk et al., 2014
Q15019	NEDD5	Siersbæk et al., 2014
P04083	ANX1	Siersbæk et al., 2014
P02545-2	LMN1	Siersbæk et al., 2014
P61026	RAB10	Siersbæk et al., 2014
Q13573	SKIP	Siersbæk et al., 2014
P51610-1	HCFC1	Siersbæk et al., 2014

Uniprot	Name	C/EBPβ publication
O15379	HDAC3	Siersbæk et al., 2014
B7Z4S9	BUD31	Siersbæk et al., 2014
P17096-2	HMGA1	Foti et al., 2003; Steinberg et al., 2012
O14979-1	HNRPDL	Siersbæk et al., 2014
P08621-4	SNRNP70	Siersbæk et al., 2014
O15514	POLR2D	Siersbæk et al., 2014
P52298	NCBP2	Siersbæk et al., 2014
Q9Y4Z0	LSM4	Siersbæk et al., 2014
P33176	KIF5B	Siersbæk et al., 2014
Q59EY7	CCAP7	Siersbæk et al., 2014
O60506-3	HNRPQ	Siersbæk et al., 2014
P61326	MAGOH	Siersbæk et al., 2014
P04899	GNAI2	Siersbæk et al., 2014
P85037	FOXK1	Siersbæk et al., 2014
P40939	HADH	Siersbæk et al., 2014
Q9UBS4	DNAJB11	Siersbæk et al., 2014
O60716-9	CTNND1	Siersbæk et al., 2014
P35222	CTNNB1	Siersbæk et al., 2014
Q8NFJ8	BHLHB5	Siersbæk et al., 2014
Q9H0E9	BRD8	Steinberg et al., 2012
Q9H2F5	EPC1	Steinberg et al., 2012
Q8N3U4	SA2	Steinberg et al., 2012
Q9BY77-2	POLDIP3	Siersbæk et al., 2014
P15927	REPA2	Steinberg et al., 2012
O14519	CDK2AP1	Steinberg et al., 2012
Q9Y580	RBM7	Steinberg et al., 2012
Q99567	NUP88	Siersbæk et al., 2014
P61956	SUMO-2	Golebiowski et al., 2009
P62979	RPS27A	Siersbæk et al., 2014
P09429	HMG1	Dintilhac et al., 2001
D3DUS9	TPI1	Siersbæk et al., 2014
Q16181	CDC10	Siersbæk et al., 2014
Q53G33	SNRPC	Siersbæk et al., 2014
Q14683	SMC1A	Steinberg et al., 2012
P10809	HSPD1	Siersbæk et al., 2014
P50991	CCT4	Siersbæk et al., 2014
P46940	IQGAP1	Siersbæk et al., 2014
Q9NR56	MBNL1	Siersbæk et al., 2014
O95232	CREAP1	Siersbæk et al., 2014
Q14157-2	UBAP2L	Siersbæk et al., 2014
P35637-1	FUS	Siersbæk et al., 2014
Q8WWM7	ATXN2L	Siersbæk et al., 2014
Q13283	G3BP1	Siersbæk et al., 2014
P35579	MYH9	Siersbæk et al., 2014
O15042	SR140	Siersbæk et al., 2014
Q14152	EIF3A	Siersbæk et al., 2014
P35637-2	FUS	Siersbæk et al., 2014
P68104	EEF1A	Siersbæk et al., 2014
P21333	FLN	Siersbæk et al., 2014
A1L0V1	ACTN1	Siersbæk et al., 2014
Q13263	TIF1B	Chang et al., 1998; Rooney et al., 2001; Siersbæk et al., 2014

Uniprot	Name	C/EBPβ publication
Q9H981	INO80N	Steinberg et al., 2012
Q9ULG1	INO80	Steinberg et al., 2012
O95619	YEATS4	Steinberg et al., 2012
Q8NBZ0	INO80E	Steinberg et al., 2012
Q6P4R8	INO80G	Steinberg et al., 2012
Q9NVC6	MED17	Siersbæk et al., 2014
Q15014	MORF4L2	Steinberg et al., 2012
Q9Y3C7	MED31	Siersbæk et al., 2014
Q96L91	EP400	Steinberg et al., 2012
O95639	CPSF4	Siersbæk et al., 2014
P31483-1	TIA	Siersbæk et al., 2014
O15294	OGT	Siersbæk et al., 2014
Q8WVM7	SA1	Steinberg et al., 2012
Q92900	RENT1	Siersbæk et al., 2014
P40616	ARL1	Siersbæk et al., 2014
O75400-3	FNBP3	Steinberg et al., 2012
Q56UN9	RAB18	Siersbæk et al., 2014
Q9NYB0	PP8000	Steinberg et al., 2012
B4DXJ1	SEC13	Siersbæk et al., 2014
Q96PU8	HKQ	Siersbæk et al., 2014
Q13952	NFYC	Steinberg et al., 2012
P27540	ARNT	Steinberg et al., 2012
Q13887	KLF5	Siersbæk et al., 2014
P08047	SP1	Siersbæk et al., 2014
Q04206	NFKB3	Xia et al., 1997; Weber et al., 2003; Zwergal et al., 2006
Q7Z3B4	NUP54	Siersbæk et al., 2014
P37198	NUP62	Siersbæk et al., 2014
Q15369	TCEB1	Siersbæk et al., 2014
P25490	INO80S	Siersbæk et al., 2014
P78406	RAE1	Siersbæk et al., 2014
O14980	XPO1	Buck et al., 2001; Steinberg et al., 2012
P40763	STAT3	Jiang et al., 2008
P54727	RAD23B	Steinberg et al., 2012
P31483-2	TIA	Siersbæk et al., 2014
Q8N1F7	NUP93	Siersbæk et al., 2014
Q9UKX7	NUP50	Siersbæk et al., 2014
Q14974	KPNB1	Siersbæk et al., 2014
Q00839-2	HNRNPU	Siersbæk et al., 2014
P0C0S5	H2AFZ	Steinberg et al., 2012
Q9UJX4	ANAPC5	Siersbæk et al., 2014
O00267	SPT5	Siersbæk et al., 2014
P05455	SSB	Siersbæk et al., 2014
Q9NRF9	CHRAC17	Steinberg et al., 2012

Uniprot	Name	C/EBPβ publication
P51148	RAB5C	Siersbæk et al., 2014
P62820	RAB1	Siersbæk et al., 2014
Q9BY77-1	POLDIP3	Siersbæk et al., 2014
Q7Z417	NUFIP2	Siersbæk et al., 2014
P19388	POLR2E	Siersbæk et al., 2014
Q8IYB3	SRM160	Siersbæk et al., 2014
Q53GS9	USP39	Siersbæk et al., 2014
Q15637	SF1	Siersbæk et al., 2014
Q99459	CDC5L	Siersbæk et al., 2014
P22087	FBL	Siersbæk et al., 2014
Q14157-1	UBAP2L	Siersbæk et al., 2014
O00571	DDX3	Siersbæk et al., 2014
B1AHD1	NHP2L1	Siersbæk et al., 2014
Q15427	SF3B4	Siersbæk et al., 2014
O14979-2	HNRPDL	Siersbæk et al., 2014
Q99729	HNRNPAB	Siersbæk et al., 2014
A0AV56	SAFB1	Siersbæk et al., 2014
P09651-1	HNRNPA1	Siersbæk et al., 2014
Q07955	SFRS1	Siersbæk et al., 2014
P49756	RBM25	Siersbæk et al., 2014
Q15393	SF3B3	Siersbæk et al., 2014
Q9UMS4	PRP19	Siersbæk et al., 2014
Q9BWF3	RBM4	Siersbæk et al., 2014
Q15287	RNPS1	Siersbæk et al., 2014
Q14011	CIRBP	Siersbæk et al., 2014
Q12905	ILF2	Siersbæk et al., 2014
P62314	SNRPD1	Siersbæk et al., 2014
Q9Y265	RUVBL1	Steinberg et al., 2012; Siersbæk et al., 2014
Q9Y230	RUVBL2	Steinberg et al., 2012; Siersbæk et al., 2014
P31943	HNRNPH1	Siersbæk et al., 2014
O43809	NUDT21	Siersbæk et al., 2014
Q9H0D6	XRN2	Siersbæk et al., 2014
Q96QC0	CAT53	Siersbæk et al., 2014
P62805	H4/A	Siersbæk et al., 2014
Q14676	MDC1	Siersbæk et al., 2014
P05388	RPLP0	Siersbæk et al., 2014
P62829	RPL23	Siersbæk et al., 2014
O75643	ASCC3L1	Siersbæk et al., 2014
P09651-2	HNRNPA1	Siersbæk et al., 2014
O60506-1	HNRPQ	Siersbæk et al., 2014
O75533	SAP155	Siersbæk et al., 2014
Q9Y2W1	TRAP150	Siersbæk et al., 2014
P52272-1	HNRNPM	Siersbæk et al., 2014

PUBLICATIONS

Kruegel, U., Robison, B., Dange, T., Kahlert, Günther, Delaney, J. R., Kotireddy, S., Tsuchiya, M., Murakami, C. J., Schleit, J., Sutphin, G., Carr, D., Tar, K., Dittmar, G., Kaeberlein, M., Kennedy, B. K., Schmidt, M. (2011). Elevated Proteasome Capacity Extends Replicative Lifespan in Saccharomyces cerevisiae. *PLOS Genetics*, 7(9), e1002253.

Mates, N., Kettner, K., Heidenreich, F., Pursche, T., Migotti, R., Kahlert, Günther, Kuhlish, E., Breunig, K.D., Schellenberger, W., Dittmar, G., Hoflack, B., Kriegel, T.M. (2014). Proteomic and functional consequences of hexokinase deficiency in glucose-repressible Kluyveromyces lactis. *Molecular & Cellular Proteomics*, 13(3), 860?875.

Böhm, J. W.*, Kahlert, Günther*, Kowenz-Leutz, E., Pless, O., Dittmar, G., and Leutz,A. (2014). A comprehensive C/EBPβ interactome.

*these authors contributed equally to this work

IN RESUBMISSION PROCESS

C/EBPβ arginine methylation pattern determines its interaction with the transcriptional coactivators P300 & CBP.

MANUSCRIPT IN PREPARATION

Protein Interaction Screen on peptide Matrices (PrISMa) , a new method to detect C/EBPβ protein interaction pattern in a PTM dependent manner.

MANUSCRIPT IN PREPARATION

Berlin, 26th March 2015

ACKNOWLEDGEMENTS

Special thanks goes to Prof. Dr. Achim Leutz for giving me the opportunity to conduct the in this thesis presented research at the Max-Delbrück-Center for Molecular Medicine, Berlin.
Special thanks goes to the Max-Delbrück-Center for Molecular Medicine and the Helmholtz-Zentrum Geesthacht / Berlin-Brandenburg Center for Regenerative Therapies for financing this PhD thesis.
Special thanks goes to Dr. Gunnar Dittmar (Mass Spectrometry Core Unit, MDC) for the supervision and constant guidance of my mass spectrometric projects.
Thanks goes to the Mass Spectrometry Core Unit team members Rebekka Migotti, Dr. Julia Kikuchi, Tamara Kanashova, Dr. Daniel Perez Hernandez, Patrick Beaudette, Dr. Rick Scavetta and Dr. Oliver Popp. I had a great time with all of you and I will dearly miss you.
Thanks goes to Dr. Elisabeth Kowenz-Leutz, Maria Knoblich, Julia W. Böhm, Dr. Daniel Perez Hernandez and Dr. Qingbin Liu. It was a pleasure working together with all of you.
Thanks goes to the entire AG Selbach for sharing their knowledge and advice about mass spectrometers with me. Special thanks goes to Christian Sommer with whom I spent countless hours in front of mass spectrometers and HPLC systems and by that learning from scratch how to troubleshoot these complex machines.
Thanks goes to all the lab members of the AG Leutz especially Dr. Susann Förster and Dr. Jörg Schönheit for lending a helping hand whenever needed.

Thanks goes to Prof. Dr. Udo Heinemann and Prof. Dr. Matthias Selbach for acting as referees of this thesis.

Thanks goes to all my friends who supported me during my years as a PhD student. Amongst them a special thanks goes to Wiebke, Sophia and Hannes.

SELBSTSTÄNDIGKEITSERKLÄRUNG

Ich erkläre hiermit, dass ich die vorliegende Arbeit selbstständig und nur unter Zuhilfenahme der angegebenen Quellen und Hilfsmittel verfasst habe.

Des Weiteren erkläre ich, mich nicht anderwärtig um einen Doktorgrad beworben zu haben beziehungweise einen entsprechenden Doktorgrad zu besitzen.

Ich habe die dem Verfahren zugrunde liegende Promotionsordnung der Mathematisch- Naturwissenschaftlichen Fakultät I und der Lebenswissenschaftlichen Fakultät der Humboldt-Universität zu Berlin zur Kenntnis genommen.

Berlin, den 27. März 2015

Günther Kahlert